EPITHERMAL ALTERATION AND GOLD MINERALIZATION IN LATE PRECAMBRIAN VOLCANIC ROCKS ON THE NORTHERN BURIN PENINSULA, SOUTHEASTERN NEWFOUNDLAND, CANADA

ALLAN ANDREW HUARD, B.Sc.(Honours)

ISBN 0-315-55019-8

Epithermal Alteration and Gold Mineralization in Late Precambrian Volcanic Rocks on the Northern Burin Peninsula, Southeastern Newfoundland, Canada

BY

Allan Andrew Huard, B. Sc. (Honours)

A thesis submitted to the school of Graduate Studies in partial fulfillment of the requirements of the degree of Master of Science

Department of Earth Sciences
Memorial University of Newfoundland
June, 1989

St. John's Newfoundland

Abstract

Alteration and gold mineralization in late Precambrian subaerial volcanic rocks on the northern Burin Peninsula of southeastern Newfoundland are compared to younger epithermal systems. Several similarities are revealed when consideration is given to the deformational and metamorphic effects of the (Devonian) Acadian orogeny.

Conspicuous erosionally resistant ridges composed of quartz, alunite, pyrophyllite, specularite, pyrite and rutile cover several thousand m^2. These include the Hickey's Pond, Tower and Bullwinkle Showings which are shown to be products of intense surficial acid leaching, a common feature of modern geothermal fields. Specularite-rich hydrothermal breccias (+/- barite) occur at Hickey's Pond and the Bullwinkle showing, and in argillic alteration zones named the Chimney Falls and Strange Showings. Silicification (*sensu stricto*) with incipient brecciation and quartz-pyrite veinlets is locally developed at Hickey's Pond.

All rock samples collected at Hickey's Pond exhibit anomalous gold concentrations, but similar rocks from the Tower and Bullwinkle showings do not. The highest gold concentrations (5.4 g/t) are in the specularite-rich breccias, followed by the silicified rock with quartz-pyrite veinlets (2.5 g/t Au). Elsewhere, the highest gold concentrations are in specularite-rich breccias at the Strange Showing (0.8 g/t Au) and Chimney Falls (0.3 g/t Au).

Two mineralizing stages are inferred. The first formed the silicified rock with quartz-pyrite veinlets and is inferred to reflect elevation of the boiling level and precious metal horizon of an ascending hydrothermal fluid into the near-surface environment at Hickey's Pond. The second formed the specularite-rich breccias, to which the only comparable mineralization noted is a barite-jarosite-goethite-gold assemblage at Summitville, Colorado. Auriferous fluids from both stages flooded the porous and permeable acid leached rocks at Hickey's Pond, creating a large, very low grade gold deposit. The surficial features were buried

by renewed volcanism, then subject to greenschist facies metamorphism and strong deformation during the Acadian orogeny.

The sites of boiling inferred to have accompanied the genesis of the Bullwinkle and Tower Showings are shown to have been favourable sites for gold deposition. Semiquantitative modelling indicates that a significant gold deposit ($>$ 6,000,000 g) could have formed in such (undiscovered) zones.

Author's Note

This thesis consists of 9 chapters in 3 logical parts of three chapters each. The first three chapters are introductory, dealing with previous work, the author's observations on general geology and a study of alteration of clearly recognizable volcanic rocks, respectively. Chapters 4, 5 and 6 comprise a detailed petrological study of several mineralogically and texturally uncommon rock types. The descriptions in Chapter 4 are supplemented by a detailed study of relevant literature in Chapter 5, followed by an interpretation of the origins of the rocks in Chapter 6. Having established independently the genesis of these rocks, the study turns to description and discussion of their precious metal geochemistry in Chapter 7. This is followed by a literature review of epithermal systems in Chapter 8 and a comparison between the features in the study area and those described in the literature in Chapter 9.

Acknowledgements

Dave Strong is thanked sincerely for his insights, suggestions and discussions pertaining to this thesis. Paul Dean and Cyril O'Driscoll anticipated the timeliness of this study and are thanked for providing the opportunity to the author. Tom Calon provided the author with an introduction to the current state of structural geology, which enabled the recognition of some important structural features in the study area. Thanks to all the above, and to Sean O'Brien, Baxter Kean, Scott Swinden, John Tuach and Derek Wilton for discussions and suggestions during and prior to the preparation of this manuscript.

Simon O'Brien (Grace Under Pressure) provided excellent field assistance in 1984 and is thanked especially for not torching the ATV. Dave Malloy is thanked for the excellent field assistance in 1985, and is here forgiven for playing the Willie Nelson tapes. Live long and prosper, guys.

Carolyn Emerson is thanked for the clear instruction in the use of the Hitachi scanning electron microscope. Gert Andrews provided some of the major element analyses, and Pam Moores did the sample preparation for the rare earth element analyses. The staff at the Department of Mines and Energy geochemistry lab are thanked for the sample preparation and additional major element analyses, and the staff of the lapidary shop at the Earth Sciences Department are thanked for the thin sections, polished sections and fluid inclusion sections. Special thanks to Dan MacInnis of Noranda Exploration in St. John's for allowing this employee access to Noranda's excellent drafting facilities.

Field work during the summers of 1984 and 1985 was funded by the Newfoundland Department of Mines and Energy. The author was funded between field seasons by a Postgraduate Fellowship from the Natural Sciences and Engineering Research Council. The study was also supported by NSERC Operating Grant No. A7975 to Dr. D.F. Strong.

This thesis is for Ellarose, Warren and Thea. And for Mouse.

Table of Contents

List of Figures

List of Tables

Chapter 1
INTRODUCTION

1.1. Introduction

The peak in gold prices in 1979 heightened exploration interest in large, low grade "epithermal" precious metal deposits, which could be profitable only with high gold prices. BP-Selco acquired mineral exploration rights to certain tracts of subaerial felsic volcanics in Newfoundland in the fall of 1982, one of which was to become the host of the Hope Brook Mine, Canada's sixth largest gold producer (McKenzie, 1986). Another property acquired by BP-Selco, at Hickey's Pond on the northern Burin Peninsula, was almost completely eclipsed by the success of the Hope Brook Mine but was recognized as an integral part of an epithermal system.

The potential for the subaerial volcanics on the Burin Peninsula to host an economic gold deposit was recognized independently by geologists of the Newfoundland Department of Mines and Energy. A two year program was devised to document mineral occurrences suspected to be related to epithermal systems, one aim of which was to attract private industry to explore the area. The first year of the program (1984) involved the area around the Swift Current Granite, which is the subject of this thesis. The second year (1985) included follow-up work in the Swift Current Granite area, and additional work farther south around the Cape Roger Mountain Batholith and the "Knee Granitoids". Preliminary reports of this program were provided by Huard and O'Driscoll (1985, 1986) but are superseded by this work.

1.1.1. Location and access

The study area is a northeasterly trending belt of rocks approximately 25 km long by up to 10 km wide, centered 20 km southwest of the community of Swift Current, at the head of Placentia Bay in southeastern Newfoundland (Figure 1-1).

A paved highway (Route 210, the Burin Highway) linking the southern end of the Burin Peninsula with the Trans-Canada highway at Goobies parallels the northwestern margin of the study area. A gravel road (214, the "Monkstown Road") runs southeast from highway 210 to the community of Monkstown, on the western shore of Placentia Bay. This road cuts through the southern part of the study area, providing excellent access to the southern half.

Field work on the southern part of the area was conducted from the Monkstown Road. The northern half was worked from a flycamp centrally located at Hickey's Pond, which was accessed via a 9 km muskeg trail from the Burin Highway.

1.1.2. Physiography and vegetation

Hickey's Pond is situated approximately 175 m above sea level, in a gently rolling area characterized by numerous small ponds. Elevations over 350 m occur in the White Hills, which run from approximately 4 km north of Hickey's Pond to Swift Current. Drainage from Hickey's Pond is southwestward for 5 km via Hickey's Brook, which flows into Sandy Harbour River, and then southeastward 7 km discharging into Placentia Bay. Sandy Harbour River runs parallel to Paradise River, site of a small hydroelectric station under construction 9 km to the southwest, and together they carry most of the drainage southeast from the study area, being fed by several smaller northeast and southwest flowing tributaries (Figure 1-2). The northeast-southwest orientation of streams is also characteristic of most ponds, and reflects a strong bedrock cleavage.

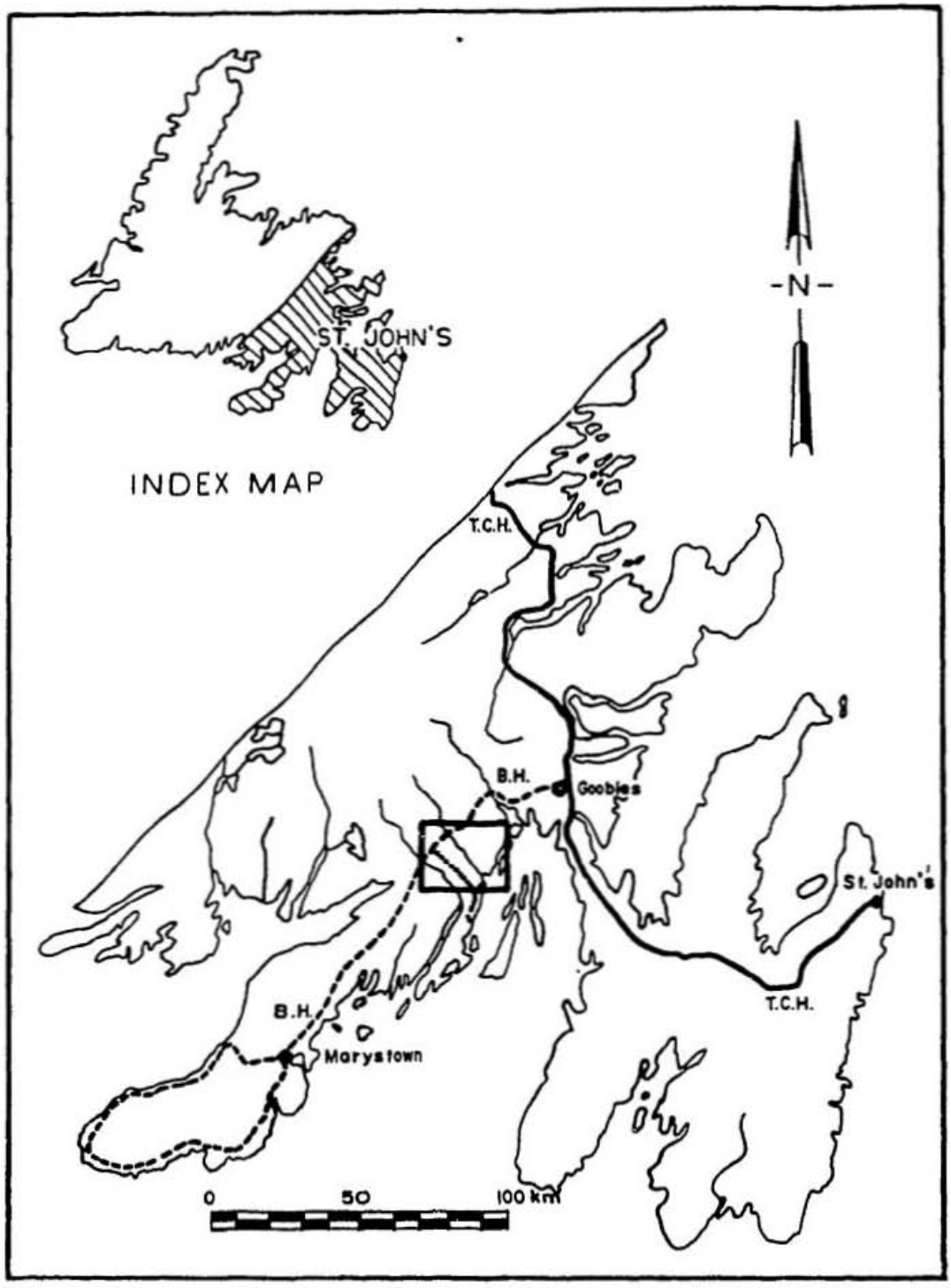

Figure 1-1: Location of study area. The box encloses the area of the appended map (Figure 2-1). T.C.H. = Trans Canada Highway, B.H. = Burin Highway, dotted line = Monkstown Road.

Figure 1-2: Physiography. View southeastward along Sandy Harbour River showing excellent outcrop availability and spruce-filled gullies in foreground.

Exposure varies from 100% over large areas in rougher parts, to 5% in muskeg-covered flatlands. Large areas are well exposed where low northeast trending barren ridges alternate with parallel boggy flats. Overburden is generally thin and allows for the identification of even very small airphoto lineaments.

Minor stands of spruce occur in the steep-walled valleys of the larger streams and airphoto lineaments, and on conspicuous glacial deposits (Section 1.1.3).

1.1.3. Glaciation

Glacial striae occur in only a few places, owing to the high fissility of the deformed rocks, but their trend where observed is consistently northwest-southeast. Drumlins up to 15 m high, 500 m across and 3000 m long occur along the Monkstown Road. They strike northwest-southeast and support the best stands of spruce in the area, one being the site of a small lumber industry and sawmill. These observations agree with the model of Tucker and McCann (1980), whereby ice moving radially outward from a central Newfoundland icecap moved southeastward across the northern Burin Peninsula.

1.1.4. Objective

The objective of this thesis is to document and explain the geological processes which formed the occurrences of gold mineralization and related alteration near the southern end of the Swift Current Granite. Such occurrences have been examined by Newfoundland Department of Mines and Energy geologists (O'Driscoll, 1984) and geologists of BP-Selco (McKenzie, 1983), following earlier suggestions that the area had features favourable for volcanic-hosted epithermal precious metal deposits (Hussey, 1978). O'Driscoll (1984) proposed additional work which might be undertaken by a temporary Department of Mines geologist. That work program, which became the initial objectives of this study, was as follows: 1) establish the volcanic stratigraphy and structure of the area, 2) examine in detail the "quartzites" outcropping on the side of Hickey's Pond and 3) intensively map and sample the surrounding area, including other known showings. These objectives would be met by mapping and sampling, complemented by petrological, geochemical, isotopic and fluid inclusion studies.

1.1.5. Procedure

Field work was conducted in the area from early June to late August, 1984, and during June, 1985. Time was divided between traverses from the Monkstown Road, when the author was staying at a cabin in Swift Current, and traverses from a fly camp established at Hickey's Pond later in the summer of 1984. Mapping at a scale of 1 : 25,000 was conducted over large areas, and more detailed mapping of the Hickey's Pond showing was undertaken at a scale of 1 : 2,500. Rock samples were collected in the field and were split where it was decided that the rock should be analyzed for Au. These splits were prepared for Au analysis at the Newfoundland Department of Mines and Energy geochemistry lab in St. John's; the analyses were performed by Chemex labs in Vancouver, British Columbia.

Thin sections and doubly polished fluid inclusion sections were prepared at Memorial University's lapidary shop in the Earth Sciences Department. These were examined by optical and scanning electron microscopes at Memorial University. Whole rock geochemistry conducted at the university included classical major element oxides, selected trace elements and rare earth elements. Major elements were also analyzed at the Department of Mines and Energy Geochemistry Lab in St. John's. Details of the analytical procedures are given in the Appendix. Additional geochemical data were acquired with an energy dispersive electron probe microanalyser. Selected whole rock powders and mineral separates were analyzed by X-ray diffraction.

1.2. History of previous work

The following report on previous work is in three parts. The first two, on general mapping and tectonic interpretations, are based mainly on work by government geologists and academics. The third section is on the economic geology of the Hickey's Pond showing, referencing promotional work dating back to 1934, government investigations and recent work by BP-Selco. Figure 1-3, the most recent geological compilation by the Newfoundland Department of Mines, is

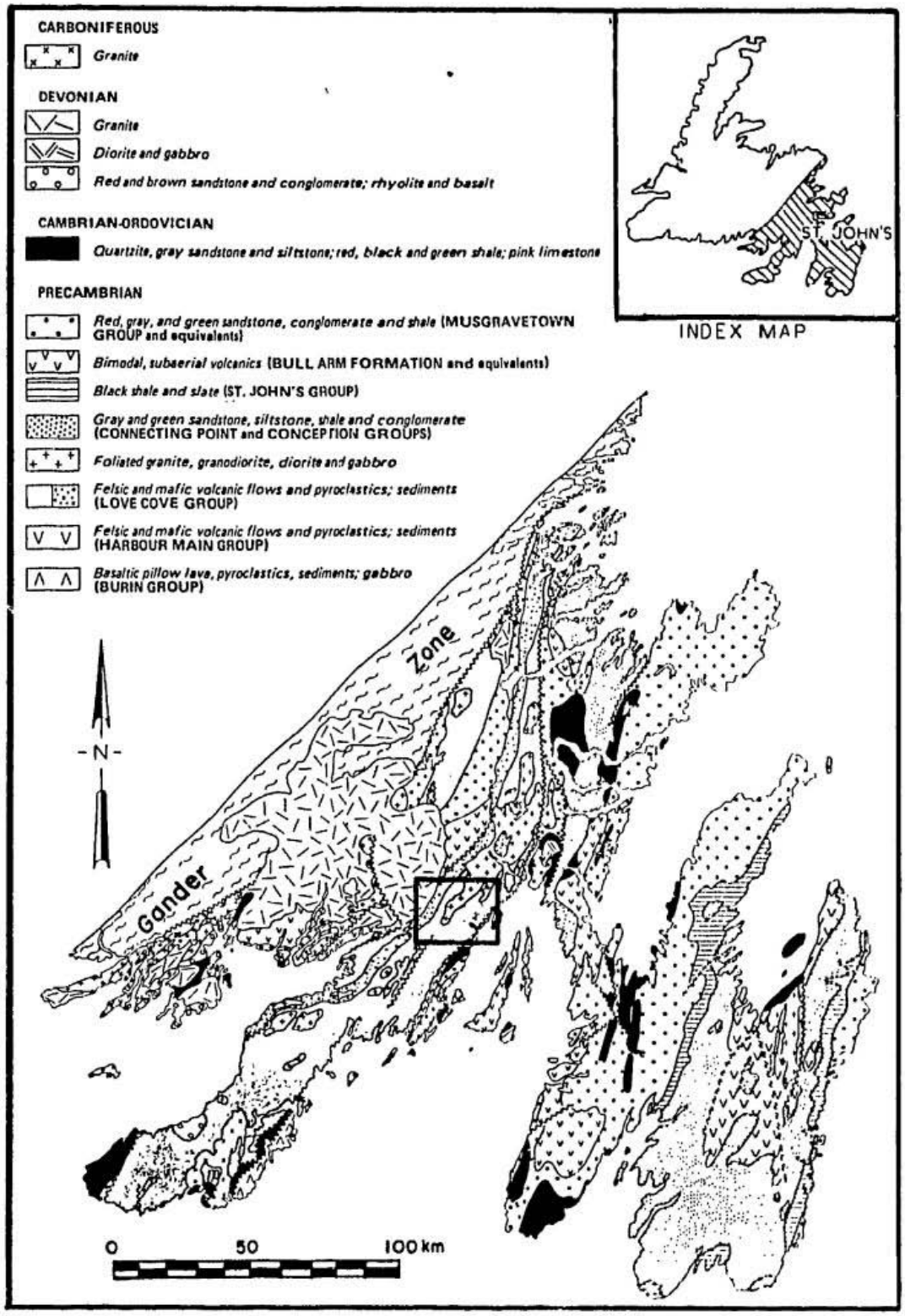

Figure 1-3: Regional geology. Prominence of felsic volcanics in the study area (box) is shown. [From Dallmeyer *et al.*, 1983.]

provided here for comparison with the historical interpretations.

1.2.1. General geology

The geology of the Burin Peninsula is now assigned to a large tectonostratigraphic package which includes the Avalon Peninsula, the namesake of the "Avalon Zone", and similar rocks which can be traced southward through the Canadian Maritime provinces and the eastern seaboard of the United States to Georgia (Williams, 1979; Williams and Hatcher, 1983). As such, a huge volume of literature is relevant to the geology of the northern Burin Peninsula. However, the aim of this section is to provide a tectonic framework for the mineralization. Therefore, only work in the area of the Northern Burin Peninsula is considered in detail. The tectonic interpretations from several syntheses (Rast *et al.*, 1976; Strong, 1979; O'Brien *et al.*, 1983A) are based on a much larger body of information than is presented here, and the reader is referred to references therein for details of Avalonian geology elsewhere.

The first geological mapping in the area was by Dahl (1934). He assigned the geology of the Hickey's Pond area to a northeasterly trending "geosynclinal" of the type described by Murray and Howley (1881). He described "Huronian slates" of sedimentary origin which strike northeast and dip almost vertically. These were in contact to the northwest with Laurentian granitoid rocks, which commonly occupy the cores of the anticlinals.

Rose (1948) did reconnaissance work to the northwest of the study area and outlined the northwestern extent of the Northern Bight (Swift Current) granite (the "Laurentian granitoid" of Dahl), which he classified only as Paleozoic. Rose included the stratified rocks to the southeast of the granite, Dahl's "Huronian slates", in his Middle (?) Cambrian Sound Island Formation. This included chlorite schist, sericite schist, pyroclastics and interbedded sediments. Rose commented on the "advanced state of metamorphism" and deformation of the rocks, which had obscured many primary features. He described a "granitized schist" composed of quartz and feldspar phenocrysts in a matrix of sericite and

fine quartz. Its occurrence near the contacts of the granite was attributed to an origin by granitization by fluids derived from the intrusive Northern Bight Granite.

Bradley (1962) mapped the Terrenceville (1M/10) map sheet, which includes the southwestern end of the study area, at a scale of 1 : 63,360. The map sheet is beyond the southern end of the "Northern Bight Granite" of Rose, but Bradley correlated the Northern Bight Granite with his Cape Roger Mountain Batholith on the basis of their being foliated. He recognized these granites as predating the deformational event that preceded the intrusion of the Ackley City Granite, and suggested that they might be Silurian.

Bradley (1962) defined two formations composed primarily of felsic volcanics; the older Southern Hills Formation and the younger, conformably overlying Deer Park Pond Formation. The Deer Park Pond Formation occurs along the southeastern margin of the Cape Roger Mountain Batholith, striking northeasterly towards the Hickey's Pond area. As such it can be correlated with Rose's Sound Island Formation, although this was not done by Bradley. He interpreted both formations to be Precambrian, on the bases of a lack of fossils and correlations with similar units which are unconformably overlain by fossiliferous Cambrian strata.

The Belleoram (1M) map sheet was mapped and compiled at 1 : 250,000 scale by Anderson (1965). He correlated the volcanic formations of Rose and Bradley, adopting Bradley's Precambrian age over Rose's Middle Cambrian age. Anderson did not adopt Bradley's correlation of the Northern Bight Granite with the Cape Roger Mountain Batholith. Instead, he characterized it as unfoliated, and correlated it with the Devonian Ackley Batholith, retaining Bradley's assignment of the Cape Roger Mountain Batholith to the Silurian.

The origin of the "Northern Bight Granite" was among the topics addressed by O'Driscoll (1973), who suggested it be renamed the Swift Current Granite for

the following reasons: 1) the village of Northern Bight no longer existed, 2) Swift Current was the largest community included in the granite and 3) it was well exposed along the road passing through Swift Current. O'Driscoll rejected Anderson's correlation of the Swift Current and the Ackley granites, citing outstanding textural and geochemical differences. He also cautioned against constraining its age to being post-Cambrian, as suggested by the occurrence of other granites intruding Cambrian sediments, until those granites were positively correlated with the Swift Current Granite. Instead, O'Driscoll accepted Bradley's correlation of the Swift Current Granite and the Cape Roger Mountain Batholith, on the bases of texture and host rock lithology. His detailed geochemical study showed the granite to be calc-alkaline, and he raised the possibility that the granite and surrounding Precambrian volcanic rocks might be comagmatic.

Substantially different radiometric dates (Rb/Sr whole rock) were determined by Bell *et al.* (1977) for the Swift Current Granite (500 +/- 30 Ma., recalculated to 514 +/- 30 Ma with $\lambda^{87}Rb = 1.42 * 10^{-11}$ year^{-1}) and the Ackley Granite (345 +/- 5 Ma., recalculated to 355 +/- 5 Ma with $\lambda^{87}Rb = 1.42 * 10^{-11}$ year^{-1}). However, a large error for the Swift Current Granite detracts from an isochron interpretation for the data.

The most recent mapping of the Harbour Buffett (1M/9) and Sound Island (1M/16) map sheets was conducted at a scale of 1 : 50,000 by O'Driscoll (1978) and O'Driscoll and Hussey (O'Driscoll and Hussey, 1978; Hussey, 1978) respectively, from which the following description is taken. They questioned the 514 Ma. age of the Swift Current Granite determined by Bell *et al.* (1977) and proposed that it is comagmatic with the Precambrian volcanic rocks. They assigned all the volcanic and sedimentary rocks to their revised Love Cove Group, which comprises two formations in the study area.

The Sound Island Formation occurs in two outcrop belts paralleling the southeastern and northwestern margins of the northeasterly trending Swift Current Granite. Its outcrop belt on the southeastern margin attains widths up

to 8 km. The southeastern extent is defined by the Paradise Sound Fault, a major northeasterly-trending fault which possibly includes a component of eastward-verging reverse movement (O'Driscoll, 1978). Relevant to this point is the observation in the Marystown map area of southeastward thrusting on northwestward- dipping fault planes (Strong *et al.*, 1978A). Southeast of the Paradise Sound Fault are sedimentary and lesser volcanic rocks of the Musgravetown Group and younger formations, which had been demonstrated to unconformably overlie the Love Cove Group in the Bonavista Bay area (Jenness, 1963). The outcrop belt of Sound Island Formation on the northwestern margin of the Swift Current Granite reaches 4 km in width.

The Sound Island Formation consists predominantly of subaerial volcanic rocks, with minor associated intrusions and sedimentary rocks. Rapidly changing depositional patterns and the tight to isoclinal folding the rocks have undergone prevent thickness estimates of the formation. Felsic volcanics were shown to predominate, with lesser mafic and intermediate rocks. The felsic varieties include porphyritic, massive and banded rhyolite flows, intrusive rhyolite porphyries, crystal and crystal-lithic tuffs. Local intense deformation has produced a schistosity marked by sericite growth. Mafic rocks in particular demonstrate lower greenschist facies metamorphism. They include porphyritic mafic to intermediate flows, tuffs and agglomerate. The mafic and felsic rocks were not subdivided on the 1 : 50,000 scale maps, but Hussey (1978) suggested a stratigraphic sequence southeast of Long Pond, whereby mafic and intermediate flows and pyroclastics are overlain by silicic tuffs which are in turn overlain by tuffaceous sediments and greywackes.

The Sandy Harbour River Formation forms a 2 km wide belt northwest of the northwestern belt of the Sound Island Formation volcanic rocks, which it parallels. It consists of tuffaceous waterlain sediments with an abundance of felsic volcanic detritus. Conglomerates commonly display severe tectonic flattening, but locally preserved facing criteria, together with spatial relations and clast lithology, lead Hussey (1978) to conclude that the sediments conformably overlie the Sound

Island Formation, notwithstanding possible lateral gradations between the two.

O'Brien *et al.* (1984) mapped the Terrenceville (1M/10) map sheet at a scale of 1 : 50,000. They adopted the name Love Cove Group used by O'Driscoll and Hussey on the maps adjacent to the northeast, and subdivided it into 3 facies, two of which are relevant to the study area and are described below.

The Deer Park Pond Facies corresponds to the Sound Island Formation of O'Driscoll (1978). It consists of felsic and subordinate mafic subaerial volcanic rocks, generally of pyroclastic origin. O'Brien *et al.* (1984) indicate that massive flows constitute less than 5% of the map area, and that welded tuffs are uncommon. Epiclastic sediments are rare east of the Cape Roger Mountain Batholith, but are more common to the west of it. This final point proves to be significant in reconstructing the paleogeography of the study area (Sections 2.2.4 and 6.8.3).

The Grandy's Pond Facies corresponds to the Sandy Harbour River Formation of O'Driscoll (1978). It consists of immature, poorly sorted sandstones and lesser polymictic conglomerate with a sandy matrix. Clasts in the conglomerate include various types of volcanic rock, and together with the feldspathic nature of the matrix and the occurrence of the Grandy's Pond Facies as intercalations within the upper levels of the Deer Park Pond Facies, it was interpreted as an epiclastic sedimentary unit by O'Brien *et al.* (1984).

Geochronologic investigations were conducted on the Swift Current Granite and Love Cove Group volcanics by Dallmeyer *et al.* (1981) to resolve apparently contradictory views on the relationship of the two. Hussey (1978) provided evidence that they were comagmatic but Bell *et al.* (1977) showed the granite to be significantly younger, although their isochron age determination was not a good linear fit.

U/Pb age determinations conducted on four zircon splits from the Swift

Current Granite were interpreted (Dallmeyer *et al.*, 1981) to define a linear trend on a concordia plot, with an upper intercept of 580 +/- 20 Ma. interpreted to be the time of crystallization. U/Pb dates for 4 splits of zircons from the Love Cove Group volcanics yielded an upper intercept of 590 +/- 30 Ma., also interpreted to be a crystallization date. These data were taken to prove a comagmatic relationship between the volcanic and intrusive rocks, a conclusion reached independently for coexisting volcanic and intrusive rocks of similar age on the Hermitage Peninsula (O'Driscoll and Strong, 1979), the southwestern end of the Burin Peninsula (Strong *et al.*, 1978A) and the eastern Avalon Peninsula (Hughes and Bruckner, 1971).

The data of Dallmeyer *et al.* (1981) were recalculated by Krogh *et al.* (1988) who showed that the samples on the concordia plot were not collinear and regressed to (unreliable) ages of 557 (+29/-16) and 597 (+87/-25) Ma for the intrusive and volcanic rocks respectively. However, radiometric dates provided by Krogh *et al.* for other rocks in the Avalon Zone support the conclusion of Dallmeyer *et al.* of comagmatic late Precambrian volcanism and plutonism.

Incremental $^{40}Ar/^{39}Ar$ heating techniques were used to date 2 hornblende separates from the Swift Current Granite. Although the low temperature fractions showed anomalously young ages, plateau dates of 560 +/- 15 Ma and 566 +/- 15 Ma were provided by the higher temperature fractions. These were interpreted to represent ages of cooling below the temperature of Ar retention for hornblende. The relatively small difference between the U/Pb (crystallization) and $^{40}Ar/^{39}Ar$ (cooling) dates was taken to indicate rapid postmagmatic cooling due to shallow levels of crustal intrusion.

1.2.2. Tectonic Interpretations

The late Precambrian rocks in the study area record a period of subaerial volcanism and associated plutonism, which gave way to epiclastic sedimentation. Similar rocks occur elsewhere in the Avalon Zone of Newfoundland (O'Driscoll and Strong, 1979; O'Brien and Taylor, 1983; O'Brien *et al.*, 1983B, 1984; Strong *et al.*, 1978A; Hughes and Bruckner, 1971) and correlatives of the Avalon Zone elsewhere (O'Brien *et al.*, 1983A, and references therein). The events they record are only a part of the history of the zone in Newfoundland, which has been summarized by Strong *et al.* (1978B), Strong (1979) and O'Brien *et al.* (1983A). The salient features of the zone manifest in Newfoundland, enumerated below, are from the summary in O'Brien *et al.* (1983A):

1. **Upper Proterozoic Oceanic Volcanism.** The Burin Group (Strong *et al.* (1978A) is a submarine volcanic sequence with alkalic affinities at the base and oceanic tholeiitic affinities at the top. Zircons from a synvolcanic gabbro sill have been dated by U/Pb at 763 +/- 2 Ma (Krogh *et al.*, 1988). Oceanic volcanism at this stage in the Avalon Zone is restricted to the Burin Group, which forms a belt approximately 60 km long.

2. **Upper Proterozoic Subaerial Volcanism and Related Plutonism.** The rocks in the study area record these events. As described above, similar rocks occur extensively across the Avalon Zone in Newfoundland and beyond. A common feature displayed by these volcanic rocks is that they are bimodal with respect to silica, lacking widespread presence of andesites.

3. **Upper Proterozoic Sedimentation.** The epiclastic sedimentary rocks described in the study area are unconformably to disconformably overlain by Precambrian marine sediments. In the eastern Avalon Zone, the Conception Group records turbidite and pelagic sedimentation. It is conformably overlain by molasse sediments of the St. John's and Signal Hill Groups.

4. **Cambrian and Younger Platformal Sedimentation.** The Upper Proterozoic sedimentary, volcanic and plutonic rocks in the eastern Avalon Zone are separated from overlying Cambrian strata by an erosional unconformity. In the western Avalon Zone, the Proterozoic sedimentary rocks are overlain unconformably to conformably by the Cambrian sedimentary rocks. The Cambrian is represented by

fossiliferous shallow marine sediments developed only in the west, which are overlain by a regionally developed quartzite which is the base of the Cambrian in the east. This is overlain by various regionally extensive platformal facies, which include limestones, fine-grained clastics and iron formation.

Two contrasting tectonic models have been proposed for the Late Proterozoic-Early Paleozoic development of the Avalon Zone. The late Precambrian volcanism has been related (Rast *et al*,1976) to subduction of oceanic crust. They suggest that Avalonian volcanics were built on a microcontinent which was separated by a back-arc basin from the North American craton at the time of northwesterly subduction of a Cadomian (Late Precambrian) ocean.

There are several problems associated with this interpretation. Evidence advanced for the Cadomian ocean and subduction zone, notably a major fault zone in Brittany marked by blueschists and interpreted to be the suture zone, has been overturned by the recognition that the rocks there are Hercynian (references in Strong, 1979). The only vestige of the oceanic crust of the back-arc basin is a Precambrian glaucophane-bearing melange in Wales. Thus evidence for the ocean and back-arc basin is limited at best, and Rast *et al.* (1976) admit that the previous work of Hughes (1970) in Newfoundland noted a conspicuous absence of compressional features. Furthermore, the bimodal character of the Avalon volcanics is not consistent with consuming plate volcanism, which would be expected to include abundant andesites. Finally, basement similar to that of the Avalon Zone is unknown to the northwest, *i.e.* in the direction of the continent from which the Avalon microcontinent was presumably rifted.

In contrast to the compressional tectonic regime proposed by Rast *et al.* (1976), Strong (1979) stressed the features which show the extensional nature of the tectonic regime under which the Avalon Zone developed. These features include local (*circa* 763 Ma) crustal rupturing and formation of limited tracts of oceanic crust followed by bimodal (basalt-rhyolite) volcanic activity. A second basalt-rhyolite association older than the Burin Group, and cited as evidence of

very long lasting extensional tectonics, was inferred by Strong on the basis of volcanic clasts in the Rock Harbour Group. The clasts have since been shown (Krogh *et al.*, 1988) to be the same age as the Marystown Group volcanics, which reduces the time period, but does not change the nature of the late Precambrian volcanism discussed by Strong (1979). He pointed out differences between the extension inferred from the Avalonian geological record and that characteristic of Paleozoic ocean-forming extension, namely the limited extent, large time interval represented and different geological characteristics of the crust formed under the former conditions. He compared these conditions to those suggested by Stewart (1976), which developed at *circa* 850 Ma in the North American craton, marking a profound change from the earlier pattern of epi-continental troughs. Finally, using a palinspastic reconstruction, he suggested this extensional event developed in local tracts of a supercontinent comprising North America, West Africa and the Baltic shield, foreshadowing its later rifting.

O'Brien *et al.* (1983A) also compare the Avalon Zone to the Precambrian Pan-African belts of North Africa. The Pan-African invites comparison because 1) the Avalon Zone, despite its continuity in the Appalachian orogen of North America does not continue into the Caledonides in Scandinavia, which are regarded as the continuation of the Appalachians, 2) probable ophiolites and "oceanized" continental crust (the product of extensive mantle magmatism which failed to produce true oceanic crust) which are the same age as the Burin Group occur in the Pan- African at Bou-Azzer (Leblanc, 1981 and references to his earlier work therein) and in the Pharusian Belt of the Hoggar Shield (Bertrand and Caby, 1978), respectively and 3) thick sequences of late upper Proterozoic calc-alkaline volcanics, laterally equivalent greywackes and related intrusive rocks occur in the Pharusian Belt (Bertrand and Caby, 1978). These volcanic rocks are overlain by thick molassic deposits.

Kroner (1979) reviewed the differences in the Pan-African belts along the eastern margin of the West African craton. His most important conclusion is that the amount of rifting as indicated by the production of oceanic crust varies

considerably along strike, from limited production of tholeiitic basalts in the Dahomeyan belt, through widespread "oceanization" in the Pharusian belt to limited production of oceanic crust in the Anti-Atlas belt. He summarized, as did Strong (1979) Pan-African tectonics as an attempt to rift a continental mass that met with variable success along strike. Limited rifting produced intracratonic basins and local, small tracts of oceanic crust (stages represented by the Rock Harbour and Burin Groups respectively). Closure of the rift was accompanied by local, limited subduction (including the subduction of continental crust), crustal thickening, melting, volcanism, and the emplacement of large calc-alkaline plutons during the late stages of volcanism.

O'Brien *et al.* (1983A) support this interpretation because it explains the *circa* 763 Ma Avalonian record and the later volcanic and intrusive events. Late Precambrian sedimentation, the Avalonian orogeny and early Cambrian sedimentation are explained as sedimentation in a shoaling basin followed by peneplanation at the height of closure, and subsequent waning of compression and transgression of the Cambrian sea.

In discussing new and old radiometric dates, Krogh *et al.* (1988) stress the similarity in age between the Burin Group and the Ophiolites at Bou Azzer, and the subaerial volcanics of the Avalon Peninsula and Pan-African terranes. They showed that the range in ages for the subaerial volcanics and associated intrusive rocks was similar to that of the Basin and Range of the southwestern United States, and suggested a comparable tectonic setting for the Avalon Zone, *i.e.* large-scale, long term epicontinental volcanism associated with very large calderas in an extensional environment.

For purposes of this thesis, the comparison between the Avalon Zone and the Pan-African is almost pointless because Pan-African history remains controversial. The fundamentally contentious issue in Pan-African history is the nature of the Pan-African "continent"; was it a coherent mass subject strictly to intracratonic processes (Kroner, 1979, 1980) or was it "assembled" during the

Pan-African (Rogers *et al.*, 1978)? This author favours the suggestion of Strong (1979) and Kroner (1979, 1980) that the Pan-African represents a temporal transition in tectonic styles, from the intraplate deformation of the Precambrian, to the plate margin deformation of the Proterozoic, where Wilson-cycle tectonics are accepted.

This thesis is primarily concerned with the economic geology of the study area, and shows that the controls on the mineralizing processes were not unique to the Pan-African. Comparisons with mineralizing systems similar to those which operated in the study area include Basin and Range tectonic settings and island arcs (Chapters 5 and 8). The former comparison is interesting in light of the same comparison made by Krogh *et al.* (1988) to explain volcanological features.

1.2.3. Economic geology

An unusual rock type at Hickey's Pond (Figure 1-4) has been assessed historically as a source of iron, potash and aluminum; most recently, attention has turned to its precious metal potential.The following sections document the work done to date at the Hickey's Pond showing and surrounding area.

1.2.3.1. Dahl: investigation of the iron potential

Specularite mineralization at Hickey's Pond had been discovered and mined at a very small scale at least several years before 1934, at which time it was included in a property comprising 4,480 acres owned by a Mr. W.H. Taylor of London, England. In January, 1934 an investigation of the Hickey's Pond showing and surroundings was undertaken by Professor O.M. Dahl, a Danish engineer and geologist (Dahl, 1934).

He reported the outcrop to be 400 by 800 feet, and contain approximately 12 "strongly mineralized" quartz veins, with a total width of 115 feet hosted by a "talcoid schist". He provided a rapid estimate of the mass of "ore" above water at the showing by multiplying the 115 foot width by the 800 foot length, the average height above water level (65 feet) and the estimated density. He

Figure 1-4: Banded rock from Hickey's Pond. Pink material is quartz, alunite, pyrophyllite and rutile; black bands are similar but contain approximately 5% specularite. No clear petrogenesis is apparent from field inspection of this common rock from Hickey's Pond. Note hammer at bottom for scale.

concluded there were 427 000 tons above water level and estimated it to contain 65% ore.

Elsewhere, Dahl reported two large outcrops within "a couple of hundred feet" of the contact with the "Laurentian Granitoids" to the northwest, where the "Huronian measures" were converted to a "talcoid schist" hosted by a "whitish slate". One of these was at Chimney Falls over 4 km to the southwest of Hickey's Pond. Both were reported to host "quartz veins of very considerable dimensions richly charged with a high grade specular ore". He also reported another outcrop of "talcoid schist" at an unspecified location which he was unable to visit, which "is reported very solid in ore". Dahl was unable to determine whether the interval between Hickey's Pond and Chimney Falls was mineralized, as it was buried under snow at the time of his inspection.

Dahl conducted detailed surveys on the drainage from the region and showed that sufficient electricity could be generated to maintain an electric smelting plant. He also appraised the area in terms of topography, overland transportation possibilities, shipping accommodation and timber resources with a view to developing the showing. He proposed simultaneous development at two places; one of which at the Hickey's Pond deposit would require concentration, the other of which "at the northeastern end of the deposit" was reported to be "so solid and high grade as not to require concentration". The location of the latter site, which was referred to as Saddle Hill, was never specified and Dahl wrote that its geology would be supplied in a supplementary report as "the field season prevented (its) detailed examination".

Dahl considered the host rocks to be sedimentary, with the protolith of the specularite mineralization being beds of "hydrous ferrous silicate or iron bearing carbonates". These strata were deformed and metamorphosed to their present appearance.

1.2.3.2. Bainbridge: promotion of the iron potential

Dahl's account of the mineralization at Hickey's Pond was heavily referenced in a report by Bainbridge (1934) to the Newfoundland Department of Agriculture and Resources. This favourable report emphasized the high Fe content, and low S and P contents of grab samples of the "ore" which had been analyzed. He misquoted Dahl in reporting the deposit to average between 3 to 400 feet over a 3 mile strike length and concluded the size of the deposit "undoubtedly runs into scores of millions of tons".

1.2.3.3. Howland: dismissal of the iron potential

Field work for the Geological Survey of Newfoundland carried out by Howland in 1938 involved the appraisal of the iron deposits in southeastern Newfoundland. Hickey's Pond was one of the deposits studied and its iron potential was quickly dismissed on the bases of 1) the iron mineralization consisted of narrow veins of high grade coarse specularite which could not be

followed along strike and 2) channel samples of the more abundant "specularitized schist" yielded low grades of iron (up to only 3.42% Fe). Howland also pointed out that the deposit terminated abruptly to the north and south, and there were no other similar occurrences in the area.

Howland did not directly address the observations reported by Dahl (1934) and Bainbridge (1934), but his observations at Hickey's Pond and other places contradicted the enthusiastic estimates of the earlier works. He reported the occurrence at Chimney falls to be "talc schist" cut by a few quartz veins containing disseminated specularite. He reported another specularite occurrence at the headwaters of Hickey's Brook, consisting of minor disseminated specularite in chlorite schist, with abundant disseminated pyrite in nearby "talc schist". It is not known whether this was one of the showings described by Dahl (1934), but no other descriptions were provided by Howland that could possibly represent the high grade mineralization reported to occur at Saddle Hill.

More important were Howland's mineralogical observations and interpretations. He identified alunite as an abundant constituent mineral at Hickey's Pond, locally constituting up to 50% of the rock there. He tentatively identified very small equant yellow crystals with very high relief as rutile (Howland; 1938, 1940).

Howland recognized the association between gold and alunite at Goldfield, Nevada and had two samples from the showing analyzed for gold, although in both samples it was below the (unspecified) detection limit available at the time. He noted differences between the mineralization at Goldfield and Hickey's Pond, including 1) the abundance of specularite at Hickey's Pond, 2) the lack of porosity at Hickey's Pond, 3) the occurrence of a shear zone of apparently deep origin there and 4) the lack of sulphosalt minerals. He concluded that the alteration responsible for the mineralization must have occurred at a greater depth than that responsible for the Goldfield mineralization, which had been categorized as epithermal.

Howland addressed the problem of the origin of the Hickey's Pond mineralization in a later paper (Howland, 1940). Two problems hampered his interpretations: 1) he did not consider the possibility that the mineralizing event could have predated the deformation; thus the lack of porosity at Hickey's was regarded as a significant difference between known deposits of near-surface origin although it could have been explained in terms of later structural events and 2) he treated the assemblage of specularite and alunite as highly unusual, having been unable to find similar examples in the literature. The latter problem was particularly unfortunate, since recent literature which is discussed in Chapter 5 has precisely documented the origin of similar rocks in a tightly constrained physicochemical regime. Although the conditions which foster such mineralization are uncommon, they are highly specialized and "pinpoint" the relative age and style of the mineralization at Hickey's Pond, as discussed in Chapter 6.

Another problem which was not resolved by Howland stems from the diverse origins which different alunite-bearing assemblages represent. In this regard, his recognition of apparently contradictory origins for different alunite occurrences in the literature was accurate, although it prevented his forming a conclusion as to the origin of the Hickey's Pond mineralization.

In terms of economic potential, he repeated his earlier dismissal of the showing as a source of iron. He related the use of alunite from Marysvale, Utah and Tolfa, Italy as a source of potash, but dismissed the potential at Hickey's Pond due to much lower alunite content. For reasons of commercial inviability elsewhere, he also dismissed the showing as a producer of aluminum and sulphuric acid.

1.2.3.4. Department of Mines and Energy: precious metal potential

The potential for the subaerial volcanics on the Burin Peninsula to host gold deposits was considered in general terms to be good by Taylor *et al.* (1979). Their favourable comment stemmed from comparison of the rocks with those in the Carolina Slate Belt of the southeastern United States, which has hosted several

small gold producers dating back to the 1800's. However, they stressed structurally controlled lode gold deposits as the most favourable target, although comparison with the Carolina Slate Belt deposits implies epithermal systems (papers in Feiss (ed.), 1985; Spence *et al.*, 1980).

Hussey (1978), using X-ray diffraction identified in the showing at Hickey's Pond the minerals named alunite and talc by Howland (1938) as natroalunite, the sodium-rich variety of alunite and pyrophyllite, respectively. He showed that the southeastern margin of the Swift Current Granite was the locus of a narrow belt of alteration which, where exposed, included quartz-sericite schists, quartz-pyrophyllite schists and specularite-quartz- pyrophyllite-natroalunite-sericite schists. Locales studied included the Hickey's Pond showing, two previously reported specularite occurrences and a new occurrence of pyrophyllite schist discovered by Hussey.

Hussey (1978) provided references which relate the association between alunite and various types of mineral deposits and related processes, *e.g.* porphyry copper deposits, gold-alunite veins, epithermal precious metal deposits and hotsprings activity. He further suggested that the Hickey's Pond mineralization had an origin similar to the pyrophyllite deposit being mined at Manuels, Newfoundland. The origin of that deposit was discussed by Papezik *et al.* (1978), who appealed to the action of acid hydrothermal fluids which possibly originated in the nearby Holyrood Granite.

Following a drill program by BP-Selco, to be discussed in the following section, O'Driscoll (1984) discussed the possible origin of the Hickey's Pond mineralization. He compared the mineralization at Hickey's Pond to hotsprings-related precious metal deposits of the Carolina Slate Belt. This was done on the basis of a correlation between the respective host rocks, the Love Cove Group and the Uwharrie Formation volcanics, which had been made by previous authors, including Williams (1979).

O'Driscoll pointed out mineralogical and geochemical similarities between deposits in the Carolina Slate Belt, as summarized by Spence *et al.* (1980), and the Hickey's Pond area, including: 1) the high-alumina alteration minerals sericite and pyrophyllite, 2) sulfides and oxides of iron, 3) the titanium-bearing mineral rutile, 4) the phosphate mineral lazulite and 5) variable quantities of gold.

O'Driscoll noted that alunite, an abundant mineral at Hickey's Pond, was absent in the gold deposits of the Carolina Slate Belt. However, he maintained the comparison on the basis that it is a common mineral in other near-surface hydrothermal regimes, e.g. Marysvale, Utah (Cunningham *et al.*, 1984). Cunningham *et al.*, however, had gold analyses performed on a suite of 72 rocks from different parts of the alunite-bearing systems they studied and demonstrated a maximum gold concentration of only 0.1 ppm. This contrasted with gold values reported by O'Driscoll for Hickey's Pond, which range from 0.1 to 0.8 ppm, averaging 0.4 ppm.

O'Driscoll also noted the uniform spacing of approximately 4 km between the Headwaters occurrence and Hickey's Pond, and the Chimney Falls occurrence and Hickey's Pond; and an 8 km spacing between Chimney Falls and a new occurrence discovered on the Monkstown Road (Tuach, 1984). He suggested the spacing could reflect a uniform spacing of hydrothermal cells which would be expected around a large, uniform cooling intrusion of the type described by Cunningham *et al.* (1984).

1.2.3.5. BP-Selco: gold exploration

Mineral exploration rights to the area surrounding the showing at Hickey's Pond were acquired in a block of 20 claims staked for BP-Selco in the fall of 1982. A geophysical survey consisting of magnetic, VLF-EM and IP surveys was conducted in the spring and summer of 1983. The magnetic and VLF-EM surveys did not define a "signature" over the known mineralization. However, the IP survey revealed moderate resistivity and chargeability highs over the known mineralization and detected other anomalies to the southwest and northeast

(Gubins, 1983).

BP-Selco completed a 423 m, four-hole diamond drill program in the fall of 1983 (McKenzie, 1983), the targets of which included down-dip extensions of the known mineralization and IP anomalies. McKenzie concluded that the showing contained only weak and erratic gold concentrations, and that no further work was warranted.

McKenzie (1983) described the rocks as having formed in a hotsprings environment as a result of the surficial accumulation of silica. The related hydrothermal system was not thought to have carried economically important concentrations of gold or other elements.

Chapter 2
GENERAL GEOLOGY

2.1. Introduction

As the primary aims of this thesis relate to alteration and mineralization, the accounts of stratigraphy, structure, metamorphism and geochemistry which follow are not intended to be comprehensive. In general, they are footnotes derived from the economic study and provide detail or corroborating evidence for the preceding review of observations (Chapter 1) on the general geology of the study area.

2.2. Stratigraphy

Volcanic and intrusive rocks were the emphasis of this study; no work was done in the belts of sedimentary rocks either southeast of the Paradise Sound Fault or northwest of the study area. The volcanics have been subdivided into predominantly mafic and predominantly felsic units, and are described in the following sections, followed by the intrusive rocks (Figure 2-1, back pocket).

2.2.1. Mafic volcanics

Mafic to intermediate flows and pyroclastic rocks are the most abundant rocks in the area, and are well represented by new exposures on the Monkstown Road. Northeast striking, steeply northwest-dipping massive, amygdaloidal and porphyritic flows are best developed farthest east, adjacent to the Paradise Sound Fault. Relationships of amygdaloidal sections to oxidized zones suggest that the flows are upright. They persist northwestward for approximately 2 km, where they gradually give way to lithic tuffs and agglomerates. Fragments in these

rocks are up to 1 m long and tend to be strongly flattened with aspect ratios up to 10:1 (Figure 2-2), although the relative importance of structural flattening *versus* syndepositional effects, *e.g.* preferred alignment of tabular fragments, is unclear.

2.2.2. Felsic volcanics

The felsic volcanics are exclusively pyroclastic and include crystal-lithic tuffs, crystal tuffs and vitric tuffs, the latter two of which are locally welded (Figure 2-3). In the porphyritic rocks, phenocrysts of quartz predominate, and may occur with lesser plagioclase or rarely sanidine. Glassy, black aphyric rhyolite dykes are common and are generally broken into cm-scale blocks by several joint sets, as opposed to displaying the penetrative cleavage taken up by the extrusive rocks. Cleavage and bedding are parallel and universally strike northeast and dip steeply northwest.

2.2.3. Intrusive rocks

The Swift Current Granite is generally an equigranular biotite granite, although locally developed phases include hornblende porphyritic granites (Figure 2-4), diorites and quartz-feldspar porphyries. It generally displays a weak foliation defined by preferred orientation of biotite, but ranges from massive to moderately sheared. It shares with the host volcanics a multitude of airphoto lineaments.

2.2.4. Interrelationships

Volcanic rocks occupy an 8 km wide belt between the eastern margin of the Swift Current Granite and the sedimentary rocks of the Musgravetown Group to the southeast. Both contacts are steeply northwest-dipping faults, the Hickey's Brook Fault (Section 2.3.1) to the northwest and the Paradise Sound fault to the southeast. The volcanics comprise a conformable sequence with a maximum true thickness of about 7000 m, but this estimate assumes no structural repetition. Evidence based on alteration patterns (Section 6.3) shows that some of the volcanics adjacent to the Hickey's Brook Fault are overturned, requiring at least

Figure 2-2: Flattened fragments in lithic tuff. Dark fragments are amygdaloidal basalt, light weathering matrix is intermediate to basaltic.

Figure 2-3: Welded tuff. Eutaxitic texture is clearly shown by flattened fragments. Photographed looking down-dip in a quarry on the Monkstown Road.

Figure 2-4: Swift Current Granite. Shown is a massive, hornblende porphyritic phase. Width of sample is 10 cm.

one fold closure in this belt of volcanics, and suggesting that the true thickness is less than 7000 m. A section through this belt reveals mafic flows giving way westward to mafic pyroclastics which are overlain by felsic pyroclastics.

This sequence is repeated with the same polarity starting at the western contact of the Swift Current Granite, northwest of Hickey's Pond, where it forms a belt about 2000 m thick. Significant differences exist between the two belts; the western belt is a thinner volcanic pile with no comparable development of the agglomeratic mafic rocks. Welding is absent in the felsic tuffs, which are overlain by sedimentary rocks and grade southward into epiclastic felsic sediments (Section 1.2.1). These differences can be explained in terms of facies changes, with the western belt representing a more distal environment removed from the (vent facies ?) agglomerates and welded tuffs farther east. As such the eastern belt of volcanics might represent a volcanic highland which was not onlapped by

sedimentary rocks.

The western contact of the Swift Current Granite is intrusive, based on the occurrence of abundant aplite dykes in the host rocks (Figure 2-5) and large xenoliths of variably resorbed, amphibolitized mafic rocks in the granite (Figure 2-6).

Given the repetition of the volcanic stratigraphy with the same polarity on opposite sides of the granite and the different types of contacts, the volcanics are interpreted to be repeated by faulting on opposite sides of the granite. It is shown in Section 2.3.1 that the eastern fault contact is a reverse fault modified by shearing, a feature illustrated in the schematic cross-section through the study area (Figure 2-7).

2.3. Structure

Airphoto examination reveals the consistent north-northeast strike of the volcanics in the study area. It is manifest on the ground as a penetrative northeast-striking, steeply northwest-dipping cleavage which is best developed in the felsic volcanics and is most poorly developed in mafic flows, which tend to be nearly massive.

The strong fabric complicates recognition of bedding in the volcanics, to the point that bedding almost everywhere appears to follow the cleavage. In only one location, on Paradise River, was a clear cleavage/bedding discordance observed, in which bedding was 011/63W and cleavage was 047/80NW (Figure 2-8). Dykes have also been rotated into the cleavage (Figure 2-9), with the exception of a very small number of east-west striking massive basalt dykes that are clearly post-tectonic. Lacking good bedding and younging criteria, the interpretation of folds from map patterns was not possible. No large scale isoclinal folds were mapped, although the degree of deformation is sufficiently high and the consistent coincidence of cleavage and bedding would permit such an interpretation. Small scale isoclinal folds are common in zones of argillic alteration (Figure 2-10), and

Figure 2-5: Aplite dykes near granite contact. Massive, pink aplite dyke (behind hammer) is boudinned in host volcanics. Photographed near granite contact in Sandy Harbour River.

Figure 2-6: Xenoliths. Mafic xenoliths near margin of Swift Current Granite. Note resorption along bottom, right margin of prominent xenolith in foreground, which is cut by a late aplite dyke.

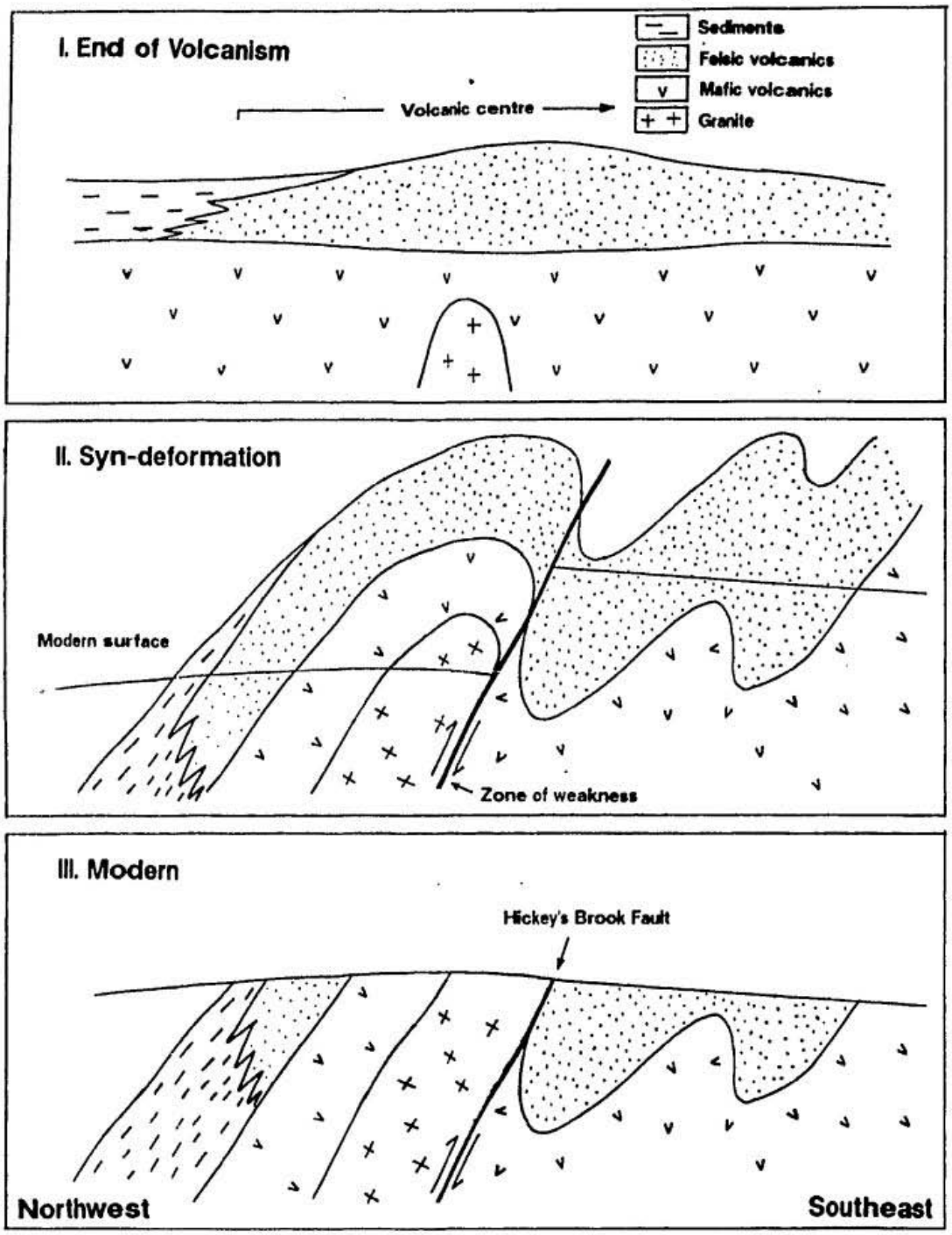

Figure 2-7: Schematic cross-section. The repetition of volcanic stratigraphy with the same polarity on opposite sides of the Swift Current Granite is explained by the thrust-faulted eastern contact of the granite, a feature inferred independently in Section 2.3.1.

Figure 2-8: Cleavage/bedding discordance. Handle of hammer lies on bedding, and pen parallels cleavage in narrow conglomeratic unit on Paradise River.

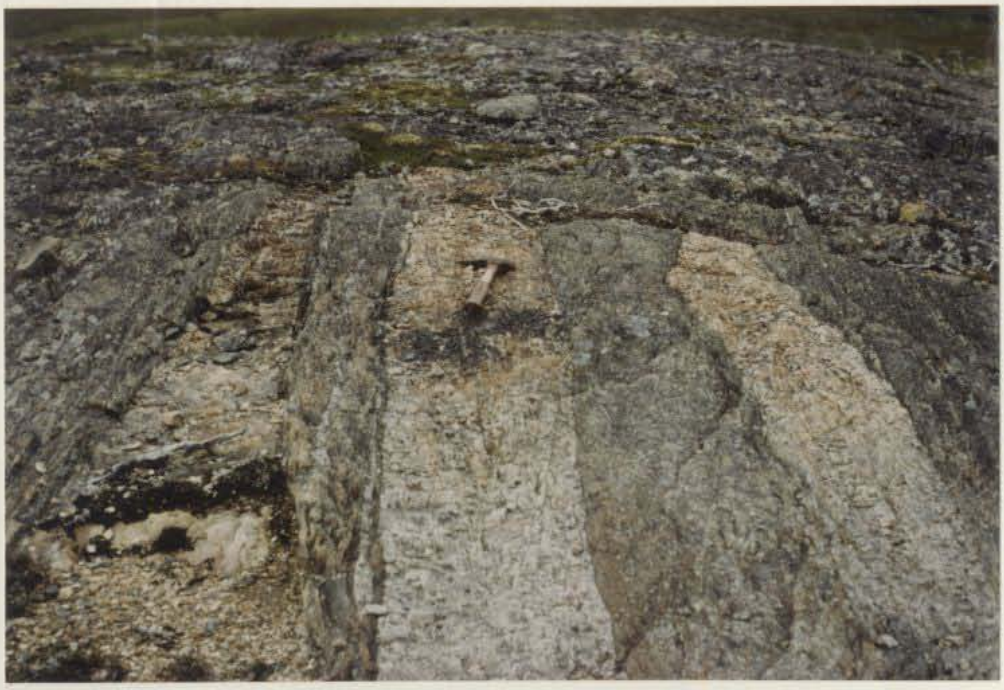

Figure 2-9: Transposed rhyolite dykes. Pink rhyolite dykes (under hammer) are structurally concordant with host volcanics.

Figure 2-10: Small-scale isoclinal folds. Folding in quartz-pyrophyllite-specularite schist is readily apparent on cut surface. "M" folds give way to (apparent) asymmetric "Z" folds towards the upper right on the cut surface.

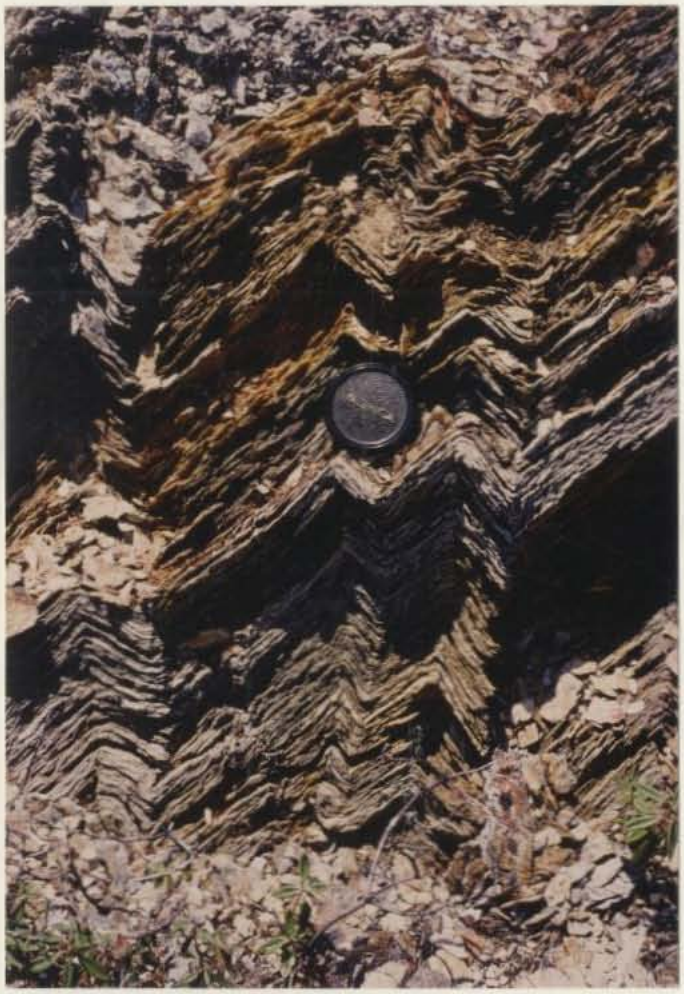

Figure 2-11: Kink bands. Northeasterly-striking schistosity in sericitized crystal tuff is "kinked" by steep, south-striking crenulation cleavage (up-down in photo). Viewed down moderately northwest-plunging fold axes.

kink bands occur rarely, also in argillic alteration zones (Figure 2-11).

2.3.1. Northeast-trending faults

Features indicating intense shearing, notably the development of "C" and "S" planes, were observed in argillically altered rocks at two different places on the eastern contact of the Swift Current Granite. At the headwaters of Hickey's Brook, the "C" planes strike 040-060/60NW, and their relationship with the "S" planes is such that they indicate dextral displacement (Figure 2-12).

Figure 2-12: "C" and "S" planes. Dextral displacement on "C" planes (parallel to hammer handle) is indicated by curvature of schistosity in argillically altered volcanic rocks at the headwaters of Hickey's Brook.

These occur in a zone at least 10 m wide which is bounded to the northwest by a sharp fault contact (035/55NW) with relatively massive granite and to the southeast by overburden. Similar relationships are observed at Chimney Falls, 7.5 km to the south-southwest along the granite contact. The nearly coplanar orientations of the "C" planes and the granite contact indicate that the granite

contact is one of the shear zone boundaries.

Figure 2-13 is a projection of pertinent data from the headwaters of Hickey's Brook onto the Wulff equal angle stereonet. The point on the "C" plane perpendicular to its intersection with the "S" planes is the direction of slip of the fault. This line plunges only 18 degrees to the south southwest, indicating that most of the displacement is strike slip. Knowing that this displacement was dextral, the geometry dictates that the dip-slip component of displacement was reverse (compressional).

The fault contact is commonly not exposed, but it was intersected by two diamond drill holes at Hickey's Pond, which is midway between the headwaters of Hickey's Brook and Chimney Falls (see Figure 2-1 in map pocket). There it is represented by a zone of schistose, argillically altered rocks at least 20 m thick, which are in contact with relatively massive granite in the hanging wall.

Given the straight course of the eastern contact of the Swift Current Granite, the occurrence of fault-related rocks along the contact and the coincidence of this contact with Hickey's Brook over much of its length, it is proposed here that the contact is a fault which is here named the Hickey's Brook Fault.

Intensely deformed rocks occur to the west of the southward projection of the western margin of the Swift Current Granite, south of Paradise River, in an alteration zone which is defined in Section 4.7 as the Strange Showing. It is at the northern end of a low, narrow northeast-trending ridge bounded by airphoto lineaments that strike 038 degrees and 054 degrees; the projections of which intersect in a swamp to the northeast of the showing.

Intensely deformed rocks, the petrography of which is discussed in detail in Section 4.7.2, occur at the Strange Showing. They feature a schistosity striking 030/85SE and a prominent lineation on the schistosity trending 185/75. Three

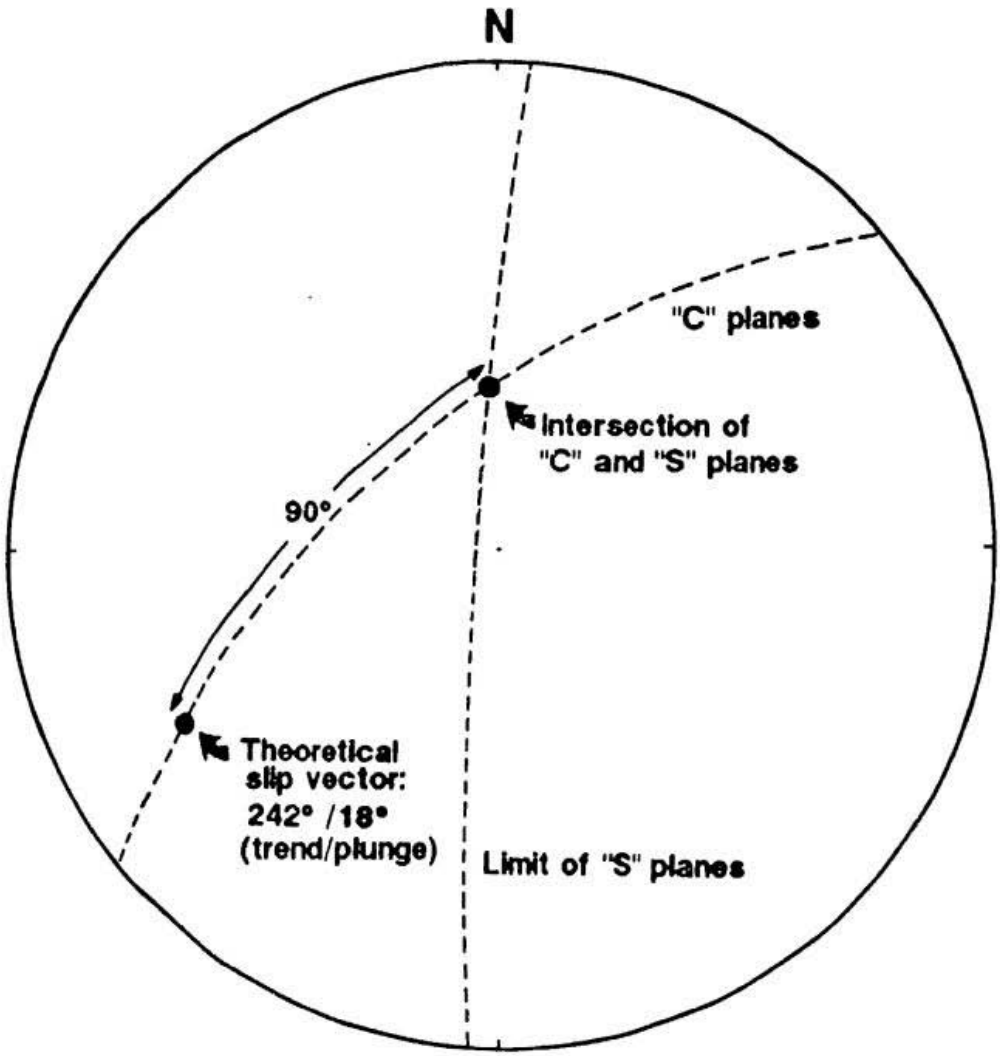

Figure 2-13: Wulff net projection. "C" planes and "S" planes define nearly horizontal slip vector in schists at the headwaters of Hickey's Brook. "Limit of "S" planes" is the orientation of schistosity at the inflections between "C" planes (see Figure 2- 12).

mutually perpendicular polished surfaces were made on one of the rocks; one surface included the plane of schistosity and one was perpendicular to the lineation. Wispy centimetre-scale "fragments" observed at the showing were revealed to be extremely elongated discs, with the long axis parallel to the lineation, and the short axis perpendicular to the schistosity.

No detailed study of the quartz fabrics was undertaken, but cursory examination showed pronounced elongation of quartz crystals and parallelism of optic axes (Figure 2-14).

Figure 2-14: Quartz microfabric at Strange Showing. Excellent parallelism of optic axes is shown by the uniform first order yellow interference colour. [Field of view 5.0mm x 3.4mm, cross polarized with quartz plate.]

They can be described as quartz ribbon mylonites (T. Calon, pers. comm.), and other features indicative of their intense deformation are described in Section 4.7.2.

2.3.2. Cross-cutting faults

The second most common trend of airphoto lineaments is 080 degrees. The most prominent such lineament crosses the point where Hickey's Brook flows into Sandy Harbour River. It becomes obscured about 2 kilometres west of this point, but remains very prominent to the east for 12 km, at which point it strikes into Placentia Bay. The otherwise straight, steep coastline has a conspicuous 500 m right-step where it is crossed by the lineament, interpreted to be a dextral strike-slip fault, near Shag Rock. The eastern contact of the Swift Current Granite, and the belt of felsic volcanics farther east have undergone approximately 1000 m of apparent right lateral displacement across the fault.

Another 080-trending lineament, 4 km long and marked by a chain of small ponds, strikes into Hickey's Pond from the west. The western shore of the pond, which is the faulted southeastern contact of the Swift Current Granite, undergoes a right-step of 200 m where the lineament intersects it (Figure 2-15 and Figure 2-1 in map pocket).

2.3.3. Summary

The intense regional cleavage and associated flattening relate to a compressional event in which thrusting from the west occurred. The Hickey's Brook fault marks the thrust contact of the Swift Current Granite over its comagmatic volcanic pile, and the Paradise Sound Fault marks the thrust contact of the lowest exposed units of the Love Cove Group over the sedimentary rocks of the Musgravetown Group. This sense of displacement is consistent with observations by O'Driscoll (1978) on the Paradise Sound Fault, and Strong *et al.* (1978A) for northeast-trending faults in the Marystown area. No large scale isoclinal folds were mapped in the study area, but their occurrence would be consistent with outcrop-scale features, *e.g.* parallelism of cleavage and bedding, strong flattening of clasts and small-scale isoclinal folds.

Compression gave way to dextral shearing, which is the last event which can

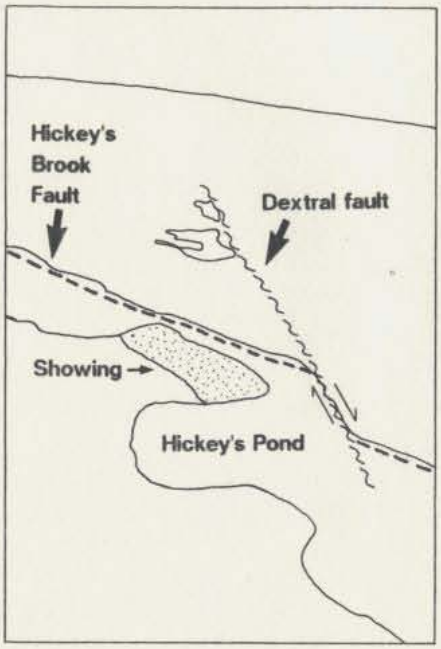

Figure 2-15: Dextral fault at Hickey's Pond. The far shore of Hickey's Pond, which is the faulted southeastern contact of the Swift Current Granite, displays a 200 m right-step which projects through chain of ponds in background (see sketch, looking west along fault).

be inferred from the Hickey's Brook Fault, although a small component of reverse dip-slip displacement persisted. Dextral faults trending 080, which occur in prominent airphoto lineaments postdate the shearing event.

2.4. Metamorphism

Two minerals associated with hydrothermally altered rocks in the study area serve as good indicators of the metamorphic history. Pyrophyllite was identified by X-ray diffraction at the Hickey's Pond showing and at three similar showings farther south, all in association with quartz, alunite, specularite, pyrite and rutile. At all of the modern occurrences (Chapter 5) where the latter group of minerals form, however, they are in equilibrium with kaolinite. Thus it is assumed that the pyrophyllite observed at the showings was derived from kaolinite by the following reaction with quartz:

$$Al_4Si_4O_{10}(OH)_8 + 4SiO_2 \rightarrow 2Al_2Si_4O_{10}(OH)_2 + 2H_2O$$

This reaction was investigated by Frey (1970) who showed that it began at sub-greenschist facies conditions and that the pyrophyllite remained stable into the greenschist facies. The upper limit for the stability of pyrophyllite was studied by Haas and Holdaway (1973) who showed it to remain stable up to the middle of the greenschist facies.

Chloritoid was observed in six places, everywhere in association with pyrophyllite and specularite. It forms porphyroblasts approximately 1 mm long which constitute less than 5% of the rock, but they are very conspicuous as black crystals imparting a "roughness" to the schistosity of the light colored quartz-pyrophyllite schists in which they occur (Figure 2-16). Thin section examination (Figure 2-17) shows the locally discordant relationship of the porphyroblasts, which are interpreted to be syntectonic, to schistosity. The appearance of chloritoid marks the onset of upper greenschist facies metamorphism (Deer, Howie and Zussman, 1966).

Figure 2-16: Chloritoid porphyroblasts. Conspicuous, black chloritoid porphyroblasts impart a roughness to quartz- pyrophyllite schist intersected in BQ drill core on the Hickey's Brook Fault at Hickey's Pond.

Figure 2-17: Chloritoid porphyroblasts (photomicrograph). Random orientation of porphyroblasts (high relief) in pyrophyllite schist (left-right schistosity) points to origin late in deformation. [Field of view 5.0mm x 3.4mm, plane polarized.]

A sample of chloritoid in thin section was analyzed with an energy dispersive microprobe, and shown to be Fe-chloritoid (Figure A-2). Given this and the minerals with which it occurs, it is believed to form by the following reaction between pyrophyllite and specularite, in which Fe^{+3} is reduced to Fe^{+2}:

$$2Al_2Si_4O_{10}(OH)_2 + Fe_2O_3 \rightarrow Fe_2Al_2O_2(SiO_4)_2(OH)_4 + 6SiO_2 + 1/2O_2$$

Widespread greenschist facies metamorphism is also implied by the universal occurrence of chlorite and epidote in recrystallized mafic rocks.

The rocks in which the chloritoid occurs had been altered under relatively oxidizing conditions, as shown by the occurrence of specularite and the association of these rocks with alunite, which is considered in detail in Chapters 4 and 5. The reduction of iron in the formation of chloritoid shows that the growth of chloritoid occurred under considerably different chemical conditions than those under which the alteration occurred. Since the chloritoid is demonstrably metamorphic, the alteration must have preceded the metamorphism. The timing of alteration is considered further in Chapters 3 and 6.

Chloritoid does not occur in all the rocks containing quartz, pyrophyllite and specularite, probably indicating that the metamorphic grade only locally reached the upper greenschist facies. Four of the occurrences define a north-northeasterly trending belt 4 km long in the western part of the study area. The other occurrences are in the Hickey's Brook Fault, approximately 12 km to the northeast, on the eastern margin of the Swift Current Granite. Other pyrophyllite occurrences on the eastern margin of the Swift Current Granite do not include chloritoid. The four occurrences in the western part of the study area are several kilometres away from outcropping Swift Current Granite, but they are closer to the large Ackley Granite farther west. These observations show that the metamorphic grade increases towards the west, in the direction of the Ackley Granite, implying a genetic relationship between the two. Furthermore, since the chloritoid was shown to be syntectonic, it roughly dates the deformation as being

the same age as the Ackley Granite.

These interpretations are consistent with the tectonochronological study of Dallmeyer *et al.* (1983). They produced $^{40}Ar/^{39}Ar$ age spectra for 11 samples of Love Cove Group rhyolites that had sericite recrystallized on the schistosity. The samples were collected over a strike length of 150 km and included two from the study area. They display consistent plateau ages averaging 378 Ma, which were interpreted to record the peak of metamorphism as inferred metamorphic temperatures did not greatly exceed the retention temperature for Argon in sericite. The metamorphic age is only slightly older than the age of the Ackley Granite determined by Dallmeyer *et al.* (1983; 352 +/-10 to 357 +/- 10 Ma) or Bell *et al.* (1977; 355 +/-5 Ma) and it is the same age as that of the deformation in the adjacent Gander Zone (Dallmeyer *et al.*, 1981). They conclude that deformation and metamorphism in the western Avalon zone (including the study area) occurred during docking of the Gander and Avalon zones, and that the Ackley Granite, which intrudes part of the intervening fault zone, was intruded at the end of the fault movement. Given these observations the apparent increase in metamorphic grade towards the west probably reflects proximity to the Ackley Granite and the former fault zone.

2.5. Geochemistry of felsic volcanics

The geochemistry and mineralogy of hydrothermal alteration in the study area is presented in chapter 3. In selecting a suite of rocks for the study, it was recognized that some fresh volcanic rocks would have to be included to provide a reference for the alteration geochemistry. Nine samples of felsic volcanic rock were thus selected, the criterion being to represent: 1) magma; thus rocks with lithic fragments were excluded and 2) a large geographic area. Microscopic studies reveal a mineralogical subdivision of the suite of fresh rocks, which corresponds to distinct geochemical features. The following sections discuss the nature of these two types of felsic volcanic rock, and relate this to processes responsible for their formation.

2.5.1. Petrographic discrimination

All 9 samples of rock contain quartz phenocrysts, commonly rounded and embayed and 6 of the samples include feldspar phenocrysts, either plagioclase or sanidine. Geochemical discrimination is provided when the rocks are grouped according to the type of feldspar present, and those samples without feldspar phenocrysts show geochemical features of one or the other group, and have been assigned to the appropriate group. Because the distinction between groups is sharp and does not depend on the percentage of feldspar present, it is believed that the geochemical features discussed below reflect features other than mixing effects between different feldspars and a common matrix.

2.5.2. Geochemical discrimination

Table 2-1 illustrates the distribution of major and trace elements between sanidine crystal tuffs and plagioclase crystal tuffs. The rare earth elements are compared in Figure 2-18. The REE patterns tend to be linear, so the relative LREE/HREE enrichments were quantified by performing a linear regression through the normalized elements with the best analytical precision. This allowed for calculated values of La^* and Yb^*, the ratios of which are provided in Table 2-1. The sanidine crystal tuffs are strongly enriched in Zr, Nb and Ni, and HREE, with a gradually decreasing enrichment of the lighter rare earths. The low concentrations of Eu make interpretation uncertain, but strong negative Eu anomalies in the sanidine crystal tuffs generally reduce its concentration below that for most plagioclase crystal tuffs. The sanidine crystal tuffs also include slight enrichments in SiO_2, Fe as Fe_2O_3 and K_2O.

Plagioclase crystal tuffs are strongly enriched in MgO, Ba and V, with lesser enrichments in Al_2O_3, TiO_2 and Sr relative to the sanidine crystal tuffs.

Table 2-1: Geochemistry of felsic volcanics. Geochemical data for sanidine and plagioclase crystal tuffs shows clear discrimination based on Mg, Ba, Y, Zr, Nb, Ni, V and La^*/Yb^*. [Data are presented split according to rock type. Major element oxides are reported in weight percent, Au in parts per billion (mg/t) and all other elements in parts per million (g/t). "0" = below detection.]

#	SiO2	Al2O3	Fe2O3	MgO	CaO	Na2O	K2O	TiO2	MnO	P2O5	LOI	Total	Cu	Pb	Zn	Au	Ag	Ba	Sr	Rb	U	Th	Y	Zr	Nb	Ga	Ni	V	La*/Yb*
	Sanidine crystal tuffs																												
133	77.90	11.70	1.53	.23	.06	2.31	4.60	.06	.05	.01	1.09	99.54	0	21	47	5	.0	139	72	138	9	39	82	312	40	23	5	0	3.9
213	78.40	10.20	2.08	.11	.62	2.77	4.17	.10	.03	.02	.69	99.19	6	9	4	0	.3	182	92	100	1	32	132	790	54	14	7	4	5.7
214	78.80	9.13	1.96	.16	1.84	3.71	1.12	.07	.05	.01	1.96	98.81	0	16	7	0	.0	74	57	35	4	29	133	572	45	14	6	1	6.4
	Plagioclase crystal tuffs																												
81	78.40	11.10	1.28	.53	2.04	2.45	2.67	.13	.06	.02	1.04	99.72	1	7	18	0	.0	583	538	52	0	5	29	142	8	13	0	1	13.6
138	73.80	13.00	1.64	.38	2.28	3.99	3.01	.10	.07	.03	.70	99.00	0	38	29	0	.0	876	281	56	3	27	21	96	10	11	0	15	27.3
149	71.60	15.10	.95	.42	.28	1.42	3.71	.51	.01	.09	3.03	97.12	0	23	12	0	.0	746	141	140	10	27	18	194	14	14	0	78	17.9
201	77.50	11.90	1.10	.42	.08	3.26	3.52	.09	.04	.01	1.14	99.06	0	9	24	0	.0	613	84	101	6	15	18	79	11	14	0	20	16.6
239	76.90	12.10	1.09	.49	.84	1.81	3.52	.11	.04	.01	2.18	99.09	72	55	18	0	.3	410	42	136	6	39	16	85	14	11	0	13	39.5
251	78.40	12.10	.85	.40	.20	3.26	2.65	.14	.03	.03	1.49	99.55	0	27	5	0	.0	577	74	68	3	34	20	91	11	14	0	11	17.7

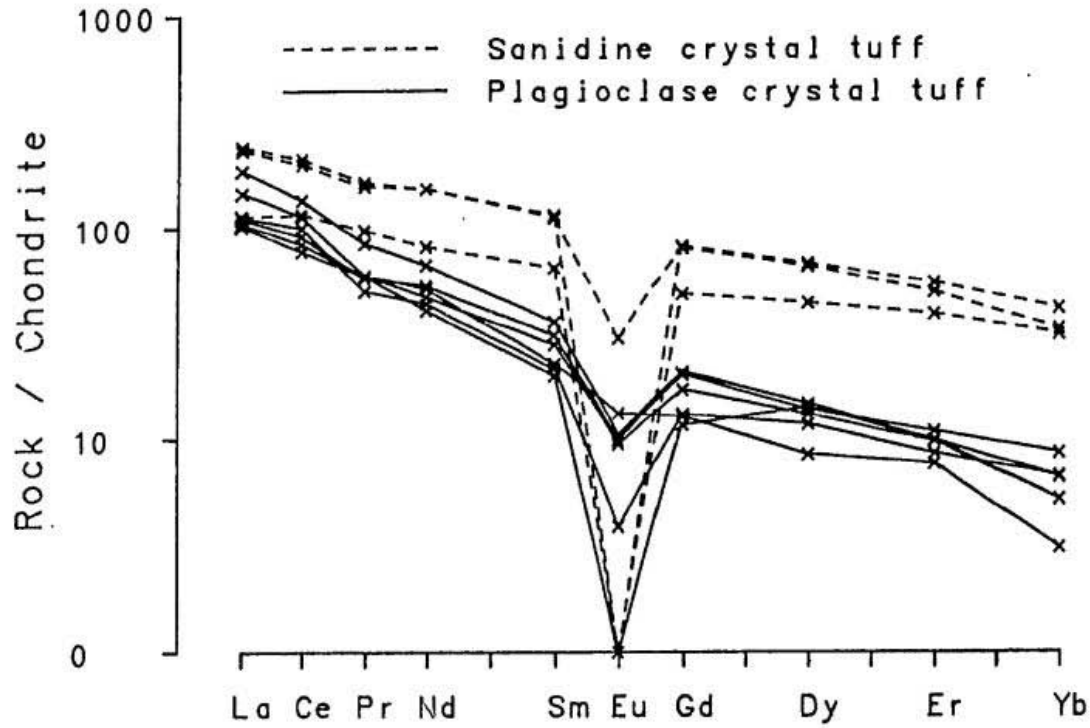

Figure 2-18: REE in felsic volcanics. Discrimination between sanidine and plagioclase crystal tuffs improves with increasing atomic number.

2.5.3. Discussion

Two features of the rare earth element patterns suggest that the sanidine crystal tuffs could have been derived from the plagioclase crystal tuffs by fractional crystallization of plagioclase. They are: 1) with the exception of Eu, the concentration of REE is greater in the sanidine crystal tuffs and 2) the very strong negative Eu anomalies in the sanidine crystal tuffs suggest fractional crystallization of plagioclase.

However, other geochemical features contradict this hypothesis. Simple fractional crystallization of plagioclase should enhance the concentration of Ba in the magma, given its low distribution coefficient in plagioclase relative to felsic melts (0.30; Hanson, 1978). Coupled with its high distribution coefficient in K-feldspar (6.12; Hanson, 1978), it would be expected to be highly concentrated in the sanidine crystal tuff if it were derived from the plagioclase crystal tuff by fractional crystallization, but the opposite behaviour is observed (Table 2-1).

Observations such as these which could not be explained by fractional crystallization have been reported by Hildreth (1981). He proposed a mechanism, thermogravitational diffusion, which could produce large gradients in trace element concentrations near the roof of a magma chamber, from which magma for volcanic rocks is commonly obtained. Thermogravitational diffusion is the diffusion of elements across temperature and volatile gradients which develop at the tops of magma chambers, and which can effect the "structure" of the melt.

Hildreth demonstrated which elements were enriched in the tops of the magma chamber from which the Bishop Tuff in California was erupted. These include Si, Zr, Nb, Y and HREE, all of which are enriched in the sanidine crystal tuffs of this study. Elements enriched in later erupted magma, sampling lower parts of the Bishop Tuff magma chamber, include Al, Mg, Ti, Sr, Ba, V and Eu (Hildreth, 1981), all of which are enriched in the plagioclase crystal tuffs of this study.

Several elements from this study, for which differences in concentration exist between the 2 types of crystal tuff, had enrichments opposite to those of the Bishop Tuff, given the equating of sanidine crystal tuffs with the top of the magma chamber and plagioclase crystal tuffs with the underlying layer, as implied by the discussion above. These elements are K, Ni and the LREE. The behaviour of K can be accounted for because it is an essential constituent in sanidine, but the behaviour of the other elements remains apparently contradictory. In addition, large differences for certain elements between each rock type which would be predicted from a consistent application of Hildreth's model were not apparent for the rocks in this study; *viz* P, U, Th, Rb and Cu. In the cases of U and Th, at least, their apparently similar concentrations in each rock type reflect inadequate analytical precision.

Nevertheless, the felsic rocks of this study do display some geochemical characteristics which can not be explained by fractional crystallization, but which are similar to features in the Bishop Tuff which have been explained by thermogravitational diffusion.

Chapter 3
ALTERATION

3.1. Introduction

Narrow schistose zones developed locally in the felsic volcanic rocks attest to intense preferential deformation in these zones. These rocks commonly occur in airphoto lineaments which may persist from a few tens of metres to several kilometres, although individual schistose zones are generally less than 100 m in length and 10 m in width. Some of the airphoto lineaments, such as that which separates the eastern margin of the Swift Current Granite from the volcanic rocks, are clearly faults. Furthermore, some of the rocks in the schistose zones have been hydrothermally altered, as indicated by the occurrence of sericite and/or pyrophyllite and/or pyrite in some of the zones (Figure 3-1). The association of hydrothermally altered rocks and fault zones can be accounted for in two ways: 1) the alteration occurred at the time of deformation or later and was localized in fault zones which focussed the fluid flow, or 2) hydrothermally altered rocks containing abundant phyllosilicates were preferentially deformed, owing to their diminished strength. In the latter case, fault zones may have "nucleated" in the high strain zones of the altered rock. The timing of events is discussed further in Section 3.7, following description of the alteration in terms of mineralogy and geochemistry.

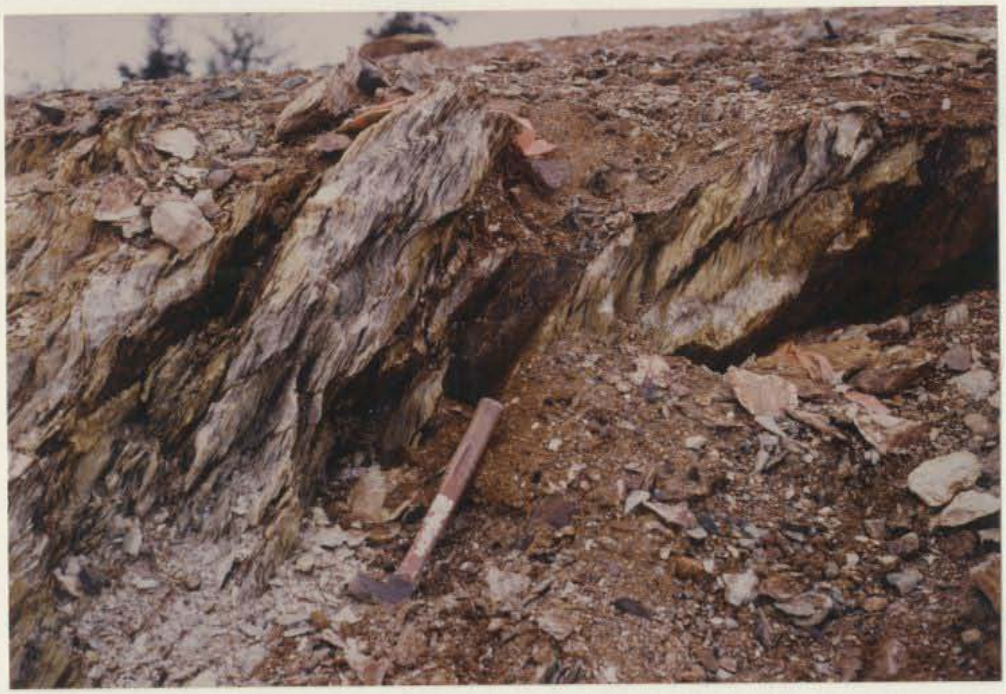

Figure 3-1: Monkstown Road schist zone. Intensely deformed and hydrothermally altered crystal tuff is represented by this pyritiferous schist. Note "flakes" of rock to left of hammer head (looking north).

3.2. Alteration mineralogy

Eighteen samples of fresh and altered rhyolites were selected from the sample collection to serve as the basis for a detailed study of the alteration. The selection was based solely on the megascopic appearance of the hand specimen, with the aim of representing the freshest rock, the most altered and all the intermediate stages. One sample of sericite schist (022) was presumably derived from basalt. It was collected from a metre-wide zone of pyritiferous sericite schist in gradational contact with basalt through an intermediate zone of chlorite schist.

3.2.1. Petrographic discrimination

Thin sections of the eighteen rocks were prepared and examined. Observations are listed here:

1. Quartz phenocrysts, commonly rounded, embayed and displaying undulatory extinction are present in most of the rocks (Figure 3-2).

Figure 3-2: Quartz phenocryst in schist. Undulose, embayed quartz phenocryst (below and to left of centre) in schistose, altered crystal tuff. Note bands of sericite. [Field of view 5.0mm x 3.4mm, cross polarized.]

Plagioclase or sanidine phenocrysts were present in half the samples; they were not observed together in any rock.

2. Sericite (?) occurs in different stages of development, from minor wisps on the cleavage to millimetre-scale bands of the material. Where best developed, no feldspars were observed in the rock.

3. The occurrence of pyrite or specularite coincides with the most intense development of sericite. Pyrite and specularite occur together in one sample (159), in which specularite had partially replaced pyrite (Figure 3-3).

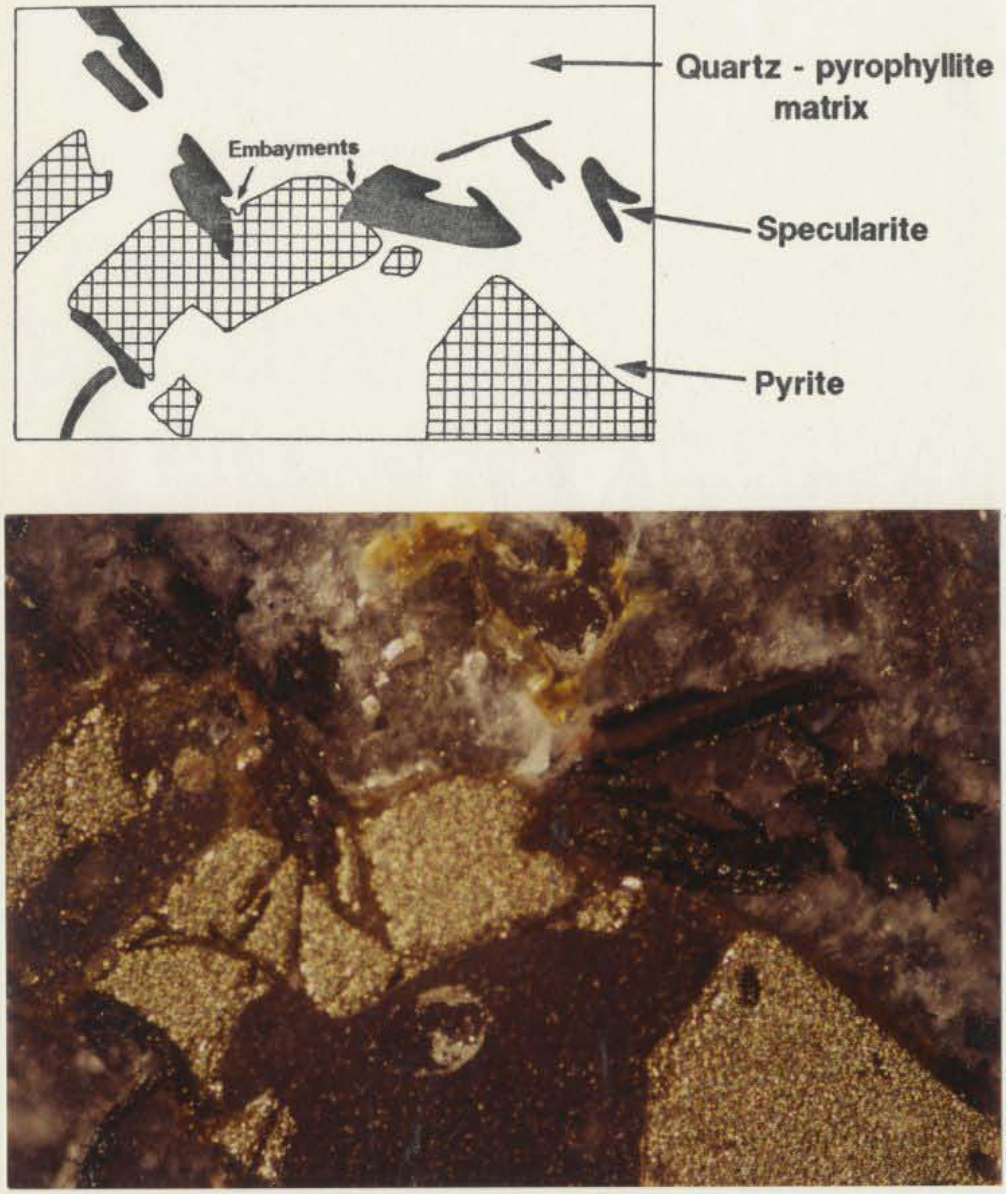

Figure 3-3: Specularite after pyrite. Black specularite fills embayments in corroded crystals of pyrite in pyrophyllite schist. [Field of view 1.2mm x 0.8mm, reflected light.]

These observations suggest a three-way subdivision of the rocks: Phyllosilicate-poor rocks, all but two of which can be subdivided into sanidine or plagioclase crystal tuffs and phyllosilicate-rich (hydrothermally altered) rocks, which do not contain feldspar. The phyllosilicate-poor rocks were the subject of the detailed discussion in Section 2.5.

3.2.2. X-Ray diffraction discrimination

The mineral tentatively identified as sericite by microscopic techniques was further investigated with the aid of X-Ray diffraction analyses. These were carried out on whole-rock powders of the most "sericite"-rich samples. Sericite produced prominent peaks in three samples and pyrophyllite in four.

Sericite and pyrophyllite do not occur together in any of the rocks in this suite. However, in the larger group of rocks that was analyzed in the course of this study, they occurred together in one sample in approximately equal modal abundance, based on the quantitative X-Ray diffraction technique of Papezik *et al.* (1978). Minor disseminated pyrite was present in all the sericite schists. It was also present in two of the pyrophyllite schists (159, 180); one occurrence of which (159) was marked by its partial replacement by specularite. Specularite occurs exclusively in pyrophyllite schists.

3.2.3. Geochemical discrimination

The distribution of Na and K in the rocks clearly defines these three groupings (Figure 3-4): 1) rocks with $>1\%$ Na_2O and $>1\%$ K_2O, 2) rocks with $<0.5\%$ Na_2O and $>3\%$ K_2O and 3) rocks with less than 0.2% combined Na_2O and K_2O.

All the rocks which contain feldspar phenocrysts belong to group 1, as do the two samples that could not be categorized according to strictly mineralogical criteria. The sericite schists make up group 2 and the pyrophyllite schists group 3 (Figure 3-4).

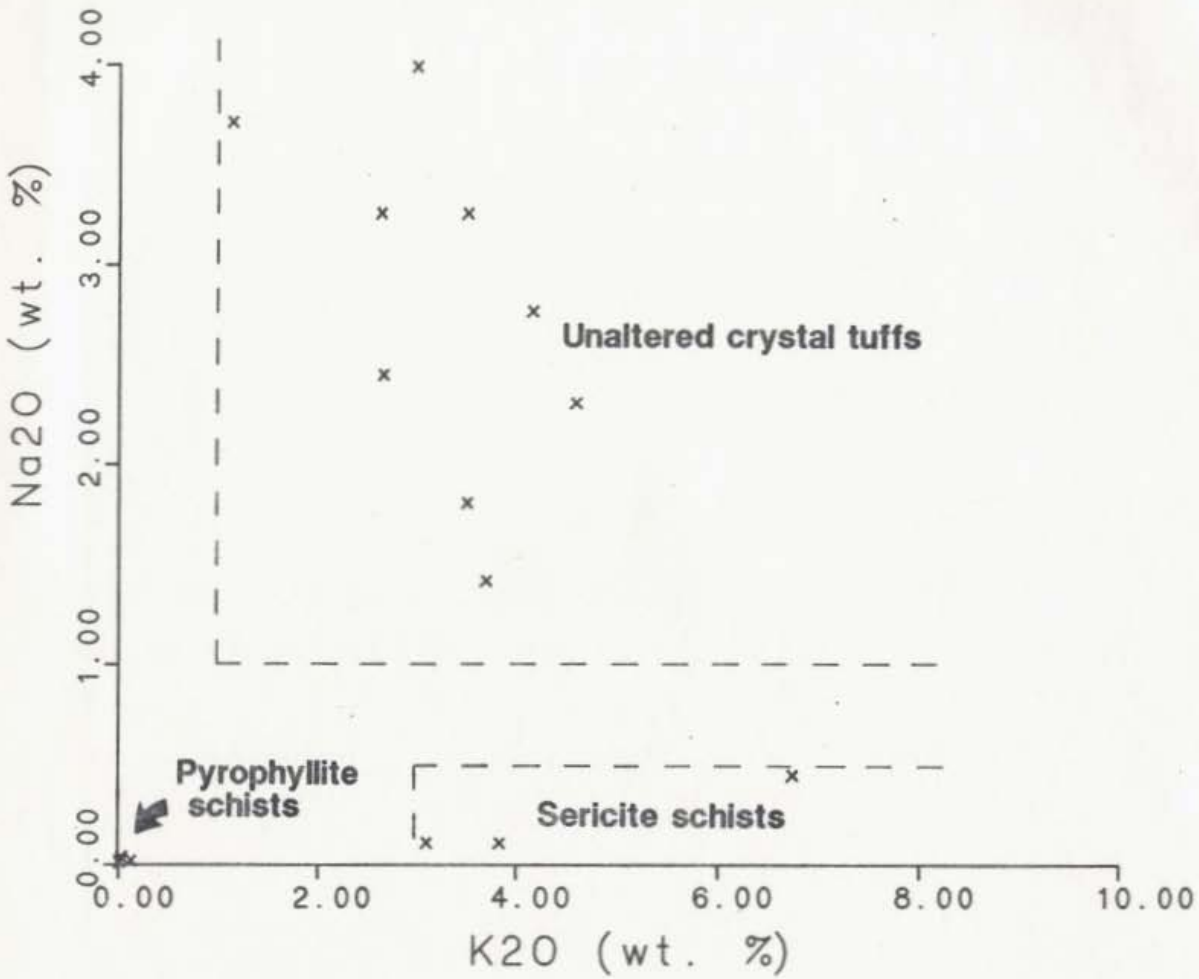

Figure 3-4: Na2O *versus* K2O in alteration suite. Unaltered rocks, sericite schists and pyrophyllite schists are clearly discriminated on the bases of Na_2O and K_2O.

3.2.4. Summary

Mineralogical criteria provide a four-way subdivision of these rocks. Rocks with feldspar phenocrysts are subdivided into plagioclase or sanidine crystal tuffs, either of which may locally contain minor sericite. Phyllosilicate-rich rocks, which are characterized by the absence of feldspar phenocrysts, are subdivided into sericite schists and pyrophyllite schists by X-ray diffraction analysis. Pyrite is most commonly associated with sericite schists and specularite is exclusively associated with pyrophyllite schists.

3.3. Alteration geochemistry: framework for discussion

3.3.1. Relationship of sericitization to pyrophyllitization

The mineralogy and geochemistry of this suite of rocks define two distinct alteration assemblages, *viz* sericitic and pyrophyllitic, not a continuous series. The observations listed below support the contention that the pyrophyllite schists are derived from the sericite schists and represent a more advanced alteration state.

1. Pyrophyllite mineralization is everywhere associated with a more widespread area of sericite mineralization, although sericite mineralization commonly occurs in the absence of pyrophyllite mineralization.

2. Sericite and pyrophyllite occur together in at least one sample, suggesting that sericite is a transitional assemblage.

3. At Chimney Falls, pyrite occurs in sericite schists and specularite occurs in pyrophyllite schists. The observed replacement of pyrite by specularite suggests that pyrophyllitization occurred at the expense of pyritiferous, sericitic rocks.

4. The concentrations of several elements in the sericite schists are intermediate between their concentrations in the fresh rocks and their concentrations in the pyrophyllite schists.

3.3.2. Effects of mass transfer

Certain features of the geochemistry of the alteration suite are discussed in this section to establish a rational framework for detailed discussion to follow in Section 3.4. It must be borne in mind that the concentration of an element in altered rocks being greater than its concentration in the fresh rock does not necessarily mean it has been added to the rock as a result of the alteration process. Such inferences must await a quantitative assessment of the net change in mass of the rock, the net loss of which can create spurious increases in trace element concentrations.

Schoen *et al.* (1974) describe an alteration system in which large changes in mass per unit volume of rock occurred as a result of alteration. However, they were able to accurately assess the net gains and losses as a result of alteration because they were able to measure the net changes in mass of each volume of rock. No such information is available to this study, owing to the deformed state of the rocks. In the absence of this information, assumptions about the behaviour of certain elements must be made before conclusions about the absolute changes in abundance of other elements can be made. For example, classical studies about the geochemical effects of weathering assume that aluminum remains constant (Krauskopf, 1979). This assumption is supported by the low mobility of aluminum in the weathering environment. Schoen *et al.* (1974) showed that for the alteration they studied, TiO_2 was less mobile than Al_2O_3, and is a better standard than aluminum for calculating absolute changes in other elements when net changes in mass are not available.

For purposes of this study, the immobility of both TiO_2 and Zr, and thus their suitability as indicators of significant changes in mass during alteration are investigated. These elements are not in significantly different concentrations in the sericite schists than in the fresh rocks (Table 3-1), so increases and decreases in the concentration of other elements in the sericite schists relative to the fresh rocks reflect additions and subtractions respectively of those elements.

Table 3-1: Geochemistry of alteration suite. Unaltered rocks are clearly discriminated from sericite schists and pyrophyllite schists by higher concentrations of Na2O. The latter rock types can be distinguished on the bases of MgO, Na2O, K2O, Sr and Rb. [Data are presented split according to rock type. Major element oxides are reported in weight percent, Au in parts per billion (mg/t) and all other elements in parts per million (g/t). "0" = below detection, " " = no analysis was conducted.]

#	SiO2	Al2O3	Fe2O3	MgO	CaO	Na2O	K2O	TiO2	MnO	P2O5	LOI	Total	Cu	Pb	Zn	Au	Ag	Ba	Sr	Rb	U	Th	Y	Zr	Nb	Ga	Ni	V	La*/Yb*
	Unaltered rocks																												
81	78.40	11.10	1.28	.53	2.04	2.45	2.67	.13	.06	.02	1.04	99.72	1	7	18	0	.0	583	538	52	0	5	29	142	8	13	0	1	.087
138	73.80	13.00	1.64	.38	2.28	3.99	3.01	.10	.07	.03	.70	99.00	0	38	29	0	.0	876	281	56	3	27	21	96	10	11	0	15	.110
149	71.60	15.10	.95	.42	.28	1.42	3.71	.51	.01	.09	3.03	97.12	0	23	12	0	.0	746	141	140	10	27	18	194	14	14	0	78	.096
201	77.50	11.90	1.10	.42	.08	3.26	3.52	.09	.04	.01	1.14	99.06	0	9	24	0	.0	613	84	101	6	15	18	79	11	14	0	20	.094
239	76.90	12.10	1.09	.49	.84	1.81	3.52	.11	.04	.01	2.18	99.09	72	55	18	0	.3	410	42	136	6	39	16	85	14	11	0	13	.123
251	78.40	12.10	.85	.40	.20	3.26	2.65	.14	.03	.03	1.49	99.55	0	27	5	0	.0	577	74	68	3	34	20	91	11	14	0	11	.096
	Sericite schists																												
22	59.20	21.60	1.29	.32	.18	.45	6.75	.53	.01	.10	4.73	95.16	3	22	4	0	.1	814	42	212	12	23	38	224	13	26	4	146	.058
51	79.10	9.60	.22	.33	.00	.11	3.12	.10	.01	.02	2.85	95.46	3	13	0	0	.4	175	2	108	3	20	18	105	10	10	0	53	.153
101													0	35	0	75	.7	153	2	97	5	24	10	84	7	10	0	43	
221	75.50	11.10	4.16	.47	.24	.11	3.85	.11	.03	.03	2.96	98.56	0	35	10	55	.8	575	24	157	16	33	7	116	16	12	0	55	.043
	Pyrophyllite schists																												
154	91.50	3.70	1.24	.02	.04	.02	.13	.47	.01	.20	1.31	98.64	2	43	0	0	.0	170	638	0	0	18	16	171	9	9	0	30	.157
159	77.50	16.99	.61	.02	.00	.04	.03	.42	.01	.16	4.17	99.95	3	35	0	5	.3	102	995	0	7	33	14	179	11	21	0	74	.137
161	85.60	9.53	.94	.01	.00	.02	.01	.26	.01	.07	2.16	98.61	0	146	0	45	.0	350	533	0	9	29	11	120	9	16	0	29	.139
180	79.10	13.88	2.00	.02	.00	.03	.02	.29	.01	.05	3.59	98.99	2	216	0			239	133	0	3	32	32	172	16	20	0	20	
244	87.30	9.42	.08	.01	.00	.01	.01	.44	.01	.11	2.29	99.68	0	24	0	0	.0	588	385	0	4	26	13	172	12	12	0	39	.164

Both Ti and Zr are enriched in the pyrophyllite schists relative to the unaltered rock. However, the degrees of enrichment for each element are substantially different. Comparisons of the simple average concentrations of each element in each rock type show that Ti increased 330% and Zr increased 165% in the pyrophyllite schists. This difference in increase is far beyond analytical uncertainty and clearly indicates either 1) preferential influx of Ti, 2) preferential removal of Zr in conjunction with correspondingly larger losses of other elements to effectively concentrate the weakly mobilized elements, or 3) a combination of the previous processes. Relevant to this question is the observation that the pyrophyllite schists contain virtually no MgO, CaO, Na_2O, K_2O or MnO, elements which constitute a total of approximately 8% of the unaltered rock. If these elements were removed from the rock as part of the alteration process and there was no introduction of mass, then Ti and Zr would effectively be concentrated in the pyrophyllite schists to approximately 107% of their concentrations in the fresh rock. Clearly, the removal of these cations alone can not account for the increased concentrations of Ti and Zr.

To approach the problem from another perspective, the amount of material that would have to be removed from the fresh rock to explain the increased concentrations of Ti and Zr was calculated. Assuming no Zr was lost, 39.5% of the fresh rock would have to have been removed to explain its concentration, and Ti would have to have been added to this rock to account for its increase. To account for the increased Ti concentration strictly in terms of the removal of other elements, fully 69.7% of the rock, including 50% of the Zr would have to have been removed. This possibility is not favoured in light of direct evidence for increases in both Ti and Zr during alteration, which is presented in Section 7.3.1.

3.4. Alteration geochemistry: description

A clear subdivision of the fresh rhyolites on the basis of minor elements, which corresponds to the type of feldspar present was discussed in Chapter 2. For the remainder of this discussion, it is assumed that the altered rocks were derived from the plagioclase crystal tuffs, as they are much more common than the sanidine crystal tuffs which are geographically removed from the altered rocks. This assumption is supported by concentrations of Y, Zr and Nb in the altered rocks that are comparable to those in the plagioclase crystal tuffs, and much lower than those in the sanidine crystal tuffs (compare Table 3-1 and Table 2-1). This solution at least addresses the "uncertainty problem" inherent in geochemical alteration studies, i.e. how much of the "alteration" characteristics may better be ascribed to pre-alteration processes.

The mineralogical subdivision established in Section 3.2 serves as a framework for a discussion of the geochemical features of the rocks. The 18 rocks in this suite have been reduced to 15, as the 3 sanidine crystal tuffs are taken to be unrelated to any of the altered rocks. The rocks were analyzed for major and selected trace elements (Table 3-1). All but one sample were analyzed for selected rare earth elements, which are plotted (normalized) in Figure 3-5, listed in the Appendix (Table A-3) and represented in Table 3-1 by La^*/Yb^*, as discussed in Section 2.5.2.

Examination of Table 3-1 reveals natural groupings of elements. In qualitative terms of enrichment and depletion, there are only four possible groupings of the elements, and these possibilities constitute Groups A through D. Elements which appear uneffected by the alteration, for analytical or genetic reasons, comprise a fifth group (E). The definitions of the groups are as follows:

1. Group A: Elements which are enriched through sericitization and pyrophyllitization.

2. Group B: Elements which are progressively depleted through sericitization and pyrophyllitization.

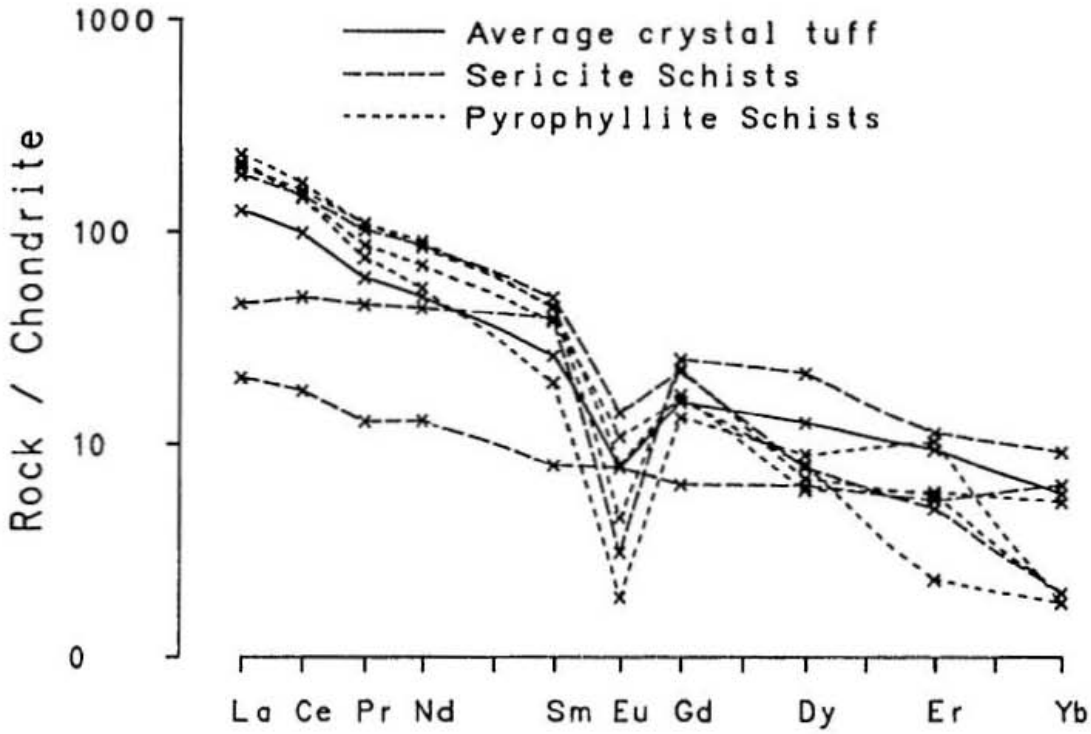

Figure 3-5: REE patterns for alteration suite. Flat patterns for two of the sericite schists, and HREE depletions and LREE enrichments in the pyrophyllite schists are apparent.

3. Group C: Elements which are enriched during sericitization and depleted during pyrophyllitization.

4. Group D: Elements which are depleted during sericitization and enriched during pyrophyllitization.

5. Group E: Elements which appear to be uneffected by both alteration processes.

The following sections identify the elements in these groups and discuss their behaviour. Reference should be made to Table 3-1 in conjunction with these sections.

3.4.1. Group A

Elements which are progressively enriched through the two alteration processes comprise Group A. These elements are Si, Ti, P and Zr, and the strongest enrichment accompanies pyrophyllitization. The small enrichment in Si during pyrophyllitization can be explained in terms of its relative immobility in the face of wholesale removal of monovalent and divalent major element cations. This process also accounts for a component of the increase in the other elements, although their strong enrichments show that they were added to the rock during pyrophyllitization.

The enrichment of the Group A elements during sericitization was much smaller.

3.4.2. Group B

Elements which are progressively depleted through the two alteration processes comprise Group B. It is here subdivided into two groups based on the degree of depletion. Group B1 elements, Na, Mg, Ca, Mn and Zn are quantitatively removed from the pyrophyllite schists. Group B2 elements, Al, Dy, Er, Yb, Y and Ba are less strongly depleted from the pyrophyllite schists.

With the exception of Mg, all the Group B1 elements suffer the greatest

depletion during sericitization. Mg is only slightly diminished during sericitization, but is eliminated during pyrophyllitization.

The behaviour of Al during pyrophyllitization seems to be highly erratic. It ranges from less than 4% to almost 17% in the pyrophyllite schists, encompassing a much greater range than in the fresh rocks or sericite schists. This apparently random behaviour probably reflects the physical segregation of pyrophyllite during deformation, *i.e.* the "squeezing out" or concentration of pyrophyllite causes depletion and concentration, respectively, of Al.

The large range of Al concentrations affords a good opportunity to study correlations with Al. In this case, a positive correlation would signify an element which is incorporated in the pyrophyllite structure. Examination of Table 3-1 shows the only such correlation with Al is Ga.

3.4.3. Group C

The elements in this group, which are enriched during sericitization and depleted during pyrophyllitization are K, U, Rb and V. The enrichments are not strong and the depletions are highly variable. U is reduced to its concentration in the fresh rocks during pyrophyllitization, whereas V remains intermediate between its concentration in the fresh rocks and the sericite schists. K and Rb are completely eliminated during pyrophyllitization; behaviour similar to the Group B1 elements.

3.4.4. Group D

The elements of Group D, which are depleted during sericitization and enriched during pyrophyllitization, are Sr, Pb, La, Ce, Pr and Nd. Sr is the most strongly depleted element during sericitization. The data set for the LREE in sericite schists is very limited. Two of the samples have La - Nd very much depleted relative to the fresh rocks, but one of these is the sample derived from a mafic rock. The REE pattern of the other sericite schist is similar to those of the

pyrophyllite schists, i.e. it is enriched in LREE and depleted in HREE relative to the fresh rocks. Thus it can not be determined whether the severely LREE-depleted pattern or the REE pattern similar to the pyrophyllite schists is the "normal" state for sericite schists derived from felsic volcanics. Notwithstanding this, the LREE are enriched in the pyrophyllite schists relative to the fresh rocks. This feature is diminished with increasing atomic number.

3.4.5. Group E

The elements of this group, Fe, Ga, Cu, Nb, Th, Sm, Eu and Gd seem uneffected by the alteration processes, but at least two non-genetic explanations can be invoked to account for this. In the case of Cu, the range in its concentration among the three rock types is too narrow to afford discrimination. The concentrations of Nb and Th are not sufficiently high in any of the rocks to surpass analytical uncertainty.

The behaviour of the rare earth elements Sm, Eu and Gd is intermediate between the behaviour of the LREE and the HREE. Whereas the LREE are concentrated in the pyrophyllite schists and the HREE are depleted in them, these intermediate REE are apparently uneffected. Their response to sericitization most closely resembles the inconsistent behaviour of the LREE.

3.5. Chemical systematics of alteration

Chemical properties of the elements ultimately underlie their responses to alteration. Much can be learned by considering the ionic radius and charge of each element, as these are the main factors which determine whether or not an element is incorporated into any of the crystal structures of the minerals that constitute the altered rocks. Figure 3-6 plots the elements discussed above in terms of ionic charge and radius. It is immediately obvious that the groups of elements defined above on the bases of enrichment and depletion in response to each alteration process reflect in part the ionic charge and radius of each element.

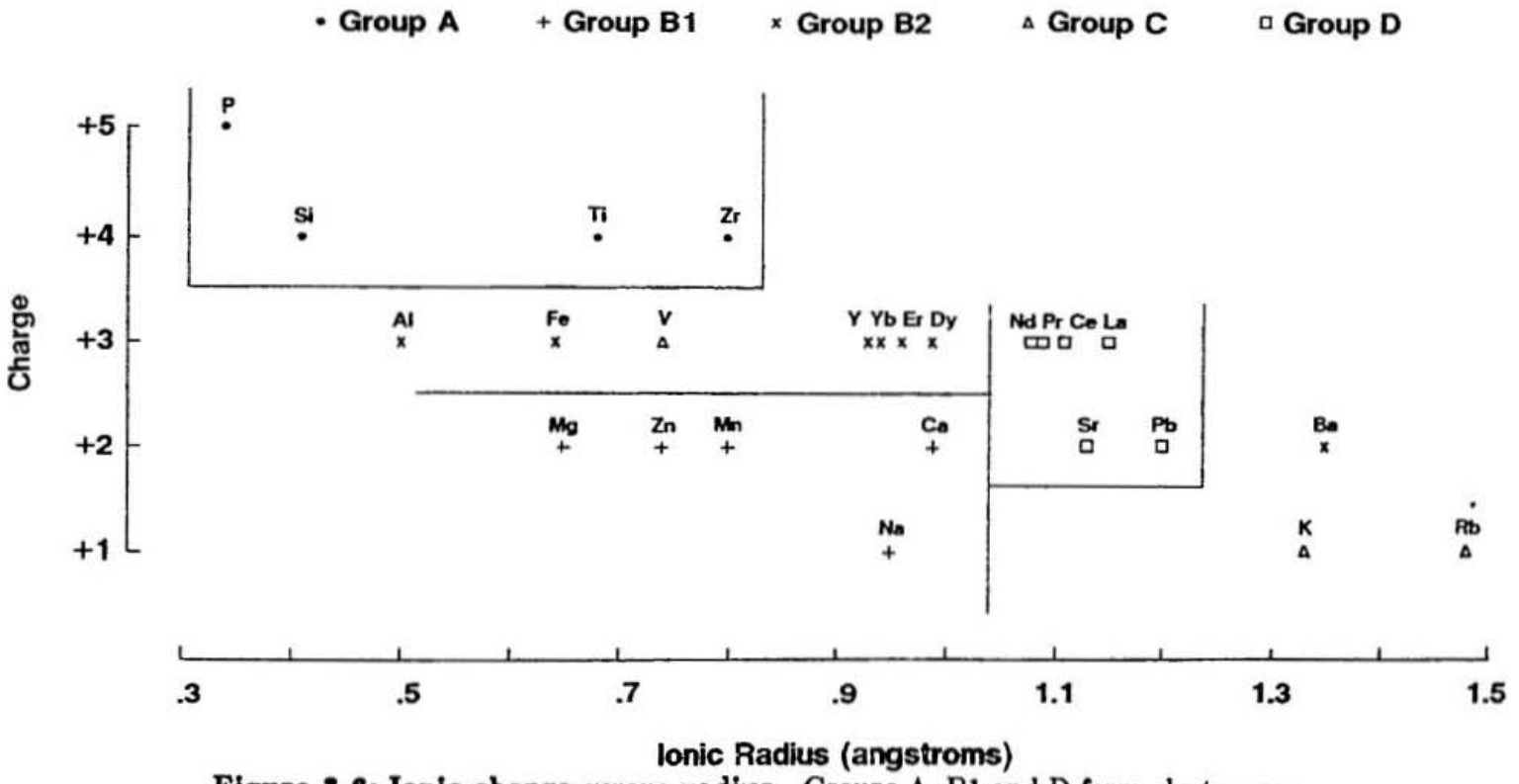

Figure 3-6: Ionic charge *versus* radius. Groups A, B1 and D form clusters on the charge/radius plot. Group A elements (•) are enriched through sericitization and pyrophyllitization. Group B elements (+ , ×) are progressively depleted through sericitization and pyrophyllitization, with elements of Group B1 (+) being quantitatively removed during pyrophyllitization. Group C elements (△) are enriched during sericitization and depleted during pyrophyllitization. Group D elements (□) are depleted during sericitization and enriched during pyrophyllitization.

The Group A elements, P, Si, Ti and Zr are all small and highly charged. Ti, Zr and P are classically regarded as relatively immobile (Pearce and Cann, 1973) but this study has shown them to be added in different proportions to the pyrophyllite schists. This enrichment is in addition to a smaller enrichment brought about by the net loss of several weight percent of other elements.

Elements of Group B1, Mg, Zn, Mn, Ca and Na are less than 1 Angstrom in radius and are divalent cations, with the exception of the monovalent Na ion. Except for Mg, they suffer the greatest depletion during sericitization, which probably reflects the destruction of plagioclase which accompanies this process. The small amount of Mg originally in the rocks may have been incorporated as a minor phase in the sericite of the sericitized rock, along with small amounts of other Group B1 elements not removed during sericitization. Alternatively, it may have remained in another phyllosilicate phase or less likely in a ferromagnesian mineral, although neither of these proposed types of minerals was observed. Small amounts of epidote observed in one of the sericite schists could account for its small concentration of Ca. All the Group B1 elements are removed during pyrophyllitization. This reflects the destruction of sericite, epidote and any Mg-bearing phase that may have occurred in the sericite schists.

The apparent "quantitative" removal of the Group B1 elements, all but one of which are major elements, during pyrophyllitization could be an artifact of the relatively high detection limits associated with their analysis as major elements. All but one of the Group B2 elements are tr ce elements and were analyzed by techniques with much lower detection limits. The only major element in Group B2 is Al, and both alteration assemblages include an aluminous phase which prevents its "quantitative" removal.

The other Group B2 elements are a cluster of the heaviest REE, the geochemically similar trivalent cation Y and Ba, which is a large divalent cation. The depletion of the trace elements of this group can also be related to feldspar breakdown, as most of the depletion corresponds to sericitization. The loss of

small quantities of Al accompanies sericitization.

The elements of Group C are scattered on the plot of ionic charge versus radius, suggesting that factors other than crystallographic control their behaviour. The enrichments these elements undergo during sericitization are variable; from weak for K, Rb and U to strong for V. It could be argued that the small increases in K, Rb and U are not statistically valid and that their presence merely indicates efficient incorporation of these elements already in the rock into sericite. However, good evidence that the increases are real is provided by sample 022, the sericite schist derived from the mafic rock. Its protolith probably had less than 1% K_2O and 50 ppm Rb, but the sericite schist derived from it has over 6% K_2O and 200 ppm Rb. These concentrations are considerably higher than those in the felsic rocks or the sericite schists derived from them. This proves that K and Rb are added to the rock during sericitization.

The sericite schist derived from the mafic rock also has a very high Al_2O_3 content, a feature probably inherited from its mafic protolith. It thus appears that the amount of K added to the rock during alteration depends on the amount of Al available to fix the K in the rock. This is supported by fairly uniform molar Al/K ratios in the sericite schists (2.96, 2.86, 2.66), which approximate the value for ideal sericite (3).

The genesis of the fluid that introduced these elements into the rock during sericitization is unknown. The association of K, Rb and U points to a magmatic contribution to the hydrothermal fluid, but it could also be explained in terms of favourable distribution coefficients for these elements in sericite.

The responses of K and Rb to pyrophyllitization are those of the Group B1 elements, i.e. they are eliminated from the rock. Their loss reflects their extreme mobility after the breakdown of sericite.

The elements of Group D form a tight cluster of divalent and trivalent

cations on the plot of ionic charge versus radius. Notable is the narrow range of ionic radii the group spans. The size-dependance of this group is well illustrated by the REE; the elements larger (lighter) than and including Nd belong to Group D, the elements smaller (heavier) than and including Dy belong to Group B2.

The elements of Group D and the other REE are depleted in response to sericitization, probably reflecting the breakdown of feldspar. The cause for the increase in LREE, Sr and Pb is less certain. The only new major phase formed during pyrophyllitization is pyrophyllite. It is unlikely, however, that these elements are incorporated into the pyrophyllite structure given the lack of correlation between any of these elements and Al in the pyrophyllite schists (Section 3.4.2). Of possible significance to this problem was the identification (in different but related rocks discussed in Chapter 7) of phosphate minerals bearing varying combinations of Ca, Sr and LREE. These minerals were identified with the SEM-EDX, which was not employed extensively in the investigation of the pyrophyllite schists. Thus, the formation of similar (unobserved) minerals in the pyrophyllite schists could account for their enrichment in Sr and LREE, especially in light of the strong enrichment in P during pyrophyllitization. Although no Pb was detected in any of the Ca-Sr-LREE phosphates, it could be a minor component in these minerals given its similar ionic radius.

Relevant to the increased concentrations of elements of Group A and Group D in the pyrophyllite schists is the sample distribution, whereby the 5 samples represent only 2 sample locations, and 4 of the samples are adjacent to a mineralized, brecciated rock which is shown in Section 6.2.1 to be a hydrothermal conduit. This breccia is strongly enriched in Ti, P and Zr, the first two of which, together with Sr are only enriched in the pyrophyllite schists adjacent to the breccia zone, implying derivation of these elements from it.

3.6. Summary

Sericitization is accompanied by the depletion of most elements with two types of exceptions: 1) no changes in the concentrations of small, highly charged immobile cations (Ti, Zr, Si, P) and 2) slight to strong enrichments in K, Rb, U and V. The depletions probably reflect the destruction of feldspars and the enrichments in K, Rb and U reflect the fixing of these elements, partially derived from the hydrothermal fluid, in sericite.

Pyrophyllitization is accompanied by further depletions of several elements, some of which are quantitatively removed. These losses reflect the breakdown of sericite. Two groups of elements are concentrated during pyrophyllitization. The small, highly charged cations (Ti, Zr, Si and P) are concentrated due both to leaching of several percent of more mobile elements and to the introduction of Ti, Zr and P from the hydrothermal fluid. The large divalent and trivalent cations Sr, Pb, La, Ce, Pr and Nd are added during pyrophyllitization where they are fixed in newly formed phosphate minerals. Enrichments of Ti, P and Sr in the pyrophyllite schists are strongest adjacent to a mineralized breccia zone, and are probably not an intrinsic characteristic of the pyrophyllitization.

3.7. Timing of alteration

The sericite and pyrophyllite schists are intensely deformed relative to the host felsic crystal tuffs, which are themselves strongly deformed. This puts a minimum Devonian age on the alteration, as it must have preceded the final deformation, which was Devonian.

Dallmeyer *et al.* (1983) determined $^{40}Ar/^{39}Ar$ age spectra for 11 samples of sericitic Love Cove Group rocks. The samples yielded variably discordant whole rock ages, but plateau dates ranging from 353 to 400 Ma were well defined. Nine of these samples had plateau dates between 370 and 390 Ma. This consistent age was interpreted (Dallmeyer *et al.*, 1983) to date the time of post-metamorphic cooling to temperatures at which radiogenic Ar would be retained in the sericite.

It was implied that the sericite formed in response to the metamorphic event. However, the study by Dallmeyer *et al.* (1983) does not preclude that the plateau ages represent "resetting" of hydrothermal sericite which could be as old as Precambrian. Older ages indicated by the highest temperature increments were attributed to outgassing of primary unrecrystallized feldspar. Alternatively, they could reflect outgassing of particularly retentive sites in pre-metamorphic, hydrothermal sericite which were not reset during the metamorphic event.

Petrographic knowledge of the rocks is essential to the resolution of this problem. This study has shown that small amounts of sericite occur in all the volcanic rocks, but large amounts occur only in rocks with no feldspar. These are interpreted here as metamorphic and hydrothermal sericite respectively. Dallmeyer *et al.* (1983) provide a general petrographic description of the rocks, which are said to consist "primarily of fine-grained white mica and minor .... primary feldspar". Feldspar phenocrysts, a common feature of the "fresh" Love Cove crystal tuffs were not reported. O'Driscoll (pers. comm.) reported that at least one of the samples in the study was from the same outcrop as one of the sericite schists discussed in this chapter, the sericite in which appeared to be hydrothermal in origin. Thus the plateau age for this sample represents the time of resetting of the sericite and the older ages defined by the highest temperature Ar fractions reflect pre-metamorphic ages for the formation of the sericite.

The geochronologic investigation of sericite in the Love Cove Group has been inconclusive with respect to dating the hydrothermal activity. There is evidence that the plateau dates represent resetting of premetamorphic hydrothermal sericite, but the age of the hydrothermal activity cannot be determined due to the metamorphic resetting. Information relating to the absolute age of the hydrothermal event is presented in Chapter 6, which shows that the two types of alteration discussed in this chapter are facies of a larger, more varied alteration system that developed synvolcanically.

Chapter 4
DESCRIPTIONS OF SHOWINGS

4.1. Introduction

This chapter describes rocks which are sufficiently unusual as to preclude immediate assignment to an origin by hydrothermal alteration of volcanic rocks. In Chapter 3 a detailed account of hydrothermal alteration of volcanic rocks was presented. The fact that those rocks are clearly alteration products, as shown by gradational relationships with, and relict textures of volcanic rocks, sets them apart from the rocks with which this chapter is concerned, which are characterized by 1) unexposed contacts with rocks of obvious volcanic origin, 2) complete lack of gradations between them and volcanic rocks, 3) lack of relict volcanic features and 4) unequivocal mineralogical makeup. The significance of the last point, which is reviewed in detail in Chapter 5, is that the mineralogy of the rocks points to an origin either by hydrothermal alteration of preexisting rocks or by precipitation of the constituents in ancient, acid hotsprings.

Nine occurrences are described in this chapter, six of which were discovered during the course of this study. Names and locations of the occurrences, which are referred to as showings (of specularite) in the following chapters, are given in Figures 2-1 and 4-1. The Hickey's Pond Showing was studied in greatest detail, and its description constitutes the largest part of this chapter. The Tower, Ridge, Bullwinkle and Paradise River Showings bear strong resemblances to the Hickey's Pond Showing, and are considered in less detail. The four other showings are described independently.

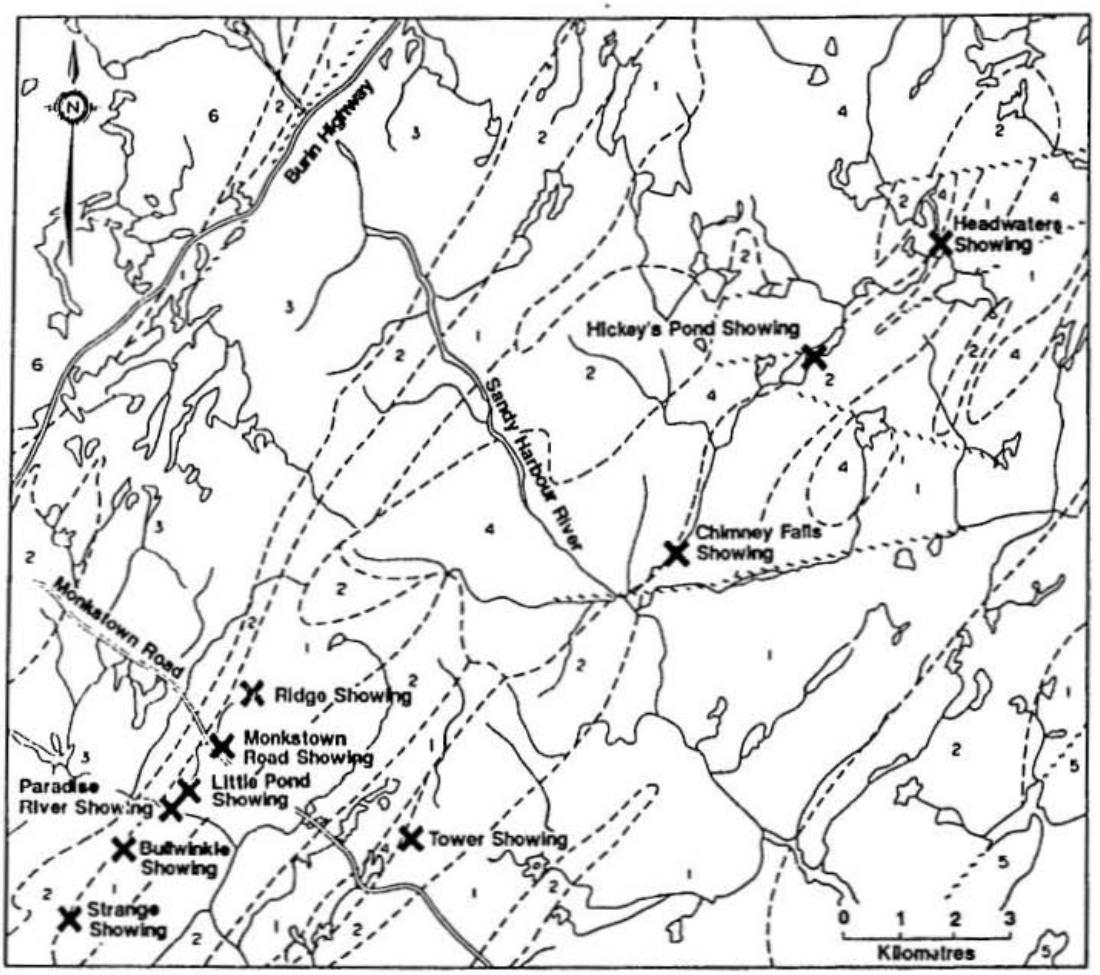

6	Ackley Granite
5	Musgravetown Group sediments
4	Swift Current Granite
	LOVE COVE GROUP
3	Graywackes and associated sediments
2	Predominantly felsic pyroclastics
1	Predominantly mafic flows

Figure 4-1: Locations of specularite showings. Note the distribution of the showings in two parallel belts. Samples from the Headwaters Showing (pyrophyllite) are discussed in Chapter 3.

4.2. Hickey's Pond Showing

4.2.1. Location

Hickey's Pond is located 15 km SW of Swift Current (NTS 1M/16 (Sound Island) map sheet). The closest point on the Burin highway is 8 km to the northwest, and the pond can be reached from this point by all terrain vehicles. The showing occupies a peninsula extending into the middle of the pond from the eastern edge. It is approximately 270 m x 110 m, with the long axis trending NNE-SSW (Figure 2-15, page 41).

The showing is bounded on three sides by the pond. To the east is a low bog approximately 30 m across that separates it from relatively fresh felsic volcanic rocks. The Swift Current Granite outcrops on the western side of the pond, which marks the site of the Hickey's Brook Fault (Section 2.3.1).

4.2.2. Petrography

Several types of rocks can be identified at Hickey's Pond. They have been subdivided on a mineralogical basis into 6 groups which are named in Table 4-1.

4.2.2.1. Specularite-banded rocks

The most common rock type at Hickey's Pond is an assemblage of quartz, alunite, pyrophyllite, specularite and rutile. A conspicuous mineralogical banding is imposed on the rocks by the occurrence of specularite in bands, which parallel a ubiquitous, variably developed tectonic fabric. Alunite forms from 5% to 35% of the rock, occurring as discrete bands of euhedral, diamond-shaped crystals up to 0.6 mm long, together with pyrophyllite, quartz, rutile and specularite (where present). Specularite occurs as slender needles (apparent in thin section) up to 0.8 mm long, which constitute up to 10% of the rock. Pyrophyllite occurs in discontinuous, sub-millimetre thick bands which account for less than 5% of the rock and define the tectonic fabric. Rutile forms approximately 1% of the rock, occurring as grains up to 1 mm long with a discernible cleavage or as tiny (0.01

Table 4-1: Definition of nomenclature. Rock names provided are to facilitate description only. No genetic implications are intended.

Rock Name	Constituent Minerals						Remarks
	quartz	alunite	pyrophyllite	specularite	pyrite	rutile	
Specularite - banded	x	x	x	x		x	Mineralogical banding common
Specularite - rich breccia	x	x	<	x	*	x	Fragments in specularite - rich matrix
Pyritiferous	x	x			x	x	
Specularite - pyrite interbanded	x	x	x	x	x	x	Rock fragments present, specularite and pyrite mutually exclusive
Silicified, pyritiferous	x	<			x	x	Massive, volcanic texture preserved, network of quartz - pyrite veinlets
Quartz - rutile rock **	x					x	
Quartz - specularite veins	x			x			Coarse - grained veins
Quartz - pyrophyllite - specularite schist ***	x		x	x		x	Soft, schistose

< denotes presence in minor amount

* present only at Chimney Falls

** present only at Tower Showing

*** present on surface at Chimney Falls and Ridge Showings, intersected in diamond drill core at Hickey's Pond

mm) equant crystals which appear bright orange under reflected light. Microcrystalline quartz constitutes the remainder of the rock, generally from 60% to 80%. In one sample, a quartz phenocryst was observed in a groundmass of fine quartz and alunite. Its irregular shape is marked by a large embayment and lobate contacts with the groundmass (Figure 4-2).

Figure 4-2: Quartz phenocryst from Hickey's Pond. Embayed quartz phenocryst (centre) stands sharply against microcrystalline groundmass of quartz and coarser euhedral alunite (first order yellow and red interference colour). [Field of view 5.0mm x 3.4mm, cross polarized.]

The interlayering is variably developed in terms of sharpness and contrast, ranging from diffuse contacts between similar bands to very sharp contacts between highly contrasting black and bright pink bands. In the diffusely banded rocks, specularite and alunite which are commonly elongated, are well-aligned parallel to the banding which is itself parallel to a variably developed schistosity. Rutile is present mostly as euhedral masses up to 1 mm long. Locally, the wispy grey bands are tightly folded about rounded fold noses (Figure 4-3).

Figure 4-3: Tight folds in diffusely banded rock from Hickey's Pond. Note more massive appearance of upper left corner.

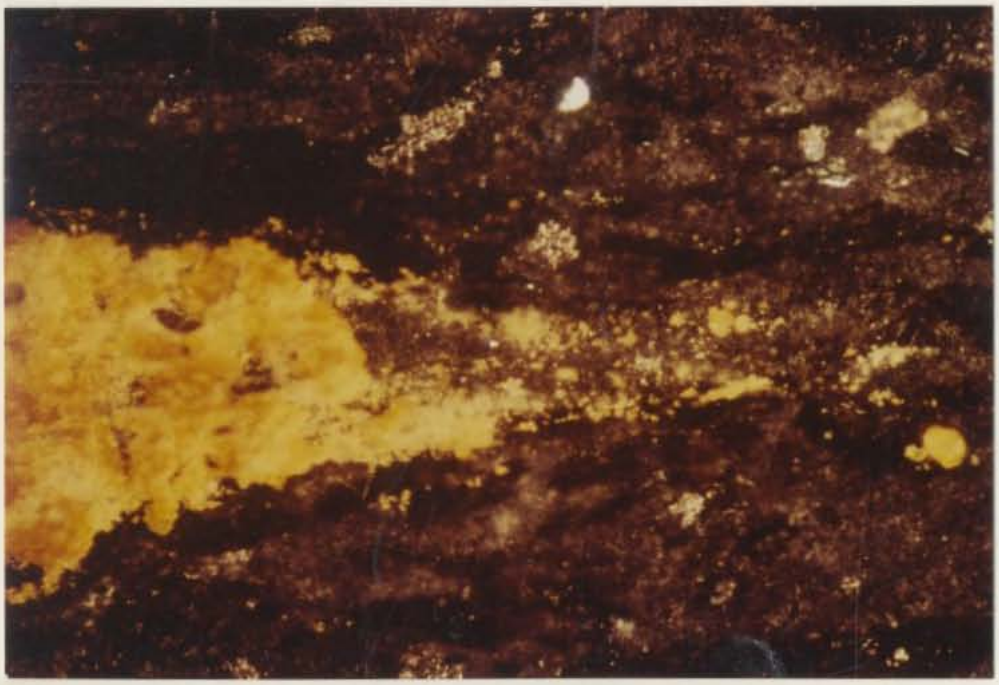

Figure 4-4: Incipient attenuation of rutile. Lensoid mass of rutile (bright orange) with "tail" of equant crystals paralleling schistosity (field of view 1.2mm x 0.8mm, reflected light).

Where the interbanding is more sharply defined, it is accompanied by other changes. Elongated minerals show a better conformity to the banding and the rutile masses assume a lensoid shape, with tails of tiny rutile crystals at each end aligned parallel to the banding and tectonic fabric (Figure 4-4). A marked reduction in crystal size, most notable in alunite and specularite, accompanies the improvement of the banding. The reduction occurs in bands which parallel the compositional banding, and the proportion of these comminuted bands increases with the improvement of the banding.

These effects are best developed in a very sharply banded type of rock that is common at Hickey's Pond, and which has been identified clearly as mylonite (T. Calon, pers. comm.). Discontinuous black bands up to a few centimetres wide have sharp contacts with intervening pink, specularite-free bands. The banding is locally tightly folded and rarely features attenuated limbs (Figure 4-5). Rutile occurs only as tiny, isolated equant crystals and discontinuous bands of these crystals (Figure 4-6).

4.2.2.2. Pyritiferous rocks

Rocks similar to those described above, *i.e.* containing quartz, alunite, pyrophyllite and rutile, but containing pyrite instead of specularite are also found at Hickey's Pond. They are light grey, and have a well-marked schistosity with lustrous pyrophyllite on cleavage surfaces. A significant difference is that pyrite tends to be disseminated throughout the rock, not concentrated in bands as is the specularite.

4.2.2.3. Specularite-pyrite interbanded rocks

Pyrite occurs in another type of rock which consists of (centimetre-scale) interbanded specularite-bearing and pyrite-bearing rock. The pyrite-bearing rock consists of euhedral alunite crystals up to 0.6 mm long that account for approximately 35% of the band. Very small (0.005-0.02 mm) equant, disseminated rutile crystals form about 1% of the bands and subangular to rounded pyrite grains up to 0.7 mm across make up about 5%. Pyrophyllite is an

Figure 4-5: Sharply banded rock from Hickey's Pond. Note attenuated limbs of isoclinal folds in polished section (right). Samples are 15cm long.

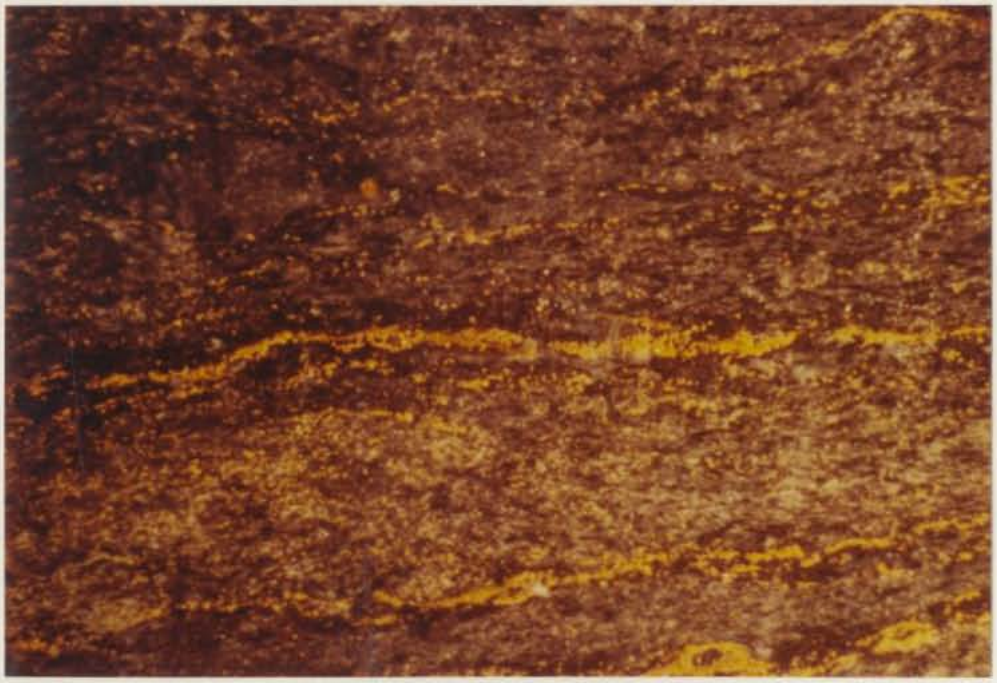

Figure 4-6: Bands of rutile crystals. Bands are composed of equant rutile crystals (bright orange) similar to those in Figure 4-4 (page 77). [Field of view 5.0mm x 3.4mm, reflected light.]

extremely minor constituent, occurring in thin, discrete, discontinuous bands. The interlayered specularite-bearing bands are similar to the pyrite-bearing bands except that specularite, instead of pyrite, is present. It occurs as slender blades up to 0.8 mm long with length to width ratios up to 10 to 1. Contacts between the pyrite-bearing and specularite-bearing bands are sharp and parallel a tectonic fabric, which is locally tightly folded (Figure 4-7).

Interbanded with the specularite and pyrite-bearing bands are grey-brown bands which feature abundant millimetre-scale rock fragments, and which lack either pyrite or specularite (Figure 4-8). Close examination of the fragments, which also occur isolated throughout the remainder of the rock, reveals that they are highly porous, consisting only of a light-colored matrix enclosing up to 70% pore space. The pores vary from ellipsoidal to circular, with fewer irregular shapes, and they are infilled with microcrystalline quartz and alunite, with lesser pyrite and rutile. The skeleton around the pores is an extremely fine-grained, dusty-appearing assemblage in which microcrystalline quartz is the only recognizable component (Figure 4-9). Unlike the massive fragment shown in Figure 4-9, most of the fragments and pores within them tend to be flattened onto the cleavage.

The mutual exclusion of pyrite and specularite within a given band was violated only rarely, where specularite was observed in isolated rock fragments within the pyritiferous rock.

4.2.2.4. Silicified pyritiferous rocks

A very distinct type of pyritiferous rock is locally developed at Hickey's Pond. It is a massive, extremely siliceous rock with irregular masses of pyrite up to 3 mm long constituting 2% of the rock. Examination of a cut surface reveals an easily discernible porphyritic texture (Figure 4-10). The matrix is light grey-brown and contrasts sharply with grey phenocrysts which have been replaced by quartz and which constitute approximately 20% of the rock.

Figure 4-7: Specularite/pyrite interbanding. Note light grey rock fragments and tight folding of banding and schistosity.

Figure 4-8: Bands of rock fragments. Pencil points to centimetre-wide band of fragments (see close-up in Figure 4-9). Grey-green bands contain pyrite, black bands contain specularite.

Figure 4-9: Rock fragment in specularite-pyrite interbanded rock. Very large pore volume of commonly ellipsoidal pores is enclosed by light grey matrix. Note sharp contacts and hairline cracks between pores. Also visible are pyrite crystals (yellow) and smaller rutile crystals (orange). [Field of view 5.0mm x 3.4mm, reflected light.]

Figure 4-10: Porphyritic texture in silicified rock. Note cross-cutting quartz veinlets and lack of tectonic fabric. Pencil points to pyrite filling a short interval in quartz veinlet.

Figure 4-11: Quartz veinlets in silicified rock. Pale grey colour of randomly oriented quartz veinlets distinguishes them from more common, milky white, syntectonically remobilized quartz veins (compare with Figure 4-18 (page 89)).

Randomly cross-cutting the rock are milky-white quartz veinlets less than 1 mm wide (Figures 4-10 and 4-11). They form a network of branching and cross-cutting veinlets that are commonly linear, but are locally curved or gently sinuous. These veinlets are locally filled with pyrite instead of quartz, for intervals up to 4 mm (Figure 4-10). Rutile occurs as discrete masses of crystals, rarely with a tabular shape, that have a very well developed layered structure (Figure 4-12).

Figure 4-12: Rutile euhedra. Distinct layered habit characterizes the masses of rutile in the competent silicified rock. Compare with the rutile in the strongly deformed rocks (Figures 4-4 (page 77) and 4-6 (page 79)). [Field of view 1.2mm x 0.8mm, reflected light.]

Alunite is very rare in these rocks, but occurs as isolated, euhedral, diamond-shaped crystals up to 0.2 mm long. Pyrophyllite is also uncommon but forms straight to gently curved, slender needles up to 0.3 mm long that are randomly oriented throughout the rock.

4.2.2.5. Specularite-rich breccias

A volumetrically minor rock-type at Hickey's Pond is a dull black, specularite-rich, relatively unfoliated featureless rock that is rarely recognizable in the field as being fragmental. On cut surfaces, however, their fragmental nature is revealed, as pale grey, generally angular fragments up to 3 cm across in a black, specularite-rich matrix (Figures 4-13 and 4-14).

Contacts between the fragments and matrix vary from sharp to diffuse, and the fragments themselves vary from recognizably volcanic to decidedly nondescript. The fragments consist primarily of microcrystalline quartz and alunite, with minor specularite, rutile and pyrophyllite. A quartz phenocryst 1.2 mm across with slightly undulatory extinction and lobate boundaries with the microcrystalline groundmass was observed in one of the breccia fragments. Other fragments displayed a very subtle, irregular banding reminiscent of flow banding. Rutile occurs as euhedral masses of crystals up to 1 mm long that display the sharp, layered habit described in Section 4.2.2.4 very well.

The matrix of the breccias is microcrystalline specularite, quartz and alunite, which occur in highly variable proportions with up to 90% specularite. Pyrophyllite, where present, is a very minor component.

Contact relations of the breccias

The specularite-rich breccia occurs as narrow pods and lenses resembling boudins which are universally enclosed by the specularite-banded rocks. The contacts are generally sharp and concordant with the banding and tectonic fabric. Locally the contact is at a high angle to, but does not cross-cut the tectonic fabric (Figure 4-15). Pyrophyllite is absent from the breccia but it occurs at the contact and throughout the banded rock as thin layers parallel to the banding and tectonic fabric.

Figure 4-16 shows another contact relationship involving the specularite-rich breccia. The country rock is a microcrystalline assemblage of quartz, alunite and

Figure 4-13: Specularite-rich breccia: outcrop. Angular, grey siliceous fragments set in a black, specularite-rich matrix. Note the unfoliated state of the outcrop and the glacial striae.

Figure 4-14: Specularite-rich breccia: polished. Note angularity of fragments and lack of tectonic fabric.

Figure 4-15: Discordant breccia contact. Light-colored pyrophyllite bands which aid in defining the fabric stop at breccia contact, but cleavage continues through the breccia.

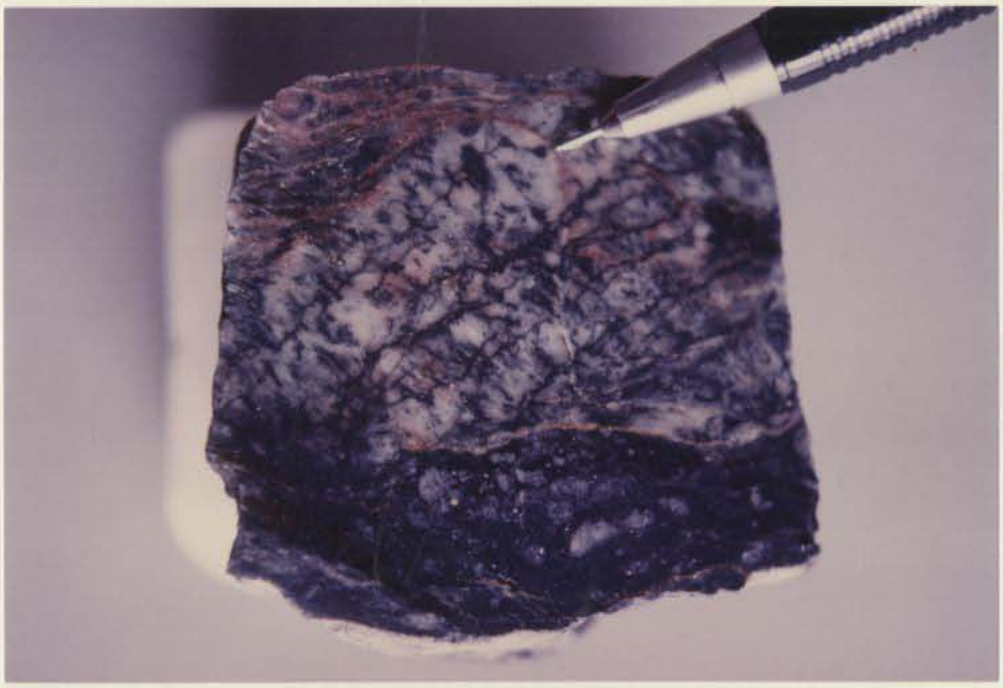

Figure 4-16: Specularite veinlets emanating from breccia. Phenocrysts in porphyritic host rock (top) are replaced by specularite. Breccia is bottom third of sample.

rutile, which displays a porphyritic texture on cut surfaces. It is dissected by a network of paper-thin specularite veinlets that originate at the contact with the breccia and continue for a few centimetres into the country rock.

Thin specularite veinlets also cross-cut a tectonic fabric in banded rock near the main occurrence of specularite-rich breccia at the showing. In Figure 4-17,

Figure 4-17: Discordant specularite veinlet. Top surface is a specularite veinlet and must not be confused with a breccia contact.

the planar top surface of the rock is fine, dark grey specularite approximately 1 mm thick that cross-cuts the banding and tectonic fabric at a high angle. The rock is a microcrystalline assemblage of quartz and alunite, with minor pyrophyllite and rutile. It was collected approximately 50 cm from the contact with the breccia.

4.2.2.6. Quartz-specularite veins

The specularite mineralization that attracted interest in the 1930's was related to quartz veins, not the more abundant banded specularite-bearing rocks. Where best developed, specularite occurs in masses of platy crystals up to approximately 3 cm across that is generally mixed with as much coarse, crystalline quartz. It occurs in a steeply northwest-dipping fault zone 30 cm across that is exposed over a vertical interval of 2 m.

Texturally and mineralogically similar veins on a smaller scale are associated with the specularite-rich fragmental rocks. Figure 4-18

Figure 4-18: Quartz-specularite veins. Milky white quartz veins with slender specularite crystals cut the fabric defined by the few pyrophyllite bands in specularite-rich breccia (compare with Figure 4-29 (page 103)).

shows small lensoid veins that are highly discordant to the fabric in the breccia. On a cut surface, specularite occurs as mm-scale needles perpendicular to the vein contacts.

4.2.3. Spatial relations

Figure 4-19 shows the distribution of the various lithologies at the Hickey's Pond showing. Pink, iron-free assemblages of quartz, alunite and rutile form the southeastern flank of the showing. Towards the west, banded specularite-rich rocks with rounded isoclinal folds give way to more tightly folded rocks with sharper banding. The extremely well-banded specularite-rich rocks with attenuated limbs occur on the extreme north-western part of the outcrop. This general increase in the "sharpness" of the banding towards the west is also apparent in drill core (Figure 4-20).

The pyritiferous alunite and pyrophyllite-bearing rocks underlie the southwestern corner of the showing. Contact relations with the more abundant specularite-bearing banded rocks are unclear, and the main contact between these rock types was not intersected by the drilling.

The specularite-pyrite interbanded rocks with lithic fragments are confined to the pit where the old mine workings are. These rocks form the core of a shallow northerly plunging antiform, each limb of which is paralleled by a fault (Figure 4-21). The fault zones and to a lesser extent the hanging walls of each fault are extensively veined with quartz and quartz-specularite veins. These are especially well developed in the steeply dipping NNE-trending fault, which was the subject of the small-scale development discussed in Section 1.2.3.1. The hanging wall of this fault is also the only occurrence of silicified pyritiferous rock on surface (Section 4.2.2.4).

All the specularite-rich fragmental rocks occur in a NNE-trending zone approximately 125 m long by 3 m wide at its widest point. The zone has a highly asymmetrical lensoid shape, with the greatest thickness achieved near the extreme southern end of the zone. This coincides with the highest elevation at the centre of the showing. Immediately west of the breccia, the banded country rock hosts numerous sub-millimetre thick specularite veins. They are nearly randomly oriented, planar features that die out within one metre of the breccia.

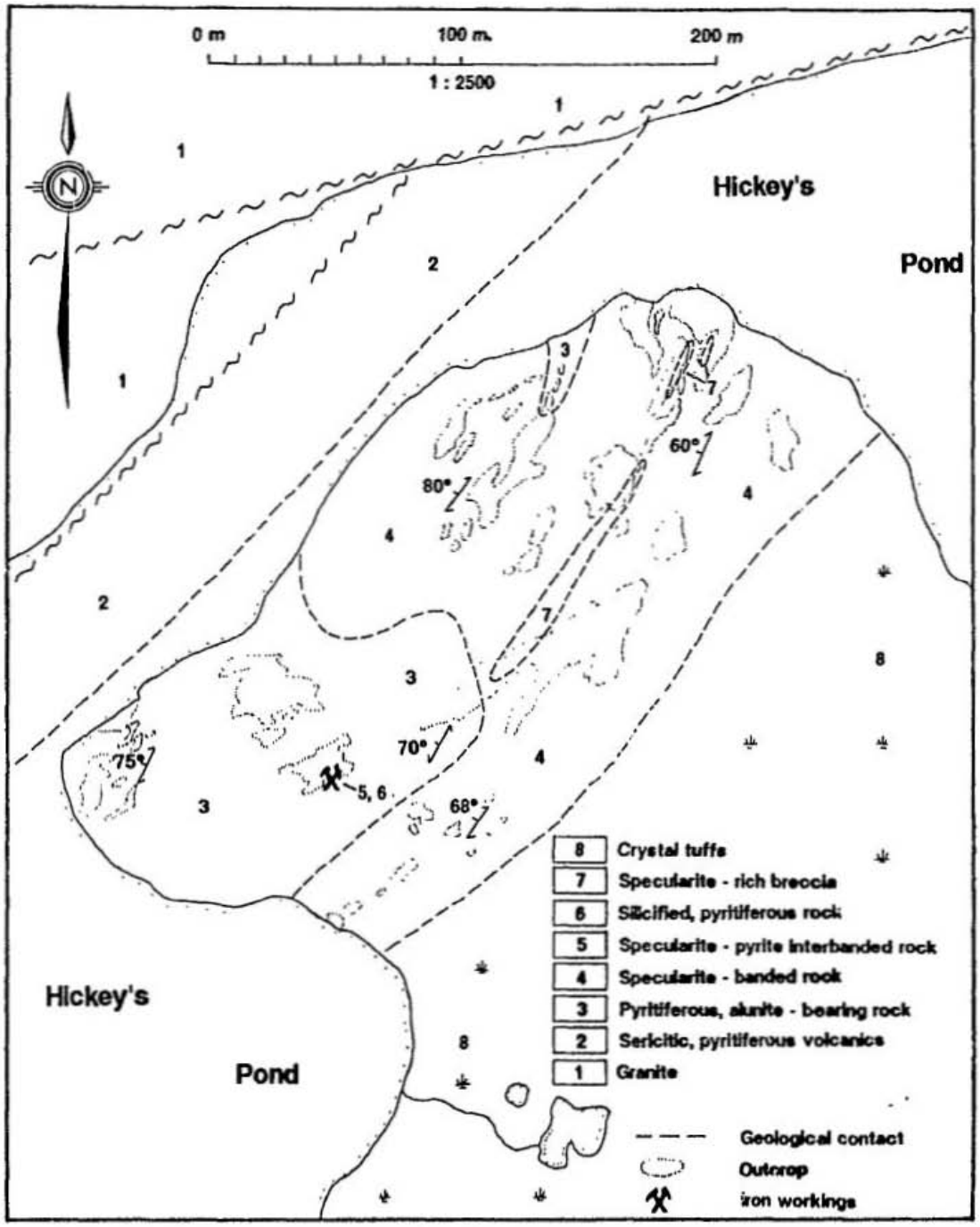

Figure 4-19: Geology of the Hickey's Pond Showing.

Figure 4-20: Sharply banded rock in drill core. Collection of samples from the top of DDH HP88-2 illustrates the sharp mineralogical banding typical of the western edge of the showing. Pink material is quartz, alunite, pyrophyllite and rutile; black bands are similar but contain approximately 5% specularite.

Figure 4-21: Site of iron workings at Hickey's Pond. Light-colored block in foreground is antiformally folded and faulted against hanging walls (top and left) which are extensively veined with quartz-specularite. Deep shadow on left marks blasting along mineralized fault contact.

4.3. Tower Showing

4.3.1. Location

The Tower showing is centered 1 km north of the microwave tower on the Monkstown Road (NTS 1M/9 (Harbour Buffet) map sheet). It comprises four resistant, siliceous mounds disposed in a NNE/SSW-trending belt. The belt is approximately 450 m long and 80 m across. On each side of this belt paralleling its trend are two continuous bogs, approximately 30 m wide. These bogs separate the rocks of the showing from the contrasting country rock (Figure 4-22).

The showing strikes northward into a pond. To the south, bedrock exposure becomes increasingly poor as a long, linear ridge of glacial till is approached. The ridge is 3 km long, averages 300 m wide and strikes NW-SE. Glacial striae striking 140 degrees were measured at the Tower showing. The showing may continue beneath this ridge, which is 400 m wide where it crosses the strike of the Tower showing approximately at right angles. The projection of the Tower showing immediately south of the ridge is coincident with a pond.

4.3.2. Petrography

Three rock types at the Tower Showing bear strong mineralogical and textural resemblances to rock types at Hickey's Pond, *viz* specularite-banded rocks, pyritiferous rocks and quartz specularite veins. Figure 4-23 illustrates dark-grey, specularite-rich bands interbanded with pink to tan bands which are isoclinally folded into small, high amplitude folds comparable to those at Hickey's Pond. However, the very sharply banded rocks at Hickey's Pond do not have counterparts at the Tower Showing. A single quartz phenocryst was observed in the specularite-banded rock, with lobate boundaries with recrystallizing microcrystalline quartz. The pyritiferous rocks are similar to those at Hickey's Pond, although rock fragments were not observed in them. The quartz-specularite veins at the Tower Showing do not exhibit the size and grade locally developed at Hickey's Pond.

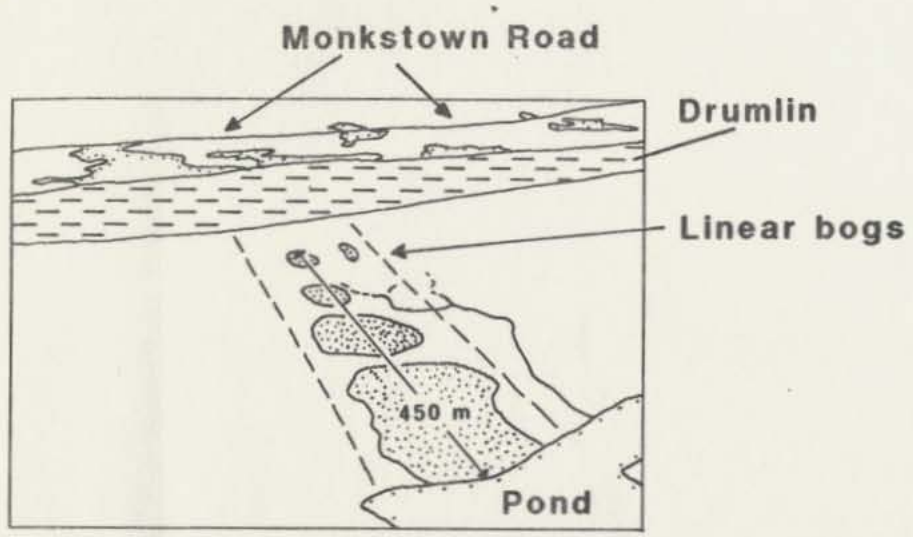

Figure 4-22: Aerial view of Tower showing. Resistant, barren mounds which constitute the showing (stippled on inset) extend from the edge of the lake (foreground) to the prominent, heavily- wooded drumlin in the background (looking southwest). The Monkstown Road is visible at the top of the photo. Compare with geology map (Figure 4-25).

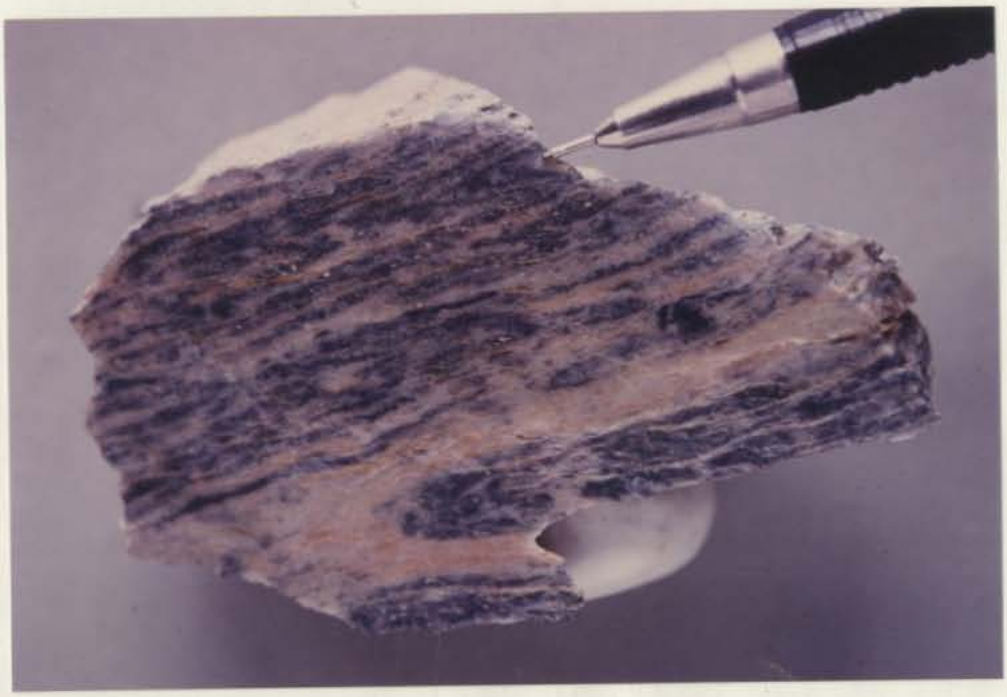

Figure 4-23: Specularite-banded rock from Tower Showing. Note fold noses throughout sample and disseminated cream-colored rutile.

A fourth rock type, which is unlike anything observed at Hickey's Pond, is described in detail in the following section.

4.3.2.1. Quartz-rutile rocks

The rock type unique to the Tower Showing consists essentially of quartz and rutile. In contrast to the pyrophyllite-bearing rocks that have developed a penetrative cleavage, these siliceous rocks are massive, being disrupted only by fine joint sets. This apparent change in structural style probably reflects the expected increased competence of these pyrophyllite-free rocks.

The rocks are grey and have a vitreous lustre, superficially resembling vein quartz. However, examination of a cut surface reveals a fragmental rock, with subtle colour changes over slightly diffuse fragment boundaries (Figure 4-24).

Figure 4-24: Quartz-rutile rock from Tower Showing. Close inspection reveals angular, fragmental nature of the rock (ignore joints and fractures).

Microscopically, rutile can be seen to be very unevenly distributed, concentrated locally in zones containing up to 10%. Quartz is microcrystalline throughout the rock. Specularite occurs rarely in these rocks, in very small irregular patches accounting for less than 1% of the rock.

4.3.3. Spatial relations

Figure 4-25 shows the distribution of various rock types at the Tower Showing. The specularite-banded rocks form the western flank of the showing and are confined to it and the quartz-rutile assemblages form the eastern flank of the showing with the exception of the northern and southern extremities, and are confined to the eastern flank. The distribution of pyritiferous rocks is not so consistent, but they form most of the southern extremity of the showing.

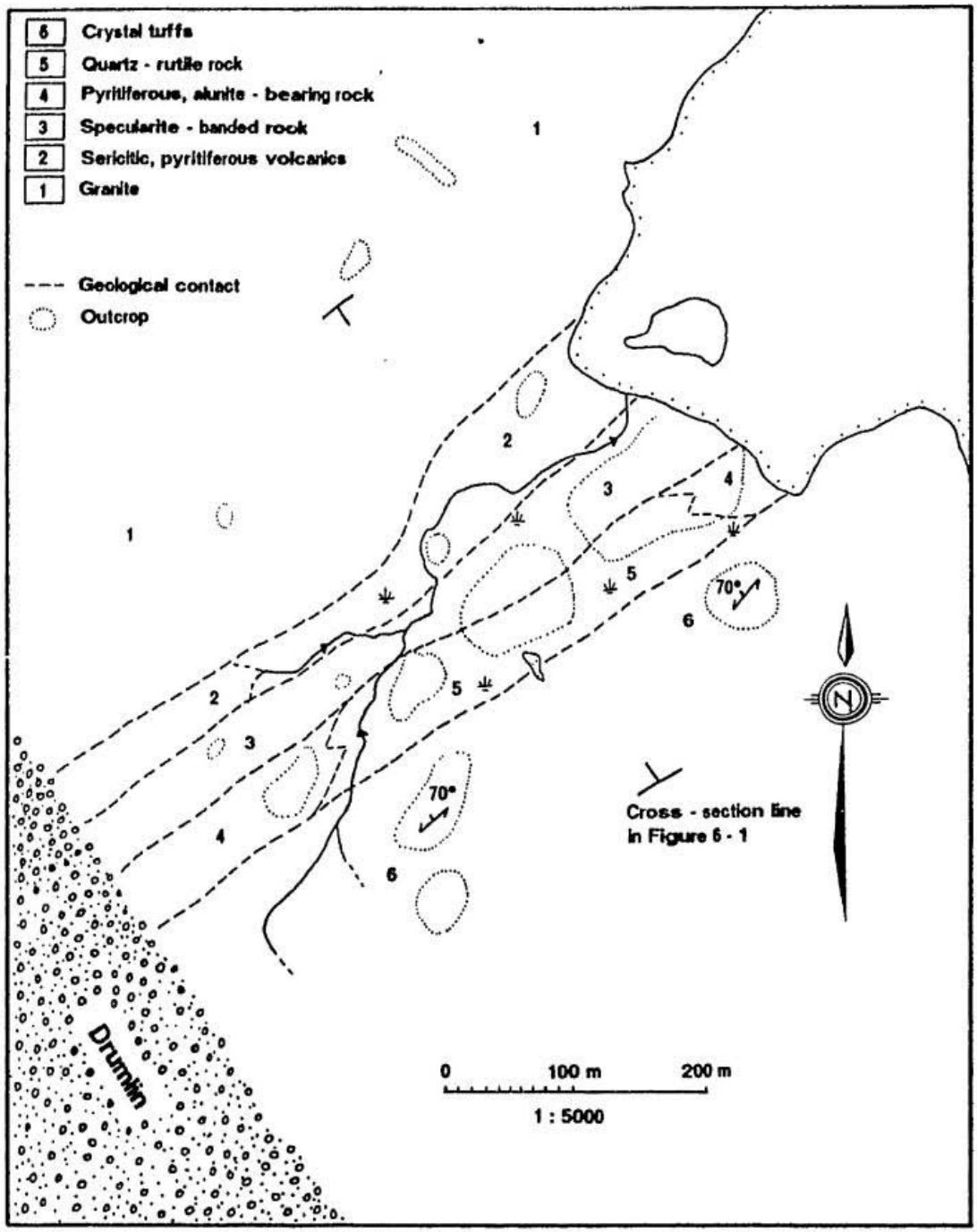

Figure 4-25: Geology of the Tower Showing.

The rocks to the east of the showing are better exposed than those to the west. They are relatively fresh felsic crystal tuffs that locally contain minor amounts of pyrite and commonly have an associated red iron hydroxide stain. West of the showing are schistose pyritiferous crystal tuffs with abundant sericite. One hundred metres west of the western edge of the showing is a small NNE-SSW trending scarp, the ground to the west of which is underlain by granite.

4.4. Bullwinkle Showing

4.4.1. Location

The Bullwinkle Showing, centered 2.5 km SSW of the Monkstown Road Specularite Showing (NTS 1M/10 (Terrenceville) map sheet), was discovered during the 1985 field season. Its extent is defined by the occurrence of variable assemblages of quartz, alunite, specularite, pyrite, pyrophyllite and rutile. It occupies a NE-trending zone 900 m by 150 m that is bounded to the NW and SE by air photo lineaments. These lineaments trend 049 and separate the showing from topographically higher volcanic rocks (Figure 4-26). A lack of outcrop exposure to the NE and SW constrains the length of the showing, although it is possible that it continues under the bogs in these areas. A prominent air photo lineament trending 124 degrees cross-cuts the low ground approximately 75 m SW of the showing.

The rocks at the showing are confined to two discontinuous NE-trending belts that occur adjacent to the lineaments that define the zone. The belts are approximately 20 m wide and they are separated from each other by a swampy lowland 100 m wide, in which bedrock exposure is very poor. A pond 250 m long occurs in the southwest end of this lowland.

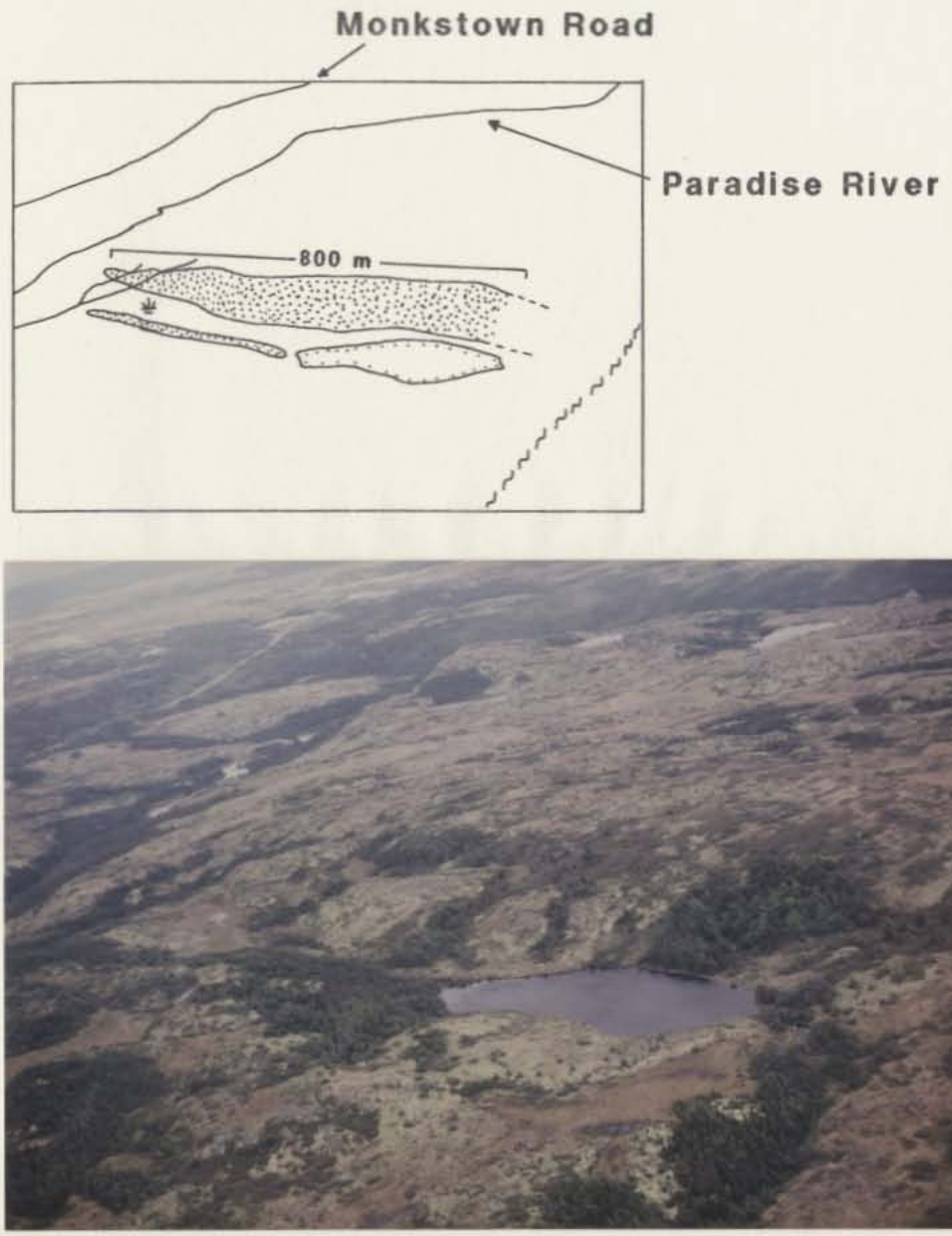

Figure 4-26: Aerial view of Bullwinkle Showing. Resistant rocks of the showing (stippled on inset) outcrop in two belts on either side of the small pond and the bog which runs northeast from the pond. The Monkstown Road is visible at the top, left corner of the photo. Compare with geology map (Figure 4-30). [Length of pond is 250m, looking east.]

4.4.2. Petrography

All the rocks at this showing have analogues at the Hickey's Pond Showing, *viz* specularite-banded rocks, pyritiferous rocks, specularite-rich breccias and quartz-specularite veins. Significant differences, where developed, are discussed below.

4.4.2.1. Specularite-banded rocks

Figure 4-27 shows a typical specularite-banded rock from the Bullwinkle Showing, for comparison with those from Hickey's Pond (*e.g.* Figure 4-5) and the Tower Showing (Figure 4-23).

A volumetrically minor variant of the specularite-banded rocks, unlike any from Hickey's Pond, contains approximately 40% pyrophyllite. The pyrophyllite forms soft, light brown bands up to 3 mm thick interbanded and contrasting sharply with black, hard bands of specularite, quartz and alunite (Figure 4-28). The banding has been chaotically folded and attenuated. Quartz occurs in the black interbands predominantly as equant crystals averaging 0.05 mm across with random optical orientations. Specularite occurs as very slender, rarely gently curved needles up to 1.2 mm long. They vary from randomly oriented to strongly preferentially arranged at a high angle to the schistosity. Alunite occurs as randomly oriented euhedral crystals that are locally pierced by needles of specularite. Rutile is confined to the pyrophyllite bands, where it occurs as scattered equant crystals averaging 0.02 mm across.

4.4.2.2. Specularite-rich breccias

Similar to the specularite-rich breccias at Hickey's Pond, these rocks are dark-grey to dull black and generally appear featureless, except on cut surfaces whereupon their fragmental nature is revealed. The most significant difference between the breccias at the Bullwinkle and Hickey's Pond Showings is that the former display a stronger tectonic fabric, indicated by lensoid fragments (Figure 4-29) and attenuated rutile crystals. One case of severe attenuation of rutile yielded a broken grain measuring 2.4 x 0.2 mm.

Figure 4-27: Specularite-banded rock from the Bullwinkle Showing. Compare with similar rocks at Hickey's Pond (Figure 4-5 (page 79)) and the Tower Showing (Figure 4-23 (page 96)). [Width of sample is 12cm.]

Figure 4-28: Pyrophyllite-rich specularite-banded rock. Note small-scale boudinage of black specularite-quartz-alunite bands in light brown pyrophyllite bands. [Width of sample is 10cm.]

Figure 4-29: Specularite-rich breccia from Bullwinkle Showing. Grey, siliceous fragments set in a black, specularite- rich matrix. Note strong tectonic fabric (left-right, compare with Figure 4-18 (page 89)), creamy, elongated high relief rutile crystals, and cross-cutting (tensional) quartz-specularite veinlets.

4.4.3. Spatial relations

Figure 4-30 shows the distribution of various rock types at the Bullwinkle Showing. The banded specularite-bearing rocks are by far the predominant lithology, accounting for approximately 90% of the showing. The pyritiferous rocks are best developed at the outcrop immediately east of the pond, although very minor amounts are found in the centre of the eastern edge and the north end of the western edge of the showing.

The specularite-rich fragmental rocks are associated with the banded specularite-bearing rocks. They are best developed in the centre of the eastern edge, where two outcrops of breccia approximately 2 m x 1 m occur. Contact relations are not visible, but the breccia appears to be in the form of lenses

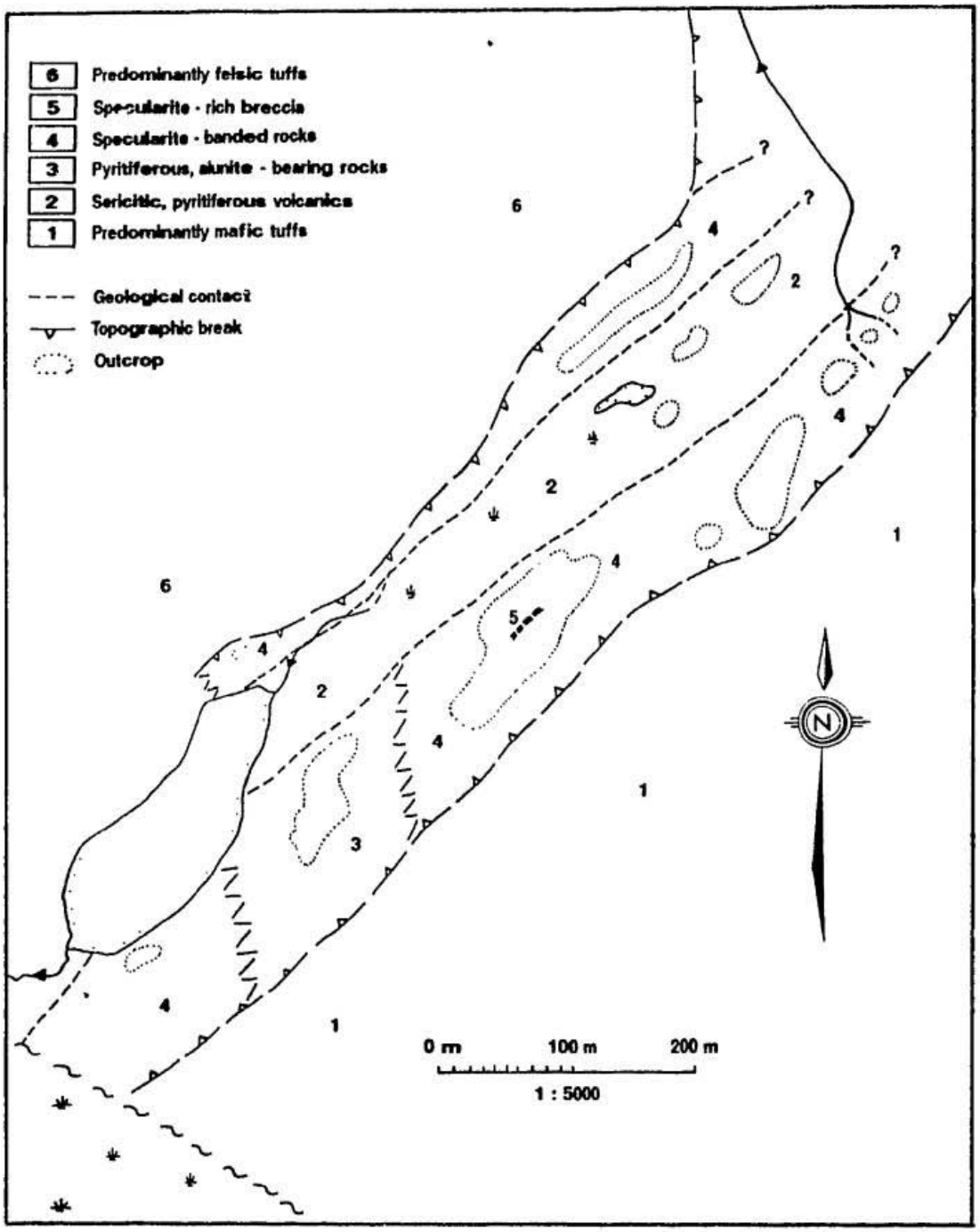

Figure 4-30: Geology of the Bullwinkle Showing.

conforming to the schistosity in the banded rock. Black, specularite-rich rock occurs within the banded, specularite-bearing rocks at the north end of the eastern edge of the showing (Figure 4-31).

Figure 4-31: Specularite-rich fragments at Bullwinkle Showing. Specularite-rich fragment (right of centre) occurs in pink, alunite-rich rock with distinct, specularite-rich bands (below fragment).

It occurs as rounded fragments up to 15 cm long that host abundant specularite veinlets, which do not cross over the contacts of the fragments, and fine-grained disseminated specularite.

The lowland in the centre of the showing, between the two belts of alunite-bearing rock is marked by a few very small outcrops of pyritiferous quartz-sericite schist. West of the showing, mafic tuffs and dykes with minor pyrite locally developed occur. A band of felsic crystal tuff 10 m wide occurs at the northern end of the eastern contact and a small outcrop of distinctive green quartz-pyrophyllite schist with abundant porphyroblastic chloritoid occurs at the centre

of the eastern margin. East of these rocks, mafic tuffs with disseminated pyrite are found.

4.5. Paradise River Showing

The Paradise River Showing is a prominent, barren resistant mound 70 m by 30 m on the north bank of Paradise River, immediately west of a small tributary which enters the river from the north. The rocks there include typical specularite-banded and pyritiferous varieties, which strongly resemble the rocks at the Builwinkle Showing, the northern end of which is only 500 m to the south. Poor exposure between the two showings allows the possibility that they are continuous, which would provide a total length of 1500 m.

4.6. Ridge Showing

4.6.1. Location

The Ridge Showing, discovered during the 1984 field season, is centered 1.2 km NNE of the Monkstown Road (NTS 1M/9 (Harbour Buffet) map sheet). It consists of varying assemblages of quartz, alunite, specularite, pyrophyllite, pyrite and rutile. These outcrops define an elongated NNE-trending zone approximately 225 m long and 35 m wide.

4.6.2. Petrography

Two of the rock types at the Ridge Showing, *viz* specularite-banded rocks and pyritiferous rocks, have analogues at the Hickey's Pond Showing. Non-banded specularite-bearing rocks which include distinctive cm-scale spheroids composed of quartz, alunite, pyrophyllite and specularite are unique to the Ridge Showing, and quartz-pyrophyllite-specularite schists occur on surface only at the Ridge and Chimney Falls showings, although they were encountered in diamond drill core at Hickey's Pond.

4.6.2.1. Spheroid-bearing rocks

These rocks are composed predominantly of light pink to white, very resistant siliceous spheroids up to 3 cm in diameter. They are generally separated by a pink to grey matrix, which may constitute up to 30% of the rock, but locally they coalesce into small masses. Thin bands of pyrophyllite are deflected around the spheroids and are commonly weathered preferentially, causing the spheroids to be highly conspicuous on a weathered surface (Figure 4-32).

Figure 4-32: Siliceous spheroids at Ridge Showing. Cleavage deflects around the spheroids, which constitute 75% of the outcrop surface.

The matrix around the spheroids consists of quartz, alunite, specularite and pyrophyllite, with very minor rutile. Quartz forms a mass of irregular crystals averaging 0.06 mm across that accounts for up to 80% of the matrix. Alunite accounts for up to 30% of the matrix, occurring as randomly oriented diamond-shaped euhedra averaging 0.15 mm in length and less commonly as crude bands in

which the crystals are recognizably oriented parallel to the band. Specularite forms randomly oriented needles and platelets averaging 0.1 mm in length and comprises approximately 5% of the matrix. Rutile is a very minor constituent, occurring as isolated equant crystals 0.01 mm across.

The spheroids are not homogeneous masses, but concentrically shelled features with coarse crystalline cores. They feature a sharp contact between the outermost shell and the matrix, but gradational contacts between shells. The shells are composed predominantly of quartz and alunite, with minor specularite concentrated in the core, the general trends outward being towards finer grain size and more siliceous material. The shells are cored by a coarse crystalline assemblage of quartz, alunite, specularite and pyrophyllite.

4.6.2.2. Quartz-pyrophyllite-specularite schists

These rocks are soft light grey to light brown schists with wispy dark grey sub-millimetre specularite-rich bands in strong contrast to the specularite-banded rocks at the showing which resemble those at Hickey's Pond. Pyrophyllite constitutes approximately 50% of these rocks, as extremely fine bands up to 2 mm thick. Rutile, which accounts for less than 1% of the rock, occurs predominantly in the pyrophyllite bands as equant crystals that average 0.01 mm across. It occurs rarely as anhedral, elongated grains up to 0.1 mm in length. Quartz comprises up to 60% of the rock, where it occurs as slightly elongated crystals averaging 0.03 mm in length that are concentrated in bands. These bands alternate with, and appear to be boudins within, the more continuous pyrophyllite bands. Quartz occurs rarely, as phenocrysts up to 0.3 mm in length. Specularite averages less than 10% of these rocks, where it occurs as slender needles up to 0.6 mm long. The specularite is most commonly in the quartz interbands.

The banding has been tightly folded on a small scale. Quartz, specularite and pyrophyllite wrap around the fold noses, retaining their conformity to the banding (Figure 4-33 and see Figure 2-10, page 34).

Figure 4-33: Tight fold in quartz-pyrophyllite-specularite schist. Note segregation of specularite into dark bands and folding of the earlier fabric. Compare with Figure 2-10 (page 34). [Field of view 5.0mm x 3.4mm, cross polarized.]

An uncommon type of pyrophyllite schist at the showing includes approximately 5% crystals of fine-grained black chloritoid, which form conspicuous porphyroblasts on the smooth, pale schistose surface of the rock. In thin section, it occurs as slender crystals up to 0.7 mm long, locally at very high angles to the schistosity.

4.6.3. Spatial relations

The banded specularite-alunite rocks and the specularite-pyrophyllite schists are confined to the western edge of the showing, where they occur in close proximity to one another. The pyritiferous, alunite-bearing rocks form the eastern edge of the showing, and the siliceous spheroid-bearing rocks are confined to a small outcrop at the extreme southwestern corner. Outcrops of pyritiferous,

weakly sericitized schistose volcanics surround the showing.

4.7. Strange Showing

4.7.1. Location

The Strange showing is located 4.1 km SSW of the Monkstown Road Specularite Showing (NTS 1M/10 (Terrenceville) map sheet). It was discovered during the 1985 field season and consists of a low, northeasterly trending outcrop approximately 10 m by 2 m. It is at the northern end of a low, narrow northeast-trending ridge bounded by two northerly converging airphoto lineaments that strike 038 degrees and 054 degrees. The projections of these lineaments intersect in a swamp to the northeast of the showing.

4.7.2. Petrography

The Strange showing is so named because of the highly contrasting rock types found there: 1) a bright pink, massive rhyolite with a hackly fracture pattern and 2% coarse grains of pyrite up to 2 mm across and 2) an intensely sheared, vitreous-lustred black rock marked by numerous highly elongated grey streaks. The pink rocks occur in a small, rubbly outcrop 3 m west of the outcrop of black, specularite-rich rock. Exposure is not complete over the short distance separating these rock types, but intervening rocks suggest there is a continuum in terms of deformation between them.

4.7.2.1. Pink rhyolite

These rocks are cut by coarse joint sets that have reduced it to angular, blocky fragments from 5 cm to 10 cm on a side. Joint surfaces are commonly heavily stained by iron hydroxides but freshly broken surfaces reveal the bright pink colour and coarse grains of pyrite.

The rocks consist of microcrystalline quartz and sanidine feldspar, which occur as a mass of irregular crystals with a poorly developed elongation. Pyrite

constitutes approximately 2% of the rock, occurring as highly corroded grains disseminated throughout the rock, which locally feature pressure shadows of coarse, elongated quartz crystals. Rutile is uniformly distributed as needle-like trains up to 0.1 mm long of equant crystals that average 0.008 mm across and constitutes less than 1% of the rock. Pyrophyllite (sericite?) also accounts for less than 1% of the rock, occurring as minor wisps parallel to the fabric. Zircons averaging 0.02 mm across are a very minor constituent.

4.7.2.2. Black rocks

These rocks have a vitreous, black colour, a good schistosity and an excellent mineral lineation on the schistosity. Close inspection reveals a fragmental appearance defined by numerous, wispy dark grey streaks in a black matrix. Several cut surfaces through the rock show that the streaks are highly elongated discs that lie on the schistosity with their long axes parallel to the lineation. The following description pertains to a thin section cut on the plane perpendicular to the schistosity and parallel to the lineation on the schistosity. On this surface, the grey streaks are most highly elongated (Figure 4-34).

Quartz constitutes approximately 90% of the rock, occurring as highly elongated threads 0.015 mm thick and up to 0.2 mm long. A description of the quartz fabrics is given in Section 2.3.1 (see Figure 2-14, page 39). Specularite accounts for approximately 2% of the rock, forming slender stringers and stockworks essentially parallel to the quartz fabric. Slightly discordant specularite veinlets were identified as infilling an extensional crenulation cleavage (T. Calon, pers. comm.).

Minerals present in amounts less than 1% include pyrite, pyrophyllite, rutile and zircon. Pyrite occurs as angular grains up to 0.3 mm across which have associated pressure shadows and as corroded grains partially replaced by and surrounded with iron hydroxides. No contact relationships between pyrite and specularite were observed. Pyrophyllite forms extremely slender needles averaging 0.004 mm across by up to 0.1 mm long, that are disposed parallel to the

Figure 4-34: Black rock from Strange Showing. Diffuse light-grey streaks and creamy, high-relief rutile smears (at pencil tip) are highly elongated parallel to schistosity.

quartz fabric. Rutile occurs as smears up to 2.5 mm long that parallel the quartz fabric. They are composed of equant crystals approximately 0.004 mm across and are readily visible on a cut surface (Figure 4-34). Equant zircons up to 0.05 mm across occur rarely throughout the rock.

4.7.2.3. Intermediate rocks

These rocks are light grey, have a good schistosity and an excellent mineral lineation on the schistosity. A thin section was cut parallel to the lineation and perpendicular to the schistosity, *i.e.* in the same orientation relative to the structure as the one described in the preceding section for the black rock. The rock is approximately 95% quartz, which occurs as highly elongated threads approximately 0.015 mm wide and up to 0.2 mm long. The crystallographic axes show excellent parallelism but the projection of the optic axes onto the plane of the thin section is 75 degrees from the mineral elongation.

Pyrite constitutes approximately 1% of the rock, occurring as euhedral polygonal to rounded corroded grains up to 0.8 mm across which locally have pressure shadows infilled with quartz. Rutile occurs as smears up to 2.7 mm long, which strongly resemble those in the black rocks described in the preceding section. Pyrophyllite constitutes less than 1% of the rock, occurring as extremely slender needles 0.002 mm wide and up to 0.1 mm long. Rare zircon crystals up to 0.7 mm across were also noted.

4.7.2.4. Summary

The black rocks and the intermediate rocks share the same structural features, *viz* a pronounced schistosity and lineation on the schistosity, highly elongated quartz crystals with well-developed parallelism of optic axes and strongly attenuated rutile crystals. These features record a much higher degree of deformation than in the adjacent pink rhyolite.

4.7.3. Field relations

The strike extent of the black, specularite-rich rock is unknown as it is lost under thin overburden towards the south. Moderately chloritized mafic tuffs with minor disseminated pyrite occur approximately 25 m farther south on the ridge. To the north, the specularite-rich rocks are in rapid gradational contact with quartz-pyrophyllite-specularite schists and the siliceous, grey pyritiferous rocks pass into pyritiferous quartz-pyrophyllite (sericite?) schists. Rhyolite dykes are common in the area, where they display a joint pattern similar to that of the pink rhyolite discussed above, i.e., coarsely spaced joint sets that have broken the rock into angular, centimetre-scale fragments.

4.8. Monkstown Road area

Three distinct outcrops of specularite-bearing rock occur along a linear trend between Paradise River and the northern side of the Monkstown Road. They are all resistant mounds covered only by a thin veneer of vegetation. The nature of contacts between them and the surroundings, and the possibility that

they are continuous in the subsurface are unknown. They are described in the following sections, in sequence from north to south.

4.8.1. Monkstown Road Specularite Showing

This showing is a resistant north-south trending linear ridge approximately 50 m by 10 m, that rises approximately 3 m above the surrounding bog. It consists of light grey and brown, generally massive, extremely siliceous rock. Chalcedonically banded silica occurs rarely, as irregular, randomly oriented veins (?) (Figure 4-35).

Specularite occurs disseminated within the siliceous rock, and in narrow bands of pyrophyllite which occur in fractures. Cutting the rocks are west-dipping veins of coarse crystalline, milky white quartz with coarse platelets of specularite and crystals of brilliant blue lazulite up to 3 cm across (Figure 4-36). On the western margin of the outcrop these veins display a strong mineral lineation in the down-dip direction.

Specularite also occurs in the matrix of a small breccia zone at the southwestern edge of the outcrop. It consists of centimetre-scale angular wallrock fragments occurring in and supported by a black matrix of quartz and specularite (Figure 4-37). The zone defines an upward-flaring cone 20 cm high that passes into narrow quartz-specularite veinlets. It is believed to be a zone of hydrothermal brecciation on the basis of its being matrix-supported, the presence of specularite and the lack of structural control.

Microscopic examination revealed the rock to consist predominantly of microcrystalline quartz, with up to 10% needles of pyrophyllite and specularite, and locally $<1\%$ chloritoid. No pyrite or alunite were observed at the showing.

Lazulite is also found at a small outcrop 500 m south of the Monkstown Road specularite showing. It occurs with plates of specularite in coarse crystalline quartz veins which cut a 5 m by 2 m zone of quartz-pyrophyllite-specularite

Figure 4-35: Chalcedonically banded silica. Note extremely fine laminations (left of pencil tip) in irregular vein or bed of silica.

Figure 4-36: Quartz-specularite-lazulite vein. Coarse crystals of brilliant blue lazulite with specularite and quartz are in sharp textural contrast to the silica in Figure 4-35.

Figure 4-37: Specularite-rich breccia. Fragments (*in situ*) of massive siliceous rock are in sharp contrast to the black, specularite-rich matrix.

schists.

4.8.2. Little Pond Specularite Showing

This showing is exposed at the north end of a prominent barren ridge 75 m long by 15 m wide, which is situated 0.75 km south of the Monkstown Road specularite showing, west of a "little pond". Specularite constitutes up to 10% of black, siliceous bands up to 40 cm thick that are interbanded with grey and brown siliceous rock (Figure 4-38). The bands are open to tightly folded about steeply north-plunging fold axes.

Microscopically, the black specularite-rich bands consist predominantly of microcrystalline quartz with 10% very fine grained specularite. Pyrophyllite occurs throughout the rock as slender needles and pure Fe-chloritoid

Figure 4-38: Specularite-rich band. Open fold is apparent in relatively massive band of siliceous, specularite-rich rock from Little Pond Showing. It bears a strong field resemblance to banded iron formation.

porphyroblasts (?) constitute approximately 3%. The intervening grey and light brown bands are composed of microcrystalline quartz with minor, very fine needles of pyrophyllite. Neither pyrite nor alunite were observed at the showing.

4.9. Chimney Falls

The Chimney Falls Showing differs from the other showings discussed in this chapter in that the bulk of the rocks there are clearly alteration products of volcanic rocks. Four of the rock samples in the alteration suite considered in Chapter 3 were from the Chimney Falls Showing. It is considered in this chapter because it hosts a narrow zone of specularite-rich breccia similar in many respects to that at Hickey's Pond, which affords valuable insights into the origins of that type of rock.

4.9.1. Location

The Chimney Falls showing is located in a deep gorge immediately downstream of a prominent waterfall on Hickey's Brook, 4 km SSW of Hickey's Pond (NTS 1M/9 (Harbour Buffet) map sheet). It is a narrow strip of outcrop, approximately 45 m long, between the eastern side of Hickey's Brook and a steep cliff that parallels the brook. An extension 200 m to the NNE, discovered in 1984, is also discussed here.

4.9.2. Petrography

4.9.2.1. Schistose rocks

Most of the rocks at this showing are schistose assemblages of quartz, pyrophyllite and rutile, with or without specularite, and/or alunite. Quartz is the predominant constituent, occurring as rounded embayed phenocrysts which commonly display undulatory extinction, and as masses of microcrystalline, interlocking crystals. Pyrophyllite occurs in thin, discontinuous mm-scale bands and minute, slender crystals. Specularite constitutes up to 5% of the rock, appearing as smears on the planes of schistosity, which appear as slender needles in thin section. Where specularite and pyrite occur together, the pyrite is corroded and surrounded by red iron hydroxide reaction rims or open spaces. Specularite commonly fills embayments in corroded pyrite grains. Rutile is present as minute, equant crystals distributed uniformly throughout the rock, or as concentrations of these crystals in rudimentary bands. Alunite occurs rarely as small euhedral crystals in specularite-bearing schists.

Quartz-sericite schists are less abundant at the showing. They contain up to 5% pyrite in the form of equant, sub-rounded to sub-angular grains with sharp boundaries, but resemble the pyrophyllite schists microscopically.

At the northern extension of the main showing, small black chloritoid crystals interrupt the schistosity, giving the rock a rough porphyroblastic appearance. They are elongate crystals that commonly parallel the cleavage, but

locally are at a high angle to it.

4.9.2.2. Specularite-rich breccias

At the main showing there is a massive, conformable lensoid body of rock approximately 1.2 m high by 0.3 m wide at its widest point (Figure 4-39). The rock is siliceous and generally black or dark grey, but contains numerous light-colored angular to subangular mm-scale rock fragments (Figure 4-40) composed of microcrystalline quartz, with lesser amounts of alunite, pyrophyllite, specularite, pyrite and rutile. The matrix surrounding the fragments contains up to 40% specularite, with quartz and much lesser alunite, pyrophyllite and rutile. Pyrite grains are commonly embayed, with specularite in the embayments, but these minerals are everywhere separated by iron hydroxides or open space.

Specularite-rich breccia also occurs at the northern extension of this showing, however no alunite or pyrite is present there.

4.9.3. Field relations

Hickey's Brook follows a prominent NNE-trending lineament at the main Chimney Falls showing. This lineament separates granite to the west from the soft, intensely deformed and easily-eroded rocks of the showing to the east, and is part of the Hickey's Brook Fault defined in Section (2.3.1). The waterfalls are developed where Hickey's Brook flows from west to east across the fault, falling approximately 7 m. Figure 4-41 shows the relationship of the lineament to the brook. The northern extension of the showing is situated at the curve in the brook where it crosses the projection of the lineament.

Alteration diminishes in intensity away from the breccia zone towards the granite, in the sequence 1) specularite-rich breccia (with alunite), 2) specularite-bearing pyrophyllite schists (+/- alunite, partially replaced pyrite), 3) pyritiferous quartz-sericite schists and 4) weakly sericitized, intensely sheared felsic tuffs.

North of the northern extension, the rocks are much less intensely altered

Figure 4-39: Lens of specularite-rich breccia at Chimney Falls. Steeply-dipping lens (black, behind hammer) is a boudin within specularite-bearing quartz-pyrophyllite schists.

Figure 4-40: Specularite-rich breccia at Chimney Falls. Light-colored fragments are quartz-alunite, black matrix contains 5% disseminated specularite.

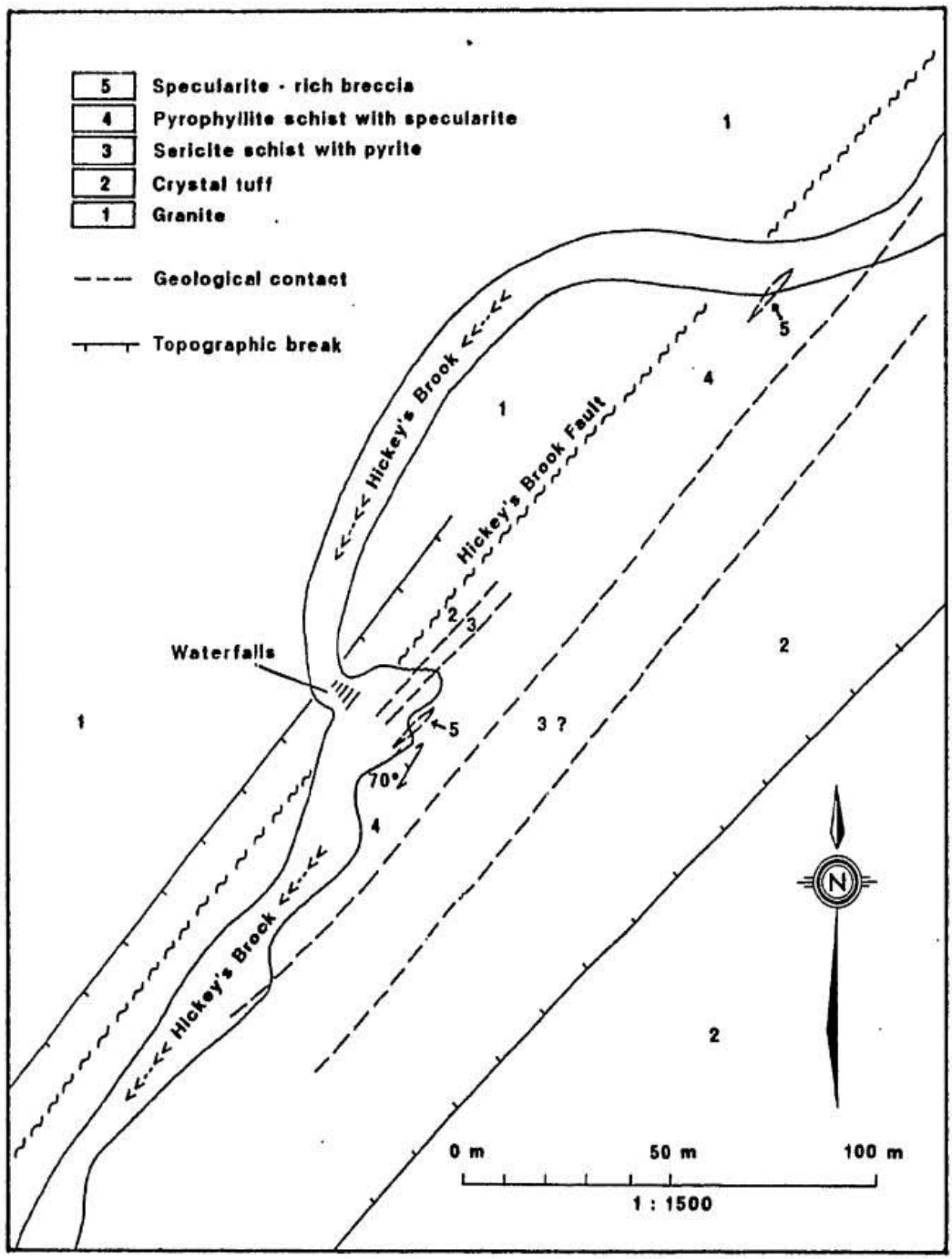

Figure 4-41: Geology of the Chimney Falls Showing.

felsic crystal tuffs. Pyrite and sericite are present, but plagioclase phenocrysts are recognizable. Beyond this are typical unaltered felsic crystal tuffs. To the south of the showing, exposure is not as good, but the same gradation from pyrophyllite through sericite to unaltered rocks may occur.

The rock immediately to the west of the fault contact resembles the Swift Current Granite. It is a competent, pink, siliceous porphyritic rock with a good foliation. Large plagioclase phenocrysts are partially altered to sericite (?). Amphibole phenocrysts up to 4 mm long are altered to magnetite, chlorite and epidote, but an excellent amphibole cleavage is locally intact. Smaller quartz phenocrysts are also abundant. The matrix is essentially fine-grained quartz.

Within this rock adjacent to the top of the falls, an angular fragment of equigranular granite occurs. It is nearly equidimensional and almost 12 cm across. The contacts of this fragment with the more foliated surrounding rock are sharp, and the foliation wraps around the fragment. This fragment resembles a granite clast in a tuffaceous volcanic rock; the implication being that the rocks to the immediate west of the fault are volcanic. However, it may also be explained as a xenolith of equigranular granite in an intrusive porphyry with an aphanitic matrix. The competence contrast between them may account for the refraction of the foliation around the more competent xenolith. The distinction between these two possible explanations is not important to this study. The salient point is that the rocks to the west of the fault are comparatively unaltered, relative to the schistose rocks to the east.

4.10. Normative mineralogy

Major element analyses were performed on 29 specularite-banded and pyritiferous rocks from the Tower, Bullwinkle and Hickey's Pond showings. These rocks are mineralogically simple, with quartz, pyrophyllite, alunite, rutile and either pyrite or specularite accounting for all the major element oxides except CaO, MnO, MgO and P_2O_5. For all of these rocks however, the sum of these

elements was <1% by weight, thus the rocks were well suited to description by normative mineralogy. A FORTRAN program was written to do the calculations. It is given in the appendix, with a flow chart illustrating its operation. A check on the suitability of the rocks for treatment with normative methods is provided by a plot of normative alunite *versus* loss on ignition (Figure 4-42), since LOI was not considered in the normative calculation, and since it is most strongly controlled by loss of sulfur in alunite. This figure shows an excellent linear relationship which matches the expected loss on ignition, confirming the validity of the assumptions underlying the norm' program. Results of the calculations are provided in Table 4-2, with the data arranged to provide the easiest comparison between the two rock types present at the three different showings. Comparison is also provided for the specularite-banded and pyritiferous rocks in double triangular diagrams (Figure 4-43 and 4-44).

Examination of Table 4-2 in conjunction with Figures 4-43 and 4-44 reveals the following:

1. The specularite-banded rocks at Hickey's Pond generally contain higher specularite concentrations than similar rocks from the other showings.

2. For the specularite-banded rocks, there is no discrimination among the showings in terms of quartz, alunite, molar K/Na ratios in alunite, pyrophyllite or rutile concentrations.

3. The pyritiferous rocks at Hickey's Pond contain consistently low concentrations of pyrophyllite relative to the other showings, a feature apparently offset by higher quartz concentrations.

4. The silicified rock with pyrite, present only at Hickey's Pond, contains very little pyrophyllite or alunite, in keeping with the petrographic observations (Section 4.2.2.4).

5. For the pyritiferous rocks, there is no discrimination among the showings in terms of alunite, molar K/Na ratios in alunite, pyrite or rutile concentrations.

The quantitative treatment which the normative mineralogy enabled has

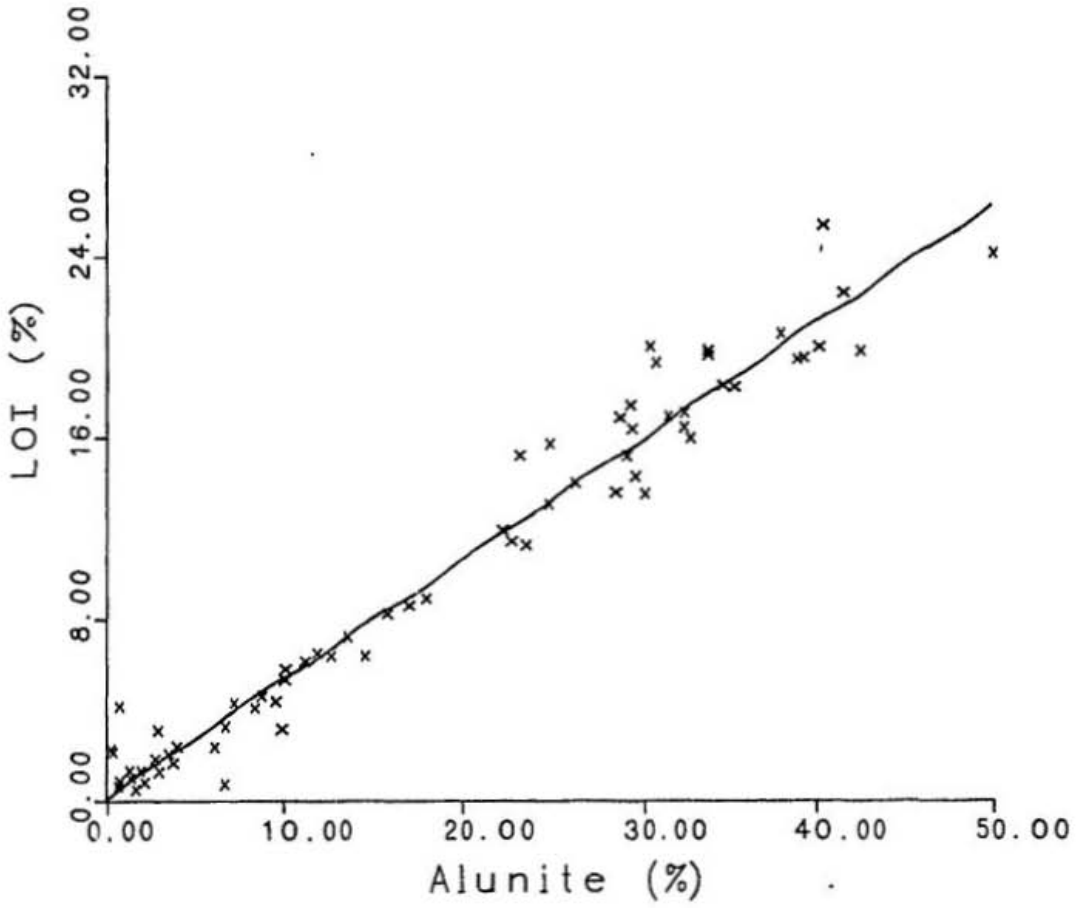

Figure 4-42: LOI *versus* normative alunite. Straight line relationship indicates that the assumptions underlying the norm program (Appendix) are valid. Solid line indicates the expected correlation for an ideal, equal mixture of Na and K alunite.

Table 4-2: Normative mineralogy. Results of calculations by the normative mineralogy computer program given in the appendix for rocks common to the three largest showings. Specularite - banded rocks are the top half, and pyritiferous rocks are the bottom half. "QTZ" = quartz, "ALUN" = alunite, "PPH" = pyrophyllite, "RUT" = rutile, "SPEC" = specularite and "PY" = pyrite, all reported in volume percent. "K/Na" is the molecular K/Na ratio in the alunite and "XTRA" is the weight percentage of elements not treated by the Norm program. Note under column titled "LOC", "HP" = Hickey's Pond Showing, "T" = Tower Showing and "B" = Bullwinkle Showing. Select mineral triplets follow on triangular diagrams.

#	LOC	QTZ	ALUN	K/Na	PPH	RUT	SPEC	PY	XTRA	
135	HP	65.05	30.08	50.2	2.33	.34	2.21	.00	.29	
228	HP	67.97	28.54	61.1	1.16	.32	2.01	.00	.31	
232	HP	62.08	33.04	45.0	1.55	.31	3.02	.00	.27	S
257	HP	61.79	29.53	34.0	4.00	.34	4.35	.00	.30	P
357	HP	66.68	24.78	45.7	3.14	.30	5.11	.00	.31	E
										C
277	T	63.53	31.58	33.9	2.83	.22	1.84	.00	.15	U
278	T	59.09	35.25	23.8	3.74	.38	1.53	.00	.20	L
283	T	56.87	38.02	42.6	4.66	.32	.13	.00	.17	A
284	T	59.12	34.71	42.5	4.15	.39	1.64	.00	.16	R
333	T	64.17	29.06	38.1	4.56	.33	1.87	.00	.36	I
										T
311	B	43.51	49.96	51.4	4.23	.41	1.89	.00	.60	E
314	B	83.87	9.71	43.4	1.64	.41	4.37	.00	.30	
319	B	61.85	3.02	46.7	30.31	.41	4.41	.00	.19	
432	B	52.51	42.27	37.0	4.02	.18	1.01	.00	.68	
436	B	74.35	22.68	30.5	1.74	.33	.89	.00	.14	
171	HP	71.62	23.39	42.5	3.33	.31	.00	1.35	.37	
263	HP	70.37	23.08	18.1	2.64	.29	.00	3.61	.25	
456	HP	48.94	40.45	51.8	1.47	.49	.00	8.65	.37	
272	T	35.41	34.00	35.9	30.03	.43	.00	.14	.36	
273	T	46.46	41.37	37.1	11.50	.39	.00	.28	.29	P
274	T	69.90	13.62	56.8	15.89	.40	.00	.18	.21	Y
275	T	56.30	33.98	40.9	7.65	.39	.00	1.69	.32	R
428	T	54.46	29.36	48.9	13.87	.39	.00	1.93	.29	I
429	T	60.13	32.66	36.6	3.58	.33	.00	3.31	.30	T
										E
313	B	55.33	30.35	31.4	9.77	.38	.00	4.18	.34	
330	B	64.19	29.27	20.3	4.56	.30	.00	1.67	.15	
435	B	53.45	39.46	41.9	5.16	.27	.00	1.67	.26	
443	B	93.76	3.86	64.2	1.24	.28	.00	.86	.07	
444	B	58.34	24.82	20.0	13.26	.31	.00	3.27	.26	
170	HP	96.59	2.31	67.6	.60	.15	.00	.35	.10	

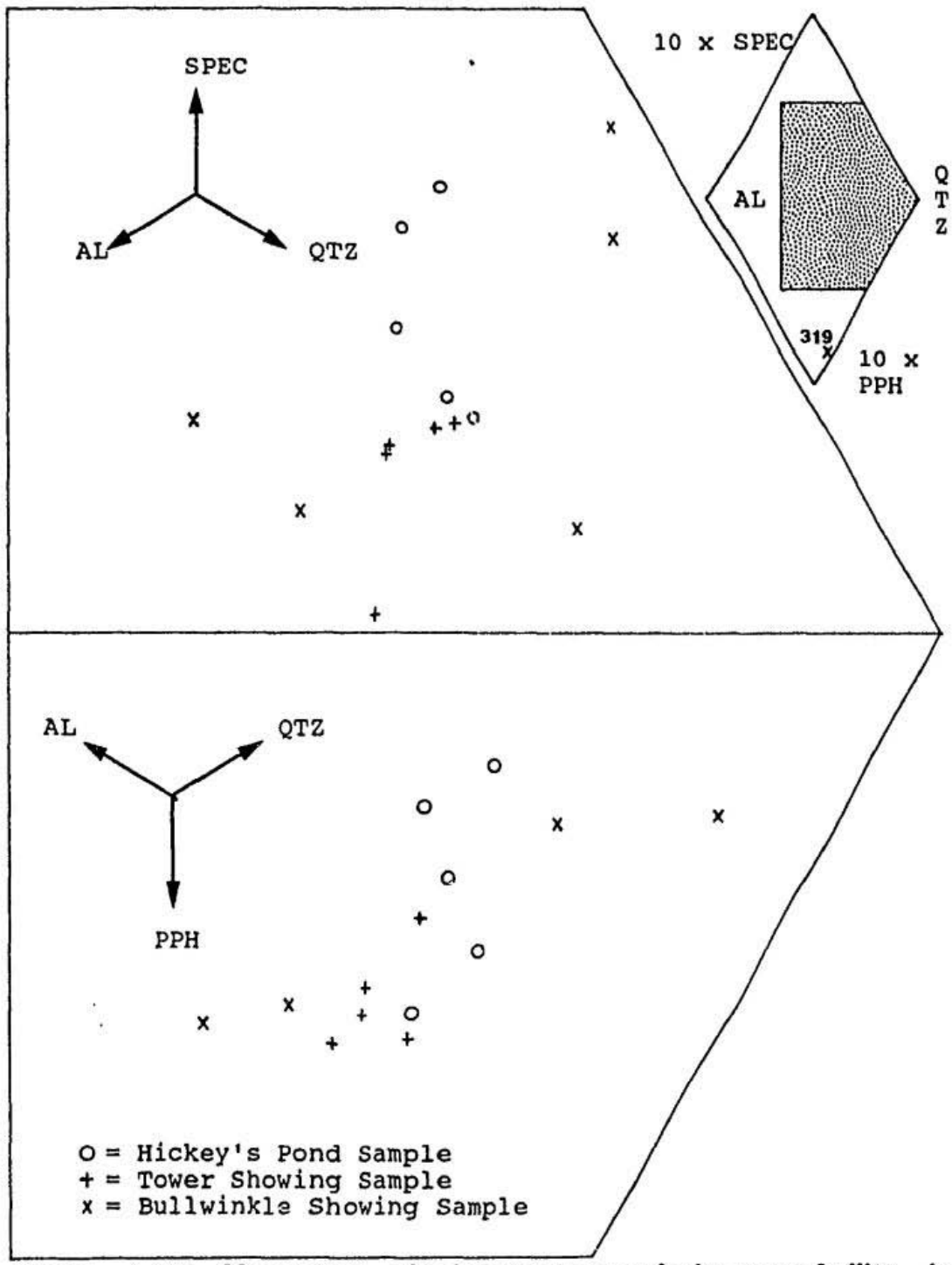

Figure 4-43: Normative alunite-quartz-specularite-pyrophyllite in specularite-banded rocks. Note the slightly higher specularite concentrations at Hickey's Pond (top half) and the overlap among showings in terms of quartz, alunite and pyrophyllite (bottom half). Sample 319, a pyrophyllite - rich specularite - banded rock from the Bullwinkle Showing is plotted on the inset figure.

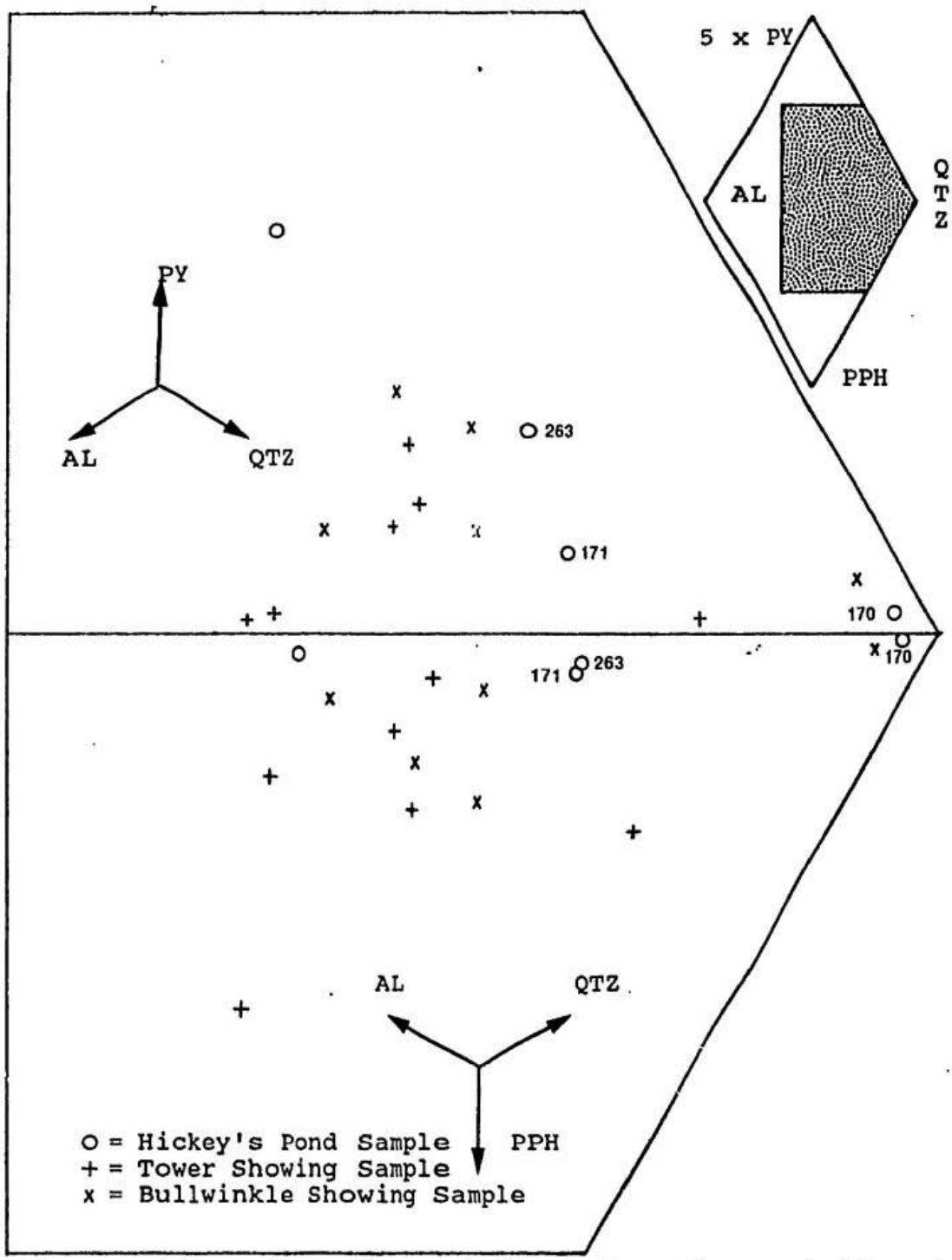

Figure 4-44: Normative alunite-quartz-pyrite-pyrophyllite in pyritiferous rocks. Note the weak enrichment in quartz in samples 263 and 161 from Hickey's Pond (top and bottom), the overlap in pyrite concentrations among the showings (top), and the consistently low pyrophyllite concentrations at Hickey's Pond (bottom). Sample 170 is a silicified rock with pyrite from Hickey's Pond for comparison.

outlined subtle differences not readily obvious from petrographic examination. The significance of these differences is discussed in Chapters 6 and 7.

4.11. Field relations

The showings described in this chapter lie in two north-northeast trending belts which are referred to as the eastern and western alteration belts (Figure 4-1), although the term "belt" is not advanced to imply continuity between the showings. The eastern belt consists, from north to south, of the Hickey's Pond, Chimney Falls and Tower Showings. If the pyrophyllite showings at the headwaters of Hickey's Brook, which also lie on the trend are considered, then the belt has a length of 15.0 km. The western alteration belt consists, from north to south, of the Ridge, Monkstown Road, Little Pond, Paradise River, Bullwinkle and Strange Showings, which extend over a length of 5.2 km.

The eastern alteration belt occurs in felsic volcanic rocks which are in fault contact with the eastern margin of the Swift Current Granite, along the Hickey's Brook fault. The western belt occurs in mixed mafic and felsic volcanics which pass upward into sedimentary rocks farther west. As such, it occupies the upper levels of the volcanic sequence, a position inferred for the eastern alteration belt also. A model to account for these spatial relations is advanced in Chapter 6, following a discussion of the origins of the showings.

Chapter 5

ALUNITE: ITS OCCURRENCE AND STABILITY RELATIONSHIPS WITH ASSOCIATED MINERALS

Quartz, alunite, pyrophyllite, specularite, pyrite and rutile occur at most of the showings described in Chapter 4. This chapter demonstrates that certain members of this group of minerals are associated with one another and with a highly specialized hydrothermal regime. The chemical conditions under which these minerals are stable, and the hydrothermal regime which fosters these chemical conditions are discussed in this chapter.

5.1. Examples and origins of alunite mineralization

The mineral most diagnostic of the conditions under which these rocks formed is alunite, $KAl_3(SO_4)_2(OH)_6$. Sodium substitutes for K in alunite, and where Na exceeds K on a molecular basis, the mineral is called natroalunite. In the following discussion, "alunite" refers to all Na/K ratios of the mineral. Four distinct modes of occurrence of alunite are recognized. In the near-surface environment, alunite occurs as a chemical precipitate in acid hotsprings (Raymahashay, 1968; Zotov, 1971; Krupp and Seward, 1987), and as a replacement mineral, commonly replacing felsic to intermediate volcanic rocks (Raymahashay, 1968; Cunningham *et al.*, 1984) but also replacing intrusive igneous rocks and sedimentary rocks (Schoen *et al.*, 1974). At deeper levels unaffected by surficial processes, alunite occurs as nearly pure veins (Cunningham *et al.*, 1984) and as a replacement mineral (Fisher and Leedy, 1973; Hayba *et al.*,1985).

5.1.1. Alunite as a chemical precipitate in hotsprings

Raymahashay (1968) describes the occurrence of alunite in freshly deposited sinters in Yellowstone National Park. It occurs as a very fine-grained, pink precipitate positively identified by means of X-ray diffraction analysis. One of the alunite-bearing sinters, and several sinters in which no alunite was noted, contained very fine-grained kaolinite.

The waters in the two springs with which the alunite is associated have pH's of 2.45 and 2.80 and temperatures of 65 and 55 degrees Celsius. The alunite at one of the springs has a mole fraction of potassium (K/(K+Na)) of 0.96. No alunite was reported at any of the nine alkaline hotsprings studied by Raymahashay.

Zotov (1971) provides new data and summarizes reports in the Russian literature which describe the precipitation of alunite in hotsprings. For the three localities described, the hotspring temperatures range from 10 to 83 degrees Celsius and the pH's from 1.8 to 2.8. The mole fractions of potassium in alunite vary from 0.45 to 0.75. Kaolinite was noted in the two sinters for which mineralogical descriptions were provided.

Krupp and Seward (1987) report alunite precipitating from hotsprings immediately northeast of Lake Rotokawa, New Zealand. This lake occupies the vent formed by a hydrothermal explosion approximately 6 000 years ago; its pH varies from 2.1 to 2.3, and its temperature is 16.4 degrees Celsius. The hotsprings from which the alunite is precipitating, together with kaolinite, native sulfur and silica minerals, have pH's from 4 to 5 and temperatures between 70 and 90 degrees Celsius.

5.1.2. Alunite as a near-surface replacement mineral

Cunningham *et al.* (1984) describe alunitization of Tertiary volcanic rocks in the Marysvale volcanic field, Utah. They present new data, and summarize the K-Ar geochronologic investigations of Steven *et al.* (1979), concluding that the age of the alteration is approximately 23 Ma.

Alunitization occurs to maximum depths of 120 m, where it abruptly gives way to propylitically altered, pyrite-bearing felsic volcanic rocks. Alunite is associated with quartz, kaolinite and minor hematite. Jarosite ($KFe_3(SO_4)_2(OH)_6$) occurs near the top of the alunite zone, above which is an assemblage dominated by hematite. Capping these assemblages is a silica zone which has a flooded texture, as opposed to the porous texture of an intensely leached rock. It includes massive quartz with minor hematite which has a conchoidal fracture and layered rock that resembles siliceous sinter. This silica cap is locally brecciated and cemented by microcrystalline quartz and locally abundant hematite.

Cunningham *et al.* interpret the abrupt transition from the assemblages of quartz, kaolinite, alunite and hematite to the underlying pyrite-bearing propylitically altered volcanic rocks to mark the paleo-groundwater table. The alteration agent was sulfuric acid derived from condensed, oxidized H_2S-rich fluids degassed from the water table.

Sillitoe *et al.* (1984) describe a feldspar destructive alteration assemblage composed of cristobalite, kaolinite and alunite with minor iron sulfides at Wau, Papua New Guinea. It is developed in an intramaar sequence approximately 2.5 million years old and occupies an area at the surface of 1.5 km by 0.9 km. The alteration occupies only topographically high areas, although the base of the alteration is essentially flat-lying, suggesting much of the altered rock was removed by erosion. The base of the alteration is marked by a zone of opal and very fine-grained iron sulfides and is overlain by up to 70 m of the alunite-bearing rock.

Sillitoe *et al.* interpret the base of the alteration to mark a boiling water table. The overlying alteration is intense acid leaching, the agent of which was produced by the interaction of groundwater and H_2S evolved from the underlying boiling water table.

Hedenquist and Henley (1985) describe the common occurrence of alunite replacing felsic volcanics at the Waiotapu geothermal field, New Zealand. It occurs with kaolinite, cristobalite, pyrite and native sulfur in zones that extend from the surface to depths of approximately 50 m. They attribute this alteration assemblage to the action of sulfuric acid produced by the condensation and oxidation of H_2S gas derived from deep hydrothermal waters.

5.1.2.1. Modern examples

The alteration of rocks to alunite-bearing assemblages is an ongoing process in restricted locales, including the Steamboat Springs geothermal area, Nevada (Schoen *et al.*, 1974) Yellowstone National Park (Raymahashay, 1968) and the Wairakei geothermal area, New Zealand (Steiner, 1953). These occurrences provide direct information about the nature of the fluids involved in the alteration.

The precipitation of alunite in acid hotsprings in the Paint Pot Hill area, Yellowstone National Park, (Raymahashay, 1968) was described in Section 5.1.1. Alteration of the felsic volcanic rocks around the acid springs has produced an assemblage of kaolinite, alunite and silica minerals with minor native sulphur. The waters at these acid springs have pH's less than 3 and sulphate ion concentrations between 150 and 200 ppm. They commonly have considerable volumes of rising gas bubbles, in which H_2S was identified. Raymahashay concludes that near-surface oxidation of H_2S gas gives rise to the acid-sulfate waters which are demonstrably the agent responsible for this alteration. The origin of the H_2S-rich fluid relates to boiling of an ascending hydrothermal fluid at depth and the partitioning of H_2S into the vapour phase, followed by near-surface condensation of this vapour (Raymahashay, 1968).

Alunite is associated with intense alteration at the silica pit in the southwest corner of the Steamboat Springs geothermal area (Schoen *et al.*, 1974). Outcropping basaltic andesites have been progressively leached, culminating in a porous residue of quartz, opal, cristobalite, and anatase, a TiO_2 polymorph. Drilling has revealed that this alteration persists to the water table, 33 m below the surface. Below the water table, alunite becomes abundant forming a 6 m thick blanket-like deposit with quartz and kaolinite. This passes downward into assemblages of montmorillonite, illite, quartz, orthoclase and plagioclase with diminishing kaolinite. Pyrite, generally concentrated in small fractures, accounts for about 3% of the rock from 20 m to 51 m below surface, beyond which it is present in diminishing quantity. Schoen *et al.* (1974) discuss a less intense style of alteration at the clay quarry, in the northwest corner of the Steamboat Springs geothermal area. Alteration of andesite in a circular area 60 m in diameter has produced an assemblage of silica minerals, kaolinite and alunite. These rocks, and the outlying andesites are buffered by an annular zone of red, iron-stained rock consisting of silica minerals, kaolinite, alunite and hematite with minor montmorillonite.

Although they describe the alteration as having ceased (Schoen *et al.*, 1974),it must have been recently active. Temperatures of 82 degrees Celsius have been recorded in fissures from which vapour was escaping at the silica pit, and the ground at the clay quarry was described as "warm to the touch" (Schoen *et al.*, 1974).

They attribute the alteration to attack by strong sulfuric acid solutions of supergene origin, as the intensity of alteration diminishes with depth. The sulfuric acid is produced by near-surface oxidation of H_2S-bearing fluids. Alunite and the various clay minerals are stable only below the permanent water table, where the descending acid is sufficiently diluted.

Steiner (1953) describes near-surface alunitization at Wairakei, New Zealand. Alunite with opal, kaolinite and leucoxene, an amorphous type of TiO_2,

is developed on the surface. H_2S gas is escaping from the ground and native sulphur is being deposited. He attributes the alteration to downward percolating sulphuric acid solutions derived from oxidation of the sulfur and entrainment in meteoric fluid. The acid leaching is strictly a surficial feature, as alunite persists to a depth of only 15 m and siderite, a phase unstable in sulfuric acid solutions, is present only 27 m below the surface.

Krupp and Seward (1987) report alunite as an alteration product of felsic volcanics, together with kaolinite, montmorillonite, native sulfur and silica minerals near Lake Rotokawa, New Zealand. It occurs on the surface and extends to shallow depths, and its origin is attributed to "steam alteration" of the type described above. The area of steam altered ground is approximately 1 km by 1.5 km, and it is pockmarked by hydrothermal explosion vents up to 600 m in diameter and smaller collapsed pits up to 10 m deep, which formed from extensive host rock dissolution. Acid hotsprings and seeps of acidic gases occur throughout the steam altered zone.

5.1.3. Origin of near-surface alunitizing fluid

The hotsprings in which alunite is forming are characterized by low pH's and high SO_4^- ion concentrations. Alunitization of the country rock near such hotsprings is apparently caused by similar acid-sulfate waters (Raymahashay, 1968). The diminishing intensity of acid alteration with depth (Schoen *et al.*, 1974; Steiner, 1953; Sillitoe *et al.*,1984; Hedenquist and Henley, 1985),the absence of SO_2 and SO_3 gases in the hotsprings environment (Schoen, 1969) and the presence instead of H_2S gas (Steiner, 1953; Raymahashay, 1968) argue for a surficial or very near surface formation of the sulfuric acid. Sulfur is derived ultimately from deep hydrothermal solutions which partition H_2S preferentially into an associated vapour phase that rises to the surface and condenses and/or mixes with shallow groundwater (Steiner, 1953; Raymahashay, 1968; Schoen *et al.*, 1974;Henley and Ellis, 1983; Cunningham *et al* , 1984; Sillitoe *et al.*,1984; Hedenquist and Henley, 1985; Krupp and Seward, 1987).

The oxidation of H_2S to H_2SO_4 requires explanation. Although H_2S readily oxidizes to elemental sulfur, the sulfur is resistant to further oxidation at temperatures compatible with a hotsprings environment (Ehrlich and Schoen, 1967). Native sulfur commonly occurs in small amounts on the surface near acid hotsprings (Raymahashay, 1968) and in acid altered rocks (Steiner, 1953; Hedenquist and Henley, 1985). Sulfur ignites in air at 260 degrees Celsius to form SO_2, which slowly oxidizes to SO_3. These gases are common in high temperature volcanic fumaroles (Henley and McNabb, 1978; Schoen, 1969).

Ehrlich and Schoen (1967) showed that sulfur-oxidizing bacteria were present in the soil 1 m from a steaming fissure at Steamboat Springs. The soil had a temperature of 36 degrees Celsius and a pH of 2.2, compared to 62 degrees Celsius and a pH of 3.4 for soil immediately adjacent to the fissure. They inoculated sulfur-bearing media with both fresh and sterilized soil. From 10 g of sulfur in the medium, over 0.24 g of SO_4^- ion was produced in 21 days at room temperature in the medium incubated with fresh soil. No SO_4^- ion production occurred in the medium inoculated with sterilized soil, proving that living organisms in the soil, not catalytic properties of the minerals in the soil, were responsible for oxidation of the sulfur. They also observed very small colorless motile rods in the cultures, which they implied could be the sulfur-oxidizing bacteria.

Krupp and Seward (1987) describe a bedded sulfur deposit which stratigraphically underlies Lake Rotokawa. The sulfur commonly displays varved bedding, indicative of seasonal variations in deposition, and direct textural evidence of bacterial deposition. Hotsprings near the lake show a pronounced seasonal variation in the concentration of SO_4^-, with greater concentrations present during the summer. Krupp and Seward interpret the bedded sulfur to have arisen in a hotspring characterized by the same type of seasonal variation apparent now, and that the underlying cause is seasonal variation in the number of sulfur-reducing bacteria in the hotsprings.

Schoen (1969) showed that the rate of sulfuric acid formation in Yellowstone Park was proportional to the surface area of acid-altered ground. This observation is consistent with a biological origin for the acid, involving aerobic bacteria living near the surface.

The elements required for bacteriogenic sulfate production, H_2S gas, native sulfur and sulfur-oxidizing bacteria have all been observed in modern hotsprings settings. It is thereby a viable process to account for the alunitizing fluid in the near-surface environment.

5.1.4. Alunite as a vein-filling

In their study of the Marysvale volcanic field Cunningham *et al.* (1984) describe veins of nearly pure, coarsely crystalline alunite up to 20 m across. They conclude that the sulfur in the alunite veins has a magmatic origin, and that the veins are related to a shallow, unexposed stock. The lack of coexisting minerals makes this type of occurrence unsuitable for study in terms of reactions with other minerals. For this reason, and because of the gross dissimilarity between alunite veins and the alunite with which this study is concerned, they are considered no further.

5.1.5. Alunite as a replacement mineral at depth

Reports on the occurrence of alunite at Summitville, Colorado have been compiled by Hayba *et al.* (1985), on whose compilation the following description is drawn. Alunite occurs with quartz in an upright, upward-flaring annular cone which extends from the present surface to a depth of approximately 240 m. This cone reaches a maximum thickness of 15 m near the surface. It encloses an upward-flaring cone of vuggy silica which has a maximum diameter of 15 m near the surface. These cones are enclosed by successively larger diameter annular cylinders of quartz-kaolinite, and illite-montmorillonite.

All these alteration assemblages formed over the vent of the host Miocene

South Mountain quartz latite porphyry. They reflect varying degrees of acid-sulphate leaching, which culminated in the core zone of vuggy silica which is the resistate after the removal of all other elements.

K-Ar dating of the host porphyry and the alunite mineralization (Mehnert, 1973) yielded ages of 22.8 and 22.9 +/- 0.6 m.y. and 22.3 and 22.4 +/- 0.5 m.y. respectively. This confirms a temporal and spatial relation between the alunite mineralization and the volcanic activity of the underlying volcanic vent.

Alunite occurs with quartz, kaolinite and pyrite at Goldfield, Nevada. This assemblage developed from Tertiary volcanic, and older plutonic and metasedimentary rocks along faults. It is exposed on the present surface and extends to depths over 300 m (Jensen *et al.*, 1971). From a study of sulfur isotopes in alunite and pyrite, Jensen *et al.* conclude that the sulfur for these minerals was derived from magmatic H_2S and that mineralization temperatures ranged from 150 to 325 degrees Celsius.

Fisher and Leedy (1973) describe occurrences of alunite in Tertiary volcanic rocks northwest of the Silverton caldera, Red Mountain District, Colorado. It occurs in intensely altered breccia pipes; the alteration of which occurred at depths up to 1500 m. They point out that this is far below the level for solfataric alteration. Alunite occurs in these 2 rock types: 1) intensely "silicified" rock and 2) argillically altered rock. The silicified rock ranges from vuggy cavernous breccias to massive very fine-grained silica. Alunite occurs with barite, leucoxene, rutile and diaspore. The silicified rocks are enveloped by argillically altered rocks, which consist of kaolinite, dickite, quartz and alunite with minor pyrophyllite, rutile, diaspore and barite.

Trace amounts of alunite formed at depths over 450 m on the northeastern and eastern sides of the Lake City caldera, Colorado (Slack, 1980). It is associated with barite, quartz, pyrite and basemetal sulphides, with which it forms veins up to 1.5 m wide and 2 000 m long. Fluid inclusion studies by Slack (1980)

conclude that the veins formed from boiling fluids with a temperature range from 206 to 280 degrees Celsius and salinities from 1.3 to 12.4% equivalent NaCl. Geological, geochronological and geochemical evidence presented by Slack show that the nearby Red Mountain quartz latite porphyry was an important source of fluid and metals for the mineralizing solution.

5.1.6. Origin of alunitizing fluid at depth

The occurrences of alunite discussed in the preceding section differ from the hotsprings related mineralization in terms of depth and temperature of formation. They represent the action of different processes, *i.e.* processes which were non-surficial and non-biological in nature.

Hayba *et al.* (1985) and Heald *et al.* (1987) reviewed the occurrences of alunite discussed in this section and concluded that highly acid, sulphate-rich fluids were responsible for the alteration. They attribute the formation of the fluids to these processes: 1) equilibration of sulfur-bearing magmatic gases with relatively oxidized magmas, conditions which would lead to production of SO_2 gas at magmatic temperatures, 2) mixing of the SO_2-rich gases with upwelling meteoric hydrothermal fluid and 3) disproportionation of SO_2 gas into H_2SO_4 and H_2S in the presence of the meteoric water according to processes described by Holland (1967). When formed, the ascending acid solution caused extensive cation leaching of the rocks, producing the common vuggy silica zones flanked by advanced argillically altered rock, described in the section above . Other observations explained by this model are 1) the higher observed mineralization temperatures than in adularia-sericite type gold deposits and 2) the association of the alunite mineralization spatially and temporally with intrusive rocks.

5.2. Phase relationships of alunite, kaolinite and pyrophyllite

The formation of the non-silicate mineral alunite in the presence of quartz requires very large H^+ and SO_4^- activities (Knight, 1977). Knight (1977) showed that at 25 degrees Celsius, a pH of less than 4 and a sulfate ion concentration greater than 100 ppm are required for its formation. This is in accord with the observations in Section 5.1, in which the alunitizing solutions were highly acidic and sulfate-rich.

The stability of alunite is governed in part by reactions with microcline, muscovite, pyrophyllite and kaolinite. These reactions have been studied by Hemley *et al.* (1969) and Knight (1977). The formation of alunite from any of these minerals involves the consumption of H^+ and SO_4^- ions and the release of SiO_2. Assemblages of alunite and either microcline or muscovite were not observed in this study, nor in the alunite deposits discussed in the above sections, nor in other literature (Hemley *et al.*, 1969). This is consistent with the findings of Hemley *et al.* that potassium concentrations in acid hotsprings are considerably smaller than those required to stabilize either potassium silicate phase in the presence of alunite (Figure 5-1).

The minimum concentrations of H^+ and SO_4^- ions required for the formation of alunite have been discussed above. A reaction by which alunite dissolves in sufficiently acid solutions is relevant to the rocks at the silica pit described by Schoen *et al.* (1974), and at Sulfur Bank, California (Hemley *et al.*, 1969). With the dissolution of alunite, only quartz and anatase (or leucoxene) remain, forming siliceous residues such as those at the silica pit in the Steamboat Springs geothermal area.

Kaolinite is associated with alunite in all the occurrences of replacement alunite discussed in the preceding section, and most of the occurrences of alunite as a hotspring precipitate. Whether kaolinite or pyrophyllite is the stable aluminosilicate phase depends on the temperature and the silica activity at the

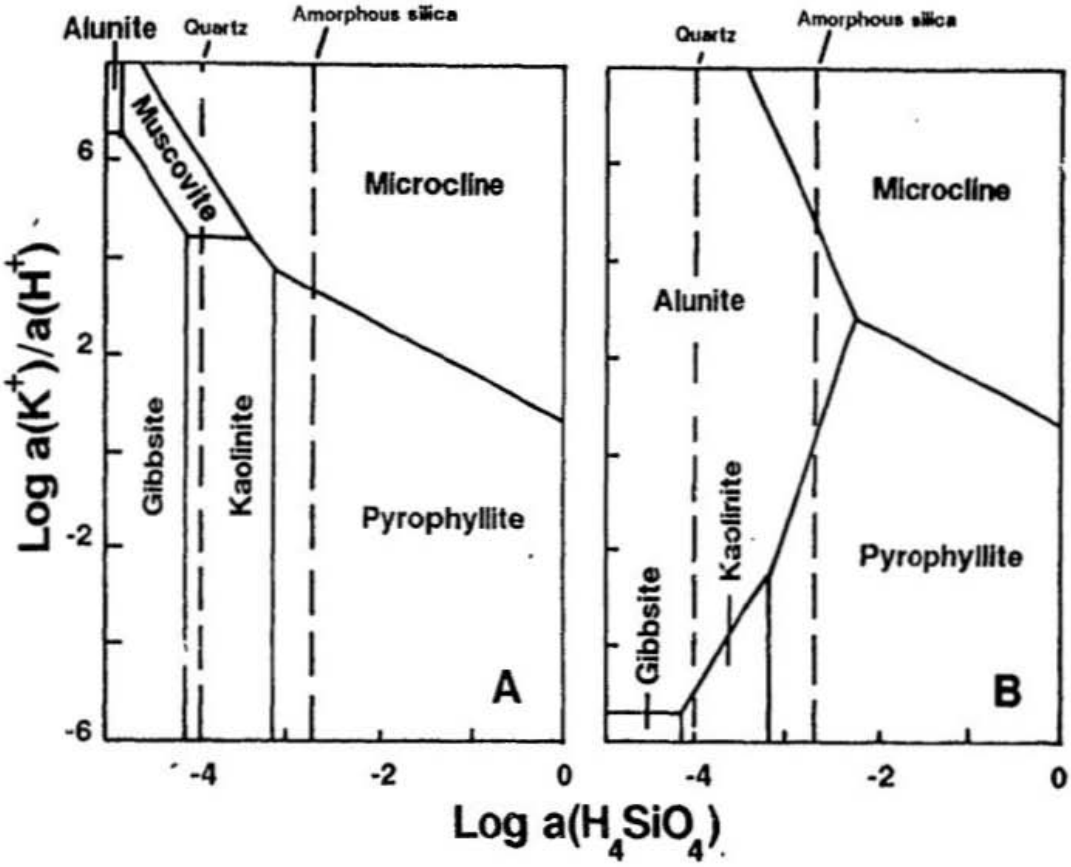

Figure 5-1: Log $a(K^+/a(H^+)$ *versus* log $a(H_4SiO_4)$.) Increased SO_4^{-2} and H^+ activities in "B" expand the alunite stability field at the expense of all other phases. Note log $a^2(H^+)$ x $a(SO_4^{-2})$ is -16 in "A" and -10 in "B". [From Knight, 1977.]

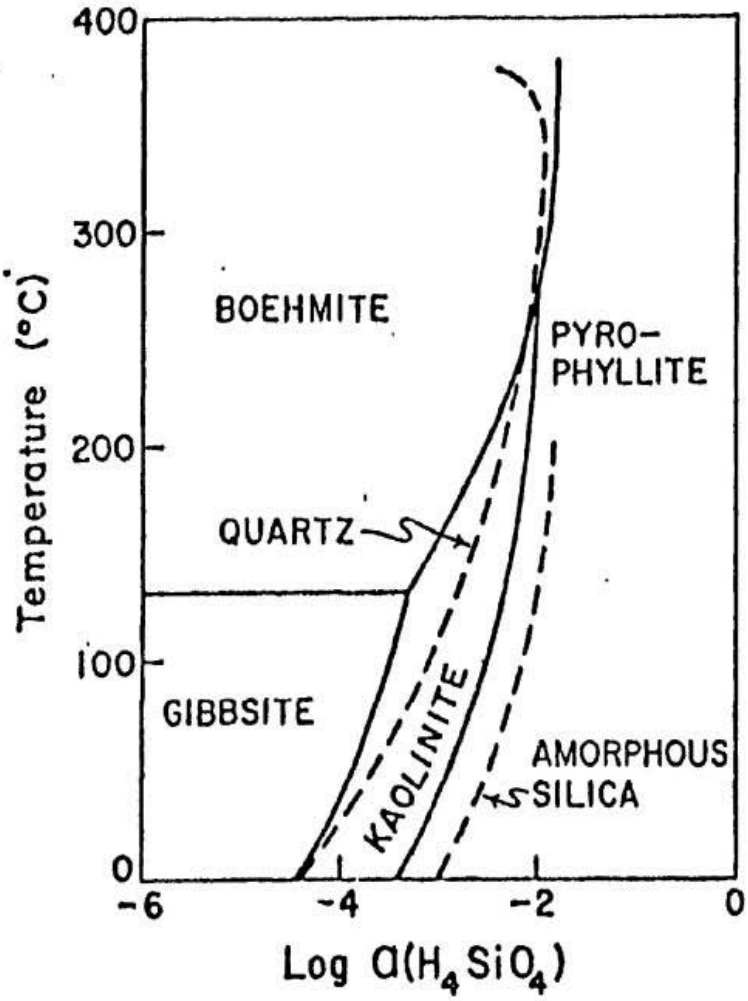

Figure 5-2: Temperature *versus* $a(H_4SiO_4)$ In unmetamorphosed rocks, pyrophyllite indicates either temperatures above 270 degrees Celsius or temperatures below 200 degrees Celsius and supersaturation with silica. Kaolinite is the stable phase in equilibrium with quartz below 270 degrees Celsius. Note solid lines are phase boundaries, dashed lines are saturation curves. [From Knight, 1977.]

time of alteration (Figure 5-2).

Knight (1977) showed that kaolinite is stable to a maximum temperature of 270 degrees Celsius at a pressure corresponding to the water vapour pressure at this temperature. Pyrophyllite is stable at temperatures above 270 degrees Celsius and at low temperatures in fluids sufficiently supersaturated with respect to quartz (Figure 5-2). He points out that supersaturation is possible only below 200 degrees Celsius; otherwise equilibrium with respect to quartz is maintained in hydrothermal fluids. Thus in unmetamorphosed rocks the presence of pyrophyllite indicates temperatures above 270 degrees Celsius if diaspore is present, or temperatures less than 200 degrees Celsius and supersaturation with respect to quartz if a metastable silica phase is present. If the rocks are unmetamorphosed, an assemblage of quartz and pyrophyllite indicates alteration pressures greater than hydrostatic, which are required to increase the solubility of silica and move its concentration into the pyrophyllite stability field (Knight, 1977).

The metamorphism to which the rocks in this study area have been subjected must be considered before the criteria established above for the conditions of formation can be applied. This is considered in the following chapter.

5.3. Behaviour of iron in association with alunite

Hematite and pyrite are important constituents at most of the showings with which this study is concerned. These minerals are common associates of alunite in the two types of near-surface alunite occurrences being considered here, *i.e.* as a replacement mineral or a chemical precipitate in hotsprings.

5.3.1. Iron phases associated with near-surface replacement alunite

Hematite associated with replacement alunite has been reported by Cunningham *et al.* (1984) and Schoen *et al.* (1974), as discussed in Section 5.3.1. At Marysvale, Utah, hematite occurs as minor dust in the alunite zone. It also forms cone-shaped concentrations, some of which were mined for their iron, between each alunite zone and its overlying silica cap (Cunningham *et al.*, 1984). They attribute this spatial relation to the release of iron from alunitizing rocks, followed by upward migration and rapid precipitation upon oxidation to the ferric state.

At the clay quarry at Steamboat Springs, hematite with alunite and kaolinite forms an annular ring on the surface around more intensely altered assemblages of alunite, kaolinite and opal (Schoen *et al.*, 1974). This reflects release and radial migration away from the most intensely altered rocks. Precipitation is caused by a rise in pH associated with the fluids' reaction with fresh rock.

As discussed above, alteration at Steamboat Springs is attributed to supergene descending waters. Schoen *et al.* suggest that an iron-bearing fluid descending through the acid altered rock could react with rising H_2S gas and precipitate pyrite. The few percent pyrite present mostly in fractures at depths greater than 20 m is ascribed to this process (Schoen *et al.*, 1974).

Pyrite associated with replacement cristobalite, kaolinite and alunite was also reported by Sillitoe *et al.* (1984) at Wau, Papua New Guinea and by Hedenquist and Henley (1985) in the Waiotapu geothermal field, New Zealand.

5.3.2. Iron phases in hotsprings deposits

Cunningham *et al.* (1984) describe flooded silica caps above the replacement alunite deposits. The caps include massive quartz and a banded variety interpreted to be siliceous sinter. They report disseminated fine-grained hematite crystals in the massive quartz but do not supply a detailed description of the sinter.

Weissberg (1969) describes an acid-sulfate hotspring at Waimangu, New Zealand. It has a pH of 3.8 and a sulfate ion concentration of 320 ppm. The lake in which the sinter is being deposited was formed in 1917 and the thin sinter developed thus far is amorphous to X-rays. Nevertheless, the chemical conditions are favourable for the precipitation of alunite. This sinter contains approximately 10% Fe_2O_3.

Pyrite has also been reported in hotsprings deposits. Weissberg (1969) detected pyrite by X-ray diffraction analysis of sinter collected from the Champagne Pool, Waiotapu, New Zealand. In 1966, this pool had a maximum temperature of 75 degrees Celsius and a pH of 5.7.

Raymahashay (1968) reported "pyritic mud" in a hotspring with a temperature of 86 degrees Celsius and a pH of 6.75 at Yellowstone National Park. Pyrite was also reported by Zotov (1971) in Lake Goryacheye, Kurile Islands; a lake in which alunite also precipitates. It has a temperature of 10 degrees Celsius and a pH of 2.8.

Zotov also describes pyrite and marcasite associated with alunite, opal, cristobalite and quartz in hotsprings and mud pots in a fumarole field east of the Ebeko volcano, Paramushir Island. These springs have temperatures up to 98 degrees Celsius and pH's as low as 0.5.

5.3.3. Iron phases associated with alunite mineralization at depth

Whereas both pyrite and specularite commonly occur as replacement minerals or chemical precipitates in the near-surface and surficial occurrences of alunite, only pyrite is commonly associated with alunite occurrences at depth.

At the Red Mountain District, Fisher and Leedy (1973) describe pyrite occurring with other basemetal sulfides and Cu-Ag sulfosalts in lenses and "chimneys"of "massive sulphide". It also occurs in the silicified core zones of the breccia pipes and in the surrounding argillically and illitically altered country rock.

A similar association is described by Slack (1980) for precious metal ore veins in the Lake City District, Colorado. The predominant minerals in the veins are pyrite and basemetal sulfides, with significant worth contributed by Ag and Ag-Au tellurides. Pyrite is also common in the sericitized country rock which surrounds the veins. In contrast, hematite and magnetite are present in only trace amounts in the veins and are demonstrably primary where they occur in the altered country rock, although they are commonly replaced by sulfide minerals.

Reviewing the mineralogy of the Summitville mining district, Hayba *et al.* (1985) characterize the main-stage mineralization as dominated by pyrite, basemetal sulphides and base and precious metal sulfosalts. In contrast, however, is a very late stage, high level assemblage of barite, jarosite and goethite in which sulfides are "extremely rare" (Hayba *et al.*, 1985).

The mineralization at Goldfield, Nevada was reviewed by Jensen *et al.* (1971), in their study of sulfur isotopes in alunite. Iron occurs as pyrite in the "silicified zones" with quartz, alunite and kaolinite. Hematite occurs where these zones are very close to surface, where it is an oxidation product of pyrite.

Sillitoe (1983) describes several cases of "massive sulfide" deposits associated with alunite (+/- pyrophyllite, kaolinite, dickite, diaspore) mineralization in

volcanic rocks overlying porphyry type hydrothermal systems. He regards the advanced argillic alteration assemblages there as having formed under conditions which foster a high-sulfur sulfide assemblage, which would include pyrite.

5.4. The association of titanium minerals and alunite

The rocks with which this study is concerned commonly contain a small amount of rutile. Anatase, a polymorph of rutile and leucoxene, an amorphous type of TiO_2 have been reported associated with replacement alunite and alunite formed as a chemical precipitate in hotsprings.

5.4.1. Titanium minerals and near-surface replacement alunite deposits

Steiner (1953) reports the occurrence of a small amount of leucoxene, derived from the alteration of titaniferous magnetite, associated with surficial replacement alunite at Wairakei, New Zealand. Schoen *et al.* (1974) report anatase in the intensely leached siliceous residues which overlie the alunite zone at the silica pit, Steamboat Springs.

5.4.2. Titanium minerals in acid hotsprings

Zotov (1971) reports leucoxene associated with very fine corroded alunite crystals and opal at the Proval'nyy Kolodets hotspring, Kurile Islands. This spring has a temperature of 83 degrees Celsius and a pH of 1.8.

5.4.3. Titanium minerals and alunite mineralization at depth

Of the four cases of deep-seated alunite mineralization referred to in this chapter (Summitville, Goldfield, Red Mountain, Lake City) detailed petrographic results are provided only by Fisher and Leedy (1973) for the Red Mountain district. They describe the occurrence of "sparse" leucoxene and rutile in the intensely "silicified" rocks in the centers of breccia pipes, and in the surrounding advanced argillic, alunite-bearing alteration zone.

5.4.4. Titanium as a petrogenetic indicator

Schoen *et al.* (1974) provide geochemical data for a series of rocks ranging from fresh basaltic andesite to the siliceous residue which is its ultimate alteration state (Section 3.3.2). With increasing alteration, silica and titanium show apparent increases to 92.42% and 4.13% respectively. All other major element oxides are virtually eliminated.

They suggest that the immobility of titanium makes it a useful criterion for distinguishing whether a highly siliceous rock is the residue from intense leaching or an open space filling. If the titanium concentration is higher than that in the fresh rock, it contains little open space filling; *i.e.*, it is a siliceous residue. If the titanium concentration is very low or less than the fresh rock, it includes some open space filling. Silica sinters and vein fillings are entirely open space fillings.

Schoen *et al.* (1974) apply this criterion to rocks of known origin at Steamboat Springs. All the demonstrably leached, porous rocks contain more TiO_2 than the basaltic andesites from which they were derived. In their discussion of its application to vein fillings they cite only two samples, which had 0.28% and 0.19% TiO_2. This clearly illustrates the low concentrations of TiO_2 that were mobilized by these fluids. However, the range of TiO_2 concentrations in vein fillings would have been significantly expanded had they included their vein sample 128-4, which contains 0.75% TiO_2. Thus, where textural evidence is lacking, the presence of even 0.75% TiO_2 in a rock of unknown origin does not preclude an origin for the rock as a chemical precipitate. Furthermore, Zotov's (1971) report of leucoxene in a freshly deposited sinter indicates that the TiO_2 concentration of a rock is not a valid criterion upon which to base its origin.

5.5. Conclusions

Alunite occurs in three genetically distinct settings: 1) as a chemical precipitate in acid hotsprings 2) as a replacement mineral in the near surface environment, having formed from fluids which originated at the surface and percolated down into the rock (primary supergene) and 3) as a deep-seated replacement mineral formed from higher temperature, non-surficial processes involving magmatic components (primary hypogene).

Chapter 6

DISCUSSION AND INTERPRETATION OF SHOWINGS

6.1. Relevance of modern alunitization to this study

There are mineralogical and textural differences between the rocks with which this study is concerned and those in modern environments of alunite formation. These differences and any mitigating circumstances are discussed in this section, to assess the relevance of these modern occurrences of alunite to this study. The remainder of the chapter discusses the genesis and interrelationships of the various showings, beginning with those whose origin is most apparent.

Kaolinite is the only aluminosilicate phase associated with alunite in the hot springs and replacement deposits discussed in the previous chapter. The only aluminosilicate associated with alunite in this study is pyrophyllite. Amorphous silica is common in modern environments of alunite formation, whereas quartz is the only silica mineral in the area of this study. Rutile is common in the rocks of this study but anatase and leucoxene are associated with modern environments of alunite formation, where they commonly occur as pseudomorphs after ilmenite. Modern occurrences of the silica-titania residues which represent intensely leached rocks are commonly highly porous. Although mineralogically similar rocks have been described in this study area, they are massive and compact.

These apparent discrepancies can be reconciled when the structural and metamorphic history of the rock is considered. As discussed in Chapter 2, these rocks have been metamorphosed to lower greenschist facies. If kaolinite were present in the rock before metamorphism, it would have been converted to

pyrophyllite (Frey, 1970). Similarly, metamorphic effects can account for recrystallization of amorphous silica and titania (leucoxene) to quartz and rutile respectively, and a polymorphic transition of anatase to rutile. Porous rocks would have been compacted and recrystallized into massive equivalents during the deformation.

Another major textural difference between modern alunite occurrences and those of this study is the mineralogical banding that is prominent at several of these showings. It is defined by black specularite-rich bands and adjacent pink, iron-free bands in the alunite-bearing specularite-banded rocks. The banding is best developed at Hickey's Pond, where it is accompanied by features which indicate that it is coincident with the most highly deformed rocks. These features include: 1) isoclinal folds with attenuated limbs in specularite-rich bands, 2) marked grain-size reduction in quartz and alunite and 3) the presence of rutile exclusively as isolated equant crystals averaging 0.01 mm across, and bands of these crystals. The rutile in these bands was probably derived from pre-existing rutile euhedra by tectonic milling. These euhedra achieve lengths of 0.5 mm in rocks with pristine volcanic texture from the Hickey's Pond showing and have been observed in various stages of fracturing, flattening and association with "tails" of the small equant crystals (Section 4.2.2.1). These features record the various stages of tectonic breakdown of the rutile, which probably was a pseudomorph after ilmenite.

The coincidence of the best development of banding with the most intense deformation, as deduced from independent indicators, suggests that the banding is at least in part a tectonic feature. The development of compositional layering during deformation is poorly understood (Hobbs, Means and Williams; 1976. pp. 250-252) but at Hickey's Pond, platy specularite could be analogous physically to sheet silicates, which tend (by poorly understood means) to segregate into layers during deformation. Thus, the fact that the rocks are banded does not favour a protolith that might have had a primary mineralogical banding, *e.g.* a hot spring precipitate, over a massive, homogeneous altered rock. Furthermore, with the

exception of the interbanding between pyritiferous and specularite-bearing rocks described in Section 4.2.2.3, no similar banding was developed in the rocks which contain pyrite. This is consistent with a tectonic origin for the banding, which would not affect equant crystals of pyrite.

Thus despite the apparent differences, the alunite-bearing rocks in this study can be successfully modelled as the deformed and metamorphosed equivalents of modern assemblages of alunite, kaolinite, quartz, amorphous silica minerals, specularite, pyrite and anatase or leucoxene. This mineral suite characterizes both acid hot springs deposits and surficial and near-surface alteration associated with very low pH acid-sulfate waters. Therefore the mineralogy alone cannot distinguish between these two possibilities. However, this is not an important distinction because the two types of mineralization are intimately associated temporally and spatially. A similar mineral suite which lacks iron oxide characterizes alunite mineralization "at depth", as discussed in Sections 5.1.5 and 5.3.3. The lack of iron oxide serves to distinguish this mineral suite from the rocks in the study area.

6.2. Chimney Falls

As discussed in Chapter 3, the pyrophyllite schists at Chimney Falls are a high alumina assemblage derived by intense alteration of volcanic rocks. The alteration is not genetically related to the Hickey's Brook Fault, which separates the intensely leached rocks of the showing from relatively fresh porphyritic rock. The presence of magnetite as an alteration product of amphibole in the porphyritic rock attests to significantly different chemical conditions during its alteration, compared to the conditions under which the rocks of the showing were altered.

6.2.1. Origin of the specularite-rich breccia

The geochemistry of the quartz-pyrophyllite schists is discussed in Chapter 3. Relevant aspects of the geochemistry of the breccia are discussed in this section to supplement a discussion of its mineralogy.

The breccia forms a competent, lensoid zone resembling a boudin in the soft, schistose rocks. Mineralogically, it varies from the schistose rock in that it contains several percent specularite and alunite and only very minor pyrophyllite. The schistose rocks are all pyrophyllite-rich and specularite and alunite, when present, are only minor constituents.

The pyrophyllite schists were shown to have greatly diminished concentrations of Na_2O, K_2O, and Fe_2O_3 relative to the felsic volcanic rocks from which they were derived. Table 6-1 shows the major element chemistry of the schists and one sample of breccia, as well as their normative mineralogy as determined by the program described in the appendix. The breccia contains over 20 times the Fe_2O_3, and significantly more Na_2O and K_2O as the schists. This translates into 10% each of normative specularite and alunite in the breccia, compared to generally less than 1% each for these minerals in the schists. The schists vary from 11% to 59% normative pyrophyllite, compared to less than 3% in the breccia. These features are in excellent agreement with the mineralogical observations.

The processes responsible for the formation of the breccia are clearly different from those implicated in the development of the pyrophyllite-rich rocks. Whereas the schists are products of intense leaching of alkalis and iron from volcanic rocks, the breccia is a site of concentration of these elements. It is interpreted to be a hydrothermal conduit through which alkali and iron-bearing acid-sulphate waters passed. Pyrophyllite was replaced by alunite (and quartz) following a reaction across a boundary such as that in Figure 5-1 (page 141). Specularite was precipitated in the matrix and it also replaced pyrite. The space in which these reactions occurred was probably not sharply defined, and stringers

Table 6-1: Major element and normative mineralogy data for Chimney Falls. Note the high specularite and alunite concentrations, and low pyrophyllite concentrations in the specularite - rich breccia. [Data are presented split according to rock type. Major element oxides are reported in weight percent and normative mineralogy in volume percent. "0" = below detection. "QTZ" = quartz, "ALUN" = alunite, "PPH" = pyrophyllite, "RUT" = rutile and "SPEC" = specularite.]

	Major Element Geochemistry											Normative mineralogy				
#	SiO2	Al2O3	Fe2O3	MgO	CaO	Na2O	K2O	TiO2	MnO	P2O5	LOI	Total	QTZ	ALUN	PPH	RUT	SPEC
Pyrophyllite schists																	
154	91.50	3.70	1.24	.02	.04	.02	.13	.47	.01	.20	1.31	98.64	86.65	1.36	11.09	0.26	0.65
159	77.50	16.99	.61	.02	.00	.04	.03	.42	.01	.16	4.17	99.95	39.80	0.76	58.88	0.24	0.32
161	85.60	9.93	.94	.01	.00	.02	.01	.26	.01	.07	2.16	98.61	65.98	0.34	33.04	0.15	0.49
244	87.30	9.47	.08	.01	.00	.01	.01	.44	.01	.11	2.29	99.68	67.07	0.21	32.43	0.25	0.04
Specularite - rich breccia																	
156	69.15	4.09	19.46	.01	.07	.30	.64	1.06	.01	.19	3.17	98.35	75.58	9.99	2.77	0.65	11.01

of specularite and local alunite mineralization probably extended outward from the main conduit. This explains the zonation present at the showing, *viz* 1) specularite-rich breccia, 2) specularite-bearing pyrophyllite schist with minor alunite and residual pyrite, 3) pyritiferous quartz-sericite schist and 4) relatively unaltered rhyolite.

A large competence contrast would be expected between a pyrophyllite-rich rock and a rock with very little pyrophyllite. This probably explains the presence of the breccia as a boudin within the highly schistose pyrophyllite-rich rock. It also mitigates against a tectonic origin for the breccia as strain would be partitioned preferentially into the easily sheared pyrophyllite-rich rocks, a demonstrable feature at this showing (see Figure 4-39, page 120).

6.2.2. Summary

The Chimney Falls Showing is the locus of intense cation leaching and accompanying pyrophyllitization. This alteration predates the fault which separates it from relatively unaltered porphyritic rocks of the Swift Current Granite which contain plagioclase and magnetite. A boudin of competent, very specularite-rich, alunite-bearing breccia marks an ancient hydrothermal conduit which developed in the pyrophyllitized rock.

6.3. Tower Showing

The quartz-rutile rocks which occur along the eastern flank of the showing are mineralogically equivalent to the silica-titania residues discussed by Schoen *et al.* (1974). At Steamboat Springs, these residues are underlain by a zone that includes alunite and kaolinite, which is underlain by less altered volcanic rocks. Pyrite and specularite occur beneath and adjacent to the silica residues. A similar zonation exists at the Tower Showing, whereby the quartz-rutile rocks pass westward into assemblages of quartz, alunite, specularite, pyrophyllite and rutile and then into pyritiferous sericite schists. Given this similarity and the westward dip of the showing, these rocks can be modelled as an overturned, steeply-dipping alteration assemblage (Figure 6-1) that represents intense acid leaching on the paleosurface and precipitation of alunite lower in the system, in response to dilution of the acid solutions. The mottled, fragmental appearance of the quartz-rutile rocks represents fragmentation and compaction of the porous rock, which could have occurred any time between its formation and the final deformation. Implicit in this "alteration model" is a tectonic origin for the banding in the specularite-banded rocks, as discussed in Section 6.1, as opposed to the inheritance of the banding from a banded chemical precipitate.

Given the asymmetry of the showing discussed above, the feeder of the hydrothermal system should have been to the west of the showing, but could have been removed by erosion. The slightly altered rocks to the east of the showing are younger, post-alteration volcanics. They have modern analogues in all the

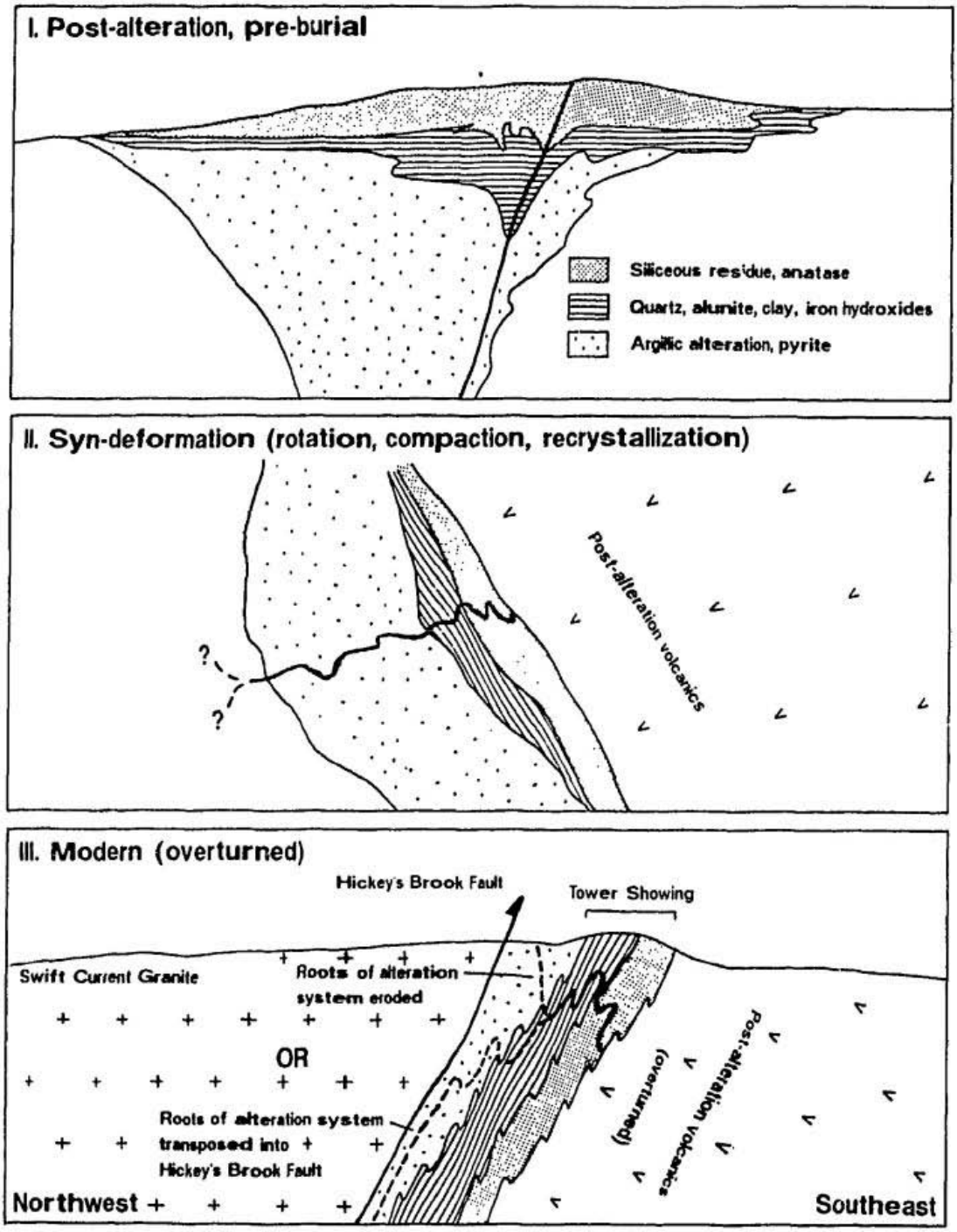

Figure 6-1: Schematic interpretation of Tower Showing. Comparison of Tower Showing (Frame III) with known zones of surficial acid leaching (Frame I, from Buchanan (1981)) indicates that the Tower Showing is overturned. The significance of the "roots" of the alteration system (Frame III) is discussed in Section 9.1.2.

volcanic rocks that have buried younger, surficially-leached rocks. The duration of the hydrothermal systems was probably small relative to that of the volcanism, occupying a short hiatus in volcanism. In this way, the type and asymmetry of the alteration dates the alteration as synvolcanic.

Silica-titania residues are also associated with the formation of alunite at depth (Section 5.1.5), where they are enveloped by alunite mineralization. Such occurrences differ from the Tower showing in that they display symmetry away from the silica residue, and they are characterized by iron as pyrite, not specularite.

Opposed to the alteration models presented above, the mineralization and all the gradations can be explained in terms of precipitation under varying chemical conditions in an acid hotspring. However, the presence of quartz phenocrysts, despite their rarity, is evidence that they are altered rocks, not chemical precipitates. Furthermore, the dimensions of the alteration zone, especially thickness, are similar to those of the acid-leached tracts discussed in Section 5.1.2. Such a large mass of chemical precipitate would be unusual for acid systems, the presence of H^+ in which tends to inhibit the polymerization of dissolved silica (Fournier, 1985).

6.4. Hickey's Pond

The bulk of the rocks at Hickey's Pond are similar to the iron-bearing rocks at the Tower showing, and by analogy may best be modelled as very near-surface acid leached volcanics. The lack of iron-free assemblages of silica and titania at Hickey's Pond could indicate: 1) they are not exposed or 2) they have been tectonically dislocated or 3) they were eroded and removed before burial or 4) alteration at this showing was not as intense and they never formed.

Lacking the zoned alteration prominent at the Tower showing, the younging direction of the Hickey's Pond showing cannot be determined. However, its spatial relations with the Swift Current Granite are similar to those of the Tower

Showing. Furthermore, the volcanic rocks to the east of the showing are relatively unaltered, and those encountered in drill core to the west are strongly altered (sericite or pyrophyllite) schists. These observations suggest that the younging direction is to the east, and the roots of the hydrothermal system may have been eroded or truncated by or transposed into the fault contact (Hickey's Brook Fault) with the Swift Current Granite to the west (see **Figure 6-1**, page 156).

Although the Hickey's Pond showing and the Tower showing seem to have had a broadly similar origin, i.e. synvolcanic, surficial to very near-surface acid leaching, there are several rock types at Hickey's Pond which require additional explanation. These are discussed in the following sections.

6.4.1. Origin of the specularite-pyrite interbanded rock

Observations relevant to the origin of these distinctively banded rocks, described in Section 4.2.2.3, are summarized here:

1. They are characterized primarily by sharply defined millimetre-scale bands of either pyritiferous or specularite-bearing rock, which also contain quartz, alunite, rutile and minor pyrophyllite.

2. They contain fragments of pumice, e.g. those in Figure 4-9 (page 82), which occur as isolated fragments or concentrated in bands interbanded with the pyritiferous and specularite-bearing bands (Figure 4-8, page 81). The various bands are locally isoclinally folded, and rarely attenuated.

3. Locally, lithic fragments containing specularite occur within pyritiferous bands.

4. Individual specularite bands less than 1 cm thick persist for up to 60 cm.

These rocks are significantly different from the more common non-fragmental, non-pyritiferous banded rocks in which the banding is defined by the presence or absence of specularite. The banding in the latter rock type reflects structural effects acting on an initially homogeneous altered rock. Such an

interpretation for the pyrite/specularite interbanded rocks is not compatible with the observations. A better interpretation is that they are chemical/clastic sediments formed in a hot spring, for these reasons:

1. The banding has locally been isoclinally folded; therefore it is pre-(final)-deformation.

2. The presence of recognizable pumice fragments can not be reconciled with a protolith in which all other volcanic features would have to have been obliterated.

3. The undeformed state of the pumice fragments, as indicated by circular pores, is not compatible with the deformation required to induce a mineralogical banding.

4. Ignoring the points made above, and assuming the specularite was derived from the pyrite by oxidation on a structural surface, the presence of specularite within fragments in the pyritiferous rock could not be explained. Furthermore, there are no replacement textures or partial reactions of specularite after pyrite.

Thus the mineralogical banding in these rocks is best considered to be primary, reflecting changing oxygen and sulfur fugacities in the fluid from which the material precipitated. The rock fragments represent clastic detritus shed into the hotspring which was not altered to the extent of the underlying volcanics.

6.4.2. Origin of the silicified, pyritiferous rock

Highly siliceous rocks have been described at the Tower showing, and their origin ascribed to intense acid leaching on the paleosurface. The very siliceous rocks at Hickey's Pond differ in that 1) they have a well-preserved porphyritic texture, 2) they are dissected by randomly oriented, thin sinuous quartz and quartz-pyrite veinlets and 3) they contain approximately 2% pyrite, occurring as grains up to 3 mm across.

The presence of pyrite indicates that the rocks have not been indiscriminantly leached since their formation. Nor is the preservation of the volcanic texture compatible with such leaching, since such a process yields porous,

easily broken rock. Sections 7.4 and 7.5 show that the highly siliceous rocks at Hickey's Pond and the Tower showing both contain over 96% SiO_2. However, the term silicification is used only with reference to the rock from Hickey's Pond, where the preserved volcanic texture proves that silica must have been added to the rock. It is in contrast to the processes responsible for the highly siliceous rock at the Tower showing, *viz* intense preferential leaching of all cations except those of Si and Ti, followed by compaction of the resulting porous residue.

The influx of silica recorded by the silicified rock may have affected some of the nearby pyritiferous rocks at Hickey's Pond. Although they are broadly similar to pyritiferous rocks at the Tower and Bullwinkle Showings (which lack true silicified rocks), their normative mineralogy distinguishes them from those at the other showings by having more silica and less pyrophyllite (Section 4-10). These differences might record distal effects of the intense silicification which developed locally at Hickey's Pond; effects which also have metallogenic implications.

6.4.3. Origin of the specularite-rich breccias

Observations relevant to the origin of the specularite-rich breccias are summarized below:

1. They contain only minor pyrophyllite, and tend to be very massive, lacking the schistosity common in the pyrophyllite-bearing rocks.

2. Locally they contain recognizable, undeformed volcanic fragments. In these rocks, rutile is present as euhedral grains up to 1 mm long.

3. Contacts with the banded country rock are sharp and commonly concordant.

4. Thin veinlets of specularite emanate from the breccia and extend into the country rock. The hosts to these veinlets include relatively undeformed rock with a recognizable porphyritic texture and banded country rock. In the latter rock type, they cross-cut a tectonic fabric.

5. The breccias are disposed in a linear, steeply westward dipping, NNE-striking zone approximately 125 m long and 5 m wide at the widest

point. This is parallel to the fault contact with the Swift Current Granite to the west.

6. The breccias contain significantly more quartz and specularite, and less alunite and pyrophyllite than the banded specularite-bearing rocks with which they are in contact.

Although hydrothermal brecciation at the time of alteration is a viable factor pertaining to the origin of these rocks, its involvement cannot be proved if all the features of the breccias can be attributed to tectonic activity. However, attempts to explain the brecciation as a wholly tectonic phenomenon are fraught with difficulties. Contacts between breccia and porphyritic or banded country rock, the presumed protolith, are sharp; there are no textural or mineralogical trends towards the breccia in the country rock.

The mineralogical differences between the breccia and country rock cannot be explained by structural events. A syntectonic hydrothermal system could be postulated to have mobilized quartz and specularite into the breccias, diluting the alunite and pyrophyllite and accounting for the normative mineralogy. However, such a model is not consistent with textural evidence. Although small, syn- or post-tectonic veinlets of specularite are found in some of the breccias, similar veinlets emanating from the breccia in the country rock prove that specularite was removed from the breccias during deformation. The only evidence for remobilized quartz is the presence of *in situ* dilational quartz and quartz-specularite veinlets.

The presence of boudins of breccia in the banded, pyrophyllite-bearing country rock shows that the breccia is pre-tectonic. Evidence of the relative competence of the breccias during deformation is that they locally contain volcanic fragments with no indications of deformation and commonly contain large masses of rutile which, in the banded rocks, were progressively milled with increasing deformation.

Thus the nature and timing of the brecciation cannot be reconciled with a

wholly tectonic origin. Hydrothermal brecciation in the hot springs environment has been documented recently owing to its commonly associated precious metal mineralization (Sillitoe *et al.*, 1984; Nelson and Giles, 1985; Hedenquist and Henley, 1985). These breccias are of two morphologies: 1) highly discordant vent breccias, which mark the subsurface channel through which the fluid flowed and 2) concordant fallout breccias, which mark the surficial accumulation of material ejected from the hydrothermal vent. Although these works show that hydrothermal brecciation can occur in the near-surface environment, there are mineralogical differences between them and the breccias at Hickey's Pond. Specularite is the diagnostic mineral in the Hickey's Pond breccias, but sulfides (Nelson and Giles, 1985; Hedenquist and Henley, 1985) and carbonates (Sillitoe *et al.*, 1984), with no oxide minerals, are present in the breccias described by the above authors.

Hydrothermal breccias described by Cunningham *et al.* (1984) have similarities with those at Hickey's Pond. They occur in the flooded silica cap, which includes minor siliceous sinter, commonly as vertical pipelike bodies composed of angular fragments of microcrystalline quartz in a hematite-bearing matrix. The breccias there, however, lack the alunite and rutile common in those from Hickey's Pond.

Whether the breccias described by Cunningham *et al* are analogues of those at Hickey's Pond also depends on whether those at Hickey's Pond are vent breccias or fallout breccias. The contacts of the breccia zone are broadly conformable with the banding in the specularite-bearing rock, suggesting it may be a fallout breccia. However, the tectonic origin of the banding renders this an equivocal line of evidence as the contacts of a vent breccia would be expected to rotate into parallelism with the tectonic banding. The occurrence of similar rocks on both sides of the breccia suggest that it is a vent breccia.

It is significant that only at Hickey's Pond was there a considerable influx of specularite into the [illegible]-leached zone, because the normative mineralogy

indicated the specularite-banded rocks which host the breccia there are enriched in specularite relative to similar rocks at the Tower and Bullwinkle Showings (Section 4-10).

6.4.4. Origin of the quartz-specularite veins

These veins are best developed in a small fault zone, with which they are roughly conformable. The presence of coarse crystalline quartz, specularite platelets up to 3 cm across and drusy cavities indicate that the veins are less deformed than the country rock, and represent syn- to post-tectonic remobilization of these minerals. This is supported by the mineralogically similar quartz-specularite veins in Figure 4-18 (page 89) which fill tension gashes which are highly discordant to the fabric.

6.4.5. Summary

The bulk of the rocks at Hickey's Pond are the product of intense near-surface acid leaching and later deformation, which produced the common banded appearance. However, silicified and pyritized volcanic rock was locally developed, possibly lower in the system. Minor chemically precipitated material, the texturally and mineralogically distinct pyrite/specularite interbanded rock formed in hot springs at the paleosurface. Breccia pipes formed in the altered rock and were cemented primarily by very fine-grained silica and iron oxides (now quartz and specularite). There is evidence that specularite also migrated beyond the conduit marked by the breccia and into the host rocks. Similarly, indications of "extra" silica in the pyritiferous rocks might relate to the influx of silica into the silicified, pyritiferous rocks. The breccias were much more competent than the more pyrophyllite-rich (originally kaolinite-rich?) country rock, and they were boudinned, locally retaining volcanic textures in the clasts. Late in the deformation, quartz and specularite were remobilized locally into veins.

6.5. Ridge Showing

The association of alunite with quartz, pyrophyllite, specularite, pyrite and rutile at this showing leads again to comparison with the Tower Showing and interpretation of the rocks as products of surficial acid leaching on the ancient paleosurface. The presence of rare quartz phenocrysts supports this interpretation.

The rocks which contain the siliceous spheroids are not encountered at any of the other showings. They resemble in shape, size and mineralogical banding the geyserite "eggs" described by Rinehart (1980) at the Narcissus geyser in Yellowstone National Park. This interpretation denotes an origin as a chemical precipitate, which is supported by the low TiO_2 concentration (0.09%) in the rock. The geyserite eggs at Narcissus are essentially pure silica and originate from an alkaline fountain geyser, chemically incapable of precipitating the minerals observed at the Ridge Showing. However, the critical factor in forming geyserite eggs is that there is a repetitive soaking of the ground with saturated fluids, as would occur adjacent an active geyser. Rinehart (1980, pp. 95-96) points out that geysering can and does occur in acid systems, despite typically poor development of silica seals required to build steam pressure (*ibid., p. 112.*

Thus at least part of the Ridge Showing owes its origin to precipitation from fluids which vented onto the paleosurface. Other parts of it represent acid leaching of the subjacent rocks, an association which would be expected.

6.5.1. Bullwinkle Showing

All of the rocks at the Bullwinkle Showing have counterparts at the Hickey's Pond Showing, in terms of mineralogy and degree of deformation. As such, the bulk of the rocks are interpreted as the result of acid-leaching on the paleosurface, and the specularite-rich breccias are interpreted to represent the emplacement of a hydrothermal breccia pipe into the near-surface levels.

A unique characteristic of the specularite-banded rocks at the Bullwinkle Showing is the much higher pyrophyllite concentration which is locally developed, a feature whose origin in different rocks was addressed in two preceding sections. The high sericite concentration in sample 022 was attributed to its derivation from a mafic rock with a higher initial concentration of Al_2O_3 than the rhyolites from which the other schists were derived (Section 3.5) and the high pyrophyllite concentration in sample 159 (Section 3.4.2) was attributed to physical segregation of the pyrophyllite during deformation. Although either of these processes might account for the high pyrophyllite concentrations locally developed at the Bullwinkle Showing, an alternative is insufficient K_2O during alteration for the formation of alunite, a characteristic which might also reflect a mafic protolith.

The occurrence of fragments of specularite-rich breccia in the banded specularite-bearing rocks (Section 4.4.3) provides additional evidence concerning the origin of both those rock types, which corroborates the interpretations given elsewhere in this section. It shows that the banded specularite-bearing rocks were exposed on the surface at the same time as the breccia, and that fragments of the latter were incorporated into the former either as erosional products or ejecta from a hydrothermal eruption. An alternative explanation that the fragments are boudinned remnants of hydrothermal breccia *in situ* is not adopted here because they lack typical boudin shape and have sharp contacts with the host rock. This evidence sheds no new light on whether the host rocks are acid-leached volcanics, as is maintained here, or chemical precipitates formed in hotsprings.

6.6. Strange Showing

Two features distinguish the rocks at the Strange Showing from the other showings discussed: 1) they are the most intensely deformed and 2) they lack alunite. The possibility that intense deformation could have remobilized alunite, which recrystallizes readily, into structurally favourable areas away from the showing can not be proved, but must be regarded as a possibility.

The most important feature revealed by the detailed petrography at the showing is that the grey, siliceous pyritiferous rocks are as deformed as the black specularite-rich rocks. This is supported by the intensely recrystallized quartz fabric and the severe attenuation of rutile observed in both rock types. Given this, the presence of specularite cannot be attributed to processes which accompanied the deformation, a conclusion further supported by the presence of pyrite in the specularite-rich rocks.

The other important observation is that the grey, pyritiferous rocks were derived from a porphyritic volcanic rock, negating the possibility that the rocks at the Strange Showing are hotsprings precipitates.

The intense deformation the rocks have undergone, the abundance of specularite in the black rocks, and their texture in which highly elongated grey streaks are separated by a black, more specularite-rich "matrix" invite comparison of these rocks with the specularite-rich breccias at the other showings. The presence of pyrite is a feature it shares with the breccia at Chimney Falls, which is also similar in that it occurs adjacent to argillically altered volcanics. The zone of argillic alteration exposed at the Strange Showing appears to be smaller than that at Chimney Falls, but this probably reflects inferior exposure and attenuation of the alteration zone along the mylonite zone in which it occurs. The breccias at Hickey's Pond and the Bullwinkle Showing are hosted by major zones of advanced argillic alteration, unlike the Strange Showing.

Consistent application of this comparison implies that the specularite-rich rocks at the Strange Showing formed by hydrothermal brecciation and infilling with specularite. The zone formed in a previously altered rock characterized by sericite and pyrite, either through evolution of the fluid or because the previous alteration had left a good "path" for the later fluid to follow. The grey, pyritiferous siliceous rocks and quartz-sericite schists represent intensely deformed versions of the early alteration. The quartz-pyrophyllite(?)-specularite schists represent limited influx of specularite into the host rock.

6.7. Monkstown Road Area

6.7.1. Monkstown Road Specularite Showing

Chalcedonically banded silica at this showing attests to open-space filling either in a hotspring or in the shallow subsurface. The lack of pyrite and alunite suggest the system is not as acidic as the other systems described, and is thus more likely to precipitate silica (Fournier, 1985; compare with Section 6.3).

The coarse, vuggy veins of quartz, specularite and lazulite are texturally incompatible with the hotsprings environment. They are modelled as syntectonically remobilized veins, analogous to those at Hickey's Pond and the Bullwinkle Showing. The presence in the veins of the phosphate mineral lazulite is unusual, and probably requires the source/host rock to be enriched in P. Although no analyses are available for this showing, such an enrichment is suggested by the presence of various phosphate minerals at the nearby Little Pond Specularite Showing. These minerals were identified with an energy dispersive microprobe, and are described in Section 7.9.2.

The small hydrothermal breccia zone infilled with specularite could be either an incipient stage, or a distal part of a larger specularite-rich breccia zone similar to those described at some of the other showings.

6.7.2. Little Pond Specularite Showing

The black, siliceous, specularite-rich bands at this showing are relatively massive and resemble primary bands of iron formation. That the banding is not of tectonic origin is supported by the lack of development of microfabrics in the quartz and the folding which the banding clearly predates. The showing is interpreted as a surficial accumulation of silica, iron and clay minerals on the paleosurface which acquired a microcrystalline texture during the regional metamorphism. The reaction of specularite and clay minerals to produce Fe-chloritoid was given in Section 2.4. For the same reasons given in the preceding

section, the lack of alunite and pyrite at this showing tend to increase the likelihood of the system to have precipitated abundant silica.

6.7.3. Paradise River Showing

Both in outcrop and microscopically, the rocks at this showing resemble the alunite-bearing rocks at the Bullwinkle Showing, the northern end of which is only 500 m to the south. As such, they are modelled as the products of intense acid leaching which occurred on the paleosurface. This is in sharp chemical contrast to the fluids responsible for the Monkstown Road and Little Pond specularite showings; a feature which resembles the lateral chemical variations in hotsprings which exhale onto the surface in active geothermal areas.

6.8. Field relations

As described in Section 4.11, all the showings discussed above can be referred to an eastern or a western belt of alteration. The orientation of these belts and their relationship with each other are considered in the following sections.

6.8.1. Western Alteration Belt

The western alteration belt consists from north to south of the Ridge, Monkstown Road, Little Pond, Paradise River, Bullwinkle and Strange Showings, which span a length of 5.2 km (Figure 4-1, page 73). The trend of the belt is north northeast which parallels the trend of stratigraphy and the pervasive regional cleavage. It maintains a fairly constant distance of 600 m from the sedimentary rocks which are higher in the stratigraphy to the northwest.

With the exception of the Strange Showing, all the alteration in the belt was ascribed to either acid leaching or chemical precipitation at or near the paleosurface, both types of which must be regarded as stratiform mineralization. Given the constant stratigraphic level of the alteration, it follows that all the showings formed contemporaneously. This is in keeping with modern geothermal

fields, which can occupy several km^2 and feature acid leaching in one locality, and the construction of silica terraces nearby. The ancient geothermal field in which these showings formed has been tipped steeply on end and flattened, such that a cross section through it is now exposed.

The Strange Showing was considered to have formed at some depth in the subsurface, but its occurrence along the trend of the western alteration belt, and the presence of argillic alteration suggest that it too was formed near the paleosurface.

6.8.2. Eastern Alteration Belt

The eastern alteration belt consists, from north to south, of the Hickey's Pond, Chimney Falls and Tower Showings. If the pyrophyllite showings at the headwaters of Hickey's Brook, which also lie on the trend, are considered then the belt has a length of 15.0 km (Figure 4-1, page 73). A consistent spatial association exists between the Eastern Alteration Belt and the eastern margin of the Swift Current Granite. This contact was shown (Section 2.3.1) to be a major fault zone and without detailed knowledge of the showings, the question arises as to whether they are genetically related to the fault zone. This possibility is rejected for the following reasons:

1. The alteration occurs only to the east of the fault, as opposed to being symmetrically distributed about the fault. Although asymmetries occur in structurally controlled alteration, the tendency is towards preferential alteration of the hanging wall (*e.g.* Buchanan, 1981), which is not the case for the eastern belt.

2. The most intense alteration at three of the showings is separated from the fault by less altered rocks. The drill core at Hickey's Pond showed over 20 m of quartz-sericite schist and small amounts of strongly sheared crystal tuff between the alunite-bearing rocks and the granite. At Chimney Falls, pyritiferous quartz-sericite schists occur between the granite and the more highly altered pyrophyllite schists and hydrothermal breccia and the Tower Showing is separated from the Swift Current Granite by 100 m of sericitized crystal tuffs.

3. Metamorphic fluids which might have accompanied the Devonian

deformation tend not to be sufficiently acid or oxidizing to account for the acid-indicator minerals at the showings.

The stratiform nature of the alteration at Hickey's Pond and the Tower Showing further disproves a genetic relationship with the fault. Unfortunately, there is no clear stratigraphic marker paralleling the course of the eastern alteration belt, comparable in function to the sedimentary rocks which overlie the western belt, to show that the stratiform alteration zones are contemporaneous. The showings occur consistently at the western edge of a steeply west dipping kilometre-wide belt of felsic volcanics which occurs between the Swift Current Granite and mafic volcanics to the east, and which might be regarded as a stratigraphic level. However, the distribution of rock types at the Tower Showing led to their interpretation as being overturned (Section 6.3), which complicates definition of the alteration belt as a stratigraphic horizon since independent evidence for a younging direction at Hickey's Pond is not available. Although it can not be shown as rigorously for the eastern belt that it is the locus of contemporaneous stratiform mineralization on the surface of an ancient geothermal field, this is assumed for the Tower and Hickey's Pond Showings by analogy with similar mineralization in the western belt. The alteration at Chimney Falls is regarded as near-surface by analogy with the Strange Showing in the western belt.

The spatial association of the eastern belt with the Hickey's Brook Fault can be explained in terms of the fault forming in structurally favourable rocks, namely the argillic and advanced argillically altered rocks which formed at and near the paleosurface. Thrusting from the west during the Acadian orogeny juxtaposed the granite with these higher stratigraphic levels, and later strike slip movement produced the shear-related fabrics which are apparent at Chimney Falls and the Headwaters Showing.

6.8.3. Interrelationship of the alteration belts

The eastern and western alteration belts have each been interpreted as stratiform mineralization which formed on the paleosurface of an ancient geothermal field. It remains to be explained whether the belts represent the same time-stratigraphic interval, or a different one. In light of the strong similarities between the two belts and the apparent repetition of stratigraphy determined independently in Section 2.2.4, the belts are modelled as structurally repeated cross sections through the time-stratigraphic level at which the geothermal systems were venting to the paleosurface.

Slightly problematical to this interpretation is the apparent difference in stratigraphic level of the two alteration belts. The western belt is in mixed mafic and felsic volcanics which mark the transition upward into a thin unit of felsic volcanics which are overlain by sedimentary rocks. The eastern belt seems to be fairly high in the felsic volcanic unit, and whether or not they were overlain by sedimentary rocks prior to being faulted against the Swift Current Granite is unknown. Assuming the alteration in both belts to be contemporaneous, it dictates the volcanic stratigraphy to be time-transgressive and subject to lateral variation, postulates which typify subaerial volcanics. In light of these assumptions, the eastern belt is considered to have formed in closer proximity to the centre of felsic volcanism and the western belt formed distal to it, in a place which developed a thinner felsic sequence before being onlapped by sediments. Supporting this interpretation are 1) proximity of the eastern belt to the Swift Current Granite, 2) the nonwelded nature of the felsic volcanics overlying the western belt (Section 2.2.4) and 3), the occurrence of possible flow banded rhyolite at Hickey's Pond, which was preserved from deformation as fragments in the competent specularite-rich breccia there. A model accounting for this distribution is presented in Figure 6-2.

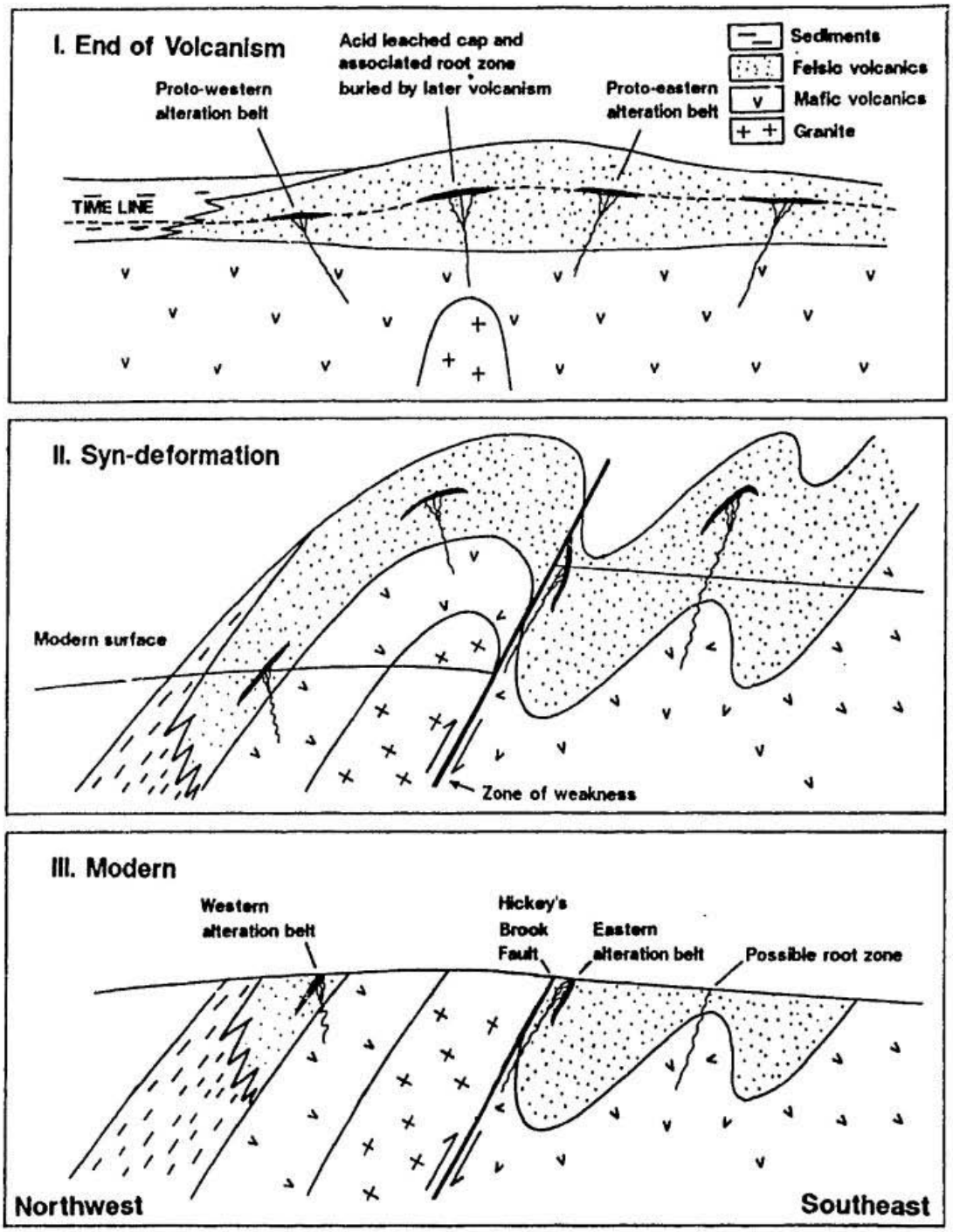

Figure 6-2: Interrelationships of the alteration belts. Two alteration belts are referred to a single alteration event by means of a reverse faulted, overturned fold (see Figure 2-7, page 32). Time line in Frame I signifies stratiform nature of acid leached caps. Root zone of eastern alteration belt is illustrated transposed into fault zone (see Figure 6-1, page 156).

6.9. Summary

Most of the showings discussed in Chapter 4 have been shown to be metamorphosed, strongly recrystallized and variably deformed versions of alteration assemblages which formed by acid leaching on the paleosurface of the ancient volcanic field. Modern analogues abound (Chapter 5) and show that this is a type of stratiform mineralization. It is closely associated with hotsprings in which chemical precipitates are forming, and hydrothermal eruption breccias which reach into shallow levels below the paleosurface, both of which processes are represented by rocks present in the study area. In the same way that the volcanic stratigraphy is structurally repeated, the time-stratigraphic interval in which the hydrothermal systems acted on the paleosurface is repeated, providing two cross-sectional views through the alteration zones and leading to its exposure as two separate belts of alteration.

Chapter 7
GOLD MINERALIZATION

7.1. Introduction

The preceding chapters document the occurrence of two fundamental types of alteration. Chapter 3 describes rocks characterized by sericite or pyrophyllite in which volcanic features are preserved, showing that these rocks are alteration products of the volcanics. Chapter 4 describes rocks characterized by alunite in which volcanic features are very rarely present, or which locally show evidence of being chemical precipitates, as opposed to altered volcanic rock. Chapters 5 and 6 show that most of the alunite bearing rocks are the product of very intense acid leaching that occurred on the paleosurface of the volcanic field, and that hot springs precipitates were locally formed and preserved. Hydrothermal breccias were shown to be associated mainly with the surficially altered rocks (particularly at Hickey's Pond), but to a lesser extent with the clay-altered rocks which formed at shallow depths.

These rock types are integral parts of epithermal systems, which are reviewed in Chapter 8, and deserve appraisal in terms of their precious metal contents. Gold analyses have been performed on all the different mineral assemblages at the showings described in Chapter 4, and on the rocks of the alteration suite described in Chapter 3. Most of these rocks have also been analyzed for Ag and selected trace elements, and selected samples from the Hickey's Pond, Tower and Bullwinkle showings were analyzed for Sb, As and Hg. Qualitative geochemical information was obtained by means of an energy dispersive electron probe microanalyser for minor mineral phases observed during examination of thin sections with a scanning electron microscope operating in

backscattered electron mode. The results of these investigations are presented in this chapter. Fluid inclusion sections were prepared for representative samples of the different rock types at Hickey's Pond. No inclusions large enough to study were observed, and it is unlikely that any primary inclusions survived the regional deformation and metamorphism.

7.2. Alteration suite

Gold and silver analyses from the 15 rocks of the alteration suite studied in Chapter 3 are presented in Table 3-1 (page 52). With the exception of a weakly elevated (0.3 ppm) Ag concentration in one of the plagioclase crystal tuffs, these elements are below detection in the unaltered rocks. Silver concentrations are elevated in 2 of the sericite schists, one of which also contains 55 ppb Au. One of the 5 samples of pyrophyllite schist contains an elevated Au concentration (45 ppb), and another sample contains 0.3 ppm Ag.

Although the data set is very small, it appears that both sericitization and pyrophyllitization in the study area were accompanied by sporadic, minor precious metal mineralization. It is noted here that the sample of pyrophyllite schist from the Headwaters Showing did not contain detectable Au or Ag concentrations. They were elevated only at Chimney Falls, where they were shown to flank a zone of hydrothermal brecciation characterized by specularite and alunite (Sections 4.9.2.2 and 6.2.1). In light of the geochemical characteristics of the breccia, described in the following section, it is cautioned here that the sporadically elevated precious metal concentrations in the pyrophyllite schists at Chimney Falls could relate to the intrusion of the breccia pipe, and not necessarily to the pyrophyllitization.

7.3. Chimney Falls

Thirteen rock samples from the Chimney Falls showing were analyzed for gold and silver (Table 7-1). Small amounts of Au and Ag, up to 105 ppb and 0.3 ppm respectively, were distributed sporadically throughout the schistose rocks. Even within groups of schistose rocks with similar mineral assemblages, e.g. pyritiferous sericite schists or specularite-bearing pyrophyllite schists, the distribution of Au and Ag is erratic. Analytical uncertainty is undoubtedly a factor contributing to the variability of Au concentration in these rocks, given the low concentrations involved.

One sample from the breccia zone at each of the main showing and the northern extension were analyzed. The sample from the main showing contains the highest Au and Ag concentrations of all the rocks from the showing: 335 ppb and 0.7 ppm respectively. The breccia from the northern extension also had an elevated Au concentration (35 ppb) although Ag was below the detection limit (0.1 ppm).

7.3.1. Trace elements

Examination of Table 7-1 shows that the breccias are enriched in K, Na, Rb, U, Th, V, Au, Ag, Cu, Ba, Ti, Zr, Fe, and Nb relative to the surrounding pyrophyllite schists. In the case of Rb, the absolute concentration is still very low, but it is significantly concentrated relative to the surrounding pyrophyllite schists, from which it had been completely removed. The concentrations of P and Sr in the breccia are approximately equal to those in the pyrophyllite schists, both being enriched relative to sericite schists or fresh volcanic rock.

Table 7-1: Geochemistry of Chimney Falls Showing samples. Note that the breccias are enriched in K, Na, Rb, U, Th, V, Au, Ag, Cu, Ba, Ti, Zr, Fe, and Nb relative to the pyrophyllite schists. [Data are presented split according to rock type. Major element oxides are reported in weight percent, Au in parts per billion (mg/t) and all other elements in parts per million (g/t). "0" = below detection, " " = no analysis was conducted.]

#	SiO2	Al2O3	Fe2O3	MgO	CaO	Na2O	K2O	TiO2	MnO	P2O5	LOI	Total	Cu	Pb	Zn	Au	Ag	Ba	Sr	Rb	U	Th	Y	Zr	Nb	Ga	Ni	V
Sericite schists																												
160													0	14	0	30	.1	263	55	8	0	14	7	135	10	4	0	51
247													8	12	205	5	.0	523	70	90	0	5	22	158	8	14	0	72
250													8	39	8	0	.0	890	168	129	0	13	19	119	10	14	0	15
Pyrophyllite schists																												
154	91.50	3.70	1.24	.02	.04	.02	.13	.47	.01	.20	1.31	98.64	2	43	0	0	.0	170	638	0	0	18	16	171	9	9	0	30
159	77.50	16.99	.61	.02	.00	.04	.03	.42	.01	.16	4.17	99.95	3	35	0	5	.3	102	995	0	7	33	14	179	11	21	0	74
161	85.60	9.53	.94	.01	.00	.02	.01	.26	.01	.07	2.16	98.61	0	146	0	45	.0	350	533	0	9	29	11	120	9	16	0	29
162													0	194	0	105	.1	396	306	6	7	18	9	95	7	11	0	101
244	87.30	9.42	.08	.01	.00	.01	.01	.44	.01	.11	2.29	99.68	0	24	0	0	.0	588	385	0	4	26	13	172	12	12	0	39
245													0	26	0	30	.0	100	212	0	9	34	27	146	10	16	0	73
246													5	10	0	0	.0	59	38	0	0	14	26	150	8	13	0	94
249													0	25	0	90	.3	51	115	0	0	20	24	84	7	12	0	44
Specularite - rich breccias																												
156	69.15	4.29	19.46	.01	.07	.30	.64	1.06	.01	.19	3.17	98.35	14	149	0	335	.7	1024	612	12	18	51	24	403	26	13	0	150
248													0	90	0	35	.0	816	373	6	13	31	13	203	13	8	0	50

7.3.2. SEM-EDX Investigation

Several elements and groups of elements, most of uncertain mineralogy were identified in the breccia from the main zone using the SEM-EDX. A compound of Ba and S (Figure A-3), undoubtedly barite, forms anhedral crystals up to 0.075 mm across. They are associated with specularite, and commonly fill interstices within and on the margins of specularite crystals (Figure 7-1).

A crystal 0.018 mm long which analyzed as Te was observed on the edge of a specularite crystal (Figures 7-1, A-4) and inferred to be native tellurium. Smaller crystals consisting of Te and Se (Figure A-5), also in contact with specularite were observed throughout the slide. They displayed varying ratios between Te and Se peak heights, which would be expected of selentellurium, the name applied to natural mixtures of the two elements. Two small (0.002 mm) crystals on the edge of specularite consist predominantly of Au and Te, with minor Se and are inferred to be calaverite ($AuTe_2$, Figures A-6, 7-2).

Other compounds noted include a crystal 0.032 mm across that consists of Cu, Se, Te and S (Figure A-7). Lacking quantitative data this mineral defies description, as copper has several telluride, selenide and sulfide forms. A small, sharply defined corner of this crystal had a stronger backscatter and an analysis of the corner showed Se, Te, Ag and S to be the main constituents, with only minor Cu (Figures 7-3, A-8).

A crystal containing Cu, As, Te and S (Figure A-9) 0.037 mm long was noted on the edge of a specularite crystal. A very similar X-ray spectrum is presented (Section 7.5.2.4) for a mineral from Hickey's Pond, which suggests that it is a single mineral, rather than a mixture. Although no references to such a mineral were found, substitution of As for Sb in goldfieldite ($Cu_{12}Sb_4Te_3S_{16}$, Palache *et al.*, 1966) would be a possibility. However, doubt remains as to whether goldfieldite is a true mineral and it has more recently been referred to as telluriferous tetrahedrite (Pierrot, 1979). Parallel reasoning suggests telluriferous tennantite as the name of the mineral from Chimney Falls.

Figure 7-1: Barite and native tellurium at Chimney Falls. Barite (light grey) fills interstices in specularite (dark grey) in specularite-rich breccia at Chimney Falls. Black matrix is quartz and alunite. Small white crystal at extreme right is native tellurium. [Field of view 0.82 mm x 0.70 mm, backscattered electron image.]

Figure 7-2: Gold telluride (Calaverite) at Chimney Falls. Small crystals of gold telluride (white, centre of photo) fill cracks on margins of specularite (light grey) and rutile (dark grey). Black matrix is quartz and alunite. [Field of view 0.048 mm x 0.041 mm, backscattered electron image.]

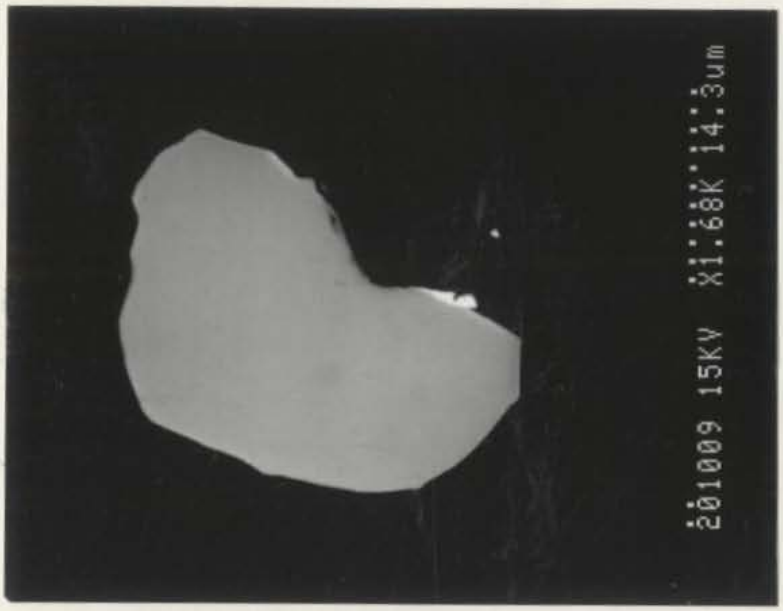

Figure 7-3: Unidentified copper and silver minerals at Chimney Falls. Large crystal in photo centre contains Cu, Se, Te and S (Figure A-7). White fringe on top right of crystal consists of Se, Te, Ag and S, with only minor Cu (Figure A-8). [Field of view 0.049 mm x 0.042 mm, backscattered electron image.]

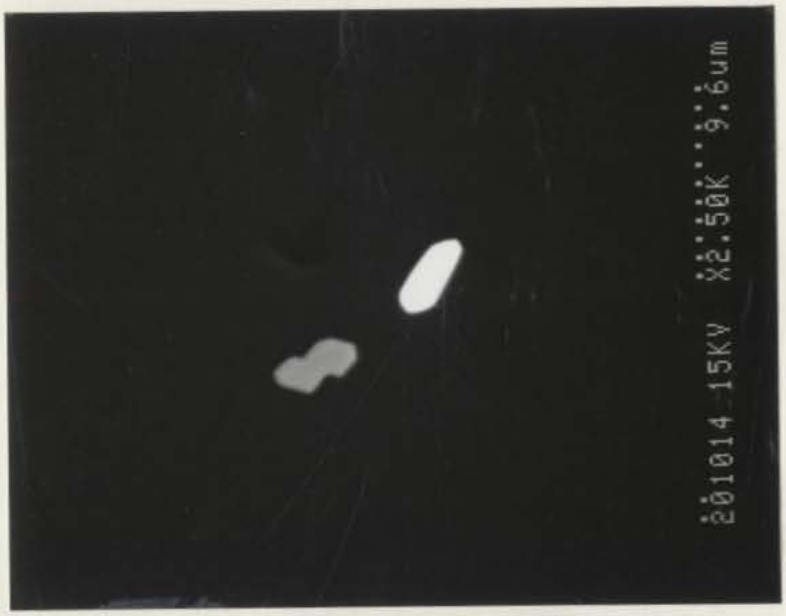

Figure 7-4: Mercury selenide (tiemannite) at Chimney Falls. Bright white crystal is mercury selenide (tiemannite, HgSe). Grey crystal below and to left is specularite. Black matrix is quartz and alunite. [Field of view 0.033 mm x 0.028 mm, backscattered electron image.]

An isolated, euhedral crystal 0.004 mm long in quartz was shown to consist primarily of Hg and Se, with minor Te and a very small Pd peak (Figures 7-4, A-10). It is probably tiemannite (HgSe), the selenide of mercury.

Several corroded pyrite grains were examined carefully but no unusual elements were detected in association with them. A random analysis of an alunite crystal showed detectable Sr, P, Ca and Ce, indicating their presence in amounts probably near 1%.

7.3.3. Discussion

The alteration of volcanic rocks up to the point of pyrophyllite schists has been dealt with in Chapter 3. It is characterized by the removal of several elements and the concentration of small, highly charged "immobile" cations (Ti, Si, P and Zr) and another group of large cations (Sr, Pb, La, Ce, Nd and Pr) which are probably stabilized in newly formed phosphate minerals in the pyrophyllite schists.

The breccia at Chimney Falls clearly resulted from a different process, as it was mineralized with abundant specularite and minor alunite. It was shown in Section 6.2.1 that the breccia marks an ancient hydrothermal conduit, and the geochemical information provided above shows that it carried elevated concentrations of K, Rb, U and V (elements added during sericite development, see Section 3.4.3), P and Sr (which are enriched in pyrophyllite schists only adjacent to the breccia (Section 3.5), implying derivation from the breccia) and very high relative concentrations of Au, Ag, Cu, Ba, Ti, Zr and Fe. Barite and compounds containing Au and Ag have been identified in the breccia, together with compounds containing Cu, Te, Se, As, S, Hg and Pd. The common spatial association of the Au-Ag-Cu compounds with the margins of specularite crystals suggests that they were exsolved from the specularite during metamorphic recrystallization. The occurrence of P, Sr, Ca and Ce in alunite and the presence of native tellurium corroborates the suggestion in Section 6.2.1 that it is primary hypogene mineralization.

7.4. Tower Showing

Eighteen rock samples from the Tower showing were analyzed for gold (Table 7-2), concentrations of which range from <5 to 36 ppb. Contrasting the pyritiferous and specularite-banded alunite-bearing rocks in terms of gold and other trace elements reveals significant differences. No gold was detected in any of the 8 specularite-banded rocks but only 2 of the 8 pyritiferous rocks contained no detected gold. The remaining samples ranged from 5 to 36 ppb Au, averaging 25 ppb. No silver was detected above the 100 ppb detection limit of the analytical process. Examination of Table 7-2 shows that the pyritiferous rocks are also enriched in Cu, Ba, Sr, Pb and P relative to the specularite-bearing rocks.

Hg, As and Sb were analyzed in 11 of the rocks discussed above. Concentrations were generally low and no significant differences exist between rock types. These three elements were also analyzed in one of the siliceous residues developed at the showing, and their concentrations are each about 10 times greater in the siliceous rock than in the alunite-bearing rock (Table 7-2).

7.4.1. Discussion

It was shown in Chapter 5 that the formation of pyrite in the acid hotsprings environment reflects the reaction of iron released from minerals undergoing breakdown with H_2S in ascending fluid. Its formation postdates that of alunite, where the two occur together, as it would not be stable in the strong sulfuric acid solutions required to produce alunite. Thus, the pyritiferous rocks at the Tower showing are distinguished genetically from the specularite-bearing rocks by a late influx of H_2S-bearing fluid and chemically by higher concentrations of Au, Cu, Ba, Sr, Pb and P. A possible explanation is that these elements were carried into the hotsprings environment by the late H_2S-bearing fluid.

Table 7-2: Geochemistry of Tower Showing samples. Note that the pyritiferous rocks are enriched in Au, Cu, Ba, Sr, Pb and P relative to the specularite-bearing rocks, and that the highest Sb, As and Hg concentrations are found in the quartz - rutile rock. [Data are presented split according to rock type. Major element oxides are reported in weight percent, Au and Hg in parts per billion (mg/t) and all other elements in parts per million (g/t). "0" = below detection, " " = no analysis was conducted.]

#	SiO2	Al2O3	Fe2O3	MgO	CaO	Na2O	K2O	TiO2	MnO	P2O5	LOI	Total	Cu	Pb	Zn	Au	Ag	Sb	As	Hg	Ba	Sr	Rb	U	Th	Y	Zr	Nb	Ga	Ni	V
	Specularite - banded rocks																														
276													6	70	0	0	.0				597	325	2	0	10	11	175	8	11	0	77
277	62.15	12.88	3.46	.01	.03	1.62	1.26	.39	.01	.10	16.97	98.88	5	91	0	0	.0	.4	2	10	678	290	4	0	12	10	163	9	10	0	68
278	59.05	14.72	2.90	.01	.05	2.11	1.00	.67	.00	.14	18.30	98.95	4	19	0	0	.0	.4	2	10	493	290	11	0	8	15	171	9	14	0	118
283	58.50	16.21	.26	.00	.09	1.73	1.95	.58	.00	.08	20.67	100.07	5	73	0	0	.0	.3	3	30	424	335	1	1	19	8	144	7	9	0	96
284	58.75	14.38	3.08	.00	.04	1.54	1.73	.67	.00	.12	18.37	98.68	6	45	0	0	.0	.4	2	20	703	274	4	0	6	5	168	9	18	0	122
285													1	50	0	0	.0				787	370	2	0	17	14	140	6	14	0	151
331	64.25	12.45	3.54	.01	.15	1.40	1.31	.58	.00	.20	15.24	99.13	4	41	0	0	.0	.1	1	10	566	374	3	0	15	10	143	9	16	0	126
334													5	30	0	0	.0				550	352	0	0	0	14	152	8	15	0	128
	Pyritiferous rocks																														
271													28	377	10	30	.0				974	573	1	0	15	6	137	8	12	0	137
272	53.20	21.32	.16	.01	.13	1.68	1.43	.74	.01	.21	19.71	98.60	9	412	0	30	.0	.3	3	10	1011	676	2	0	5	6	188	7	19	0	117
273	51.80	19.08	.33	.01	.10	2.02	1.81	.68	.01	.17	22.50	98.51	8	209	0	0	.0	.3	3	10	777	686	0	0	3	9	176	8	14	0	116
274	79.90	10.01	.22	.01	.09	.47	.94	.73	.01	.10	7.23	99.71	10	202	0	25	.0	.8	4	10	633	302	4	0	0	12	203	11	6	0	46
275	58.00	14.99	1.99	.00	.14	1.54	1.62	.67	.00	.18	19.93	99.06	13	103	0	0	.0	.2	2	10	888	521	3	1	12	10	165	9	6	0	118
282													12	146	0	5	.0				645	379	3	0	11	7	148	9	13	0	104
428	61.10	15.12	2.30	.01	.07	1.16	1.69	.68	.00	.21	16.44	98.78	10	337	0	36		.3	3	30	841	450	4	0	5	7	152	7	15	0	125
429	60.00	13.62	3.97	.01	.09	1.62	1.42	.58	.01	.19	17.15	98.66	8	71	0	23		.2	2	30	535	354	5	0	10	13	151	7	16	0	142
	Quartz - rutile rocks																														
279	94.85	1.20	.42	.01	.00	.03	.13	.64	.01	.01	.99	98.29	5	22	0	15	.0	3.2	19	110	0	33	2	0	2	6	169	12	3	0	0
280													15	135	0	0	.0				83	109	2	0	18	7	172	10	5	0	12

7.5. Hickey's Pond

Gold analyses performed on 36 rocks from the Hickey's Pond showing are presented in Table 7-3. With the exception of a few quartz veins, all the rocks contain elevated gold concentrations including a few samples of ore grade material. The following are a few observations on the gold distribution in the samples:

1. The three samples which contain the highest gold concentrations, near 5000 ppb, are specularite-rich breccias, although this rock type does not consistently contain concentrations so high.

2. The next highest gold concentration (2530 ppb) occurs in the silicified, pyritiferous rock.

3. The range and average gold concentrations are comparable for the specularite-banded and pyritiferous rocks. Typical gold concentrations are a few hundred ppb.

4. The milky quartz (+/- specularite) veins, interpreted to have been remobilized during metamorphism, contain only sporadically elevated gold concentrations. A sample of massive, coarse crystalline (remobilized) specularite contains 105 ppb Au.

Silver analyses were conducted on all the rocks and its distribution has marked differences from that of gold, leading to important differences in Au/Ag ratios. The highest silver concentration, 11.3 ppm, is in the silicified rock with coarse pyrite. This leads to a Au/Ag ratio of 0.2 for that rock type. The specularite-rich breccias have poor but positive correlations between Au and Ag, but Au/Ag ratios are generally >1, reaching 5.4. Silver concentrations in the alunite bearing rocks with pyrite are comparable to those containing specularite, and Au/Ag ratios are with few exceptions <1.

Table 7-3: Geochemistry of Hickey's Pond samples. Note that all rock types display elevated gold concentrations, with the highest concentrations associated with the specularite - rich breccias and the silicified, pyritiferous rocks. See text for additional discussion. [Data are presented split according to rock type. Major element oxides are reported in weight percent, Au and Hg in parts per billion (mg/t) and all other elements in parts per million (g/t). "0" = below detection, " " = no analysis was conducted.]

#	SiO2	Al2O3	Fe2O3	MgO	CaO	Na2O	K2O	TiO2	MnO	P2O5	LOI	Total	Cu	Pb	Zn	Au	Ag	Sb	As	Hg	Ba	Sr	Rb	U	Th	Y	Zr	Nb	Ga	Ni	V
	Specularite - banded rocks																														
135	64.10	12.25	4.20	.01	.09	1.17	1.79	.60	.00	.19	13.60	98.00	0	200	0	350	.3	1.0	3	30	526	377	0	0	18	29	188	12	30	0	94
228	65.85	11.23	3.82	.01	.09	.86	2.05	.56	.00	.21	13.64	98.32	3	157	0	325	.4	1.0	4	150	611	716	0	13	33	22	182	10	23	0	74
229													1	114	0	105	.7				638	556	0	2	23	27	185	11	23	0	94
232	59.40	12.91	5.62	.00	.07	1.39	1.73	.33	.01	.19	16.02	97.87	0	283	0	170	.6	1.2	4	250	672	693	0	9	26	19	181	13	32	0	84
257	59.60	12.08	7.95	.02	.09	1.47	1.15	.57	.00	.19	14.36	97.48	7	56	0	270	.3	2.4	6	40	744	456	0	2	17	21	175	13	21	0	91
261													10	163	0	180	.3				731	635	3	0	13	13	174	10	22	0	77
357	62.95	9.94	9.25	.00	.09	1.00	1.28	.50	.01	.21	13.12	98.35	6	136	0	1300	.8	4.4	15	130	490	394	5	3	29	13	162	10	29	0	93
	Pyritiferous rocks																														
134													32	243	0	230	.0				639	473	0	1	13	29	149	10	30	0	81
171	72.20	10.14	1.65	.03	.14	1.07	1.20	.55	.01	.19	11.32	98.50	17	371	0	200	.4	2.0	9	120	527	358	0	3	23	20	164	10	22	0	66
218													22	267	0	1850	2.2				436	448	0	13	39	18	160	11	18	0	54
231													0	100	0	110	.3				690	795	0	0	15	23	178	11	23	0	80
236													0	63	0	45	.2				988	141	0	0	16	32	175	10	23	0	67
263	67.80	9.53	4.25	.00	.12	1.46	.49	.50	.01	.12	15.25	99.53	21	81	0	90	.1	.6	6	60	372	272	0	0	12	15	150	11	20	0	92
266													6	302	0		.6				359	269	2	0	7	13	152	7	39	0	80
456	44.25	14.73	9.60	.02	.13	1.40	2.29	.79	.00	.22	25.49	98.92																			
	Specularite - pyrite interbanded rocks																														
172	61.10	13.64	3.70	.02	.13	1.70	1.30	.93	.01	.18	16.50	99.21	46	606	0	275	.4	4.0	19	120	323	425	0	0	12	12	99	7	52	0	166
339													25	408	0						778	1296	2	0	7	9	97	5	36	0	154
340	60.40	12.54	4.38	.00	.12	1.70	.95	.55	.00	.12	19.36	100.12	46	283	0	75	.3				205	161	0	0	6	14	159	12	23	0	71
	Silicified pyritiferous rocks																														
169													54	108	0						151	165	3	0	0	15	114	7	8	0	34
170	96.30	1.09	.41	.01	.08	.06	.19	.27	.01	.00	.80	99.22	311	34	0	2530	11.3	4.0	19	60	25	58	0	6	31	2	57	5	4	0	12
	Specularite - rich breccias																														
235	86.50	1.56	8.12	.00	.05	.16	.18	.57	.01	.09	2.07	99.31	0	115	0	5400	1.0	9.8	12	240	149	145	0	8	17	25	177	14	8	0	47
254	77.60	4.82	7.73	.00	.14	.63	.40	.83	.01	.18	6.54	98.88	2	32	0	45	.1	4.0	14	190	599	126	0	2	20	48	243	14	11	0	98
255	33.70	3.23	50.49	.00	.28	.28	.28	.46	.00	.42	4.09	93.23	0	79	0	4710	1.5	20.0	14	5500	257	249	35	27	104	21	151	1	10	0	219
341	78.05	2.49	12.88	.01	.04	.19	.39	.53	.00	.11	2.37	97.06	4	144	0	4950	3.3	8.2	15	300	239	163	16	4	19	18	163	13	11	0	69
345													6	317	0						418	316	3	0	16	4	70	3	25	0	97
346	67.35	3.86	18.35	.01	.05	.53	.28	.44	.01	.14	5.34	96.36	0	189	0	200	.2	3.4	7	320	336	234	13	0	11	15	145	12	14	0	139
347	63.20	6.72	16.62	.01	.09	.87	.51	.48	.00	.23	8.63	97.36				143	.3	2.6	6	890											
350													6	225	0						423	277	3	0	1	7	76	3	25	0	72
351	67.15	5.78	16.42	.01	.09	.55	.78	.28	.00	.19	6.39	97.64	0	493	0	470	2.2	8.6	9	510	541	299	15	0	6	10	80	7	28	0	160
352	83.55	1.70	9.86	.00	.02	.20	.16	.36	.01	.07	2.40	98.33	4	150	0	1250	.5	5.0	7	320	135	128	7	0	15	5	127	10	8	0	68
353	70.55	7.41	9.12	.00	.12	.78	.85	.63	.01	.27	8.95	98.69	5	54	0	200	.1	4.0	10	1800	740	245	3	0	19	32	200	14	16	0	109
355	75.90	2.93	12.46	.00	.03	.34	.30	.61	.01	.11	4.31	97.00	0	32	0	85	.1	2.8	11	220	227	93	4	0	7	28	198	15	8	0	82
	Quartz veins with specularite																														
167													0	14	0	100	.1				0	4	0	3	18	4	0	3	0	0	1
174													5	31	0	60	.0				23	74	0	9	3	10	134	5	1	0	9
217													0	74	0	5	.2				107	191	0	0	10	6	0	5	3	0	0
233													0	58	0	405	.4				141	139	0	0	22	9	20	7	5	0	79
237													0	23	0	15	.0				14	32	0	0	8	2	0	5	0	0	13
238													2	39	0	5	.0				26	34	0	0	2	7	5	6	6	0	35
256																0	.0														
259																0	.0														
	Massive, platy specularite																														
168													0	0	0	105	.5				27	0	12	0	0	0	0	8	0	0	700
175													0	1	0	10	.3				14	5	37	3	3	0	0	8	0	4	991

7.5.1. Trace elements

Selected trace element concentrations were determined for most of the rocks from Hickey's Pond and are also presented in Table 7-3. Observations regarding their distribution are listed below.

1. The specularite-rich breccias have fairly consistently elevated concentrations of Rb (reaching 35 ppm) and sporadically high concentrations of P, U and Th, but have lower concentrations of Sr and Ba than most of the rocks.

2. Copper concentrations are uniformly low in the specularite-rich breccias.

3. The silicified, pyritiferous rocks have highly anomalous copper concentrations (up to 311 ppm), and low concentrations of Rb, Sr, Zr, Ti and Ba. The concentration of P is below the detection limit.

4. The concentrations of most trace elements, with the exception of copper, are in the same range for the alunite-bearing rocks containing specularite compared to those containing pyrite.

5. The highest concentration of arsenic occurs in the silicified rock with pyrite, but concentrations are generally low and there is a positive correlation with gold transcending all rock types.

6. Mercury and antimony reach their highest concentrations in the specularite-rich breccias, but neither element is particularly enriched in the silicified rock.

7.5.2. SEM-EDX investigation

Several thin sections were examined using a scanning electron microscope operating under backscattered electron mode. The following observations are categorized according to rock type.

7.5.2.1. Specularite-rich breccias

Native gold occurs in discrete grains up to 0.038 mm long in these rocks, where it is universally in contact with specularite (Figure 7-5). Microanalyses of the grains reveal only very low concentrations of silver (Figure A-11).

Native (?) bismuth occurs in isolated, irregular blebs up to 0.1 mm across in the breccias (Figure A-12). Other analyses revealed appreciable quantities of Te with Bi (Figure A-13), which might represent admixed native tellurium which is commonly associated with native bismuth or one of several bismuth tellurides, *e.g.* tellurobismuthite (Bi_2Te_3).

Analysis of a crystal only 0.0015 mm across on the margin of a specularite crystal revealed it to consist of Hg, Ag, I and Cl (Figure A-14). Both Hg and Ag each have chloride and iodide forms, and this crystal is probably a mixture of them.

Millimetre-thick specularite veins that emanate from the specularite-rich breccia were described in Section 4.4.2.2. A thin section was prepared parallel to one such veinlet and included in the SEM examination. A grain of native gold 0.008 mm across was observed on the edge of a specularite crystal (Figure 7-6). A crystal of xenotime (YPO_4) 0.12 mm across was shown to contain very small amounts of Dy and Er (Figure A-15).

7.5.2.2. Silicified rock

Gold was identified as a probable telluride (calaverite?) forming crystals up to 0.030 mm across in pyrite grains in these rocks (Figures 7-7, A-16).

A compound containing Cu, Fe, As and S, with minor Sb was observed as a thin rim 0.013 mm long on a pyrite crystal (Figures 7-8, A-17). The mineral could be tennantite or enargite, but the former is favoured because of the relatively high iron content suggested by the peak heights.

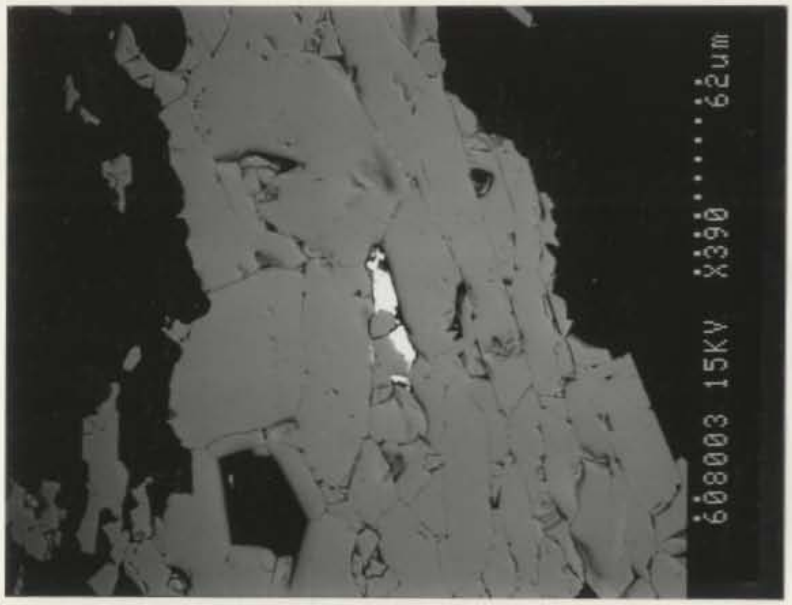

Figure 7-5: Gold in Hickey's Pond breccia. Native gold (white, photo centre) occurs within specularite (grey) in specularite-rich breccia at Hickey's Pond. Black matrix is quartz and alunite. [Field of view 0.21 mm x 0.18 mm, backscattered electron image.]

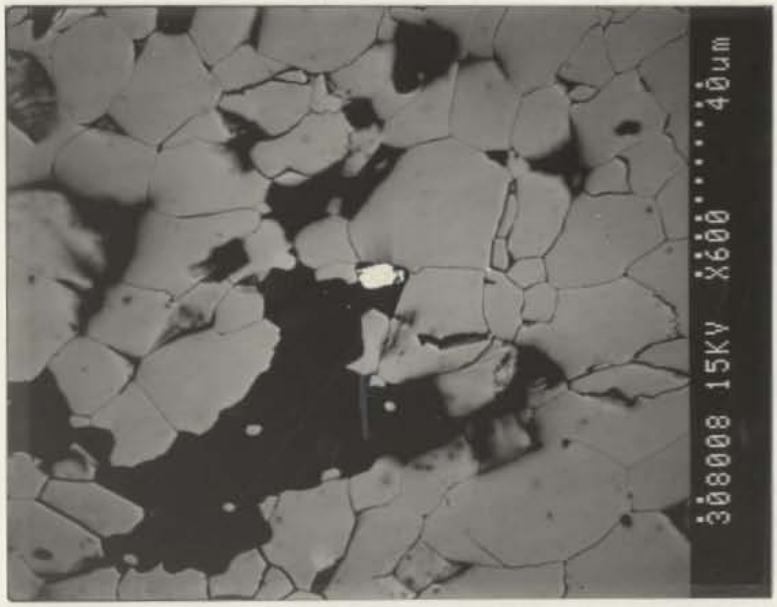

Figure 7-6: Gold in specularite veinlet at Hickey's Pond. Native gold (white) occurs in millimetre-thick specularite (grey) veinlet emanating from specularite-rich breccia at Hickey's Pond (see Figure 4-17). [Field of view 0.14 mm x 0.12 mm, backscattered electron image.]

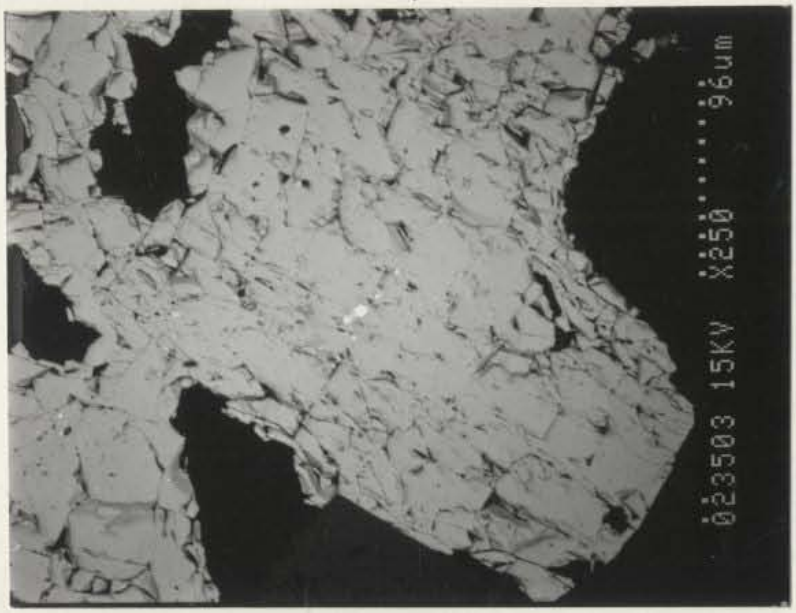

Figure 7-7: Gold telluride (Calaverite) at Hickey's Pond. Gold telluride (white, photo centre) occurs within pyrite crystal (grey) in silicified, pyritiferous rock at Hickey's Pond. [Field of view 0.33 mm x 0.28 mm, backscattered electron image.]

Figure 7-8: Tennantite at Hickey's Pond. Tennantite (white, photo centre) occurs on margin of and within a crack in pyrite (grey) in silicified pyritiferous rock at Hickey's Pond. Microanalysis of this crystal revealed a significant concentration of Se (Figure A-17). [Field of view 0.10 mm x 0.087mm, backscattered electron image.]

A crystal only 0.003 mm long and completely enclosed by pyrite consists of Pb, Ag, S and Se (Figure A-18), which probably is a mixture of galena and silver selenide (naumannite, Ag_2Se).

Chalcopyrite grains up to 0.025 mm long were noted in the pyrite crystals. Very small (0.0025 mm) crystals, which were shown to consist of Bi, Se and Ag (Figure A-19), were observed locally on interfaces between chalcopyrite and pyrite (Figure 7-9). Differences in the proportions of these elements were indicated by varying peak height ratios, which suggests a mixture of selenide minerals, possibly naumannite (Ag_2Se) and guanajuatite (Bi_2Se_3).

Other chalcopyrite grains (in pyrite) have distinct fringes which consist of Cu, S, Te, Sb, Fe and minor Se (Figure A-20). If the mineral is tetrahedrite, it contains considerable concentrations of Te and Se.

7.5.2.3. Specularite-banded rocks

Attempts to identify gold in this common rock type were not successful, but other interesting compounds were noted. Xenotime (YPO_4) with minor amounts of Dy and Er was observed in embayments in specularite crystals and as isolated, elongated crystals up to 0.04 m long (Figure 7-10). Microanalyses of zircon crystals revealed a significant quantity of Sc (Figure A-21).

An isolated, euhedral crystal 0.006 mm across in pyrite was shown to consist of Bi and Se, with minor concentrations of Cu and Ag (guanajuatite (?, Bi_2Se_3), Figure A-22).

7.5.2.4. Chemical precipitates

The rocks inferred to be hotsprings precipitates contain minor irregularly shaped crystals of barite, locally with significant Sr concentrations, up to 0.012 mm across. A crystal 0.012 mm across intergrown among a cluster of small pyrite crystals consists of Cu, As, Te and S (Figures 7-11, A-23). This compound has peak height ratios nearly identical to those measured for a compound of the same

Figure 7-9: Silver and bismuth selenides at Hickey's Pond. Chalcopyrite crystals (grey) within pyrite (black) host two crystals of silver-bismuth selenide (white dots at cp-py interfaces, photo centre and lower right). [Field of view 0.17 mm x 0.14 mm, backscattered electron image.]

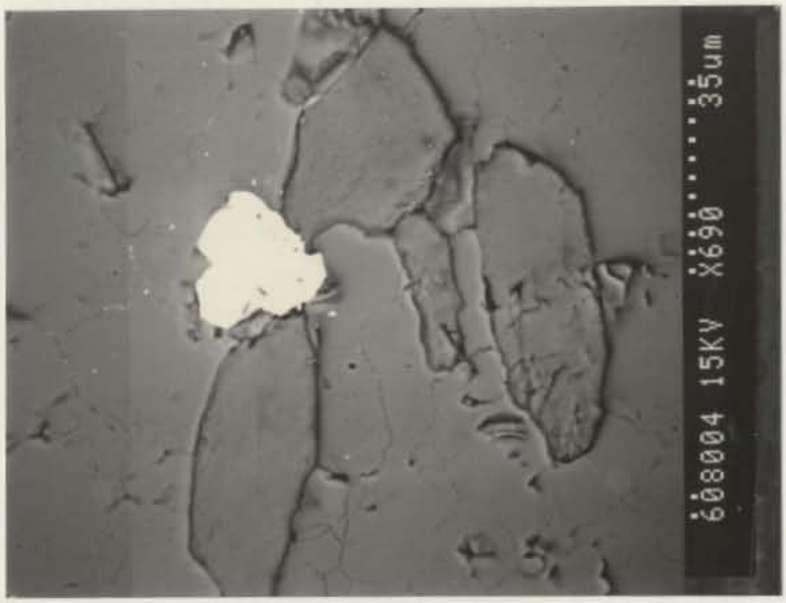

Figure 7-10: Xenotime with HREE at Hickey's Pond. Xenotime crystal (white) in specularite-banded rock at Hickey's Pond was shown to contain heavy REE. Alunite crystals stand in relief against quartz in the matrix. [Field of view 0.12 mm x 0.10 mm, backscattered electron image.]

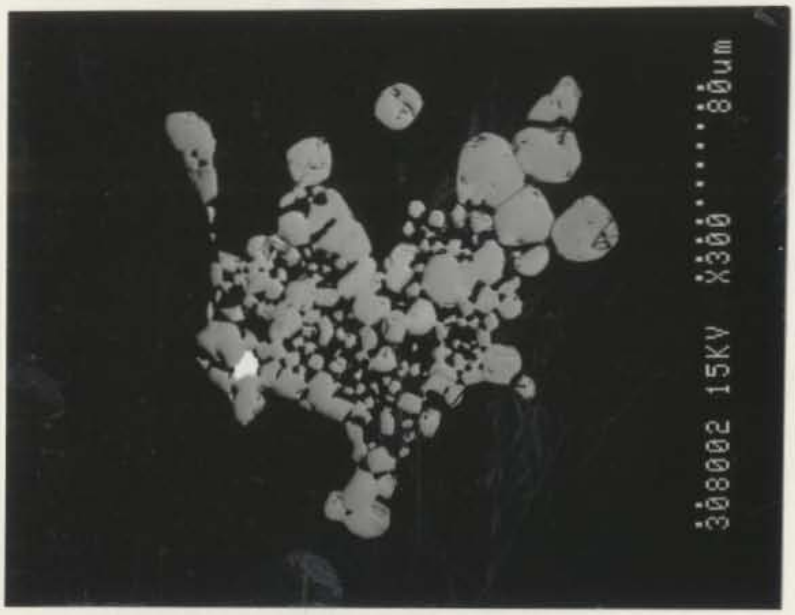

Figure 7-11: Telluriferous tennantite at Hickey's Pond. Telluriferous tennantite (white) fills interstices among pyrite crystals (grey) in rock inferred to be hotsprings precipitate at Hickey's Pond. Black matrix is quartz and alunite. [Field of view 0.27 mm x 0.23 mm, backscattered electron image.]

elements at the Chimney Falls showing, where it was described as telluriferous tennantite (Section 7.3.2).

7.5.3. Discussion

7.5.3.1. Geochemical comparison of breccias at Hickey's Pond and Chimney Falls

Textural evidence discussed in Chapter 6 showed that the specularite-rich breccias at Hickey's Pond and Chimney Falls formed by hydrothermal brecciation. Mineralogical similarities suggest that they formed either in the same, or in similar hydrothermal systems, and this interpretation is supported by geochemical similarities.

Certain geochemical similarities reflect obvious mineralogical similarities,

e.g., the high iron concentrations in the breccias at Hickey's Pond and Chimney Falls (up to 50.40% and 19.46% Fe_2O_3, respectively) are the result of high specularite contents. High phosphorous concentrations reflect less obvious Y-HREE-phosphate minerals at Hickey's Pond and P-bearing alunite at Chimney Falls.

The most important similarity among trace elements is the high concentration of gold, which is at its maximum at each showing in the breccias. Comparisons between most of the other trace elements are complicated because the respective host rocks are different mineralogically, and at the time of mineralization, they were probably very different in physical terms as host rocks to the hydrothermal conduits, *viz* the fluids in the breccia pipe at Chimney Falls probably were better contained in the "pipe" than those which erupted into the porous and permeable acid leached zone on the paleosurface at Hickey's Pond.

Thus, the list of elements which are enriched in the breccias at Chimney Falls can be reconciled with those enriched in the breccias at Hickey's Pond in the following manner:

1. Fe, P, Au, Ag, Rb, Th, U and V are enriched, at least locally, in both breccias.

2. K occurs in similar concentrations in the breccias from both showings, but it is not anomalous at Hickey's Pond where the host rock contains the K-bearing mineral alunite.

3. The classically immobile elements Ti, Zr and Nb, which are enriched in the breccia pipe at Chimney Falls, may have exhausted their limited mobility and precipitated at that depth due to changing physical and chemical conditions.

4. Cu, Ba and Sr are enriched in the host rocks of the breccia at Hickey's Pond, but not in the breccia itself. This might indicate that these elements were transported in the breccia pipe, but migrated beyond it into the porous and permeable host rock.

Opportunities abound to reasonably account for minor geochemical

differences between the two breccias, given the differences in host rocks, depth of the systems and the capacity of hydrothermal systems to evolve. As the list above has shown, all the geochemical features can be reconciled. More important, however, in proving the equivalence of the systems responsible for the breccias at each showing, are the overwhelming similarities in terms of texture and mineralogy, which are complemented by the high concentrations of certain elements, foremost among which is gold.

7.5.3.2. Evidence for two mineralising processes

The highest gold concentrations at the showing are related to two different rock types, *viz* specularite-rich breccias and silicified rocks with pyrite, which can be distinguished on the bases of texture, mineralogy and trace element geochemistry, including Au/Ag ratios (Table 7-4).

Table 7-4: Evidence for two mineralising processes. The chart summarizes the differences between the two contrasting rock types at the Hickey's Pond Showing with the highest gold concentrations. Although different processes were responsible for their formation, they are inferred to have formed at approximately the same time and could reflect a non-continuous evolution of one system. Note that "high" and "low" trace element concentrations are relative to the other rock type.

	Silicified, pyritiferous rocks	Specularite - rich breccias
Color	Pale grey	Black, deep purple with white fragments
Texture	Massive, volcanic textures preserved, network of quartz-pyrite veinlets	Brecciated fragments in fine - grained matrix
Alteration minerals	Quartz	Quartz, alunite
Vein minerals	Quartz, pyrite	Quartz, specularite
Iron phase	Pyrite	Specularite
Gold	Gold telluride	Native gold
Trace elements: "high" "low"	Cu, Ag P, Hg, Ba, Sr	P, Hg, Rb Cu, Ag
Au / Ag ratio	< 1	> 1

These observations suggest that two different mineralizing systems acted at Hickey's Pond.

7.5.3.3. Source of gold in specularite-banded and pyritiferous rocks

For purposes of the discussion to follow, the gold mineralization associated with the silicified, pyrite-bearing rocks is called (arbitrarily) Stage I and that associated with the specularite-rich breccias is called Stage II. Given that these two mineralizing processes have recognizable geochemical signatures, the question is raised: can either or both of the mineralizing events, Stage I or Stage II be implicated in the mineralization of the more abundant pyritiferous and specularite-banded rocks?

Comparison of Tables 7-2 and 7-3 shows that the specularite-banded rocks at Hickey's Pond contain more P, Hg and Au than the (unmineralized) specularite-bearing rock at the Tower showing. This element suite is diagnostic of the specularite-rich breccias at Hickey's Pond, which are herein implicated in the gold mineralization process of the specularite-banded rocks at Hickey's Pond. The mechanism of this interaction was a migration of gold and other elements away from the breccia pipe into the porous and permeable acid-leached rock on the paleosurface. Such an interaction was inferred independently from the normative mineralogy introduced in Section 4-10. Following similar reasoning, the relatively high copper concentrations in the pyritiferous rocks suggests the involvement of the Stage I fluids in their mineralization, an interaction which was also deduced independently from the normative mineralogy described in Section 4-10. The mechanism of this interaction would be similar to that involving the Stage II fluid, *viz* the lateral migration of Au and Cu outward from the zone of intense silicification, which served as a conduit as indicated by its extensive quartz veining.

Very uniform gold concentrations, and a lack of visible (to the SEM) gold suggests a thorough saturation of the rock with the mineralizing fluid, as opposed to a vein or fracture controlled type of mineralization. This is consistent with the

processes proposed above for the mineralization of the alunite-bearing rocks.

7.6. Ridge Showing

Gold, silver and selected trace elements were analyzed in 9 samples from the Ridge Showing (Table 7-5).

Table 7-5: Geochemistry of Ridge Showing samples. Note the higher concentrations of Sr, TiO_2, Zr and V in the quartz - pyrophyllite schists with specularite compared to those without specularite, and the lack of Au which transcends all rock types. [Data are presented split according to rock type. All elements are reported in parts per million (g/t) except Au in parts per billion (mg/t) and TiO_2 in weight percent. "0" = below detection]

#	Cu	Pb	Zn	Au	Ag	Ba	Sr	Rb	U	Th	Y	TiO2	Zr	Nb	Ga	Ni	V
	Specularite - banded rocks																
295	5	57	0	0	.0	615	699	0	0	15	14	.72	220	13	10	0	72
296	6	50	0	0	.0	317	490	1	0	13	22	.39	230	12	13	0	31
	Pyritiferous rocks																
291	12	44	0	0	.1	695	827	4	0	23	19	.57	228	12	11	0	37
299	4	9	0	0	.0	459	319	0	0	13	13	.12	194	16	11	0	1
	Quartz - pyrophyllite - specularite schists																
100	0	16	0	0	.0	81	372	0	0	16	63	1.00	288	17	17	0	101
294	6	39	0	0	.0	38	468	0	6	17	50	.58	351	18	16	0	44
	Quartz - pyrophyllite schists																
293	3	11	1	0	.0	81	30	18	0	21	30	.10	170	16	14	0	0
292	3	20	0	0	.0	0	25	4	0	33	15	.08	169	15	14	0	0
	Geyserite																
297	5	31	0	5	.1	265	196	0	0	22	25	.09	165	16	9	0	7

Ag reached the 0.1 ppm detection limit in only 2 samples, and Au reached the 5 ppb detection limit in 1 sample. One of the weakly elevated Ag concentrations corresponded to the only sample of pyritiferous alunite-bearing rock analyzed, the other Ag value and the 5 ppb Au concentration came from the sample of geyserite eggs.

These data are too few to allow discussion of the precious metal concentrations, although it is interesting that the sample of pyritiferous rock, the

rock type which contains the only elevated gold concentrations at the Tower Showing, had a detectable Ag concentration.

7.7. Bullwinkle Showing

Gold and selected trace elements were analyzed in 18 samples collected at the Bullwinkle Showing, and Ag and major elements were analyzed in half of these. Data are given in Table 7-6, grouped according to rock type.

Most samples did not contain detectable gold concentrations, but 4 of the 6 pyritiferous rocks had elevated concentrations ranging from 30 to 110 ppb. The only other elevated concentrations were 15 and 121 ppb, which represent 2 of the 8 samples of banded, specularite-bearing rocks that were analyzed. Thus, the clear difference in gold concentrations in the pyritiferous and specularite-banded rocks at the Tower Showing is scarcely apparent at the Bullwinkle showing. Similarly, other elements which provided discrimination between these rock types at the Tower Showing, *viz* Cu, Ba, Sr, Pb, Ti and P, are in similar concentrations in both rock types at the Bullwinkle Showing. The only element which serves to contrast the rock types is As, which is slightly higher in the pyritiferous rocks (2 to 9 ppm) than in the specularite-banded rocks (2 to 4 ppm).

The only trace elements in remarkable concentrations are Pb, which is sporadically anomalous (to 750 ppm) in the pyritiferous rocks; Sr, which is locally very anomalous (to 1240 ppm) in the banded specularite-banded rocks; Ba, which is locally anomalous (to 1550 ppm) in either of the above rock types and Zn, which was not detected (<1 ppm) in 23 of the 24 samples in which it was analyzed.

Table 7-6: Geochemistry of Bullwinkle Showing samples. Note that no clear subdivision of specularite - banded and pyritiferous rocks, comparable to those at the Tower Showing, is possible. Low concentrations of gold appear to be more commonly associated with the pyritiferous rocks, and the specularite - rich breccias at this showing are barren of gold. [Data are presented split according to rock type. Major element oxides are reported in weight percent, Au and Hg in parts per billion (mg/t) and all other elements in parts per million (g/t). "0" = below detection, " " = no analysis was conducted.]

#	SiO2	Al2O3	Fe2O3	MgO	CaO	Na2O	K2O	TiO2	MnO	P2O5	LOI	Total	Cu	Pb	Zn	Au	Ag	Sb	As	Hg	Ba	Sr	Rb	U	Th	Y	Zr	Nb	Ga	Ni	V
Specularite - banded rocks																															
311	43.40	19.86	3.50	.00	.21	1.84	2.96	.71	.00	.39	24.26	97.13	9	86	0	0	.0	.7	4	10	1550	1160	0	3	30	12	238	14	31	0	125
314	79.85	4.12	8.13	.00	.08	.42	.49	.70	.01	.21	4.39	98.40	4	109	0	0	.0	.4	2	10	639	387	0	0	14	20	258	16	13	0	110
315													0	175	0	0	.0				1127	601	11	0	27	17	272	18	21	0	253
316													5	78	0	0	.0				669	363	2	0	6	17	162	12	4	0	35
319	76.25	9.35	8.03	.01	.05	.12	.16	.69	.01	.12	3.10	97.89	5	58	0	0	.0	.5	2	10	206	236	2	2	15	41	256	16	21	0	103
326													16	219	0	15	.1				927	739	2	0	23	18	181	12	21	0	59
432	52.45	17.27	1.90	.01	.21	2.06	1.84	.32	.00	.46	19.93	96.45	10	67	0	0		.2	3	30	1240	1240	3	0	13	7	110	6	19	0	128
436	73.80	9.45	1.72	.00	.04	1.26	.84	.59	.01	.09	11.47	99.27	5	103	0	121		.4	3	10	561	218	3	0	25	16	195	10	19	0	61
438													6	23	0	0					505	337	0	0	19	18	124	6	12	0	69
Pyritiferous rocks																															
313	57.25	13.95	4.82	.00	.13	1.57	1.09	.64	.01	.20	20.10	99.76	10	750	0	0	.0	.6	9	30	777	381	0	0	15	9	195	12	15	0	69
325													1	18	0	0	.0				1149	59	0	5	3	23	138	10	4	0	0
330	63.60	12.48	1.98	.00	.03	1.81	.70	.52	.00	.12	17.49	98.73	6	310	0	45	.1	.5	9	10	897	373	0	0	13	11	218	12	20	0	31
435	54.65	16.66	2.00	.01	.06	1.79	1.96	.47	.01	.18	19.60	97.39	11	94	0	47		.6	9	20	854	491	3	4	22	9	148	8	18	0	80
443	93.30	1.88	1.06	.01	.01	.11	.30	.50	.01	.04	1.67	98.89	6	64	0	110		.2	2	10	382	104	7	0	7	11	184	10	3	0	18
444	63.35	13.11	3.84	.01	.05	1.53	.58	.53	.01	.19	15.77	98.97	9	525	0	30		.4	9	20	865	450	3	5	16	18	230	12	17	0	58
Specularite - rich breccias																															
320	73.00	5.17	11.52	.00	.09	.57	.27	.62	.01	.22	5.79	97.26	0	172	0	0	.0	.4	4	10	893	363	6	1	9	23	231	17	8	0	122
321	92.45	1.20	2.38	.00	.00	.14	.13	.64	.00	.03	1.84	98.81	0	24	0	0	.1	.6	2	10	70	42	0	0	6	18	192	16	2	0	0
329	84.15	4.73	2.06	.00	.09	.66	.33	.56	.00	.06	6.15	98.79	3	20	0	0	.0	.4	1	10	213	179	0	2	14	23	208	13	7	0	36

7.7.1. Specularite-rich breccias

No Au was detected in any of the 3 samples of specularite-rich breccia analyzed at the Bullwinkle Showing. Comparing the breccias to those at Hickey's Pond, they also have very low concentrations of Ag, Hg, As, Sb, Rb, U, Th, V and P.

7.7.2. SEM-EDX investigation

One thin section of specularite-rich breccia, and one of banded specularite-bearing rock were examined with the SEM under the backscattered electron mode. No unusual compounds were noted.

7.7.3. Discussion

7.7.3.1. Specularite-rich breccias

Section 7.7.1 describes specularite-rich breccias which contrast sharply with those at Chimney Falls and Hickey's Pond by having gold concentrations below detection, despite their textural and mineralogical similarities. The barren state of the breccias at the Bullwinkle Showing can be explained as the result of gold precipitation lower in the system. Although proof of this would require mapping the breccias in three dimensions, the explanation is reasonable because the breccias at Hickey's Pond (a much smaller showing) underlie a much larger area. Since the breccias at both showings represent intrusions onto the paleosurface, it can be said that the boiling level was higher at the Hickey's Pond showing. A corollary of this is that similar mineralized breccias occur stratigraphically under the Bullwinkle Showing.

7.7.3.2. Non-brecciated rocks

The more common pyritiferous and specularite-banded rocks at the Bullwinkle Showing are characterized by relatively low precious metal concentrations. This feature allies them more closely with those at the Tower Showing than those at Hickey's Pond. It was suggested in Section 7.5.3.3 that the

gold in the non-brecciated rocks at Hickey's Pond moved laterally away from the two types of auriferous "conduits" (now specularite-rich breccia and silicified, pyritiferous rocks) into the porous and permeable acid-leached host. Such a process did not happen at the Bullwinkle Showing as the breccias there are volumetrically minor and geochemically barren of Au, nor are there silicified *sensu stricto*, pyritiferous rocks.

The rocks at the Bullwinkle Showing which most commonly contain elevated gold concentrations contain pyrite as opposed to specularite. This distinction is not as consistent as at the Tower Showing, but suggests the same source of mineralizing fluid, namely the late, H_2S-bearing fluid which was responsible for the formation of pyrite. The possibility remains that this fluid represents the final stage of the original fluid which boiled at an unknown depth to produce the alunite mineralization on the paleosurface. Implicit in this is the possibility of mineralized zones at the depth of boiling.

7.8. Strange Showing

Gold analyses were performed on four rocks from the Strange Showing, including 3 specularite-rich rocks (Table 7-7). All the specularite-rich rocks have elevated gold concentrations, ranging from 276 to 813 ppb. No gold was detected in the one sample of pink rhyolite with disseminated pyrite that was analyzed for gold. Only two Ag analyses were performed; one on a specularite-rich rock and the other on a pink, pyritiferous rock, but no Ag was detected in either sample.

Table 7-7 also includes major element geochemistry and selected trace elements. Relative to the host rhyolite, the specularite-rich breccias contain significantly more SiO_2, Fe_2O_3, Au and possibly V, and significantly less Al_2O_3, Na_2O, K_2O, Ba, Sr and Rb. Although the loss of the latter group of elements tends to distinguish the breccias at the Strange Showing geochemically from those at other showings, their absence probably reflects the lack of alunite at the showing, which may itself reflect a structurally imposed segregation (Section 6.6).

Table 7-7: Geochemistry of Strange Showing samples. Note the consistently elevated gold concentrations in the specularite - rich breccias, and the relatively low concentrations of Na2O, K2O, Ba, Sr and Rb which tend to distinguish the breccias at this showing geochemically from the others. [Data are presented split according to rock type. Major element oxides are reported in weight percent, Au in parts per billion (mg/t) and all other elements in parts per million (g/t). "0" = below detection, " " = no analysis was conducted.]

#	SiO2	Al2O3	Fe2O3	MgO	CaO	Na2O	K2O	TiO2	MnO	P2O5	LOI	Total	Cu	Pb	Zn	Au	Ag	Ba	Sr	Rb	U	Th	Y	Zr	Nb	Ga	Ni	V
Specularite - rich breccias																												
327	91.70	1.08	5.40	.07	.04	.04	.03	.48	.01	.03	.88	99.76	3	2	0	800	.0	0	6	0	0	1	11	177	14	6	0	0
440													3	12	0	276		131	11	14	1	10	19	204	10	5	0	82
441	96.00	.26	2.47	.00	.01	.05	.05	.42	.00	.03	.66	99.95	6	23	0	813		0	3	4	1	12	10	153	7	1	0	20
Pink rhyolite																												
328	76.80	10.32	2.16	.02	.09	3.70	3.76	.20	.01	.02	2.09	99.17	0	20	0	0	.0	147	52	87	2	20	55	520	51	17	0	0

7.8.1. SEM-EDX investigation

A rounded crystal 0.005 mm in diameter consists primarily of Bi, Al and P, with minor concentrations of Ag, Ca, Ba, Si and Fe (Figures 7-12, A-24).

Figure 7-12: Bi-Al phosphate at Strange Showing. Grey, semicircular crystal is a phosphate of Bi and Al (Waylandite?, Zairite?). Small black circle in centre of crystal represents decrepitation under the electron beam during spot analysis. White, semicircular rim is native bismuth. Significant concentrations of Ag, Ca and Ba occur in the phosphate (Figure A-24) and Se and Te occur in the bismuth (Figure A-25). [Field of view 0.014 mm x 0.012 mm, backscattered electron image.]

During spot analysis, it decrepitated under the electron beam (see Figure 7-12), behaviour common in sulfates and phosphates. Possible phosphate minerals it might represent include Waylandite ($(Bi,Ca)Al_3(PO_4,SiO_4)_2(OH)_6$) and Zairite ($(Bi(Fe,Al)_3(PO_4)_2(OH)_6$). An irregular, ragged rim around half of this crystal displayed a stronger backscatter (Figure 7-12) and was shown to consist primarily of Bi, but low concentrations of Se, Te, P and Fe were detected (native Bi?, Figure A-25). A prominent Si peak is inferred to represent quartz "sampled" by the beam adjacent to the target mineral which was only 0.001 mm across.

Very small apatite crystals were noted throughout the slide. An irregular

crystal 0.02 mm across was shown to be native Au, with only minor Ag peaks present on the spectrum.

7.8.2. Discussion

It was shown in Section 2.3.1 that the Strange Showing was a mylonite zone, but a possible relict breccia texture, together with the abundance of specularite suggested that it may be a mylonitized equivalent of the breccia zone at Chimney Falls (Section 6.6). The presence of native Au and Bi (?), together with the phosphate mineral containing Se, Te, Ag and Ba strengthens the similarity with the other mineralized breccia zones. Section 7.7.3.1 alluded to the possibility of mineralized specularite-rich breccias stratigraphically underlying the Bullwinkle Showing. In light of the intense compression and shearing the area underwent, and the east-west striking faults which intervene between the Bullwinkle and Strange Showings, it is proposed that the Strange Showing represents part of this hypothesized zone. It is not inferred to be the mineralized zone postulated in Section 7.7.3.2.

7.9. Monkstown Road Area

7.9.1. Monkstown Road Specularite Showing

Gold analyses were performed on 5 samples from this showing, and silver concentrations determined on 2 samples. Neither element reached the detection limit in any of the samples.

7.9.2. Little Pond Specularite Showing

Two samples from this showing were analyzed for gold and silver, but neither element was present above the detection limit.

A thin section of one of the specularite-rich bands was prepared and examined under the SEM under backscattered electron mode. Several scattered, euhedral crystals of apatite and monazite up to 0.015 mm across were noted.

Other crystals of a compound containing Bi and Te with lesser Se were noted (Figure A-26). They are inferred to be tellurobismuthite (Bi_2Te_3) on the bases of a clear hexagonal outline of one crystal (Figure 7-13) and the presence of Se.

Figure 7-13: Tellurobismuthite at Little Pond Showing. White crystal to right of centre is tellurobismuthite (note perfect hexagonal outline). Other white crystals are xenotime, grey crystals are specularite. Black matrix is quartz and pyrophyllite. [Field of view 0.28 mm x 0.24 mm, backscattered electron image.]

The occurrence of tellurobismuthite serves to link this showing with the auriferous specularite-rich breccias at Hickey's Pond, Chimney Falls and the Strange showings, where similar compounds occur. As such, it indicates that gold could have been precipitated lower in the hydrothermal system responsible for the exhalite at the Little Pond Showing. Phosphates have also been noted in the breccia pipes and in the acid leached alunite-bearing rocks, serving as another potential link with the system elsewhere.

7.9.3. Paradise River Showing

Three samples from this showing were analyzed for gold and silver. None of the samples contains even the detection limit for either element.

7.9.4. Conclusion

The most significant aspect of the geochemical data presented above is that rocks at the Hickey's Pond Showing, which are mineralogically and texturally similar to certain rocks present at the Tower, Ridge and Bullwinkle showings, contain consistently elevated gold concentrations whereas the other rocks are virtually barren. The following chapter, a discussion of epithermal systems, shows that the presence of gold in rocks such as those at Hickey's Pond is unusual. However, this chapter also suggests that the presence of gold at Hickey's Pond relates not to the essential processes which formed the rock, but to later intrusions of auriferous fluids into the near surface environment, their passageways marked by specularite-rich hydrothermal breccias and zones of intense silicification with pyrite. Two occurrences of specularite-rich breccias at deeper stratigraphic levels (Chimney Falls and the Strange Showing) contain the highest gold concentrations away from Hickey's Pond. .

Chapter 8
EPITHERMAL GOLD DEPOSITS

8.1. Introduction

The term epithermal was introduced by Lindgren in 1911 to describe precious metal deposits that form veins and breccias at shallow levels in association with extrusive and intrusive igneous rocks. A substantial volume of literature has described these deposits in terms of the time of formation relative to the host rock, and the origin, temperature and chemical characteristics of the mineralizing fluid (Henley and Ellis, 1983; Buchanan, 1981; Sillitoe, 1977; Panteleyev, 1986; papers in Berger and Bethke (editors), 1985). It has been shown that these deposits reflect the action of relatively cool (250 degrees Celsius), dilute saline (3% equivalent NaCl) waters of predominantly meteoric origin that were active shortly after the eruption of their host rocks. This description applies equally well to modern geothermal systems, which are now considered modern analogues of ancient epithermal systems (White, 1955; Henley and Ellis, 1983; Henley, 1985).

Possibly the most contentious issue regarding these deposits is the source of ore metals, which amounts to a question of the importance of a magmatic component to the hydrothermal fluid. This debate is not considered here, because epithermal fluids need not be especially rich to lead to rich mineralization. Ewers and Keays (1977) summarize data for metal concentrations in geothermal waters discharged from two wells at Broadlands, New Zealand (BR 2 and BR 7). The concentration of gold in discharges from BR 2 is 0.04 ppb Au, and from BR 7 it varies from 0.1 to 1 ppb. Brown (1986) observed and attempted to correct for gold deposition in geothermal apparatus similar to that from which the authors

cited above collected their samples. His corrected gold concentration was 1.5 ppb, which despite the correction, remains a small concentration. Despite the low concentration in the fluid, precipitates from the fluid at BR 2 contain 55 000 ppb Au (Weissberg, 1969), which would constitute a very rich ore.

Much of the diversity apparent in epithermal systems stems from the geological factors which cause the entrained gold to precipitate. Deposition of gold occurs in response to chemical and physical changes in the gold-bearing solution, foremost among which are changes in temperature, pressure, pH, oxidation potential and total sulfur concentration. Geological processes which can lead to rapid changes in these parameters are: 1) boiling of the mineralizing solution 2) mixing of the mineralizing solution with a different solution and 3) changes caused by interactions of the fluid and the surficial environment. Epithermal "models" have been developed to illustrate the effects each of these geological processes has on the fluid. These models, which follow the threefold subdivision employed by Berger and Eimon (1983), are discussed in the following sections.

8.2. Boiling model

The significant chemical effects of boiling in reference to the deposition of metals were expounded by Drummond and Ohmoto (1985). They show that the most immediate chemical changes in the solution reflect the loss of CO_2, H_2S, CH_4, SO_2 and H_2 to the vapour phase. Factors which promote this are 1) low solution temperatures because the partitioning of volatiles into the gas, the volatility ratio, is larger at low temperatures, 2) boiling in open systems, in which the gases are removed from the system to prohibit their interaction with the liquid and 3) isoenthalpic boiling, because the diminishing temperature is accompanied by increasing volatility ratios.

The most significant effect of this devolatilization is the consumption of H^+ ions, primarily by recombination with bicarbonate ion to replenish the CO_2. The

consumption of H^+ ions is recorded as a rise in pH and is a suitable mechanism for the precipitation of chloride complexed metals. Factors which promote the rise in pH include the three factors which promote devolatilization, discussed above, and large initial $[CO_2]/[H^+]$ ratios (Drummond and Ohmoto, 1985). A factor which inhibits the pH rise for a given amount of devolatilization is a large initial concentration of incompletely dissociated acid, in particular the HSO_4^- species.

The response of thio complexed metals to increasing pH, when the initial pH is near neutral, is opposite that of chloride complexed metals (Drummond and Ohmoto, 1985; Hedenquist and Henley, 1985), i.e., their solubility is enhanced. However, other chemical changes which accompany boiling tend to counteract this, foremost among which is the reduction in reduced sulfur species which accompanies H_2S outgassing. The strong partitioning of H_2S into the vapour can lead to the loss of 97% of the H_2S from the solution under geologically reasonable conditions, which can lead to a reduction in gold solubility by a factor of 100 (Hedenquist and Henley, 1985). Brown (1986) illustrates the efficacy of boiling as a mechanism for gold deposition by documenting the occurrence of precipitates containing up to 7.3% Au and 20.9% Ag on the steam separation equipment at geothermal plants at Broadlands and Kawerau, New Zealand.

Another chemical change which accompanies boiling and which tends to destabilize thio complexed metals is an increase in oxygen fugacity. This reflects the preferential outgassing of the reduced forms of C (CH_4 relative to CO_2), S (H_2S relative to SO_2) and H (H_2 relative to H_2O) (Buchanan, 1981; Drummond and Ohmoto, 1985). Drummond and Ohmoto, however, question the ability of the solution to re-equilibrate its redox state in a reasonable time after boiling. Similarly, Henley (1985) cautioned against attempts to model the sluggish redox reactions in the highly disequilibrated boiling process. Citing Brown's (1986) observation that gold deposition occurs seconds after boiling of the solution, Henley concluded that non-redox reactions, such as the conversion and loss of HS^- as H_2S or HCO_3^- as CO_2) and the attendant sulfur concentration and pH changes

are more important in causing gold precipitation than are redox changes.

The final effect of boiling which could lead to the precipitation of gold is cooling of the solution. Given that boiling in geothermal systems occurs in response to decreased lithostatic pressure associated with upward flow, as opposed to an increased temperature caused by an influx of heat, the boiling is approximately adiabatic and must result in cooling. The importance of cooling as a depositional process has been questioned by Buchanan (1981). He suggested that reductions in temperature would be buffered by the thermal "reservoir" of the wall rock.

Buchanan (1981) attributed several features of epithermal systems to boiling of the mineralizing fluid, the most important of which is the distribution of base and precious metals. A salient feature of his compilation of 60 epithermal deposits is the vertical zonation (in ascending order) of a basemetal-rich zone, a silver-rich zone and a gold-rich zone (Figure 8-1). This zonation is attributed to sequential destabilization of complexed basemetals, silver and gold in a boiling system that progressively lost CO_2 and H_2S. Adding to the spatial separation of the precious metals from the basemetals, as opposed to a strictly temporal (paragenetic) separation, is the physical transport upward of the precious metals in the boiling, effervescing solution (Buchanan, 1981).

Buchanan offers fluid inclusion evidence that boiling occurs in natural hydrothermal systems. In a 2.1 cm wide banded veinlet from Guanajuato, he documented 6 distinct episodes of boiling of the fluid. Similarly, he attributes the occurrence of 81 alternating bands of quartz-chlorite and quartz-adularia in a 10 cm slab of a mineralized vein from Oatman, Arizona, to episodic boiling of the fluid. The episodic nature of the boiling reflects a cycle of boiling, mineral precipitation in the conduits causing pressure increases and the cessation of boiling, to be followed by the rupturing of the seal by tectonism or hydrofracturing and the start of another boiling episode.

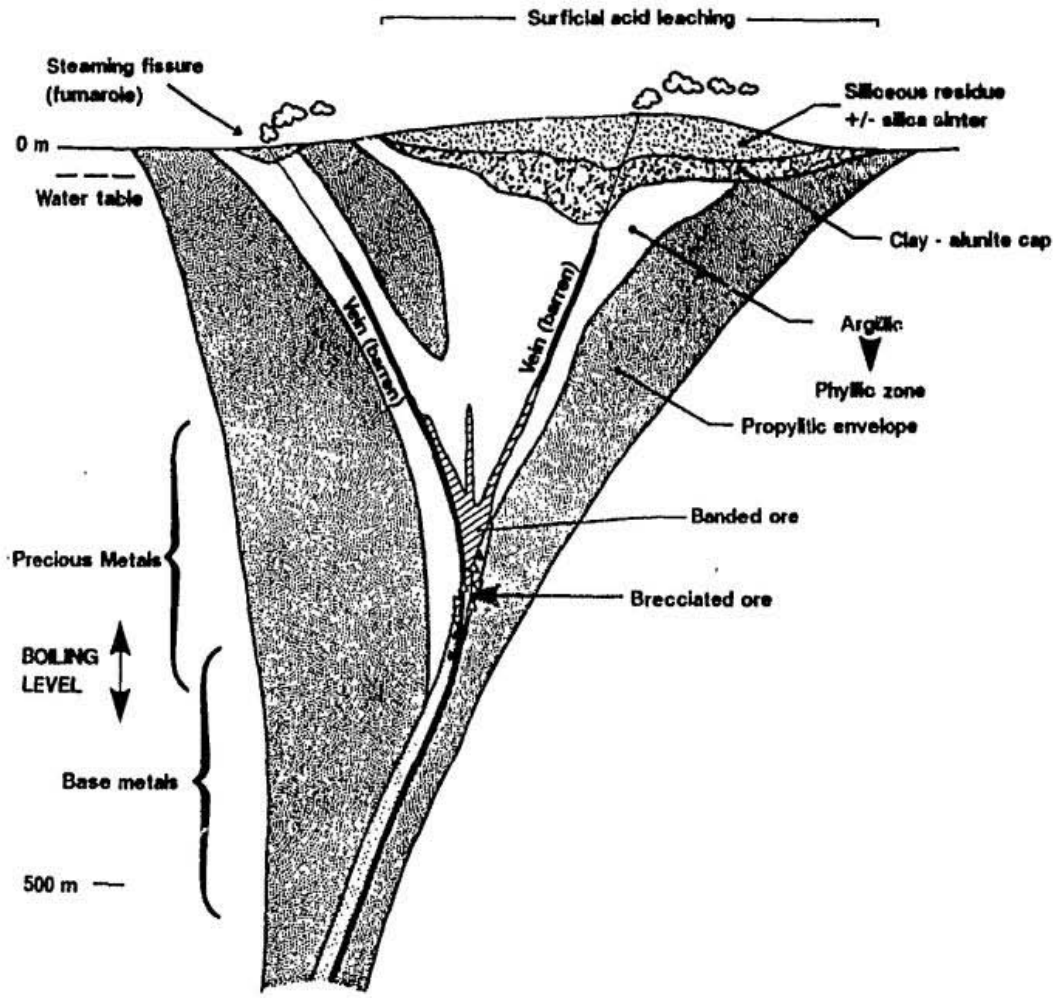

Figure 8-1: Epithermal system - boiling model. Distribution of alteration zones around boiling, ascending fluid is idealized. Note the separation between the ore zone and the silica and alunite-bearing cap rocks of the acid-leached zone. [From Buchanan, 1981.]

Ewers and Keays (1977) invoke boiling of an ascending fluid to account for anomalously high concentrations of Au, As and Sb at certain depths in the Broadlands geothermal field, New Zealand. They correlate the anomalous zones with regions of formerly high porosity and permeability and suggest that boiling occurred in these zones due to their inability to contain the fluids' vapour pressure.

8.3. Mixing model

A second geological process which can lead to the precipitation of gold entrained in a rising hydrothermal fluid is mixing. Physical and chemical parameters relevant to the transport of gold which can change as a result of mixing are temperature, oxidation state, pH and total sulfur. The efficiency of the process depends on the contrasts between the fluids and the proportions in which they mix.

Evidence of fluid mixing is best documented at the Creede mining district, Colorado (Figure 8-2). Hayba *et al.* (1985) provide a thorough summary of metallogenic investigations there, including their own previous works (Hayba, 1984; Foley *et al.*, 1982; Bethke *et al.*, 1973). The following descriptions of the different lines of evidence for mixing are from Hayba *et al.* (1985).

The orebodies occur in flat-lying, fractured welded tuffs which are overlain by soft, unwelded, impermeable tuffs. They also occur in the porous, clastic caldera fill sedimentary rocks of the Creede Formation, where they abut against the fractured, mineralized welded tuffs. This distribution shows that the ore-bearing fluids were moving laterally beneath the aquitard of the soft impermeable tuffs towards the caldera, approximately from north to south. At the time of mineralization, there was a strong topographic gradient between the collapsed caldera and a chain of volcanoes 10 km to the north on the present continental divide. The difference in elevations of approximately 1000 m (Steven and Eaton, 1975) would have imparted a strong lateral pressure gradient to the groundwater,

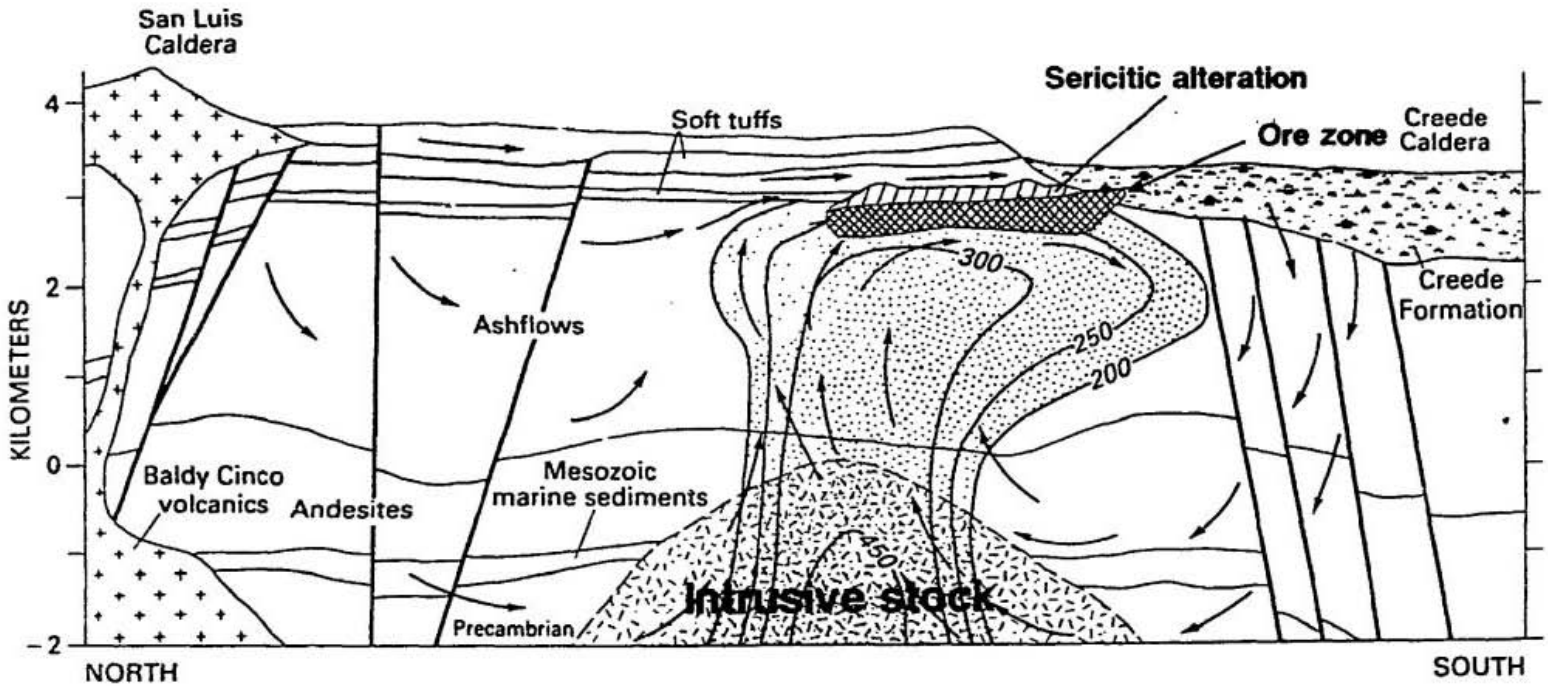

Figure 8-2: Epithermal system - mixing model. Schematic cross-section of the Creede, Colorado system illustrates mixing between ascending hydrothermal fluid (stippled) and groundwater flowing north to south. Note that the system does not discharge onto the surface, preventing the formation of an acid-leached cap. [From Hayba *et al.*, 1985.]

causing north to south movement. Hayba *et al.* cite the numerical models of Hanaoka (1980), which predict a deep convecting system overlain by a cooler groundwater cap for areas in which strong lateral hydraulic gradients are present in the groundwater overlying an upwelling hydrothermal fluid. Fluid flow would be approximately parallel at the interface of the two fluid types but conductive heat transfer and physical mixing would occur.

Thus, there is circumstantial evidence that mixing of cool groundwater and hydrothermal waters could have taken place. Evidence that this mixing did take place is provided by the detailed isotopic study of Foley *et al.* (1982). They describe two isotopically distinct waters in fluid inclusions in quartz: 1) primary fluid inclusions which are similar in terms of salinity, homogenization temperature and hydrogen isotope composition to primary fluid inclusions in sphalerite and 2) pseudosecondary inclusions of "fresh" water (relative to the saline fluids in the primary inclusions) with slightly lower homogenization temperatures and hydrogen isotope compositions 30 permil lighter than those of the primary inclusions. Their interpretation is that the latter fluid was part of the cooler, unevolved regional groundwater that periodically mixed with the mineralizing fluid. They suggest that its incorporation as pseudosecondary inclusions reflects fracturing resulting from the thermal shock associated with its introduction.

Additional evidence for mixing of different fluids is given in fluid inclusion studies by Roedder (1977), Hayba (1984) and Robinson and Norman (1984). Roedder measured freezing and homogenization temperatures of 221 fluid inclusions in 20 separate growth zones of a sample of banded sphalerite from Creede. Hayba *et al.* (1985) plotted these data as equivalent chloride content and heat content respectively. They showed that the mineralizing "fluid" could be successfully modelled as different proportions of two end members: 1) fresh surface water at approximately 160 degrees Celsius and 2) mineralizing fluid with approximately 10 equivalent weight % NaCl at 270 degrees Celsius. Boiling of the fluid would cause cooling and increases in salinity, a trend which is opposite to that defined by the data. Although small amounts of (pre-mixing) boiling of

the hot, saline end member could be inferred for the data, most of the waters' characteristics derive from mixing (Hayba *et al.*, 1985).

Hayba (1984) studied the variation in fluid inclusion characteristics over a strike length of 1000 m of the OH vein at Creede. His study pertained to a distinctive phase of sphalerite growth which was recognizable throughout the vein; therefore his observations record purely spatial variations, as opposed to temporal. He documented progressive north to south decreases in temperature and salinity. These were interpreted to represent progressive mixing of a hot, saline mineralizing fluid and cooler, slightly preheated fresh water.

Robinson and Norman (1984) studied the variation in the vertical dimension of fluid inclusions in quartz at the Amethyst vein at Creede. They demonstrated decreasing temperatures and salinities with increasing elevation and appealed to mixing of the ascending ore fluid and cooler, overlying fresh waters to explain their observations.

8.4. Hotsprings model

Unlike the boiling and mixing models discussed above, several geological processes can be active in the hotsprings model (Figure 8-3), including boiling and mixing. Its salient characteristic is that processes which act to cause the precipitation of gold do so in response to contact with the surface (Berger and Eimon, 1983). Boiling and mixing in the hotsprings environment change the same physical and chemical parameters as they do when active at greater depths. However, unique characteristics of their action in the hotsprings environment are discussed here, where it is shown that processes responsible for precipitating gold in the hotsprings environment can be more efficient than similar processes acting at depth. This does not mean however, that hotsprings gold deposits are richer or larger than deeper ones. **An essential requirement for gold deposition in the hotsprings environment is that the gold was not precipitated from the solution at depth.** This requirement is commonly not satisfied, as

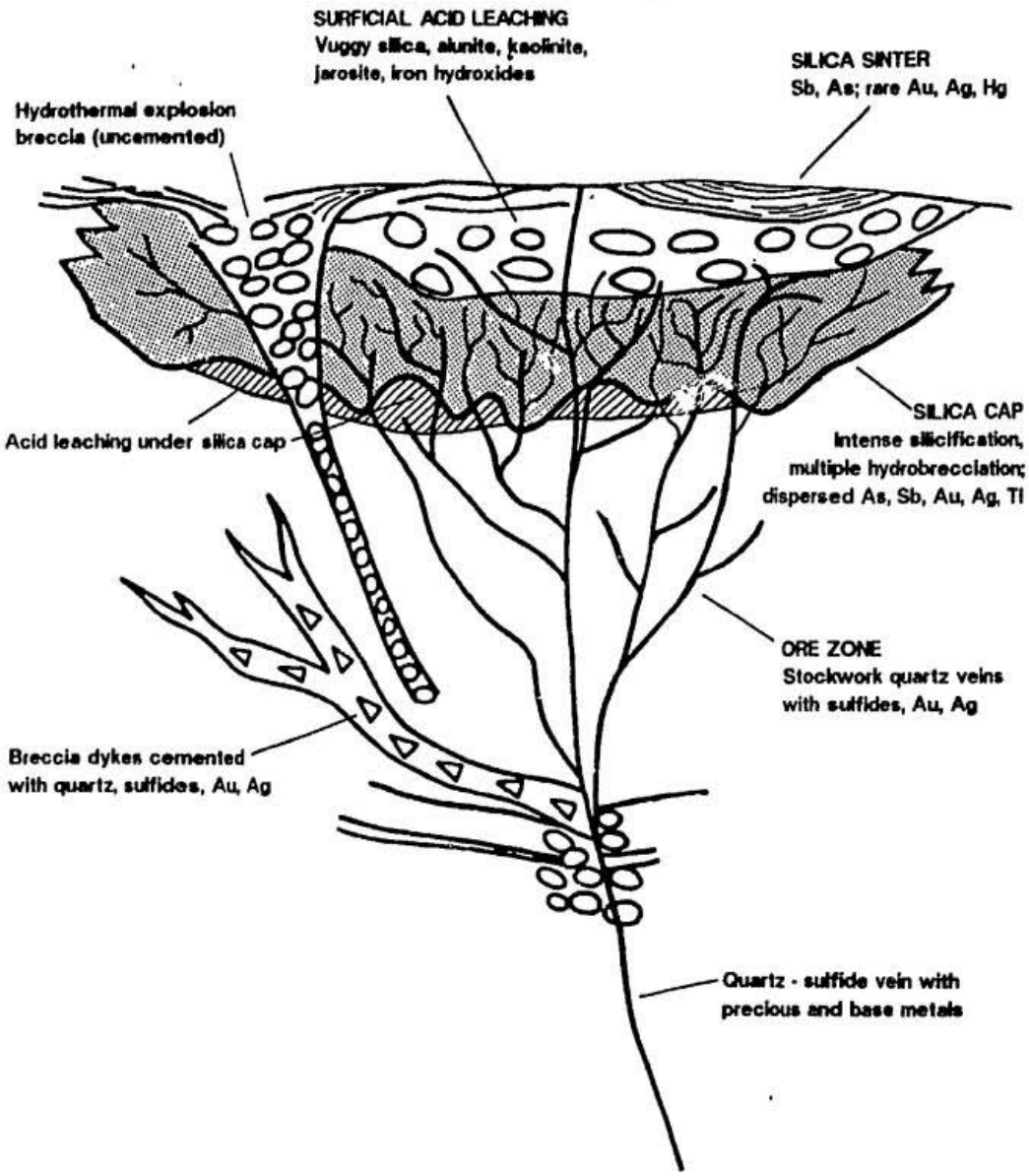

Figure 8-3: Epithermal system - hotsprings model. Distribution of alteration mineralogy and morphologies is idealized for a hydrothermal fluid ascending to surface. Note "compression" of ore zone into close proximity with acid-leached zone (compare with Figure 8-1), which can develop under silica cap following condensation and oxidation there of ascending acidic gases. Not shown is "channelling" of fluid into hydrothermal explosion breccia "conduits". [From Berger and Eimon, 1983.]

demonstrated by the common occurrence of barren sinters and surficial alteration features. For purposes of the discussion to follow, however, it is assumed that the ascending fluid has not precipitated its dissolved gold. The following sections discuss the processes in the hotsprings environment which lead to gold deposition. It should be borne in mind that all of these processes can act in concert.

8.4.1. Boiling

The chemical parameter changed during boiling which serves most to cause gold precipitation is the concentration of sulphide species. The feature of boiling in the hotsprings environment which increases the efficiency of their loss (through evolution of H_2S gas) is that boiling occurs in an approximately open system (Hedenquist and Henley, 1985). Hedenquist and Henley show that the small vapour loss associated with boiling in deep, closed systems may be sufficient to lead to precipitation of base metals, but would probably not cause gold deposition. Gold solubility could actually increase where the effects of pH increase outweigh those of decreasing sulphide concentration. Where boiling occurs above throttle points, i.e. where lithostatic pressure is negligible, the loss of H_2S can be nearly complete and gold solubility is decreased by a factor of over 100 (Hedenquist and Henley, 1985).

One geological feature which promotes open boiling of an ascending fluid is a hydrothermal eruption vent. The formation of these features is described by Hedenquist and Henley (1985), Nelson and Giles (1985) and Sillitoe *et al.* (1984). These authors question the generally held theory for the origin of hydrothermal eruptions, which involves a gradual increase in fluid overpressure, i.e. pressure greater than hydrostatic, until the sum of hydrostatic, lithostatic and rock tensile strength are exceeded. Under these circumstances, the rocks fracture and enormous volume increases ensue in the suddenly depressurized fluid. Nelson and Giles (1985) and Sillitoe *et al.* (1984) favour influxes of magmatic heat and magma respectively to cause rapid pressure increases. These overwhelm the ability of the fluid to migrate down pressure gradients and a hydrothermal explosion results.

Hedenquist and Henley (1985) proposed that reservoirs of compressed gas would form in locally sealed areas above boiling ascending fluids. Rupturing of these reservoirs due to seismicity would allow the gas cap to expand rapidly and breach the surface.

Regardless of origin, hydrothermal explosions occur forming breccia pipes and commonly fallout aprons of transported material. The breccia pipes commonly host gold deposits, an association described by Sillitoe *et al.* (1984), Nelson and Giles (1985) and Hedenquist and Henley (1985). This association occurs because hydrothermal eruptions reflect the action of upwelling fluids which may be gas-rich and metal-rich. These fluids are focussed into the breccia pipes where boiling and gold precipitation occur in the shallow subsurface.

8.4.2. Mixing

The general effects of fluid mixing were discussed in Section 8.3. Mixing in the hotsprings environment can be more efficient than mixing at deeper levels because of the nature of the near-surface fluids with which the mineralizing fluid is likely to mix. Surficial waters tend to be cool and highly oxidized, either feature of which would promote gold deposition. Two subtypes of surficial fluid are recognized, *viz* fresh and steam-heated. The origin of the latter fluid was treated in detail in Chapter 5, where it was shown to relate to surficial oxidation of sulfur-rich vapours evolved from boiling fluids at depth. Although the steam-heated waters by themselves do not form gold deposits, gold mineralization occurs in the surficial acid leached zone where mineralizing fluids mix with steam-heated waters. Deposition of gold is favoured by the mixing of these fluids due to the very low pH's typical of the steam-heated waters. This process is invoked by Krupp and Seward to account for the very high concentrations of gold, up to 50 ppm, precipitating in alunite-bearing sulfide-rich muds in acid hotsprings near Lake Rotokawa, New Zealand.

8.4.3. Cooling

Geothermal gradients tend to steepen as the surface is approached, and cooling decreases the solubility of gold complexed in hydrothermal solutions. Ewers and Keays (1977) studied the zoning of precious and trace elements to a depth of 1400 m in a geothermal well at Broadlands, New Zealand. Of the elements analyzed, it was concluded that only Tl was precipitated solely in response to decreasing temperature. Other elements, including gold were precipitated owing to the combined effects of decreasing temperature and minor amounts of boiling. Similarly, Hedenquist and Henley (1985) concluded that cooling in the Champagne Pool, New Zealand was not an important direct factor in the precipitation of gold there, although indirectly its importance increased where gold coprecipitated with sulphides destabilized by cooling. Thus, although cooling is most important in the hotsprings model, its effects are largely overshadowed by those of boiling and mixing.

8.5. Ore characteristics

The characterization of ore in adularia-sericite type epithermal deposits can be subdivided according to their mechanism of precipitation. Common to all of them is a very low content of basemetals.

Deep boiling gives rise to the classic, banded bonanza veins. The veins commonly mark the positions of paleofaults which localized the mineralizing fluid. They are repetitively banded with fine-grained quartz, adularia and sericite and may contain large amounts of calcite or chlorite. Native gold is commonly associated with electrum, argentite and sulfosalts of Ag and Cu (Buchanan, 1981; Silberman and Berger, 1985; Giles and Nelson, 1982). Pyrite is the predominant sulphide mineral. The veins persist over large vertical intervals; generally larger than the contained ore zones. Basemetal contents increase as gold decreases near the bottom of the ore zone, and barren quartz veins with increasing calcite extend upward from the ore zone (Buchanan, 1981).

The Creede deposit, which formed from mixing solutions is characterized by a large lateral extent. Mining in one vein occurred over a 3 km length but a vertical interval of only 200-400 m. The ore occurs predominantly in veins localized in radial faults which run north from the Creede caldera. Disseminated mineralization occurs where the mineralized faults intersect the sedimentary sequences of the intracaldera Creede Formation. Silver is much more abundant than gold (Ag:Au = 400) and the deposit is unusual because of its high basemetal content (7.5% total Cu-Pb-Zn). The veins consist of quartz and adularia with much lesser basemetal sulphides, fluorite, barite, chlorite, tetrahedrite, native silver and silver sulfosalts. Vein textures reflect open space fillings (Hayba *et al.*, 1985; Berger and Eimon, 1983).

In marked contrast to the relatively deep-seated vein deposits described above, ore deposits formed in the hotsprings environment are characterized by abundant hydrothermal brecciation (Berger and Eimon, 1983). Ore occurs commonly in pipe or funnel-shaped breccia bodies of silicified fragments in a matrix of quartz, adularia and pyrite. Evidence for several episodes of brecciation and cementation is common. Native gold occurs with electrum and silver sulfosalts. Highly anomalous concentrations of Hg, As, Sb and Tl are reflected in part by the local presence of cinnabar and stibnite.

Ore-grade concentrations of gold and silver (85 and 500 ppm respectively) have been described in sinters precipitating from alkaline-chloride waters in the Broadlands geothermal field, New Zealand (Weissberg, 1969). They are also highly enriched in As (2%), Sb (30%), Hg (2000 ppm) and Tl (0.5%). Although no economic gold mineralization has been recognized in modern or undeformed ancient sinters, the deformed and metamorphosed Precambrian gold mines at Haile, South Carolina and Marathon (Hemlo), Ontario have been interpreted as sinter (Spence *et al.*, 1980; Goldie, 1985).

8.5.1. Hydrothermal alteration

Adularia is a common gangue mineral in the ore zones of these deposits, and sericite is a common mineral in surrounding and especially overlying hydrothermally altered rocks. Buchanan (1981) described the most common alteration patterns associated with his boiling model (Figure 8-1, page 210). Surrounding the mineralized vein are silicified and adularized country rock, which thins out above the ore zone. As this assemblage thins out, a surrounding zone of sericite, illite and quartz thickens and expands in volume to near the palcosurface. These assemblages are surrounded by propylitically altered rock; an assemblage of chlorite, illite, carbonate, pyrite, montmorillonite and epidote.

Overlying these alteration zones Buchanan (1981) illustrates a surficial zone of siliceous residue which is the product of intense acid leaching. This is underlain by assemblages of alunite, quartz and kaolinite.

These two surficial assemblages record the effects of acids produced in the surficial environment from ascending acidic gases boiled off the hydrothermal fluids at depth, and are equivalent to those described in detail in Chapter 5. Buchanan (1981) states that these surficial alteration features serve as "excellent guides to non-outcropping ore shoots", because they are genetically related to gold mineralization through the common process of boiling.

In the hotsprings environment, silicification is a common alteration feature, especially near mineralized breccia zones. Silicified zones are surrounded by argillic alteration zones consisting of quartz, illite-montmorillonite and locally kaolinite (Berger and Eimon, 1983; Hedenquist and Henley, 1985).

8.6. Acid-sulphate gold deposits

Hypogene alunite deposits, discussed in Sections 5.1.5 and 5.1.6 relate to the production of acid-sulphate waters from magmatic gases and meteoric water. This occurs at depths far greater than the groundwater table, which is the approximate lower level for the formation of alunite in the hotsprings environment, also discussed in Chapter 5. Gold mineralization is known to be associated with hypogene alunite deposits at Goldfield, Nevada and Summitville, Colorado, among others. These acid-sulphate gold deposits (term of Hayba *et al.*, 1985) are smaller and less numerous than the adularia-sericite gold deposits discussed above. Their unique features (Figure 8-4) are commonly not discussed in review papers or included in models of epithermal gold deposits, with notable exceptions including Hayba *et al.* (1985), Silberman and Berger (1985) and Panteleyev (1986). This section discusses the precious metal mineralization associated with hypogene acid-sulphate alteration, at the four areas of hypogene alunite mineralization described in Chapter 5.

8.6.1. Summitville, Colorado

The Summitville deposit is hosted by a quartz latite porphyry erupted into the collapsed Summitville caldera of the San Juan caldera complex, Colorado. Production at small operations from 1870 to closure in 1947 included 113 000 oz of gold and 240 000 oz of silver. A large open pit operation developed during the mid 1980's produced 52 000 oz and 88 000 oz of gold in 1896 and 1987 respectively.

The ore zone minerals, pyrite, covellite, enargite and gold among others occur over a vertical interval of 400 m in intensely leached siliceous residue and quartz-alunite rocks. These rocks form the core of an upward-flaring pipe which was clearly a major hydrothermal conduit. Stoffregen (1985) stressed that the main stage of mineralization postdates the alteration and suggested that it could have occurred at lower salinities. Salinities for the acid-sulfate alteration are approximately 10% equivalent NaCl and temperatures are approximately 250

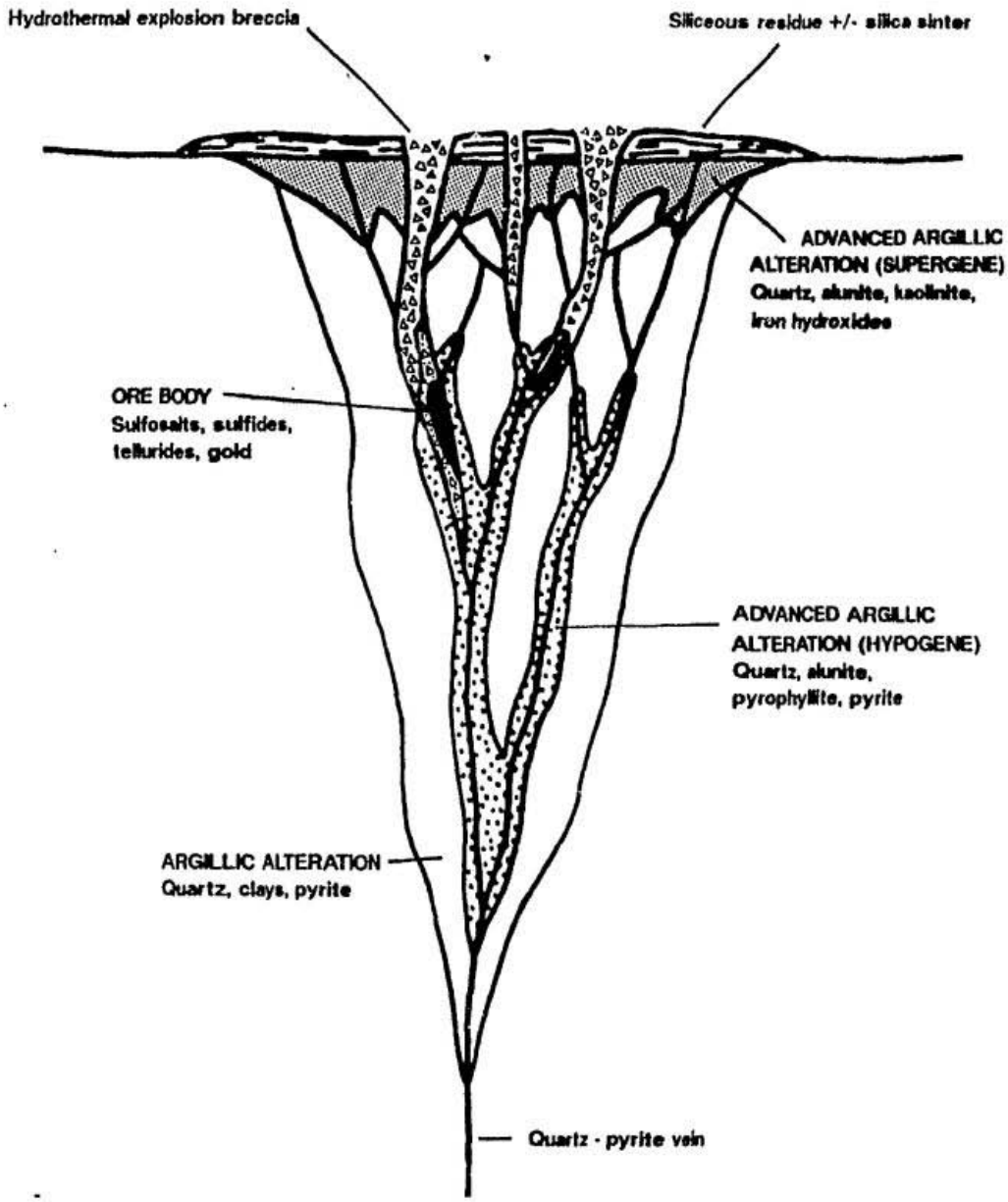

Figure 8-4: Epithermal system - acid-sulphate model. Schematic cross-section showing location of orebody with respect to alteration features. Note its occurrence within sulphide-bearing hypogene advanced argillic alteration zone (unlike systems in Figures 8-1, 8-2 and 8-3) which is separate from supergene advanced argillic (acid-leached) zone. [From Silberman and Berger, 1985.]

degrees Celsius.

A late mineralizing event at Summitville is characterized by veins of **barite-jarosite-goethite with native gold** (Stoffregen, 1985). Sulphides are extremely rare, and the assemblage occurs only in the uppermost levels at Summitville. Comparisons are made in Section 9.1.2 between this assemblage and certain auriferous assemblages in the study area described in Chapter 8.

8.6.2. Goldfield, Nevada

Zones of quartz-alunite-kaolinite-pyrite developed along fractures at the expense of volcanic, plutonic and metasedimentary rocks at Goldfield, Nevada. These "silicified zones" (Ransome, 1909; see section 6.4.2) host irregularly shaped gold-silver orebodies which apparently formed during the hydrothermal alteration (Jensen *et al.*, 1971). Goldfield has produced 4 200 000 oz of Au and 1 700 000 oz of Ag from 5 500 000 tons of ore.

8.6.3. Silverton Caldera, Colorado

The geology of the gold mineralization near the Silverton Caldera, Colorado is reviewed by Fisher and Leedy (1973) in their study of the geochemical features of the mineralization. Gold occurs with pyrite, silver and copper sulfosalts, and base metal sulfides within irregularly shaped orebodies within the "silicified" alunite-bearing breccia pipes described in Chapter 5. The orebodies range from metre-scale pods and lenses to vertical "chimneys" over 100 m in height, which were mined from the late 1800's by small operations.

Fisher and Leedy stress the control which caldera-related fault surfaces have on the localization of the breccia pipes. The timing of alteration and mineralization is regarded as contemporaneous with a late stage of magmatic activity, given a spatial association between the mineralized breccia pipes and late quartz-latite stocks, and the occurrence of such stocks crosscutting the breccia pipes. However, details of the mineralization are not discussed.

8.6.4. Lake City District, Colorado

Alunite is a minor gangue mineral in certain paragenetic sequences of precious metal vein mineralization in the Lake City District, Colorado. The regional and local geology are reviewed by Slack (1980), from whom the following description is taken. The veins with the richest precious metal concentrations are radially disposed around the northeastern corner of the Lake City caldera. Barite is everywhere present in these veins, together with the other gangue minerals quartz and minor rhodochrosite. Ore minerals include Ag-rich tetrahedrite, Ag-Cu-Pb sulfosalts, electrum and Au-Ag tellurides. Basemetal minerals include galena, sphalerite, chalcopyrite and hinsdalite, a hydrated Pb-Sr phosphate. The veins' radial distribution is centred on the Red Mountain dome, a quartz-latite porphyry which intruded the caldera fill shortly after its deposition. Geochronologic investigations summarized by Slack show that the precious metal vein systems were formed contemporaneously with the intrusion of the Red Mountain dome. These spatial and temporal relationships, and comparisons with other types of vein mineralization associated with the Lake City caldera lead Slack to imply that the Red Mountain Dome magma was a source of metals for the veins. Precious metal (and alunite) mineralization occurred at a minimum depth of 450 m, temperatures from 206 to 280 degrees Celsius and salinities from 1.3 to 12.4% NaCl.

8.7. Conclusion

Two distinct types of epithermal volcanic-hosted precious metal deposits have been described, *viz* adularia-sericite and acid-sulphate type. Alunite occurs in both types, and the relationship between alunite and gold mineralization in each type is essential in interpreting the gold mineralization on the Burin Peninsula. In the adularia-sericite type deposit, alunite forms at and near the paleosurface around acid hotsprings, which may form at the top of the hydrothermal system. Its occurrence points to processes acting at deeper levels in the system, *viz* boiling and loss of H_2S, that favour the precipitation of gold there. In acid-sulfate type gold deposits, alunite can occur at much deeper levels, clearly

below the level of oxidation by atmospheric oxygen. Although gold commonly is associated with rocks from which even alunite has been leached, it is also associated with the surrounding alunite-bearing rocks.

Chapter 9
CONCLUSIONS

9.1. Comparison of the study area with "epithermal mineralization"

Given the observations on the distribution of gold in the study area (Chapter 7) and knowledge of volcanic hosted epithermal precious metal deposits (Chapter 8), it is immediately obvious that most of the observed mineralization does not fit any subtype of either the adularia-sericite type or the acid-sulphate type deposit. The two sections to follow consider first the differences, and then similarities between the rocks in the study area and known epithermal gold deposits.

9.1.1. Discrimination

The foremost inconsistency is the universal association of the highest gold concentrations with specularite in the study area; gold is overwhelmingly associated with sulphide mineralization in all types of epithermal systems. The association of gold and alunite is also problematical. This association is best developed at Hickey's Pond, where a large area of alunite-bearing rock is characterized by gold concentrations in the range of a few hundred ppb. Although alunite is an integral part of certain epithermal systems (see clay-alunite cap, Figure 8-1, page 210) it forms on the barren acid-leached paleosurface due to boiling and gold precipitation at depth, followed by ascent and oxidation of H_2S to H_2SO_4. Primary hypogene alunite and sulphide mineralization are diagnostic of acid-sulphate type deposits, but the alunite at Hickey's Pond was shown in Section 6.4 to be primary supergene. Although the alunite-gold

association at Chimney Falls is probably hypogene, the abundance of specularite distinguishes it from most known acid-sulphate deposits.

9.1.2. Reconciliation

The only mineralized rocks that "fit" known epithermal models are the (Stage I) silicified pyritiferous rocks at Hickey's Pond, that contain 2.5 ppm Au. The preservation of volcanic texture in these rocks with over 96% SiO_2 proves that silica was added, and the abundance of quartz (+/- pyrite) veins attests to mechanical failure of the rock, possibly at a stage of incipient brecciation or peripheral to a breccia zone. These observations are compatible with the hotsprings precipitation model, in which shallow boiling is accompanied by silicification, brecciation and pyrite and precious metal mineralization (see silica cap in Figure 8-3, page 215). The part of the system exposed at Hickey's Pond must have been active at very shallow levels, and the hotsprings model would predict higher grade gold concentrations in an underlying stockwork of quartz-sulfide veins.

Other rocks in the study area which "fit" an epithermal model are the acid leached rocks at the Tower, Bullwinkle and Ridge Showings. The important difference between these rocks and similar ones at Hickey's Pond, a distinction essential to the successful comparison with epithermal systems, is that they are barren of significant gold mineralization. It was shown in Chapters 5 and 6, independently of precious metal potential, that these showings reflect boiling and steam separation at depth, conditions shown in Chapter 8 to favour gold mineralization at the level of boiling. Thus the zones in which boiling must have occurred, and in which mineralization would be expected, have not been recognized near these showings. Although the specularite-rich breccias record the effects of boiling, their mineralogy is unlike that in known epithermal deposits and they are not believed to be the "missing" boiling zones inferred from the surficial features.

The only reference noted in the literature to a mineral assemblage

comparable to that of the specularite-rich breccias is to a late mineralizing stage at Summitville, Colorado, characterized by barite-jarosite-goethite-gold and described in Section 8.6.1. Similarities with the specularite-rich breccias at Hickey's Pond include the extreme rarity of sulfides, the presence of gold in the native state and the occurrence of the assemblage only in the uppermost levels at Summitville. The "fit" is not perfect, as barite occurs only at Chimney Falls, there is no jarosite present at Hickey's Pond (only alunite) and specularite is inferred to be a metamorphosed equivalent of goethite. The significance is that it is an occurrence of gold in association with an acid, oxide mineral assemblage. As such, it lends the gold mineralization related to specularite-rich breccias (Stage II) in the study area to comparison with the acid-sulphate type of gold mineralization. This is supported by the occurrence of hinsdalite (hydrated Pb-Sr phosphate) in acid-sulphate type deposits in the Lake City District (Section 8.6.4), because Sr and P are present in the breccia at Chimney Falls (Section 7.3.3).

The occurrence of acid-sulphate type mineralization in the acid-leached cap of an ancient adularia-sericite type system is unprecedented. The reasons for the temporal and spatial convergence of the two types of systems is unknown, but probably reflects mutual adherence to porosity-permeability considerations, i.e., both fluids followed the easiest path. It also suggests a relationship between the deposit types, which has not been encountered at the deposits reported in the literature, whereby the adularia-sericite system may have evolved into a high sulfur type system. The specularite-rich breccias formed late in the paragenesis, and are considered to have had no bearing on the implications of the earlier process, *i.e.*, that the surficial acid leaching is related genetically to undiscovered parts of the system where models of adularia-sericite type epithermal deposits would predict gold mineralization to occur.

A significant mass of gold was deposited in the specularite-banded and pyritiferous rocks at Hickey's Pond, a feature which is inconsistent with modern epithermal models. However, this mineralization must be considered epithermal insofar as it represents a hitherto unreported interaction of epithermal

mineralizing fluids (the Stage I and II fluids of this study) with an epithermal alteration package classically regarded as barren (the surficial acid-leached zone).

9.1.3. Speculations on the controls of gold mineralization at Hickey's Pond

Two gold mineralizing processes have been identified at the Hickey's Pond Showing (Section 7.5.3.2), *viz* Stage I, a sulphide Cu-Ag-Au assemblage; and Stage II, an acid, oxide association with native gold. The question of why gold associated with Stage I (adularia-sericite type, hotsprings style) mineralization reached the paleosurface at Hickey's Pond but was (presumably) precipitated at depth under the precursors of the Tower and Bullwinkle showings has not been addressed. This relates to the more fundamental question not addressed in Chapter 8, which is: what controls whether an ascending hydrothermal fluid will lead to a classic boiling model type deposit (*"at depth"*) or a hotsprings type deposit?

Reed and Spycher (1985) show with the aid of numerical models that where the ratio of metals (Fe, Cu, Pb and Zn) to sulfur is low, boiling can occur without appreciable gold precipitation. When higher concentrations of metals are precipitated as sulphides, they act as sinks for sulfur, the loss of which causes gold precipitation. Underlying the metal content of the fluid is its salinity, high values of which are seen by Reed and Spycher as the key to the high metal contents required to remove sufficient sulfur from the boiling system to precipitate gold.

Non-equilibrium processes might also be important to this question. Given a suitable conduit through which to pass, sufficiently high flow velocities could raise the level of gold precipitation into the hotsprings setting. A major caldera-related fault is the main fluid channel at the Rotokawa geothermal field in New Zealand, in which high grade gold concentrations occur in a hotsprings setting (Krupp and Seward, 1987).

Neither of these features can be rigorously evaluated to account for the

significantly higher gold concentrations at Hickey's Pond compared to other similar showings. However, the proximal setting of the Hickey's Pond Showing to a volcanic centre (Section 6.8.3), and the suggestion that the felsic volcanics relate to a caldera (Section 2.5.3) suggest that the Hickey's Pond Showing would have been closer to caldera-related faults which could have served as hydrothermal conduits.

The Stage II acid, oxide mineralized assemblage with native gold represents the richest mineralization at Hickey's Pond and elsewhere, and is also implicated in the (low grade) mineralization of the specularite-banded rocks at Hickey's Pond. These systems are not as well understood as the adularia-sericite type deposits. The only apparent control stems from the proximity of the Stage I and Stage II fluids at Hickey's Pond, *i.e.* that the Stage II fluids also moved along possible caldera-related faults.

9.2. Speculations on undiscovered gold mineralization

It was shown above that in a qualitative sense, the occurrence of surficial acid leached rocks is indicative of conditions favourable for gold deposition at deeper levels in the hydrothermal system. Semiquantitative estimates of the amount of gold moved by the hydrothermal systems responsible for the alunite mineralization in the study area can be made given 1) the size and mineralogy of the alunite showings, 2) a qualitative understanding of the processes responsible for their formation, and 3) quantitative estimates of relevant chemical concentrations (e.g. gold solubility) and physical processes (*e.g.* percentage of sulfur partitioned into the vapour phase) which characterized the systems.

The approach taken in the following sections is to 1) calculate the mass of sulfur in a representative alunite showing 2) estimate the mass of hydrothermal fluid required to move the sulfur and 3) estimate the quantity of gold which such a fluid could have deposited. For quantitative evaluation of each process, two estimates and two corresponding calculations are performed, representing the

worst reasonable possible scenario and the best reasonable possible scenario from the viewpoint of forming a gold deposit. The Tower showing serves as the basis for this discussion, as its size is intermediate between the larger Bullwinkle showing and the smaller Hickey's Pond showing.

Note that the following discussion pertains to "missing" parts of an adularia-sericite system. The occurrences of auriferous specularite-rich breccias *"at depth"* at Chimney Falls and the Strange Showing have been referred to a paragenetically later acid-sulphate type of system and are not considered to be these "missing parts".

9.2.1. Mass of sulfur at the Tower Showing

The Tower showing is 450 m long and 80 m wide. For purposes of calculating its volume, it is modelled as the remaining half of a cylinder that had been 450 m in diameter and 80 m in thickness. This assumption probably underestimates its volume because a random horizontal section (the modern ground surface) through a horizontal cylinder (the showing) probably does not correspond to its true diameter. For this reason and since the rocks dip steeply to the northwest, no correction for true thickness is made here. If the cross section of the showing is an ellipse (due to tectonism or primary controls), its volume is overestimated if the long axis is horizontal or underestimated if the long axis is vertical. Notwithstanding these possibilities, the approximate volume of rock at the Tower showing prior to erosion to its present state is 12.7 million m^3. Given a specific gravity of 2.4, this is a mass of 30 million tonnes of acid leached rock.

Normative mineralogy is available for 12 rock samples from the Tower showing. Normative alunite ranges from 1.5% in the quartz-rutile rock to between 13.6% and 41.4% in the other rocks, in agreement with modal estimates. The variation is large and strongly controlled by the proportion of alunite-bearing rocks to quartz-rutile rocks. The simple average of the maximum and minimum alunite concentrations will be taken as a global average for the showing. Together with the mass of rock (30 MT) and the percentage of sulfur in alunite

(15.4%), there are 1.3 million tonnes of sulfur in alunite at the Tower showing. Additional sulfur is present in pyrite but its mass is probably much less and is not considered here.

This mass of sulfur is reasonable by the standards of some modern systems. Krupp and Seward (1987) describe a bedded sulfur deposit under Lake Rotokawa, New Zealand. The deposit formed in approximately 1 500 years, starting 6 000 years ago and contains 2.6 million tonnes of elemental sulfur above a cutoff grade of 10%.

9.2.2. Mass of hydrothermal fluid

The sulfur present at the Tower showing was probably derived from a boiling hydrothermal fluid. Several chemical parameters and physical processes must be estimated in order to determine the mass of hydrothermal fluid responsible for the sulfur. These are be discussed in the following paragraphs, which are arranged in sequence of occurrence.

Concentration of sulfur in hydrothermal fluid

The following sections borrow heavily from comparisons of ancient epithermal systems to modern geothermal systems, the connections between which were discussed in Section 8.1. The concentration of H_2S in modern New Zealand geothermal waters is discussed by Weissberg (1969) and Mahon and Finlayson (1972). Values for deep waters span over 2 orders of magnitude; from approximately 10 ppm at Wairakei to over 800 ppm at Rotokawa. In their detailed study of gold mineralization associated with the geothermal system at Rotokawa, Krupp and Seward (1987) present observed concentrations ranging from 29 to 248 ppm H_2S, and suggest that 229 ppm is most representative of the deep fluid in the system. At Broadlands and Waiotapu, 5 measurements cluster at approximately 100 ppm. For the calculations, the worst and best possible scenarios assume 400 ppm and 50 ppm respectively, of H_2S in the ascending hydrothermal fluid. Since S accounts for almost all the mass in H_2S, no correction for the mass of H is be performed.

Percentage of sulfur partitioned into vapour phase

The smaller the percentage of sulfur partitioned into the vapour phase, the larger is the hydrothermal system required to explain the sulfur at the Tower showing and the larger is the potential gold deposit. However, since effective partitioning of H_2S into the vapour phase is required to cause gold precipitation, a high percentage is assumed; implying the smallest possible hydrothermal system. For the calculations, the worst and best possible scenarios for partitioning of H_2S into the vapour phase are 90% and 80% respectively.

Percentage of sulfur incorporated into alunite

Incorporation into alunite is only one possible fate of the sulfur released into the vapour phase. It could be bound in sulfide minerals formed above the boiling level, dissolved in groundwaters and dispersed or exhaled into the atmosphere and dispersed. For the calculations, the worst and best possible scenarios for incorporation of H_2S vapour into alunite are 75% and 40% respectively.

Given the estimates discussed above and the mass of sulfur determined in the preceding section, the mass of water required to yield the sulfur at the Tower showing could vary from 4.8 to 81.2 billion tonnes. Weissberg (1969) showed that the Wairakei geothermal system could discharge 800 billion tonnes of water in 57 000 years, a figure which could be modest for the lifespan of a geothermal system. Thus, even the maximum fluid volume calculated for the Tower showing is small in comparison to modern geothermal systems. This could indicate that the trapping of hydrothermal sulfur in alunite is much less efficient than assumed in the preceding section, or that all the alunite showings in the area, together with undiscovered and non-outcropping showings should be considered in calculating the size of the hydrothermal system. Even the maximum estimate of gold mineralization could underestimate the potential by a factor of 10.

Mass of gold deposited

Given the mass of hydrothermal fluid from which the Tower Showing was derived, the concentration of gold in the hydrothermal fluid is required to estimate the mass of gold such a system could have deposited. Weissberg (1969)

showed that the discharge waters from one of the Broadlands geothermal wells (BR 2) contained 0.04 ppb Au, which is only 10 times its concentration in seawater. Ewers and Keays (1977) reviewed data from a different well at Broadlands, where the gold concentration varied from 0.1 to 1.0 ppb. For the calculations, the worst and best possible scenarios assume gold concentrations of 0.04 and 0.4 ppb.

A case for higher than observed gold concentrations is put forward by Brown (1986). Having observed significant precipitation of gold and other metals in the surface piping through which the geothermal fluid at Broadlands drillhole BR 22 is transported, he provided a corrected gold concentration (1.5 ppb), which takes the loss into account. This highlighted a shortcoming of previous estimates, including those cited above, but is only regarded here as semi-quantitative since detailed measurements of the thickness of the deposit along the length of the pipe could not be determined. Nevertheless, Brown's research shows that even the maximum gold concentration assumed in this calculation could underestimate the true value by a factor up to 4.

The final consideration is the efficiency of the gold depositional process. Weissberg (1969) showed that 4% of the gold in the solution discharged from a geothermal well at Broadlands was precipitated with silica and metastibnite onto a concrete runoff apron. The fluid temperature was approximately 60 degrees Celsius and it flowed rapidly across the apron, having little time to precipitate gold. A potentially more efficient mechanism is described by Hedenquist and Henley (1985). It involves open boiling in a hydrothermal eruption vent coupled with almost complete loss of H_2S and CO_2, causing the gold solubility to be reduced by a factor of 100. However, they assume for their modelling that the solution was initially saturated with gold, which implies a concentration of 6 ppb. This is considerably higher than observed gold concentrations elsewhere in New Zealand and no new data are provided to substantiate it. Since boiling is considered to be a better mechanism for gold precipitation than cooling, oxidation and coprecipitation (processes which may have caused gold precipitation in the

short time available on the concrete runoff pad), then an efficiency greater than 4% is probable for deposition in response to boiling. For the calculations, the worst and best possible scenarios for depositional efficiency are 4% and 20%, respectively.

Given the mass of hydrothermal fluid (Section 9.2.2), its gold concentration and the efficiency of the gold depositional process (this section), the quantity of gold which could have been deposited ranges from 7 680 g (270 oz) to 6 500 000 g (229 000 oz). The processes and calculations described in the preceding sections are summarized in Figure 9-1.

9.2.3. Discussion

The assumptions and calculations performed above indicate that an economically viable gold deposit could be related genetically to the alunite mineralization at the Tower showing. Given that the Tower showing is neither the only nor the largest such showing, the potential is multiplied several times. Of greater importance, however, than the results of the calculations is the qualitative interpretation which shows that the alunite showings are related genetically to a process, boiling, which is a viable mechanism for the formation of an epithermal gold deposit.

9.3. A Model of Epithermal Alteration and Gold Mineralisation on the Northern Burin Peninsula

A schematic model of the following description is provided in Figure 9-2. The eruption of subaerial volcanics onto continental basement began at circa 600 Ma, in an extensional tectonic regime possibly of Pan-African affinity. The earliest erupted units were basalt and basaltic andesite flows, which progressively gave way to mafic pyroclastics and felsic volcanics. The felsic volcanics formed extensive sheets of tuff and welded tuff, and relate to large magma chambers, given their large volume and certain geochemical features. They were comagmatic with the Swift Current Granite, which intruded at least into the

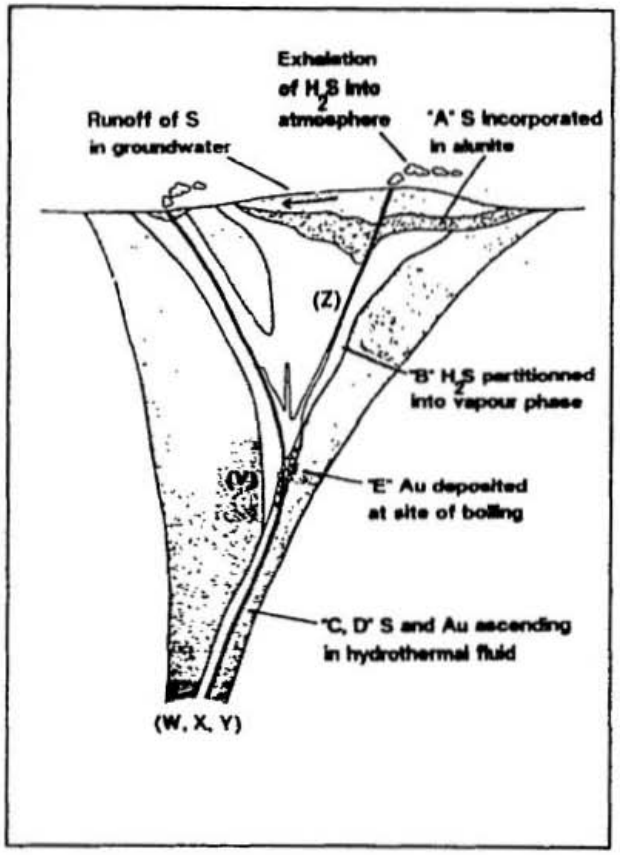

Given mass of S at Tower showing = 1.3 Mt, let:
A = fraction of S in ascending vapour incorporated in alunite
B = fraction of S partitionned into vapour phase during boiling
C = concentration (ppm) of S in hydrothermal fluid
D = concentration of Au in ascending hydrothermal fluid
E = fraction of Au in fluid deposited during boiling

TO CALCULATE	EQUATION	WORST POSSIBLE SCENARIO	BEST POSSIBLE SCENARIO
(Z) Mass of S in ascending vapour (after boiling)	Z = 1.3 Mt / A	A = 0.75 Z = 1.73 Mt	A = 0.40 Z = 3.25 Mt
(Y) Mass of S in ascending hydro-thermal fluid (before boiling)	Y = Z / B	B = 0.90 Y = 1.92 Mt	B = 0.80 Y = 4.06 Mt
(X) Mass of ascending hydro-thermal fluid	X = Y / C	C = 400 ppm X = 4.80 Gt	C = 50 ppm X = 81.2 Gt
(W) Mass of Au in ascending hydrothermal fluid	W = X * D	D = 0.04 ppb W = 192 Kg (6,760 oz)	D = 0.4 ppb W = 32,500 Kg (1,140,000 oz)
(V) Mass of Au deposited during boiling	V = W * E	E = 0.04 V = 7.68 Kg (270 oz)	E = 0.20 V = 6,500 Kg (229,000 oz)

Figure 9-1: Speculations on potential gold mineralization. Given the mass of sulfur in the acid leached cap of a representative showing, the processes it represents and quantitative estimates of the characteristics of the system, the mass of gold potentially associated with the showing can be estimated.

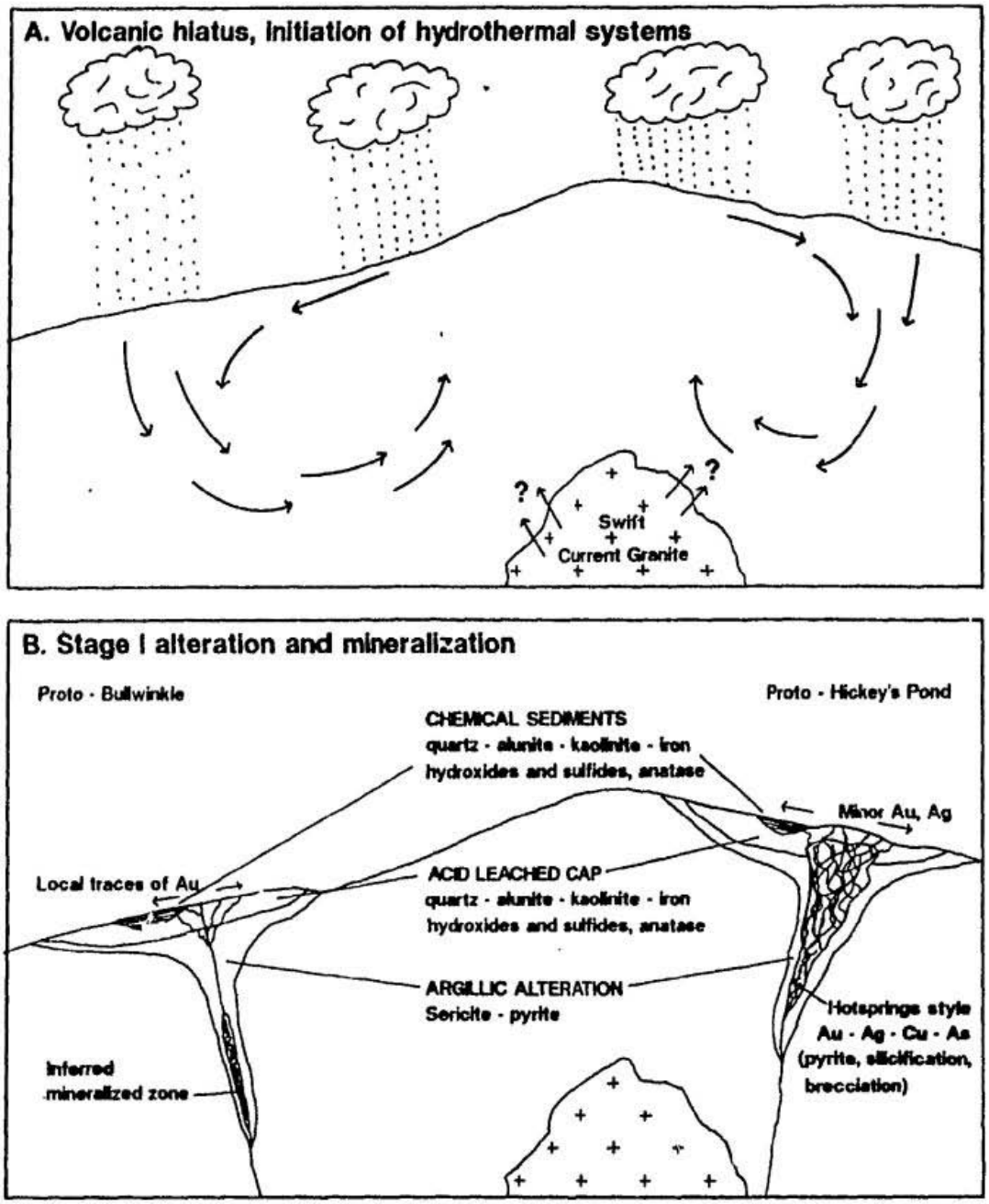

Figure 9-2: Model of epithermal alteration and gold mineralization on the northern Burin Peninsula. A. Convection cells of meteoric water +/- magmatic fluids are driven by the high level Swift Current Granite, during a hiatus in the last stages of volcanism. B. Gases and fluids from boiling hydrothermal systems at depth attain the surface and produce large areas of surficial acid leaching and minor chemical sediments. Higher boiling level at proto - Hickey's Pond Showing brings gold, pyrite, silicification and incipient brecciation into acid leached cap at Hickey's Pond. Mineralized zones could have formed at the boiling levels of all such systems. Note alteration cells are spaced apart and exaggerated in size for clarity. (continued....)

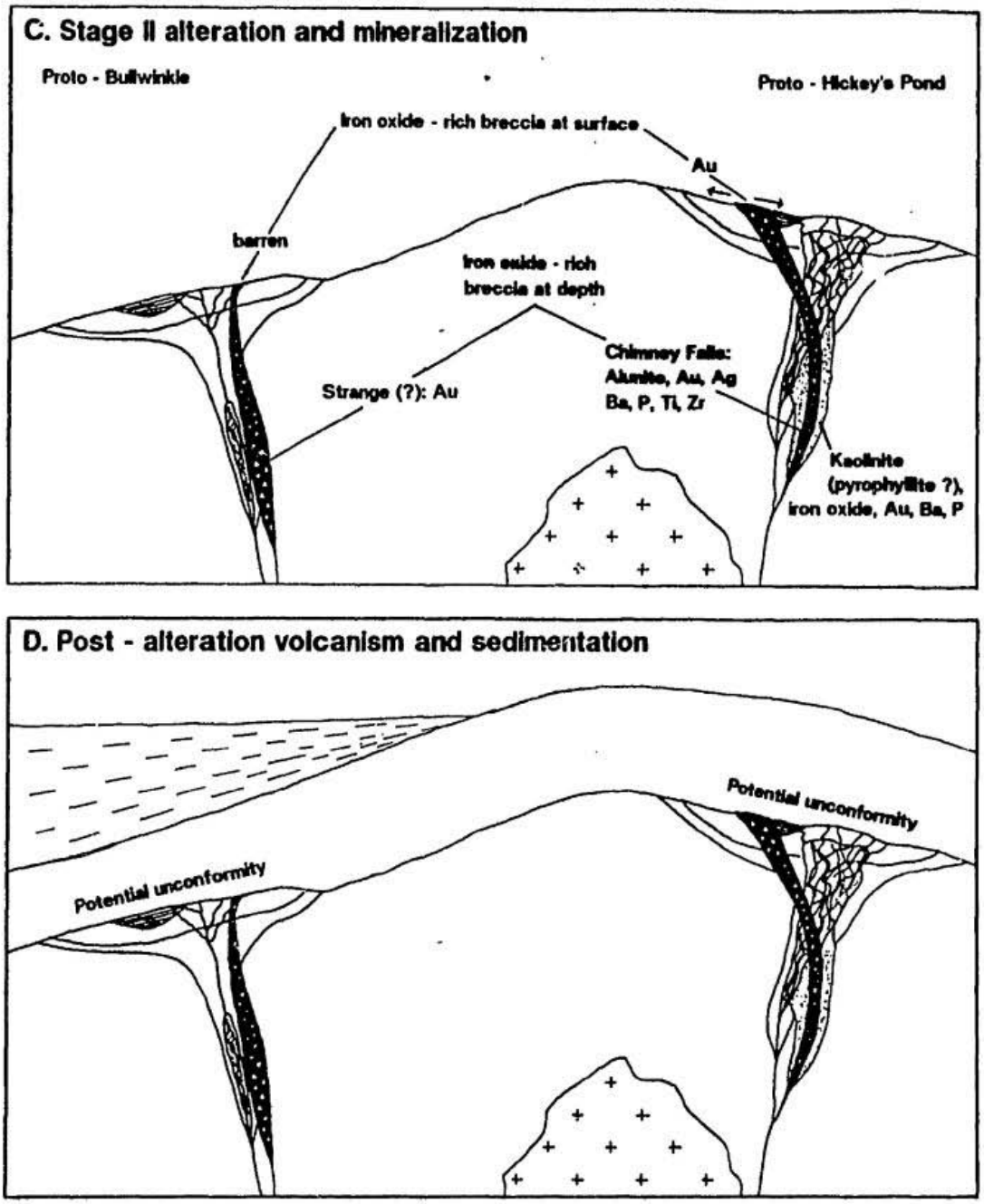

Figure 9-2 (....continued) C. Hydrothermal breccias characterized by iron oxides explode to surface at Hickey's Pond and the Bullwinkle Showings. They carry gold and iron oxides into the acid leached zone at Hickey's Pond, and they are also characterized by gold at deeper levels (Strange and Chimney Falls Showings), where they are flanked by kaolinite (or pyrophyllite?). D. Post - alteration volcanism buries the surficial features, but erosion prior to burial could have occurred. (continued....)

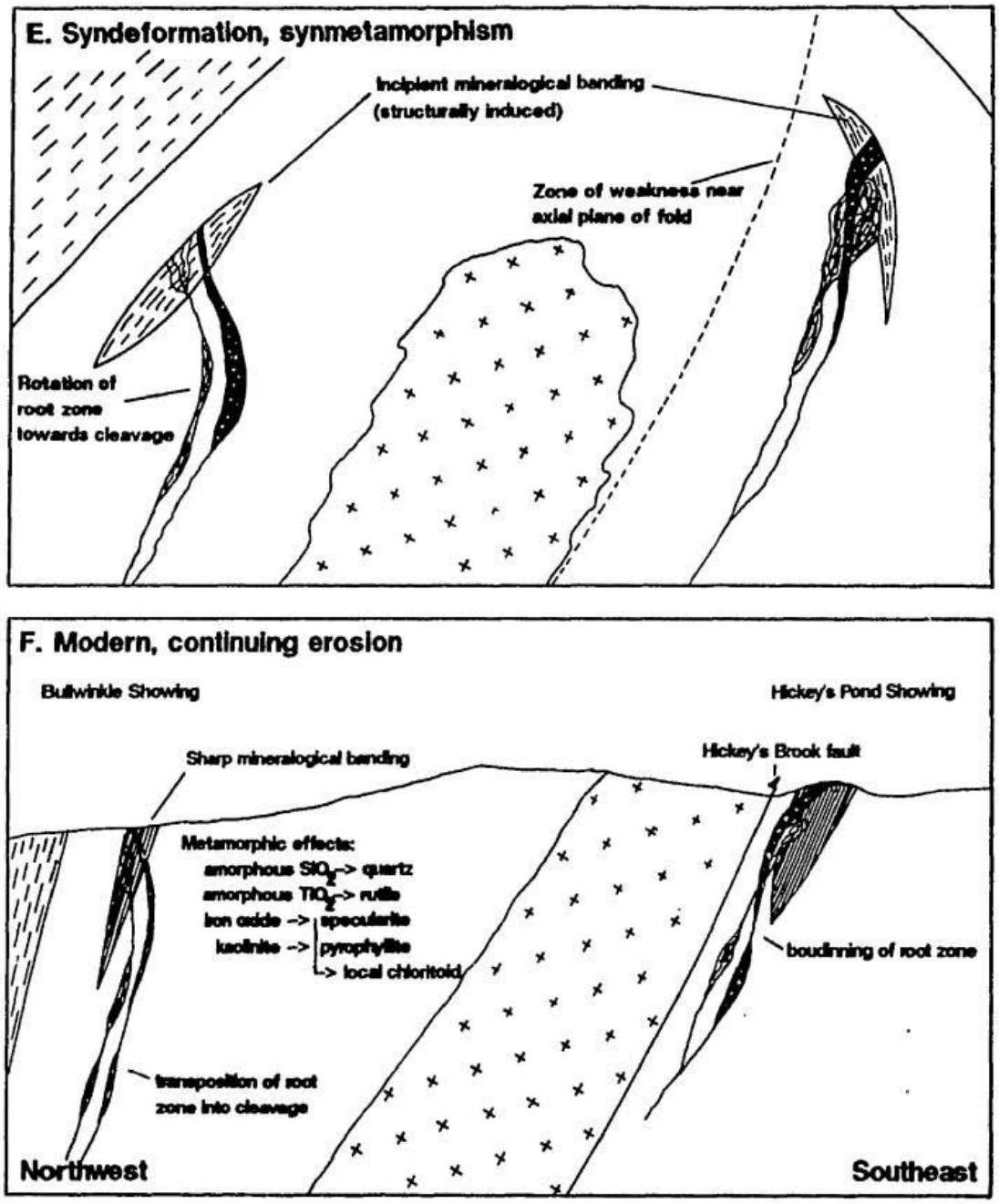

Figure 9-2 (continued....) E. Deformation begins with major anticlinorium overturned to the east. Note that root zones of hydrothermal systems could have rotated in sense opposite to that illustrated. F. Continued compression causes failure along the "underside" of the granite, which leads to its being reverse faulted into contact with the surficial alteration zones. Compression and shearing transpose (and boudin) root zones into the regional cleavage, and impose a distinct mineralogical banding on the formerly massive rocks. Metamorphic changes accompany the deformation, which is followed by (ongoing) erosion.

basal mafic part of the volcanic sequence.

Hydrothermal fluids, probably of meteoric origin but with possible magmatic components began to circulate. Local intense sericitization and pyrite mineralization with small concentrations of Au and Ag mark the passage of these fluids. Enrichments in K, Rb, U and Th in these rocks might indicate a magmatic component in the fluid. Chemical evolution of the fluids lead to kaolinite or pyrophyllite mineralization.

At the same time, ascending hydrothermal fluids, possibly the same fluids responsible for the sericitization were boiling and partitioning large quantities of sulfur into H_2S in a vapour phase. This process led to precipitation of precious metals at the level of boiling, as discussed in Section 8.2. The H_2S-rich vapours attained the paleosurface where they were oxidized to sulphuric acid, and percolated downward into the rock. This produced large areas on the paleosurface of intensely acid-leached ground, characterized by silica minerals, oxides of Ti and Fe, kaolinite and alunite. Pyrite formed by reaction of ascending H_2S and Fe liberated from phases undergoing breakdown. Locally, the same minerals were precipitated in acid hotsprings.

At what was to become the Hickey's Pond showing, the level of boiling was sufficiently high to bring silicification, incipient brecciation, quartz-pyrite veinlets and precious metal mineralization into the very near surface environment.

A second gold-bearing assemblage, characterized mineralogically by specularite, barite and alunite (similar to late stage mineralization at Summitville) and geochemically by high concentrations of Fe, Ti, P, Rb, Ba, Cu and Hg was developed in close proximity to the other alteration features. It formed auriferous breccia pipes in the subsurface at what are now the Chimney Falls and the Strange showings, and similar pipes erupted through to the paleosurfaces of the present Bullwinkle and Hickey's Pond showings. Local ore-grade material was thus developed at Hickey's Pond, and lateral migration of the fluids out of the

conduit into the porous and permeable acid leached rocks constituted a second pulse of mineralizing fluid into the hotsprings environment. The breccias at the Bullwinkle Showing were not mineralized, but could indicate mineralization lower in the system.

Resumption of volcanism buried and preserved the surficial alteration features. Volcanism gave way to marine sedimentation, followed by local uplift and Cambrian sedimentation.

Intense deformation and greenschist facies metamorphism accompanied the Acadian Orogeny. Structural effects record compression and southeastward verging thrusts, associated with "docking" of the Avalon and Gander Zones, and later shearing. Metamorphism peaked at or slightly after the deformation, and relates in part to the intrusion of the Ackley City Granite west of the study area.

Cryptocrystalline textures were obliterated, and any remaining porosity of the acid leached rocks was eliminated by recrystallization and compression. Tectonism induced a mineralogical banding on the alunite and specularite-bearing assemblages at all the showings, due to the platy habit of the specularite. Volcanic features of the acid leached and clay altered rocks were lost, with the exception of primary quartz phenocrysts. Volcanic features were locally preserved in the competent silicified rocks and in fragments in the specularite-rich breccias, both of which contain only minor pyrophyllite. The latter were boudinned, especially in the case of the breccia pipe in the incompetent, clay-altered rocks at Chimney Falls.

Veins of coarse, milky quartz and platy specularite (textures incompatible with epithermal systems) were "sweated out" at the specularite showings, but gold was only poorly remobilized into these. It was however, precipitated in the native state in post-tectonic millimetre-scale specularite veinlets emanating from the specularite-rich breccia at Hickey's Pond.

Mineralogical changes which accompanied the metamorphism include kaolinite --> pyrophyllite; leucoxene, anatase --> rutile; goethite --> specularite and pyrophyllite + specularite --> chloritoid + quartz.

9.4. Recommendations for additional work

Geochemical surveys and prospecting could be conducted near the major zones of acid leaching with the aim of discovering the gold mineralization which this study has predicted to occur. A recently released lake sediment survey (Davenport *et al.*, 1989) which covers the northern part of the study area (NTS sheets 1M/15 and 1M/16) provides useful information for the planning of further lake sediment and other geochemical surveys. It shows that sediment from Hickey's Pond does not contain even weakly elevated concentrations of Au or As, but that Cu, Ba and Sb are present in anomalous concentrations. Further lake sediment sampling could provide coarse evaluation of the precious metal potential of all the similar subaerial volcanics from the southwestern tip of the Burin Peninsula to Bonavista Bay.

The Hickey's Pond Showing displays a wide range in intensity of tectonic segregation. It is well suited to a study of this poorly understood phenomenon because of the lateral variation, presence of independent kinematic indicators and excellent exposure at the showing which is complemented by diamond drill core. Detailed crystallographic studies of quartz at the Strange Showing could determine the nature of deformation there, and the excellent shear features visible along the Hickey's Brook Fault could be studied in more detail. Structural study will be essential in determining the fate of the root zones of the exposed epithermal alteration zones, which could host economic gold deposits.

References

Anderson, F. D. Geology of Belleoram map sheet. Geological Survey of Canada, Map 8-1965.

Bainbridge, T. Memoranda relating to iron deposits at Placentia Bay, Newfoundland. Davenport and Company, Aldwych, W.C.2, London, England. Unpublished Report, 11 pages, 1934.

Bell, K., Blenkinsop, J. and Strong, D. F. The geochronology of some granitic rocks from eastern Newfoundland and its bearing on Appalachian evolution. *Canadian Journal of Earth Sciences*, 1977, *14*, 456-476.

Berger, B. R. and Eimon, P. I. Conceptual models of epithermal precious-metals deposits. In Shanks, W. C. (Ed.), *Cameron Volume on Unconventional Mineral Deposits*, Society of Mining Engineers, 1983.

Berger, B. R. and Bethke, P. M. Geology and Geochemistry of Epithermal Systems. Society of Economic Geologists. Edited by Berger, B. R. and Bethke, P. M., 1985.

Bertrand, J.M.L. and Caby, R. Geodynamic evolution of the Pan-African orogenic belt: A new interpretation of the Hoggar Shield (Algerian Sahara). *Geologischen Rundschau*, 1978, *67*, 357-388.

Bethke, P. M., Barton Jr., P. B. and Rye, R. O. Hydrogen, oxygen and sulphur isotopic compositions of ore fluids in the Creede District, Mineral County, Colorado (abstract). *Economic Geology*, 1973, *68*, 1205.

Bradley, D.A. *Gisborne Lake and Terrenceville Map-Areas, Newfoundland (1M/15 and 10.* Technical Report, Geological Survey of Canada, Memoir 321, 1962.

Brown, Kevin L. Gold deposition from geothermal discharges in New Zealand. *Economic Geology*, 1986, *81*, 979-983.

Buchanan, Larry J. *Precious metal deposits associated with volcanic environments in the southwest.* Technical Report Volume 14, Arizona Geological Society Digest, 1981.

Cunningham, Charles G., Rye, Robert O., Steven, Thomas A., and Mehnert, H. H. Origins and exploration significance of replacement and vein-type alunite deposits in the Marysvale Volcanic Field, West Central Utah. *Economic Geology*, 1984, *79*, 50-71.

Dahl, Otto M. Third report on the iron deposits at Hickey's Pond, Placentia Bay, Newfoundland. Davenport and Company, Aldwych, W.C. 2, London. Unpublished report, 9 pages, 1934.

Dallmeyer, R. D., Odom, A. L., O'Driscoll, C. F. and Hussey, E. M.

Geochronology of the Swift Current granite and host volcanic rocks of the Love Cove Group, southwestern Avalon zone, Newfoundland: Evidence of a late Proterozoic volcanic-subvolcanic association. *Canadian Journal of Earth Sciences*, 1981, *18*, 699-707.

Dallmeyer, R. D., Hussey, E. M., O'Brien, S. J. and O'Driscoll, C. F. Chronology of tectonothermal activity in the western Avalon Zone of the Newfoundland Appalachians . *Canadian Journal of Earth Sciences*, 1983, *20*, 355-363.

Davenport, P. H., Nolan, L. W. and Hayes, J. P. *Gold and associated elements from lake sediment from regional surveys in the northwestern part of the Belleoram map area (1M/5, 11-16.* Technical Report Open File Report 1M/276, 25 pages, 4 appendices and 15 maps, Newfoundland Department of Mines, 1989.

Deer, W. A., Howie, R. A. and Zussman, J. *An Introduction to the Rock Forming Minerals.* Longman Group Limited, London, 1966.

Drummond, S. E. and Ohmoto, H. Chemical evolution and mineral deposition in boiling hydrothermal systems. *Economic Geology*, 1985, *80*, 126-147.

Ehrlich, Garry G., and Schoen, Robert. *Possible role of sulfur oxidizing bacteria in surficial acid alteration near hot springs.* Technical Report, U. S. Geological Survey Professional Paper 575-C, 1967.

Ewers, G. R. and Keays, Reid R. Volatile and precious metal zoning in the Broadlands geothermal field, New Zealand. *Economic Geology*, 1977, *72*, 1337-1354.

Feiss, P. Geoffrey. Volcanic-hosted gold and high alumina rocks of the Carolina Slate Belt. Guidebook for the Field Trip held in conjunction with the 1985 fall meeting of the Society of Economic Geologists. Edited by P. G. Feiss, 1985.

Fisher, Frederick S. and Leedy, Willard P. *Geochemical Characteristics of Mineralized Breccia pipes in the Red Mountain District, San Juan Mountains, Colorado.* Technical Report Bulletin 1381, United States Geological Survey, 1973.

Foley, N. K., Bethke, P. M. and Rye, R. O. A reinterpretation of D(H2O) values of inclusion fluids in quartz from shallow ore bodies (abstract). *Geological Society of America, Abstracts with Programs*, 1982, *14*, 489.

Fournier, Robert O. The behaviour of silica in hydrothermal solutions. In Berger, B. R. and Bethke, P. M. (Ed.), *Geology and Geochemistry of Epithermal Systems,* Society of Economic Geologists, 1985.

Frey, M. The step from diagenesis to metamorphism in pelitic rocks during Alpine orogenesis. *Sedimentology*, 1970, *15*, 261-279.

Giles, D. L. and Nelson, C. E. *Epithermal lode gold deposits of the circum-Pacific rim*, pages 273-278. American Association of Petroleum Geologists, 1982.

Goldie, Raymond. The sinters of the Ohaki and Champagne pools, New Zealand: Possible modern analogues of the Hemlo gold deposit, northern Ontario . *Geoscience Canada*, 1985, *12*, 60-64.

Gubins, A. First Year Assessment Report on Geophysical Surveys, Licence 2268, 1983.

Haas, Herbert and Holdaway. M. J. Equilibria in the system Al2O3-SiO2-H2O involving the stability limits of pyrophyllite, and thermodynamic data of pyrophyllite. *American Journal of Science*, 1973, *273*, 449-464.

Hanaoka, N. Numerical model experiment of hydrothermal system - topographic effects. *Bulletin Geological Survey Japan*, 1980, *31*, 321-332.

Hanson, Gilbert N. The application of trace elements to the petrogenesis of igneous rocks of granitic composition. *Earth and Planetary Science Letters*, 1978, *38*, 26-43.

Hayba, D. O. Documentation of thermal and salinity gradients and interpretation of the hydrologic conditions in the OH vein, Creede, Colorado. *Geological Society of America, Abstracts with Programs*, 1984, *16*, 534.

Hayba, Daniel O., Bethke, Philip M., Heald, Pamela and Foley, Nora K. Geologic, mineralogic and geochemical characteristics of volcanic-hosted epithermal precious-metal deposits. In Berger, B. R. and Bethke, P. M. (Ed.), *Geology and Geochemistry of Epithermal Systems*, Society of Economic Geologists, 1985.

Heald, Pamela, Foley, Nora K. and Hayba, Daniel O. Comparative anatomy of volcanic-hosted epithermal deposits: Acid-sulfate and adularia-sericite types. *Economic Geology*, 1987, *82*, 1-26.

Hedenquist, Jeffrey W. and Henley, Richard W. Hydrothermal eruptions in the Waiotapu geothermal system, New Zealand: Their origin, associated breccias, and relation to precious metal mineralization. *Economic Geology*, 1985, *80*, 1640-1668.

Hemley, J. J., Hostetler, P. B., Gude, A. J., and Mountjoy, W. T. Some stability relations of alunite. *Economic Geology*, 196[illegible] *64*, 599-612.

Henley, R. W., and McNabb, Alex. Magmatic vapor plumes and ground-water interaction in porphyry copper emplacement. *Economic Geology*, 1978, *73*, 1-20.

Henley, R. W., and Ellis, A. J. Geothermal systems ancient and modern: a geochemical review . *Earth-Science Reviews*, 1983, *19*, 1-50.

Henley, R. W. The geothermal framework of epithermal deposits. In Berger, B. R. and Bethke, P. M. (Ed.), *Geology and Geochemistry of Epithermal Systems,* Society of Economic Geologists, 1985.

Hildreth, W. Gradients in silicic magma chambers: implications for lithospheric magmatism. *Journal of Geophysical Research*, 1981, *86*, 10153-10192.

Hobbs, Bruce E., Means, Winthrop D. and Williams, Paul F. *An Outline of Structural Geology.* John Wiley & Sons, Inc., 1976.

Holland, H. D. Gangue minerals in hydrothermal deposits. In Barnes, H. L. (Ed.), *Geochemistry of Hydrothermal Ore Deposits,* Holt, Rinehart, and Winston, Inc., New York, 1967.

Howland, Arthur L. Precambrian iron bearing deposits of southeastern Newfoundland. Geological Survey of Newfoundland, unpublished report, 1938.

Howland, Arthur L. Specularite - Alunite mineralization at Hickeys Pond, Newfoundland. *American Mineralogist*, 1940, *25*, 34-45.

Huard, Allan A. and O'Driscoll, Cyril F. Auriferous specularite-alunite-pyrophyllite deposits of the Hickey's Pond area, northern Burin Peninsula, Newfoundland. In Brewer, K., Walsh, D. and Gibbons, R. V. (Ed.), *Current Research,* Mineral Development Division, Department of Mines and Energy, Government of Newfoundland and Labrador, 1985.

Huard, Allan A. and O'Driscoll, Cyril F. Epithermal gold mineralization in late Precambrian volcanic rocks on the Burin Peninsula. In Blackwood, R. F., Walsh, D. G. and Gibbons, R. V. (Ed.), *Current Research,* Mineral Development Division, Department of Mines and Energy, Government of Newfoundland and Labrador, 1986.

Hughes, C. J. The late Precambrian Avalonian orogeny in the Avalon Peninsula, SE Newfoundland. *American Journal of Science*, 1970, *269*, 183-190.

Hughes, C. J. and Bruckner, W. D. Late Precambrian rocks of Eastern Avalon Peninsula, Newfoundland - a volcanic island complex. *Canadian Journal of Earth Sciences*, 1971, *8*, 899-915.

Hussey, E. M. Sound Island Map-area (West Half). Newfoundland Department of Mines and Energy. Mineral Development Division, Open File Report 1M/16 (212), 39 pages, 1978.

Jenness, S. E. *Terra Nova and Bonavista map areas, Newfoundland.* Technical Report, Geological Survey of Canada, Memoir 327, 1963.

Jensen, M. L., Ashley, R. P. and Albers, John P. Primary and secondary sulphates at Goldfield, Nevada. *Economic Geology*, 1971, *66*, 618-626.

Knight, Jerry E. A thermochemical study of alunite, enargite, luzonite, and tennantite deposits. *Economic.Geology*, 1977, *72*, 1321-1336.

Krauskopf, Konrad B. *Introduction to Geochemistry*. McGraw-Hill Inc., 1979.

Krogh, T. E., Strong, D. F., O'Brien, S. J. and Papezik, V. S. Precise U-Pb zircon dates from the Avalon terrane in Newfoundland. *Canadian Journal of Earth Sciences*, 1988, *25*, 442-453.

Kroner, Alfred. Pan-African plate tectonics and its repercussions on the crust of northeast Africa. *Geologischen Rundschau*, 1979, *69*, 565-583.

Kroner, Alfred. Pan-African Crustal Evolution. *Episodes*, 1980, , 3-8.

Krupp, K. E. and Seward, T. M. The Rotokawa geothermal system, New Zealand: An active epithermal gold-depositing environment. *Economic Geology*, 1987, *82*, 1109-1129.

Leblanc, M. The Late Proterozoic ophiolites of Bou Azzer (Morocco): Evidence for Pan-African plate tectonics. In A. Kroner (Ed.), *Precambrian Plate Tectonics*, Elsevier Scientific Publishing Company, Amsterdam, 1981.

Mahon, William A. J. and Finlayson, James B. The chemistry of the Broadlands geothermal area, New Zealand. *American Journal of Science*, 1972, *272*, 48-68.

McKenzie, C. B. First Year Assessment Report - Diamond Drilling, C.B. 3317, Licence 2268, 1983.

McKenzie, Colin B. Geology and mineralization of the Chetwynd deposit, Southwestern Newfoundland, Canada, pages 137-148. Proceedings of Gold '86 Symposium, Toronto, 1986.

Mehnert, Harald H., Lipman, Peter W. and Steven, Thomas A. Age of Mineralization at Summitville, Colorado, as indicated by K-Ar dating of alunite. *Economic Geology*, 1973, *68*, 399-401.

Murray, Alexander and Howley, James P. Reports for 1868 and 1869. In *Geological Society of Newfoundland*, Edward Stanford, London, 1881.

Nelson, Carl E. and Giles, David L. Hydrothermal eruption mechanisms and hot spring gold deposits. *Economic Geology*, 1985, *80*, 1633-1639.

O'Brien, S. J., Wardle, R. J. and King, A. F. The Avalon Zone: A Pan-African terrane in the African Orogen of Canada. *Geological Journal*, 1983A, *18*, 195-222.

O'Brien, S. J. and Taylor, S. W. *Baine Harbour (1M/7) and Point Enragee (1M/6) map areas, Southeastern Newfoundland*. Technical Report 83-5, Mineral Development Division, Department of Mines and Energy,

Government of Newfoundland and Labrador, 1983B.

O'Brien, S. J., Nunn, G. A. G., Dickson, W. L. and Tuach, J. *Geology of the Terrenceville (1M/10) and Gisborne Lake (1M/15) map areas, Southeast Newfoundland.* Technical Report 84-4, Mineral Development Division, Department of Mines and Energy, Government of Newfoundland and Labrador, 1984.

O'Driscoll, Cyril F. Geology and Petrochemistry of the Swift Current Granite, Newfoundland. B. Sc. thesis, April, 1973. Memorial University of Newfoundland, St. John's, 84 pages.

O'Driscoll, C. F. Harbour Buffett map sheet (1M/9). Newfoundland Department of Mines and Energy, Mineral Development Division, Map 7873, 1978.

O'Driscoll, C. F. and Hussey, E. M. Sound Island map sheet (1M/16). Newfoundland Department of Mines and Energy, Mineral Development Division, Map 7863, 1978.

O'Driscoll, C. F. and Strong, D. F. Geology and geochemistry of late Precambrian volcanic and intrusive rocks of southwestern Avalon zone in Newfoundland. *Precambrian Research*, 1978, *8*, 19-48.

O'Driscoll, Cyril F. *The Hickey's Pond belt: auriferous specularite - alunite - pyrophyllite - sericite mineralization.* Technical Report, Newfoundland Department of Mines and Energy, Mineral Development Division, Open File Report 1M/16 (221), 12 pages, 1984.

Palache, Charles; Berman, Harry and Frondel, Clifford. *Dana's System of Mineralogy, Volume I.* John Wiley and sons, Inc., 1944.

Panteleyev, Andrejs. A Canadian Cordilleran model for epithermal gold- silver deposits. *Geoscience Canada*, 1986, *13*, 101-111.

Papezik, V.S., Keats, H.F. and Vahtra, J. Geology of the Foxtrap pyrophyllite deposit, Avalon Peninsula, Newfoundland. *The Canadian Mining and Metallurgical Bulletin*, 1978, *71*, 152-160.

Pearce, J. A. and Cann, J. R. Tectonic setting of basic volcanic rocks determined using trace element analyses. *Earth and Planetary Science Letters*, 1973, *19*, 290-300.

Pierrot, Roland M. *Chemical and Determinative Tables of Mineralogy (without the silicates).* Masson Publishing USA, Inc., 1979.

Ransome, F. L. *The geology and ore deposits of Goldfield, Nevada.* Technical Report, United States Geological Survey, Professional Paper 66, 1909.

Rast, N., O'Brien, B. H. and Wardle, R. J. Relationships between Precambrian and Lower Paleozoic rocks of the "Avalon Platform" in New Brunswick, the

Northeast Appalachians and the British Isles. *Tectonophysics*, 1976, *30*, 315-338.

Raymahashay, Bikash C. A geochemical study of rock alteration by hot springs in the Paint Pot Hill area, Yellowstone Park. *Geochimica et Cosmochimica Acta*, 1968, *32*, 499-522.

Reed, Mark H. and Spycher, Nicholas F. Boiling, cooling and oxidation in epithermal systems: A numerical modeling approach. In Berger, B. R. and Bethke, P. M. (Ed.), *Geology and Geochemistry of Epithermal Systems*, Society of Economic Geologists, 1985.

Rinehart, John S. *Geysers and Geothermal Energy*. Springer-Verlag, 1980.

Robinson, R. W. and Norman, D. I. Mineralogy and fluid-inclusion study of the southern Amethyst vein system, Creede mining district, Colorado. *Economic Geology*, 1984, *79*, 439-447.

Roedder, E. *Changes in ore fluid with time, from fluid inclusion studies at Creede, Colorado*, pages 179-185. International Association Genesis Ore Deposits, 1977.

Rogers, John W., Ghuma, Mohamed A., Nagy, Richard M., Greenberg, Jeffrey K. and Fullagar, Paul D. Plutonism in Pan-African belts and the geological evolution of northeastern Africa. *Earth and Planetary Science Letters*, 1978, *39*, 109-117.

Rose, E.R. *Bulletin No. 32, Part II: Geology of the Area Between Bonavista, Trinity and Placentia Bays, Eastern Newfoundland*. Technical Report, Geological Survey of Newfoundland, 1948.

Schoen, Robert. Rate of sulfuric acid formation in Yellowstone National Park. *Geological Society of America Bulletin*, 1969, *80*, 643-650.

Schoen, Robert, White, Donald E., and Hemley, J. J. Argillization by descending acid at Steamboat Springs, Nevada. *Clays and Clay Minerals*, 1974, *22*, 1-22.

Silberman, Miles L. and Berger, Byron R. Relationship of trace-element patterns to alteration and morphology in epithermal precious-metal deposits. In Berger, B. R. and Bethke, P. M. (Ed.), *Geology and Geochemistry of Epithermal Systems*, Society of Economic Geologists, 1985.

Sillitoe, R. H. Metallic Mineralization affiliated to subaerial volcanism: a review. In *Volcanic Processes in Ore Genesis*, Geological Society of London, Special Publication no. 7, 1977.

Sillitoe, Richard H. Enargite-bearing massive sulfide deposits high in porphyry copper systems. *Economic Geology*, 1983, *78*, 348-352.

Sillitoe, Richard H., Baker, Max E., and Brook, William A. Gold deposits and hydrothermal eruption breccias associated with a maar volcano at Wau, Papua New Guinea. *Economic Geology*, 1984, *79*, 638-655.

Slack, John F. Multistage vein ores of the Lake City District, western San Juan mountains, Colorado. *Economic Geology*, 1980, *75*, 963-991.

Spence, W. H., Worthington, J. E., Jones, E. M. and Kiff, I. T. Origin of the gold mineralization at the Haile mine, Lancaster County, South Carolina. *Mining Engineering*, 1980, *32*, 70-73.

Steiner, A. Hydrothermal rock alteration at Wairakei, New Zealand. *Economic Geology*, 1953, *48*, 1-13.

Steven, Thomas A. and Eaton, Gordon P. Environment of ore deposition in the Creede mining district, San Juan mountains, Colorado: I. Geologic, hydrologic, and geophysical setting . *Economic Geology*, 1975, *70*, 1023-1037.

Steven, T. A., Charles, C. G., Naeser, C. W. and Mehnert, H. H. *Revised stratigraphy and radiometric ages of volcanic rocks and mineral deposits in the Marysvale area, west-central Utah.* Technical Report, United States Geological Survey Bulletin 1469, 1979.

Stewart, J. H. Late Precambrian evolution of North America: plate tectonics implications. *Geology*, 1976, *4*, 11-15.

Stoffregen, R. *Genesis of acid-sulphate alteration and Au-Cu-Ag mineralization at Summitville, Colorado.* PhD thesis, University of California (Berkeley), 1985.

Strong, D. F., O'Brien, S. J., Taylor, S. W., Strong, P. G. and Wilton, D. H. *Marystown (1M/3) and St. Lawrence (1L/14) map areas, Newfoundland.* Technical Report, Mineral Development Division, Department of Mines and Energy, Report 77-8, 1978A.

Strong, D. F., O'Brien, S. J., Taylor, S. W., Strong, P. G. and Wilton, D. H. Aborted Proterozoic rifting in eastern Newfoundland. *Canadian Journal of Earth Sciences*, 1978B, *15*, 117-131.

Strong, David F. Proterozoic tectonics of Northwestern Gondwanaland: New evidence from eastern Newfoundland. *Tectonophysics*, 1979, *54*, 81-101.

Taylor, S. W., O'Brien, S. J. and Swinden, H. S. *Geology and mineral potential of the Avalon Zone and granitoid rocks of Eastern Newfoundland.* Technical Report, Mineral Development Division, Department of Mines and Energy, Report 79-3, 1979.

Tuach, J. Metallogenic studies of granite associated mineralization in the Ackley Granite and the Cross Hills Plutonic Complex. In Murray, M. J., Whelan,

J. G. and Gibbons, R. V. (Ed.), *Current Research,* Newfoundland Department of Mines and Energy, Mineral Development Division, Report 84-1, 1984.

Tucker, C. M. and McCann, S. B. Quaternary Events on the Burin Peninsula,and the islands of St. Pierre and Miquelon, France. *Canadian Journal of Earth Sciences*, 1980, *17*, 1462-1479.

Weissberg, B. G. Gold-silver ore-grade precipitates from New Zealand Thermal Waters. *Economic Geology*, 1969, *64*, 95-108.

White, D. E. Thermal springs and epithermal ore deposits. In Bateman, A. M. (Ed.), *Economic Geology 50th Anniversary Volume*, Society of Economic Geologists, 1955.

Williams, Harold. Appalachian orogen in Canada. *Canadian Journal of Earth Science*, 1979, *16*, 792-807.

Williams, Harold and Hatcher, Jr., Robert D. Appalachian suspect terranes. *Geological Society of America*, 1983, *158*, 33-53.

Zotov, A. V. Dependance of the composition of alunite on the temperature of its formation. *Geochemistry International*, 1971, , 71-75.

Appendix

A.1. Sample preparation

Samples collected for geochemical study were approximately 2 kg, one quarter of which was broken off and kept separately for reference or thin sectioning. Care was taken to collect unweathered samples, and only in the schistose, altered rocks was this criterion difficult to fulfill.

Samples were crushed by personnel at the (then) Department of Mines and Energy sample preparation lab in St. John's. Primary crushing to -2 cm was done with a jaw crusher, which was followed by pulverization on a swing mill using a tungsten carbide bowl and puck. Splits of the pulps remain in storage at the facility.

A.2. Analysis of major elements

Major element oxides were initially analyzed by atomic absorption spectrometry following acid dissolution at Memorial University. It was noted, however, that samples of the alunite-bearing rocks were leaving a red precipitate on dissolution, which was shown to be TiO_2 by electron probe microanalysis and specifically rutile by X-ray diffraction analysis. Complete dissolution was achieved, however by alkali carbonate fusion at the Department of Mines and Energy geochemical lab in St. John's, which repeated the analyses on the rutile-bearing rocks and performed all subsequent major element determinations.

Table A-1 lists the standard samples run with the thesis samples and their

accepted values.

A.3. Normative mineralogy

As discussed in Section 4-10, the rocks selected for normative mineralogy determination were the mineralogically simple rocks from the Tower, Bullwinkle and Hickey's Pond showings. They contain quartz, pyrophyllite, alunite, rutile and either pyrite or specularite, which account for all the major element oxides except CaO, MnO, MgO and P_2O_5. For all of these rocks however, the sum of these elements was $<1\%$ by weight. A FORTRAN program was written to do the calculations. It is provided after Figure A-1, which is a flow chart illustrating its operation.

Table A-1: Comparison of major element data with published data for standard samples. "DME" is analysis of standard within a batch of samples for this study and "pub" is published value of the standard (Abbey, 1983).

	DR-N		GSP-1		BCR-1		BX-N	
	DME	pub	DME	pub	DME	pub	DME	pub
SiO2	53.65	52.85	67.00	67.32	54.60	54.53	7.55	7.40
Al2O3	18.39	17.52	15.18	15.28	13.70	13.72	55.05	54.21
Fe2O3	9.62	9.70	4.33	4.30	13.48	13.41	22.54	23.17
MgO	4.27	4.40	.97	.97	3.53	3.48	.07	.11
CaO	6.87	7.05	1.95	2.03	7.07	6.97	.14	.17
Na2O	3.00	2.99	2.75	2.81	3.29	3.30	.02	.04
K2O	1.70	1.70	5.51	5.51	1.73	1.70	.04	.05
TiO2	.1.09	1.09	.67	.66	2.32	2.26	2.19	2.37
MnO	.23	.22	.05	.04	.20	.18	.05	.05
P2O5	.24	.25	.29	.28	.38	.36	.15	.13

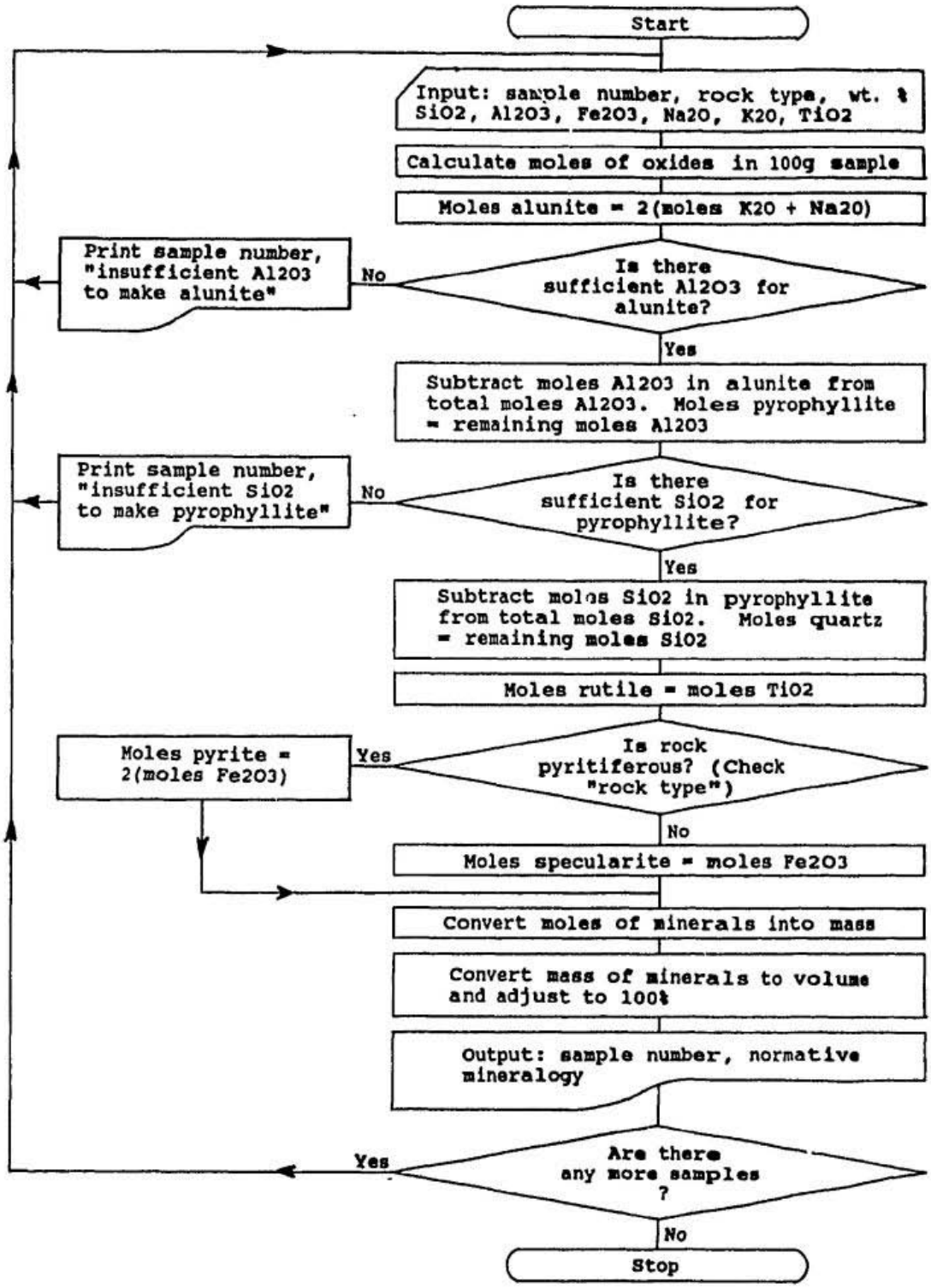

Figure A-1: Normative mineralogy computer program flowchart. Figure illustrates operation of the program which produced the data in Tables 4-2 and 6-1.

NORMATIVE MINERALOGY PROGRAM
FORTRAN 77

```
      integer rktype
c     rktype is 3 if pyritiferous
      real masal, maspph, masqtz, masrut, maspec, maspy
c     real variables above correspond to mass of alunite,
c     pyrophyllite, quartz, rutile, specularite and pyrite
10    Read (1, 100) name, rktype, loc, xsi, xal, xfe,
     +xna, xk, xti, xloi, xtotal
c     'name' is sample number, this statement inputs major
c     element data
100   format (i3, i2, i2, /, 13x, f5.2, 1x, f5.2,
     +1x, f5.2, 10x, 2f5.2, 1x, f4.2, 11x, f5.2, 2x, f6.2,/,/)
      if (name .eq. 999) goto 900
c     this tests for end of data
      diff = xtotal - (xsi + xal + xfe + xna + xk + xti + xloi)
c     'diff' is the mass of elements not in normative minerals
      xmolsi = xsi/60.0848
      xmolal = xal/101.9612
      xmolfe = xfe/159.6922
      xmolna = xna/61.979
      xmolk = xk/94.2034
      xk2o = 0.00
      if ((xmolk + xmolna) .eq. 0.0) goto 120
      xk2o = (100.0 * xmolk)/(xmolk + xmolna)
120   xmolti = xti/79.8988
c     the "xmol" variables convert percentage of each oxide into
c     number of moles, assuming a 100 g sample
      ymolal = (xmolna + xmolk)*2.0
      if ((xmolna + xmolk) .gt. (xmolal/3.0)) goto 450
      xmolal = xmolal - (1.5 * ymolal)
      ymolpph = xmolal
      if (xmolal .gt. (xmolsi/4.0)) goto 470
      xmolsi = xmolsi - (4.0 * ymolpph)
      ymolqtz = xmolsi
      ymolrut = xmolti
      if (rktype .eq. 3) goto 300
      ymolpy = 0.0
      ymolspec = xmolfe
      goto 350
300   ymolspec = 0.0
      ymolpy = 2.0 * xmolfe
c     the "ymol" variables convert moles of oxides into moles
c     of minerals
```

```
350   masal = ymolal * (398.09 + (xk2o * 0.1611))
      maspph = ymolpph * 360.31574
      masqtz = ymolqtz * 60.0848
      masrut = ymolrut * 79.8988
      masspec = ymolspec * 159.6922
      maspy = ymolpy * 120.0
      totmas = masal + maspph + masqtz + masrut + masspec + maspy
c     the "mas" variables convert moles of minerals into the mass
c     each mineral
      volal = masal/2.82
      volpph = maspph/2.77
      volqtz = masqtz/2.65
      volrut = masrut/4.86
      volspec = masspec/5.25
      volpy = maspy/4.99
c     the "vol" variables convert mass of minerals into volume
c     and the following statements recast the volume to 100%
      totvol = volal + volpph + volqtz + volrut + volspec + volpy
      if (totvol .eq. 0.0) goto 10
      volal = 100.0 * (volal/totvol)
      volpph = 100.0 * (volpph/totvol)
      volqtz = 100.0 * (volqtz/totvol)
      volrut = 100.0 * (volrut/totvol)
      volspec = 100.0 * (volspec/totvol)
      volpy = 100.0 * (volpy/totvol)
c     data are outputted with the following write statement
      write (2, 400) name, volqtz, volal, xk2o,
     +volpph,volrut,volspec,volpy, diff
400   format (3x, i3, 2x,
f5.2,1x,f5.2,1x,f4.1,1x,f5.2,1x,f4.2,1x,f5.2,1x,
     +f4.2,1x,f4.2)
      goto 10
450   write (2, 460) name
460   format (3x, i3, 3x, 27hinsufficient Al for alunite)
      goto 10
470   write (2, 480) name
480   format (  3x, i3,  3x, 32hinsufficient Si for pyrophyllite)
      goto 10
900   stop
      end
```

A.4. Analysis of trace elements

Concentrations of Cu, Pb, Zn, Ba, Sr, Rb, U, Th, Y, Zr, Nb, Ga, Ni and V were determined by X-ray fluorescence spectrometry at Memorial University. Samples were first pelletized by subjecting 10 g of sample mixed with 1.25 g of a binding agent (Union Carbide phenolic resin TR-16933) to a 50 MPa pressure in a 40 mm die for approximately one minute, followed by baking at 200 C for ten minutes. The pellets were analyzed in a Phillips 1450 automatic X-ray fluorescence spectrometer calibrated against international standards. Table A-2 lists the range, mean and accepted value for a standard sample (G2) which was analyzed with every batch of 10 samples from the thesis.

Gold concentrations were determined at Chemex Labs Ltd. in Vancouver. Most samples were analyzed by atomic absorption spectrometry following a fire assay concentration, but the fire assay for some samples was (at the request of the lab) followed by neutron activation analysis.

Silver analyses were performed by atomic absorption spectrometry by personnel at the Department of Mines' geochemical lab in St. John's, and As, Sb and Hg were analyzed by various techniques at Chemex Labs Ltd. in Vancouver.

A.5. Analysis of rare earth elements

Rare earth elements were analyzed by the thin-film X-ray fluorescence technique outlined by Fryer (1977), which involves separation of REE in cation exchange columns followed by precipitation onto filter paper and analysis. A Tm spike monitored the efficiency of the REE separation and provided a correction factor for loss. This factor (yield) is provided with the corrected data and chondrite normalizing factors in Table A-3. Fryer reports accuracy of +/- 10% or +/- 0.1ppm, whichever is greater.

Table A-2: Comparison of trace element data with published data for standard sample. Standard sample G2 was analyzed in every batch of 10 samples. "Accepted" value is from Flanagan (1970), "Mean", "Low" and "High" are based on 20 analyses of G2.

	Accepted	Mean	Low	High
Cu	10	24	18	27
Pb	30	35	22	47
Zn	84	84	79	88
Ba	1900	1826	1756	1899
Sr	480	466	445	487
Rb	170	165	153	173
U	2	2	0	8
Th	25	28	10	45
Y	11	13	7	17
Zr	300	302	295	307
Nb	13	14	11	19
Ga	23	22	20	23
Ni	4	8	5	10
V	36	37	32	41

Table A-3: Rare earth element data. Concentrations are reported in parts per million, N. F. is the normalizing factor used to construct the plots in Figures 2-18 and 3-5 and "yield" is the fraction of the Tm spike measured during analysis.

-#-	La	Ce	Pr	Nd	Sm	Eu	Gd	Dy	Er	Yb	Yield
22	14.7	40.5	5.3	26.5	7.8	0.2	6.6	7.1	2.4	1.9	.26
51	58.3	121.2	11.9	52.4	9.8	1.0	5.8	2.5	1.1	0.4	.34
81	34.5	74.1	6.7	31.7	6.1	0.7	5.2	4.5	2.3	1.8	.52
133	35.7	93.3	11.3	48.6	12.7	0.0	12.5	14.3	8.3	6.5	.44
138	58.5	109.3	9.7	39.7	7.0	0.8	5.4	4.8	2.1	1.4	.51
149	32.6	67.7	6.9	28.1	5.5	0.7	4.4	4.3	2.1	1.1	.52
154	73.2	138.0	12.7	54.5	8.8	0.3	5.9	2.3	1.2	0.4	.49
159	63.2	127.9	12.8	51.3	9.0	0.6	4.5	2.0	1.3	1.1	.53
161	64.9	118.2	8.8	32.9	3.9	0.1	3.5	2.9	2.2	0.4	.35
201	31.6	62.7	6.8	24.2	3.9	0.0	3.9	4.6	2.1	1.1	.27
213	75.7	171.0	18.9	90.9	22.5	0.0	21.1	21.9	11.7	8.6	.44
214	73.0	161.8	18.1	90.8	21.9	2.2	20.7	21.3	10.6	6.8	.44
221	6.5	14.6	1.5	7.7	1.6	0.6	1.7	2.1	1.2	1.3	.50
239	45.6	91.4	6.9	30.7	4.5	1.0	3.3	2.7	1.6	0.6	.36
244	67.0	118.4	10.2	42.0	7.6	0.8	4.2	2.6	0.5	0.4	.40
251	35.0	80.9	5.8	26.2	4.2	0.3	3.4	3.8	1.8	1.4	.41
N.F.	.315	.813	.116	.597	.197	.0722	.259	.325	.213	.208	

A.6. Electron probe microanalyser technique

Polished carbon-coated thin sections were examined in a Hitachi S570 scanning electron microscope at an accelerating voltage of 15 kV. Backscattered electron imaging was obtained with a GW Electronics Type 113 solid state backscattered electron detector. X-ray analysis was performed on beam spot mode with a Tracor Northern 5500 energy dispersive X-ray analyzer equipped with a Microtrace silicon X-ray spectrometer (Model 70152) with a spectral resolution of 145 eV. X-ray spectra referenced throughout the text appear on the following pages. Detector/sample positioning gave an effective take-off angle of 30 degrees. Backscattered electron images were recorded on Polaroid Type 665 positive/negative film.

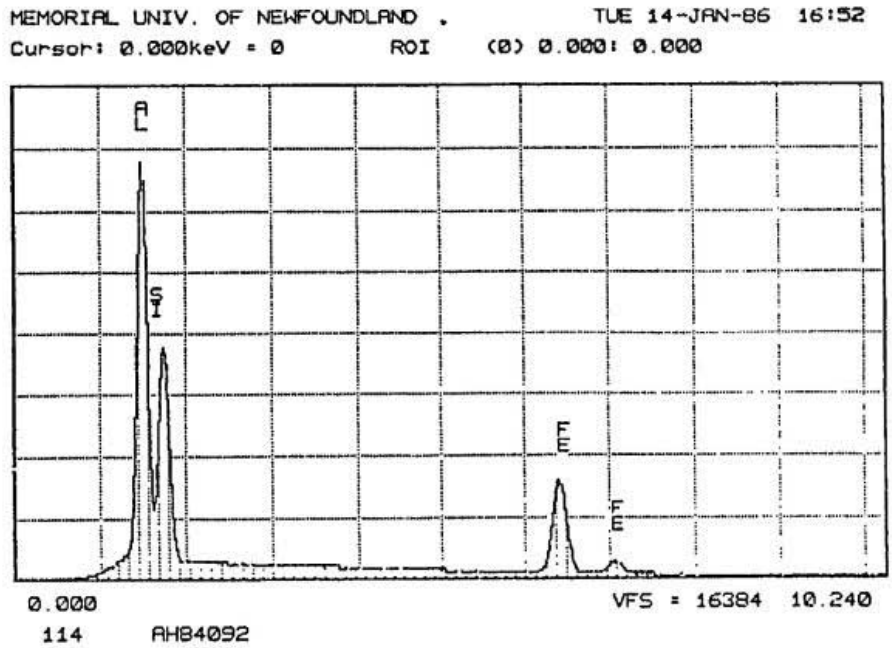

Figure A-2: Fe-chloritoid at Little Pond Showing. Note lack of Mg.

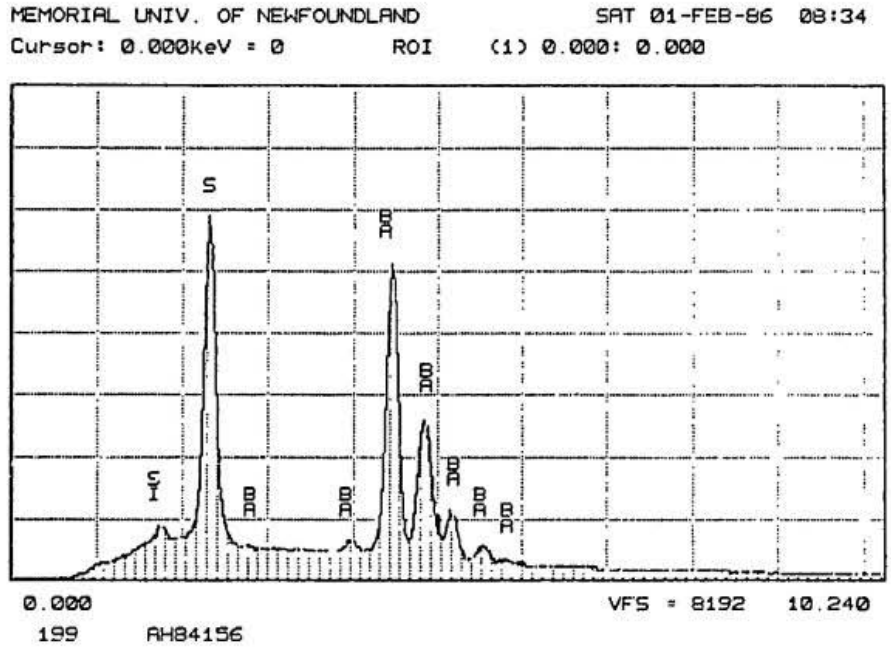

Figure A-3: Barite in specularite-rich breccia at Chimney Falls.

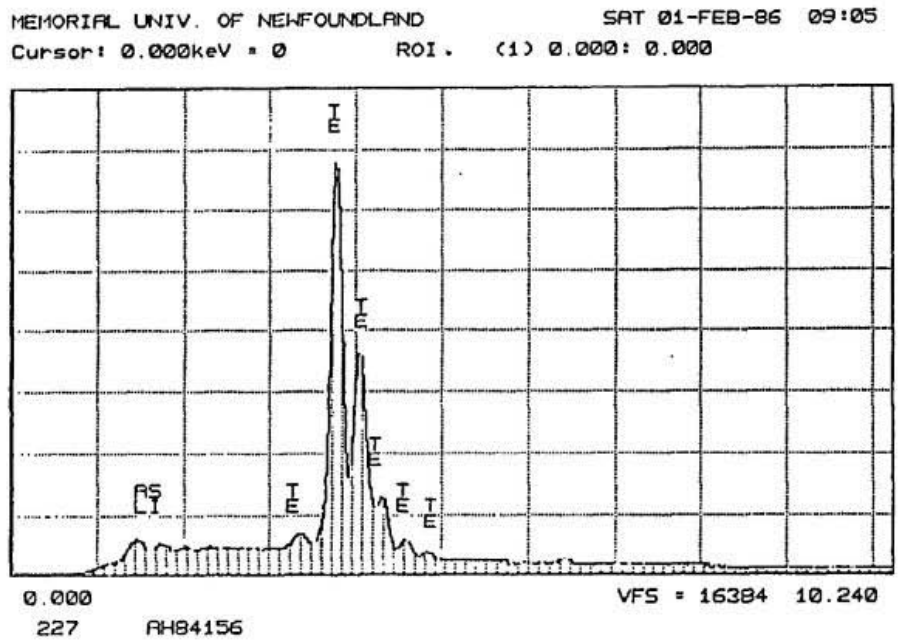

Figure A-4: Native tellurium in specularite-rich breccia at Chimney Falls.

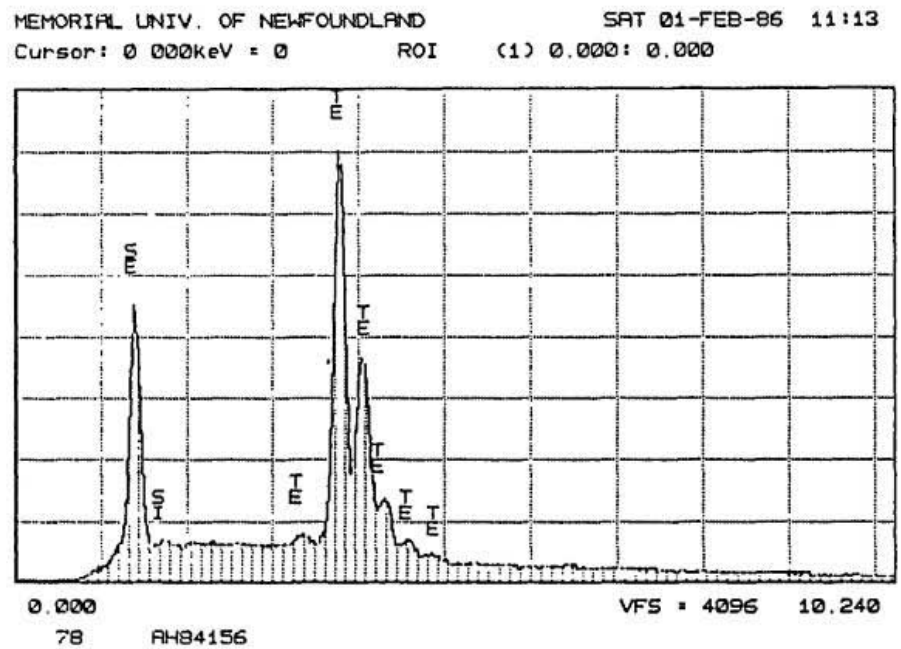

Figure A-5: Selentellurium in specularite-rich breccia at Chimney Falls.

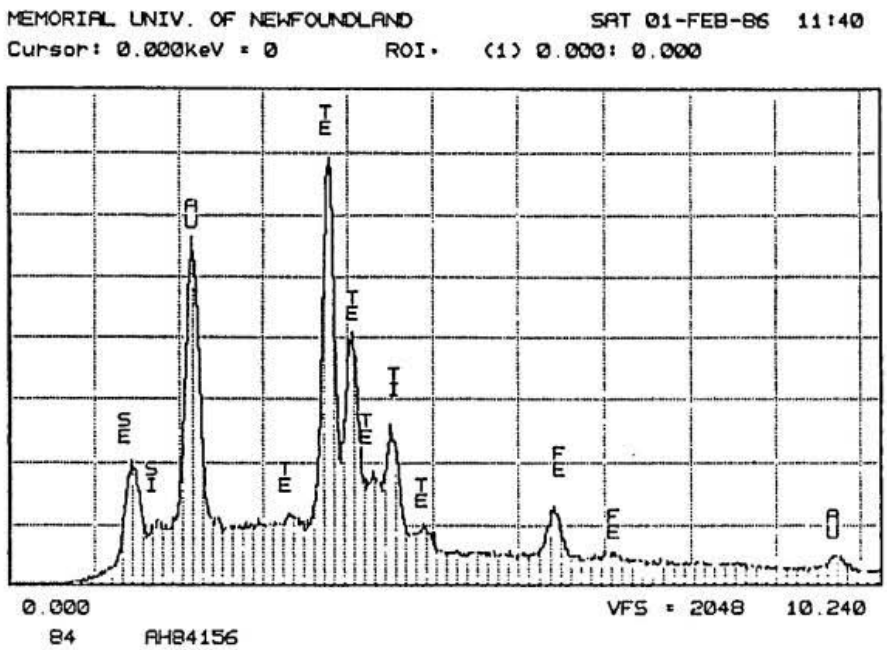

Figure A-6: Gold telluride (calaverite) in specularite-rich breccia at Chimney Falls. Note presence of Se and Fe, the latter of which could be from specularite inadvertently "sampled" by the electron beam.

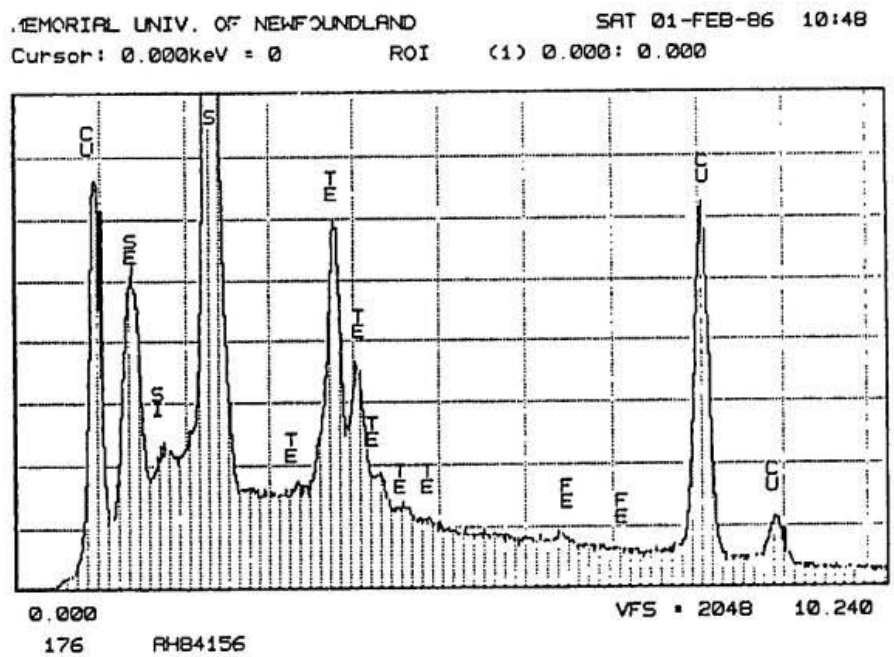

Figure A-7: Unidentified copper mineral in specularite-rich breccia at Chimney Falls.

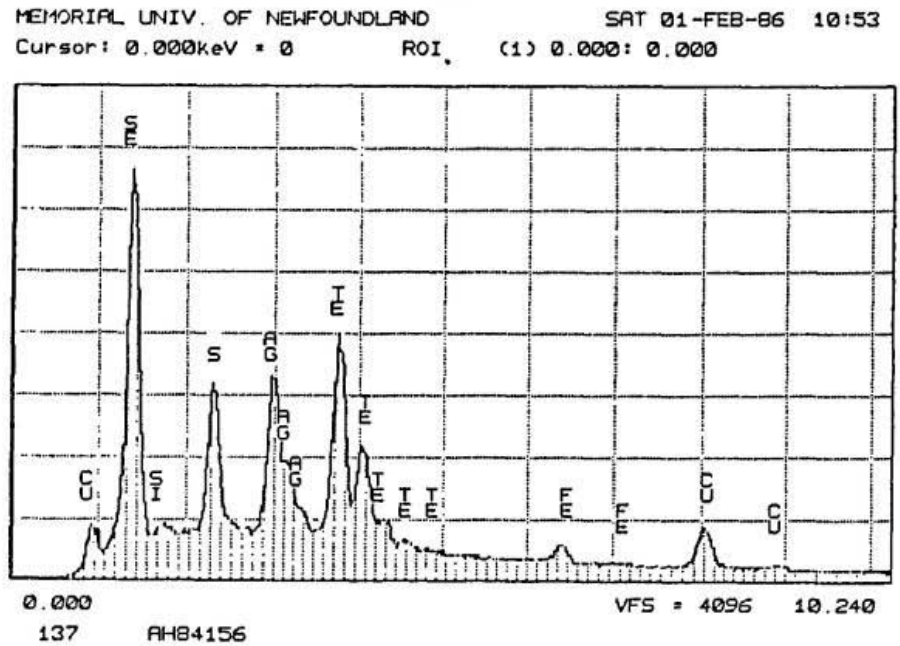

Figure A-8: Unidentified silver mineral in specularite-rich breccia at Chimney Falls.

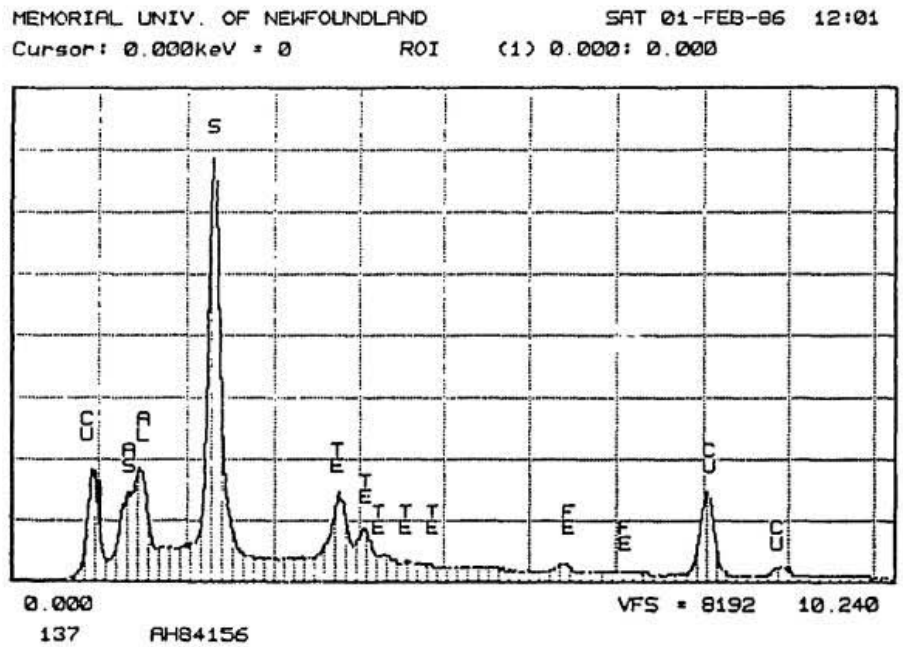

Figure A-9: Telluriferous tennantite in specularite-rich breccia at Chimney Falls. Aluminum peak is probably from an adjacent mineral. Spectrum is nearly identical to one obtained from a mineral in hotsprings precipitate at Hickey's Pond (Figure A-23).

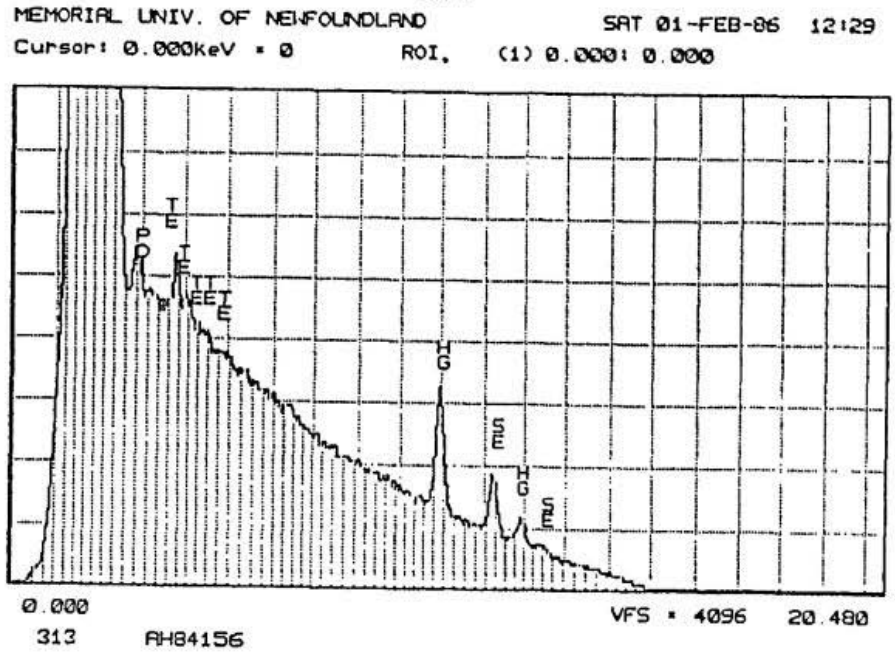

Figure A-10: Mercury selenide (tiemannite) in specularite- rich breccia at Chimney Falls. Vertical expansion shows the presence of Te and Pd, but pushes the main peaks of Hg and Se far offscale. [20 KeV accelerating voltage.]

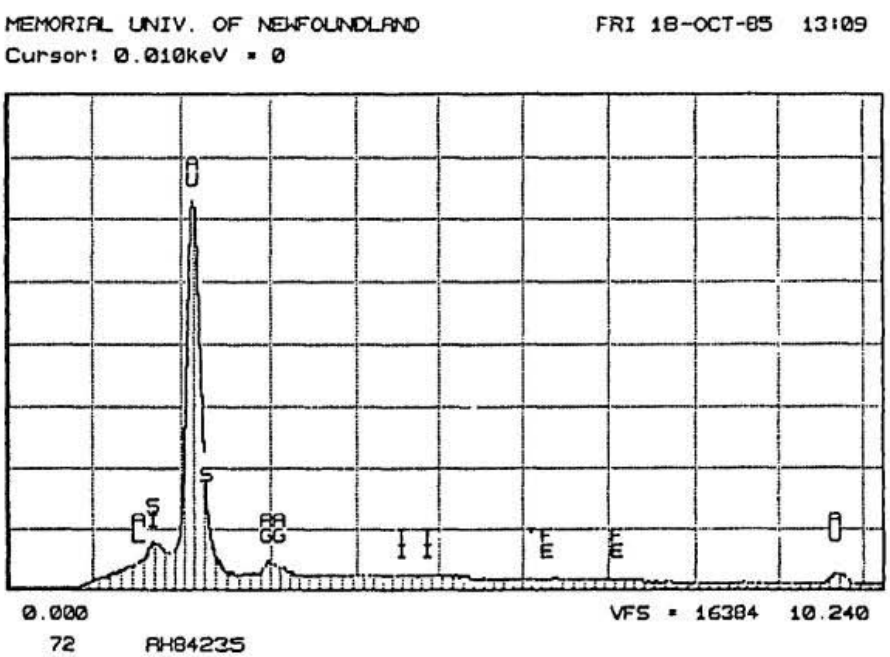

Figure A-11: Gold in specularite-rich breccia at Hickey's Pond. Note very small peaks for Ag.

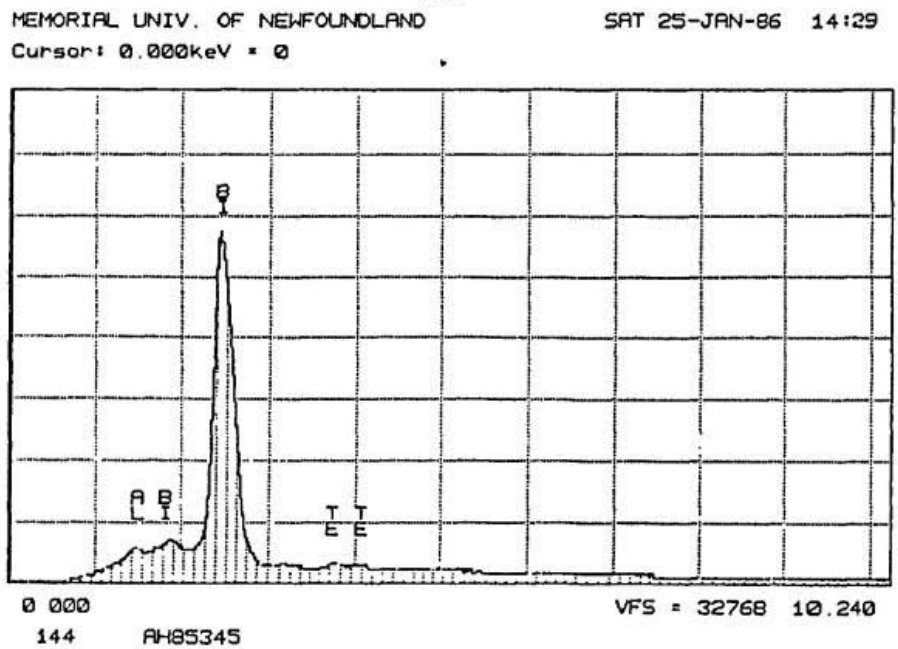

Figure A-12: Native bismuth in specularite-rich breccia at Hickey's Pond.

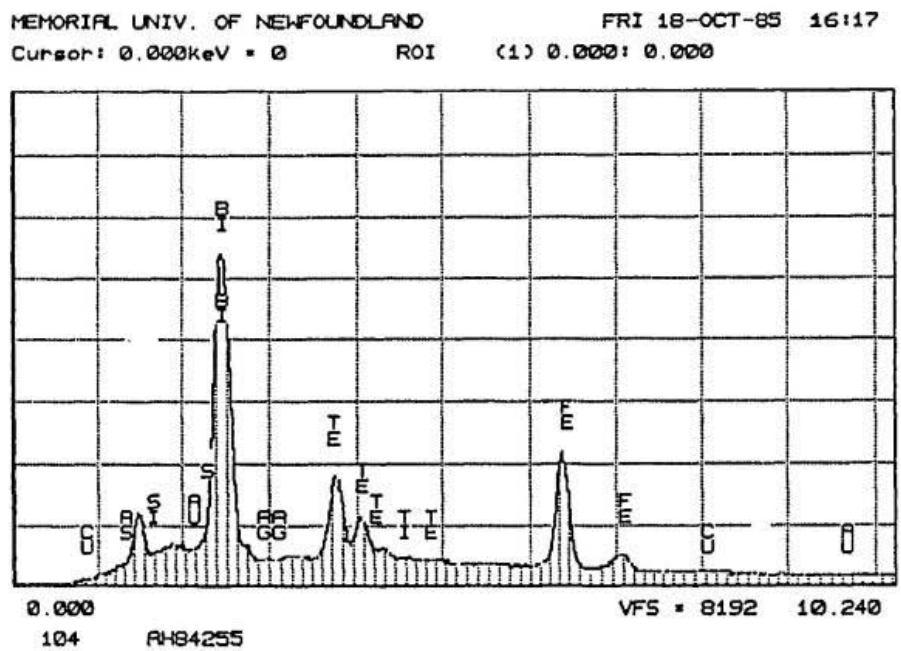

Figure A-13: Tellurobismuthite in specularite-rich breccia at Hickey's Pond. Iron in spectrum reflects "sampling" of host specularite crystal.

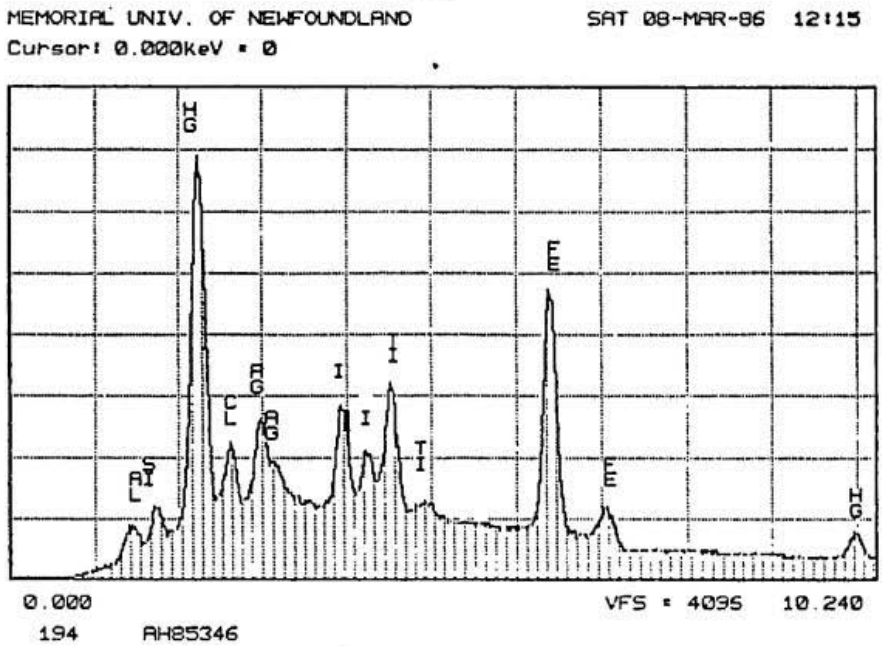

Figure A-14: Mercury and silver halides in specularite-rich breccia at Hickey's Pond. Crystal was only 0.0015 mm across and Fe, Ti, Al and Si in spectrum probably reflect inadvertent sampling of host material.

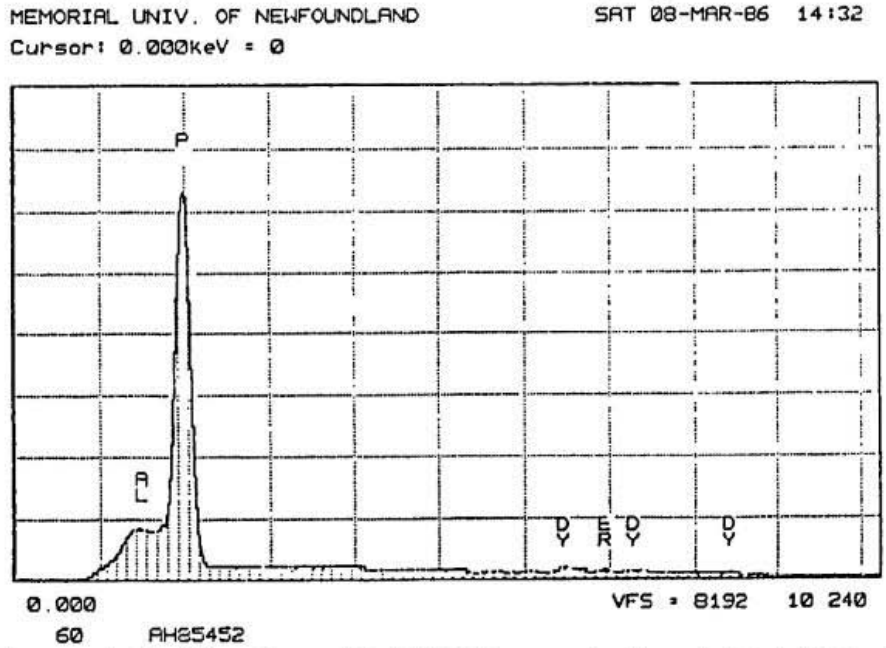

Figure A-15: Xenotime with HREE in specularite veinlet at Hickey's Pond. Note that P completely obscures Y peak. Among the REE, only Dy and Er (even atomic numbers, high chondritic concentration) were detected, but other HREE, *viz* Tb, Ho and Tm, if present at a comparable normalized concentration, would be at too low an absolute concentration to be detected.

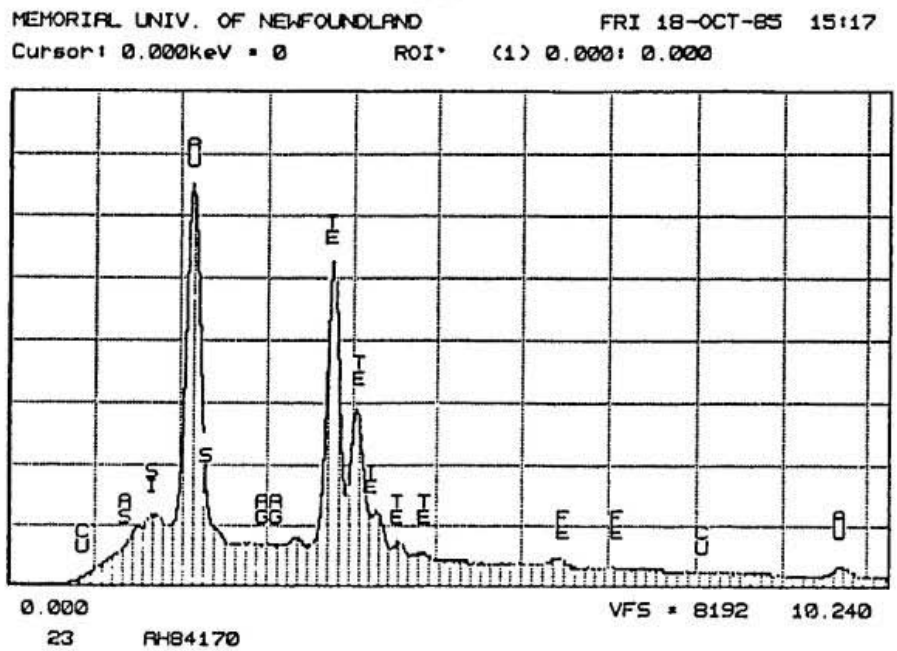

Figure A-16: Gold telluride (calaverite) in silicified, pyritiferous rock at Hickey's Pond.

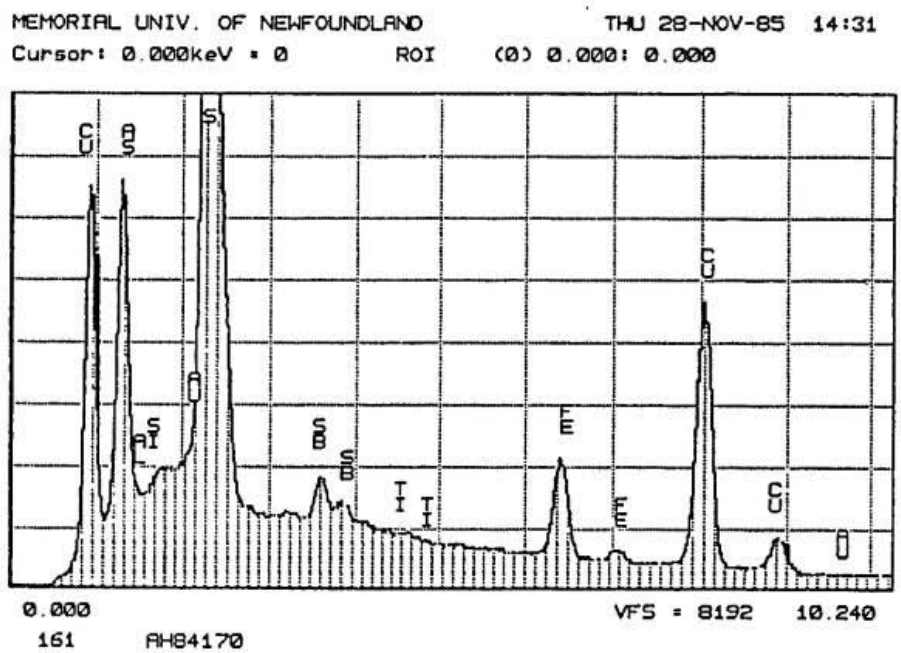

Figure A-17: Tennantite in silicified, pyritiferous rock at Hickey's Pond. Note presence of Sb.

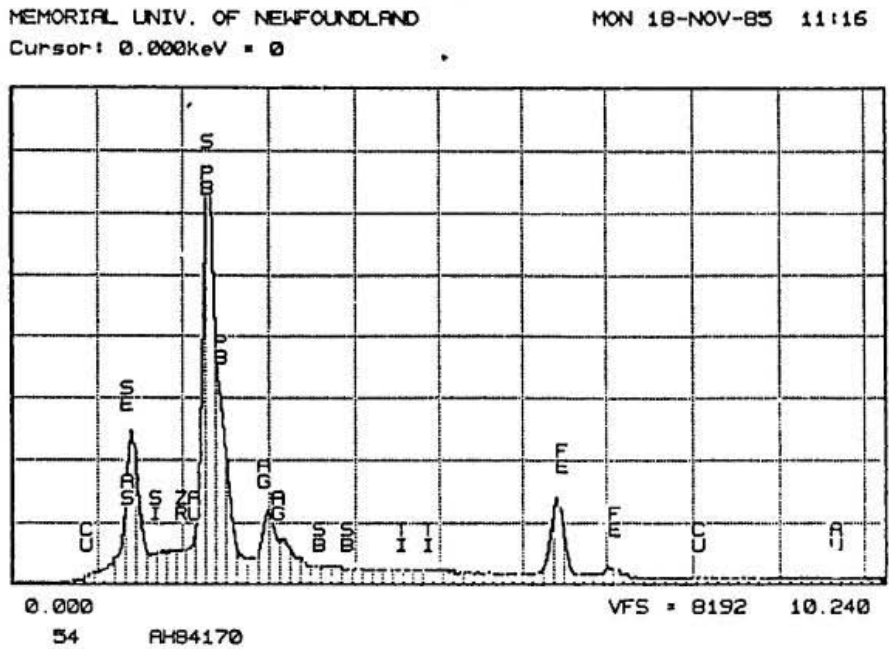

Figure A-18: Galena and silver selenide in silicified, pyritiferous rock at Hickey's Pond. Iron in spectrum probably reflects host pyrite.

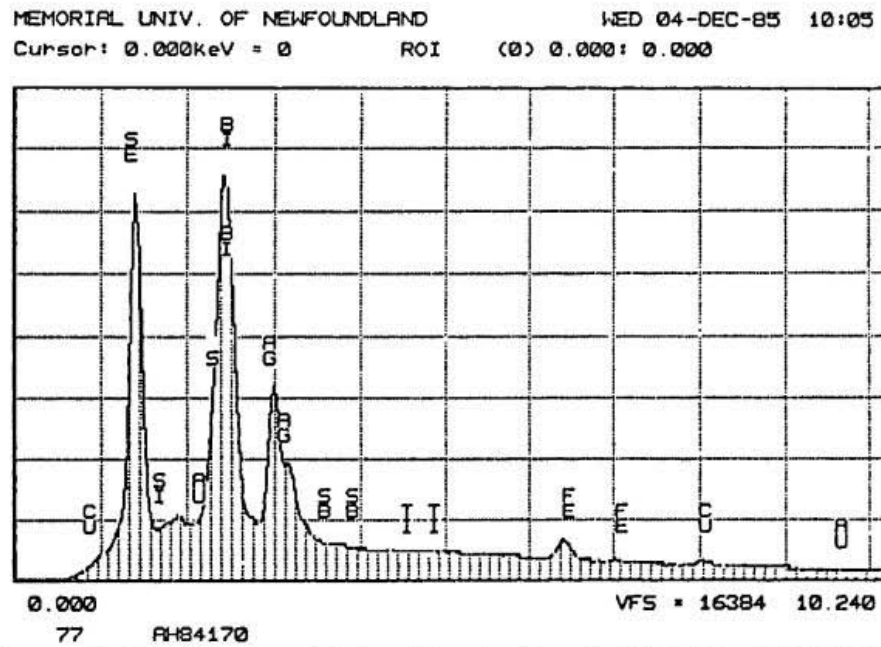

Figure A-19: Silver and bismuth selenides in silicified, pyritiferous rock at Hickey's Pond.

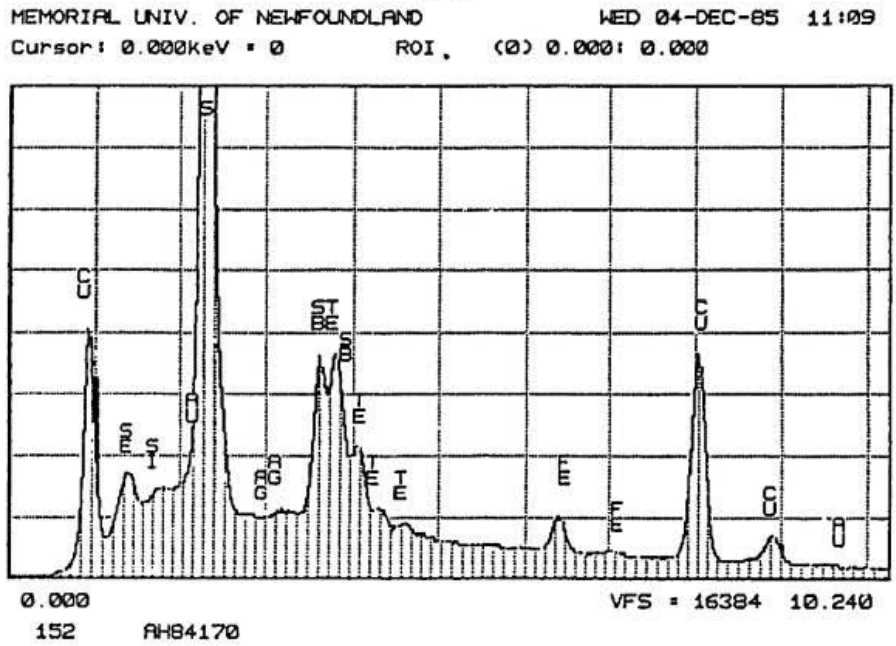

Figure A-20: Unidentified copper sulfosalt in silicified, pyritiferous rock at Hickey's Pond.

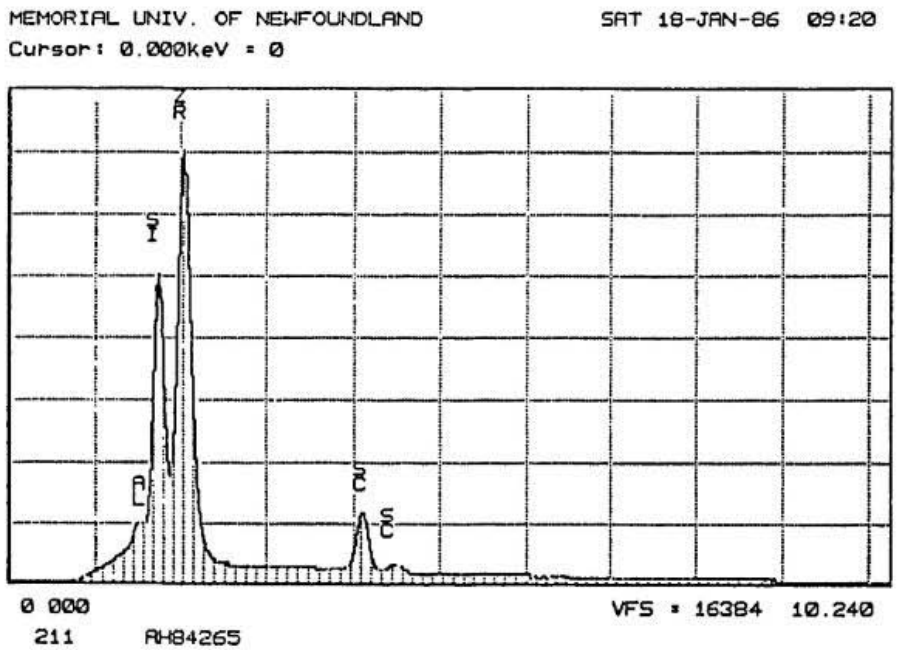

Figure A-21: Sc in zircon in specularite-banded rock at Hickey's Pond.

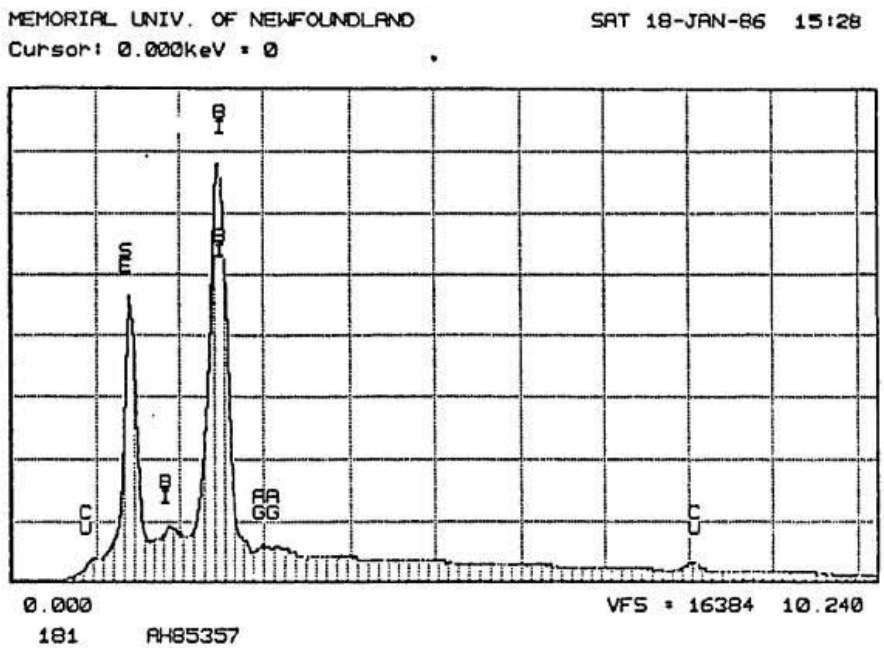

Figure A-22: Guanajuatite (Bi_2Se_3) in specularite- banded rock at Hickey's Pond.

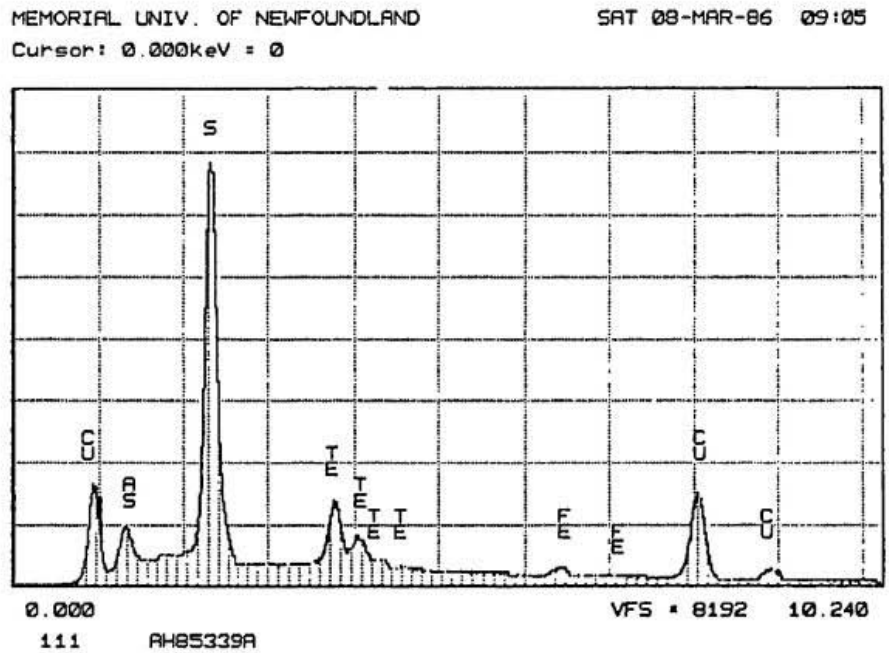

Figure A-23: Telluriferous tennantite in hotsprings precipitate at Hickey's Pond. Spectrum is nearly identical to one obtained from a mineral in specularite-rich breccia at Chimney Falls (Figure A-9).

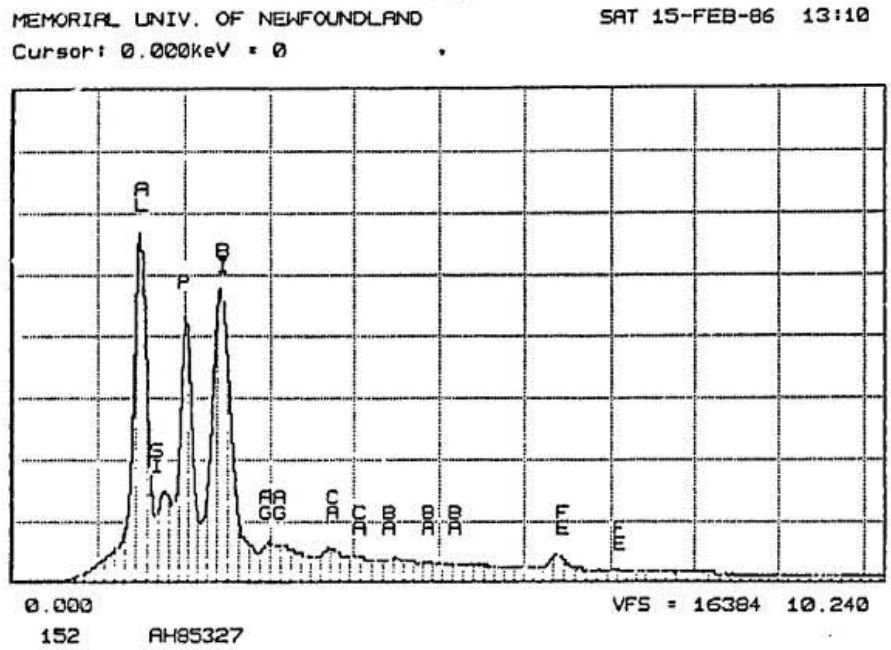

Figure A-24: Bi-Al phosphate in black, specularite-rich rock at Strange Showing. Vertical expansion (not shown) reveals Ag, Ca and Ba in the spectrum.

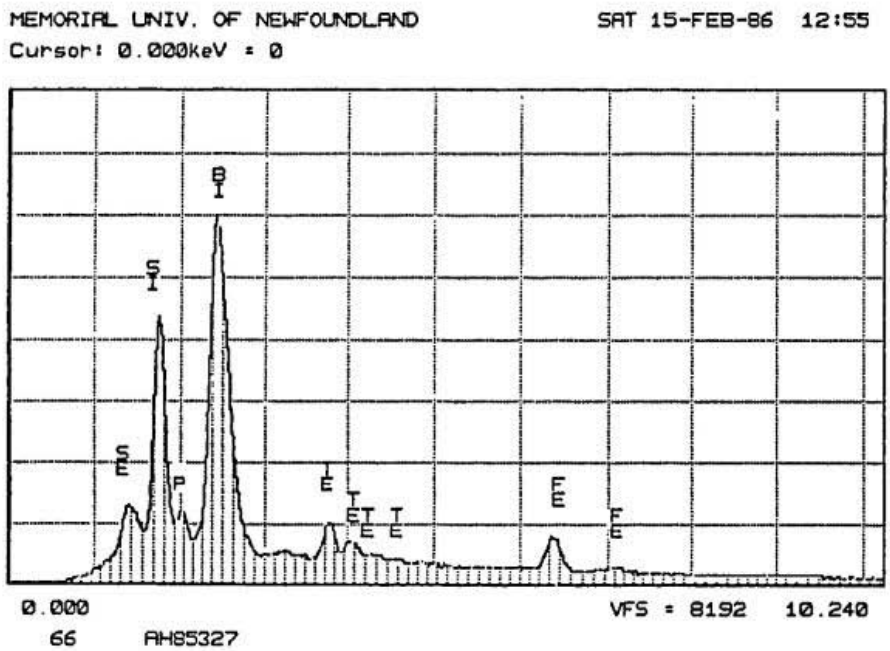

Figure A-25: Native bismuth in black, specularite-rich rock at Strange Showing. Spectrum also reveals Se, P, Te and Fe. Prominent Si peak is inferred to represent adjacent quartz.

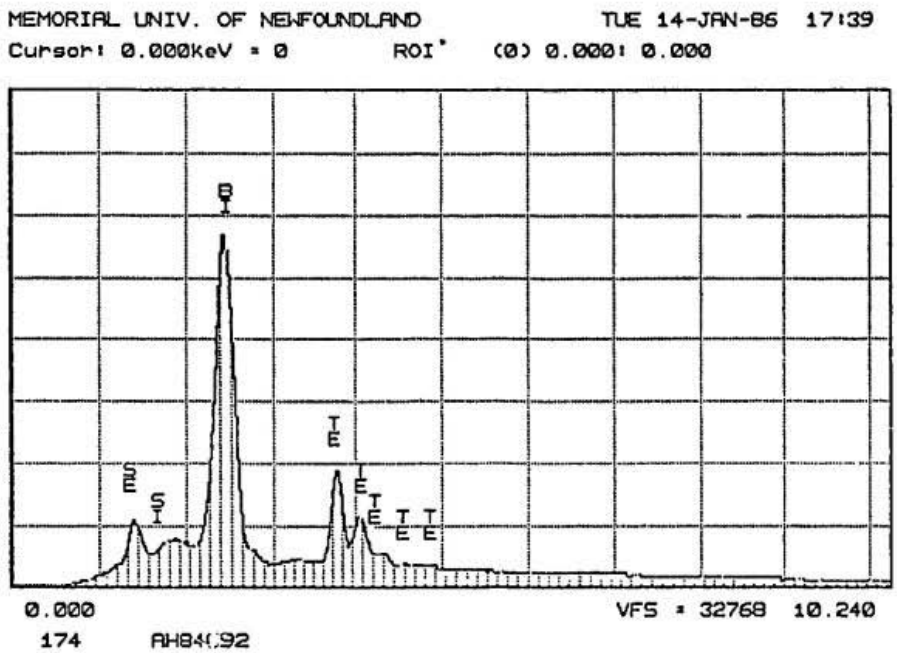

Figure A-26: Tellurobismuthite at Little Pond Showing. Note presence of Se.

References

Abbey, Sydney. *Studies in 'standard samples' of silicate rocks and minerals.* Technical Report Paper 83-15, Geological Survey of Canada, 1983.

Flanagan, F. J. Sources of Geochemical Standards - II. *Geochimica et Cosmochimica Acta*, 1970, *34*, 121-125.

Fryer, B. J. Rare earth evidence in iron formation for changing oxidation states. *Geochimica et Cosmochimica Acta*, 1977, *41*, 361-367.

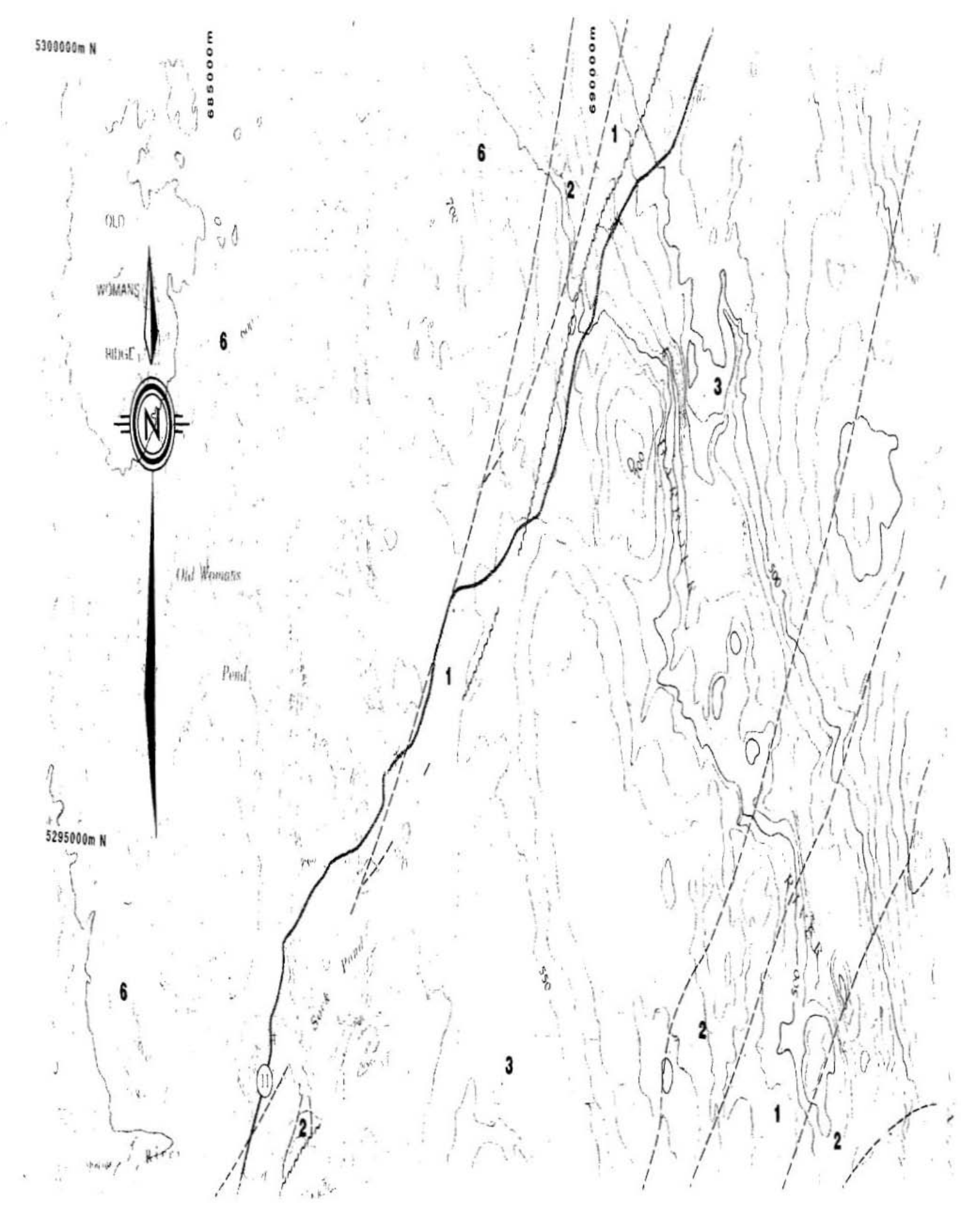
5300000m N
6850000m
6900000m
OLD
WOMANS
HIGH
Old Womans
Pond
5295000m N

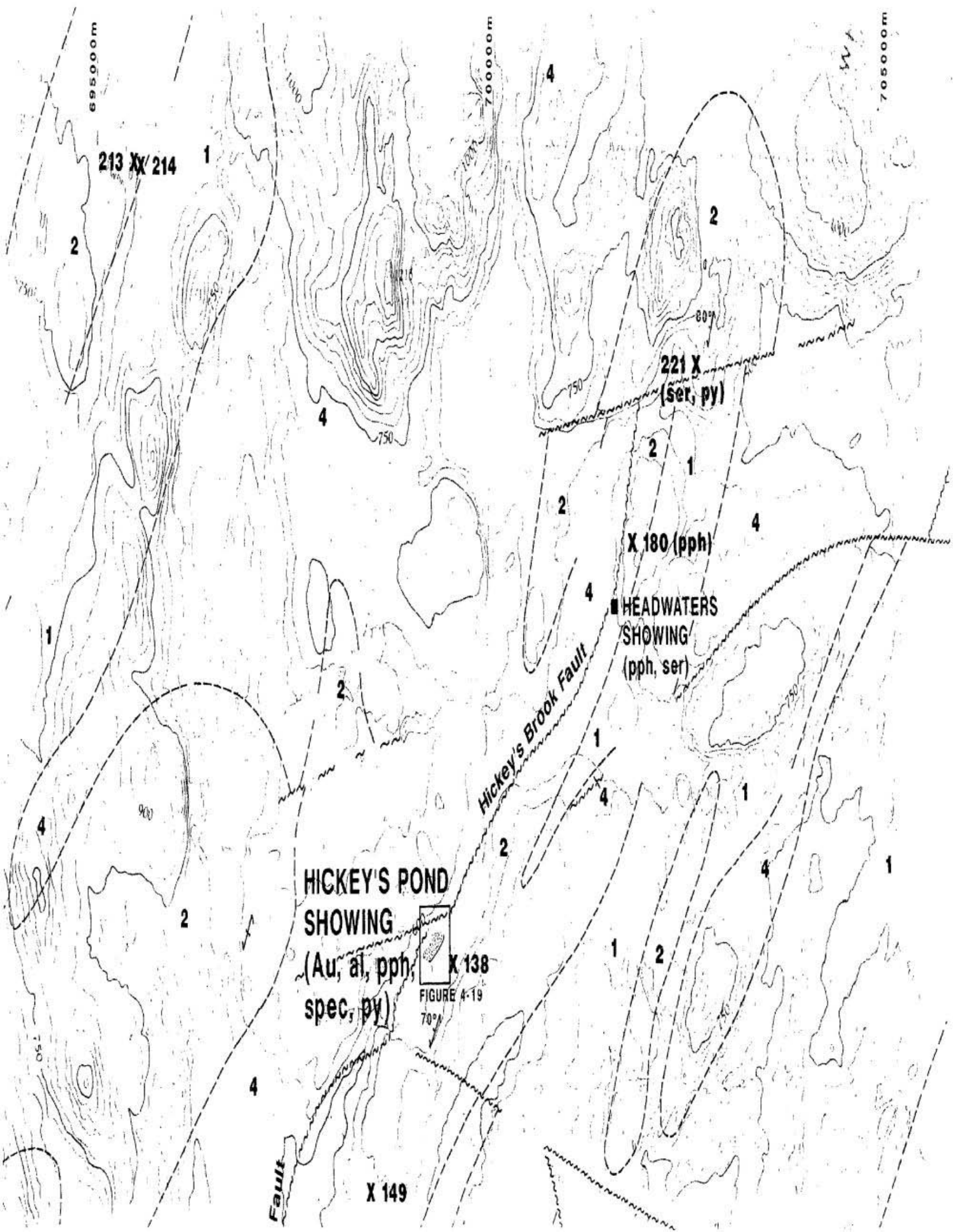
695000m
700000m
705000m
213 X
X 214
221 X
(ser, py)
X 180 (pph)
HEADWATERS
SHOWING
(pph, ser)
Hickey's Brook Fault
HICKEY'S POND
SHOWING
(Au, ai, pph,
spec, py)
X 138
X 149
Fault
FIGURE 4-19

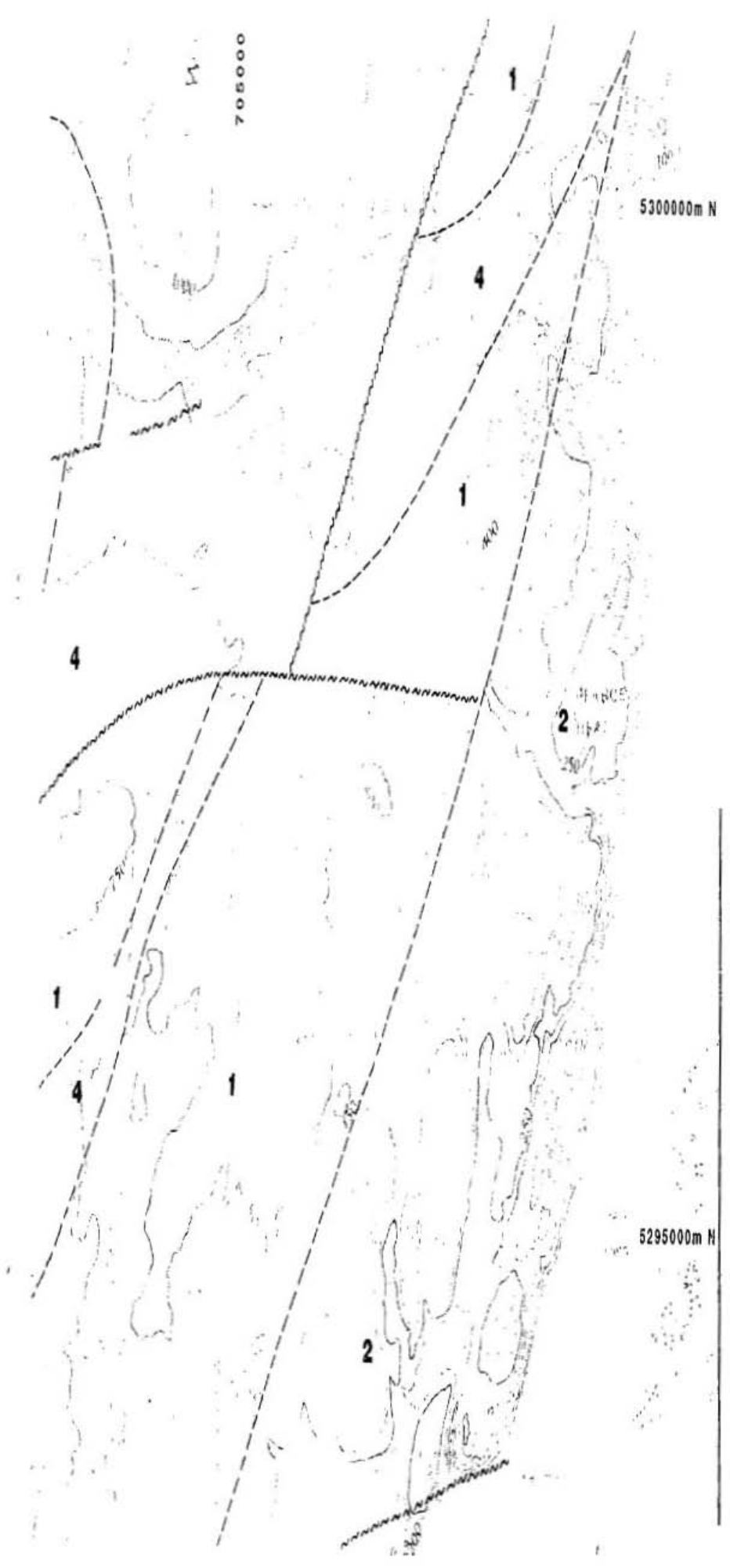
705000
5300000m N
5295000m N
1
4
1
4
2
1
4
1
2

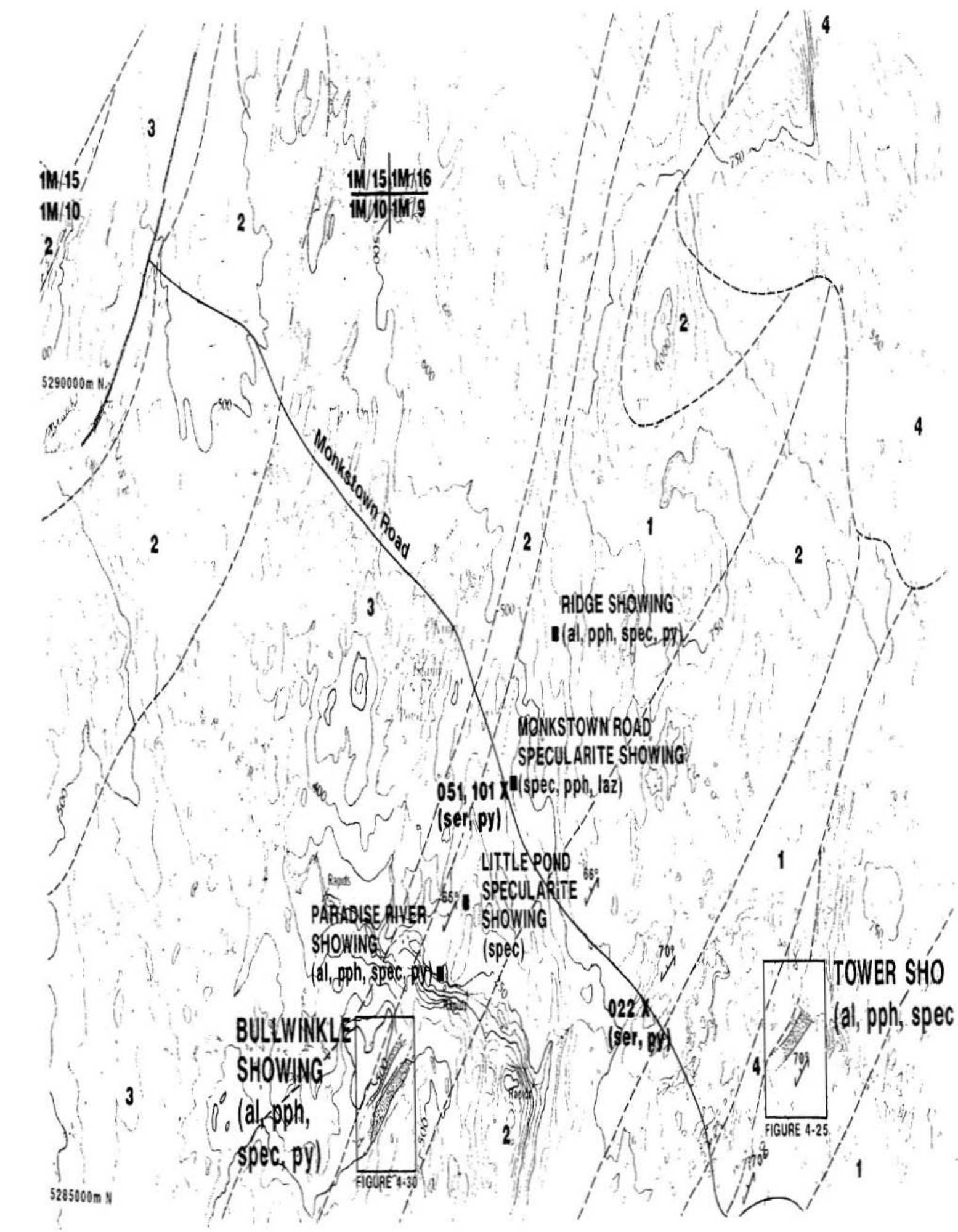
1M/15
1M/10
1M/15 1M/16
1M/10 1M/9
5290000m N
Monkstown Road
RIDGE SHOWING
(al, pph, spec, py)
MONKSTOWN ROAD
SPECULARITE SHOWING
(spec, pph, laz)
051, 101 X
(ser, py)
LITTLE POND
SPECULARITE
SHOWING
(spec)
PARADISE RIVER
SHOWING
(al, pph, spec, py)
BULLWINKLE
SHOWING
(al, pph,
spec, py)
022 X
(ser, py)
TOWER SHO
(al, pph, spec
FIGURE 4-30
FIGURE 4-25
5285000m N

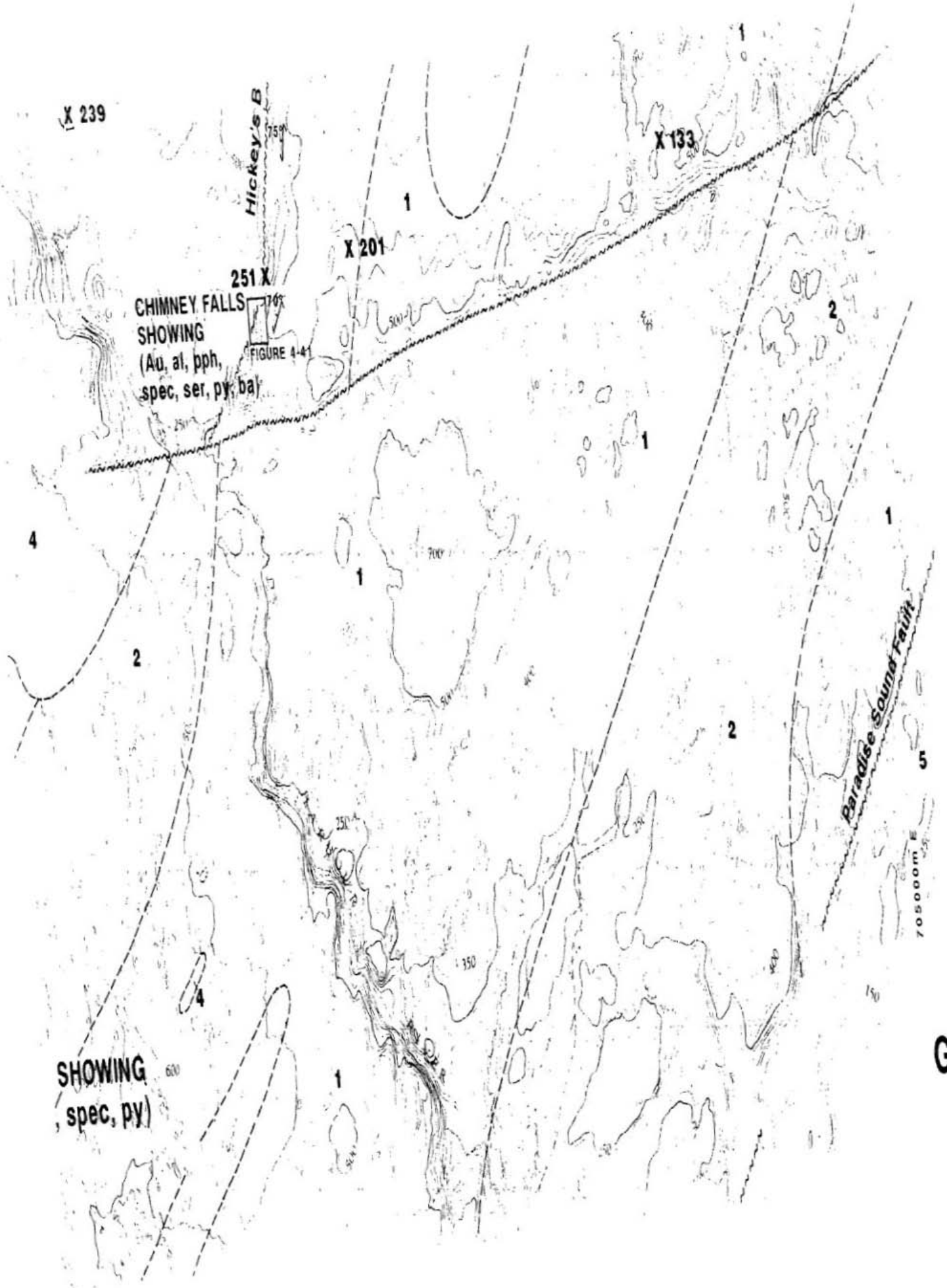
X 239
Hickey's B
X 133
X 201
251 X
CHIMNEY FALLS
SHOWING
(Au, al, pph,
spec, ser, py, ba)
FIGURE 4-41
Paradise Sound Fault
SHOWING
, spec, py)
GE

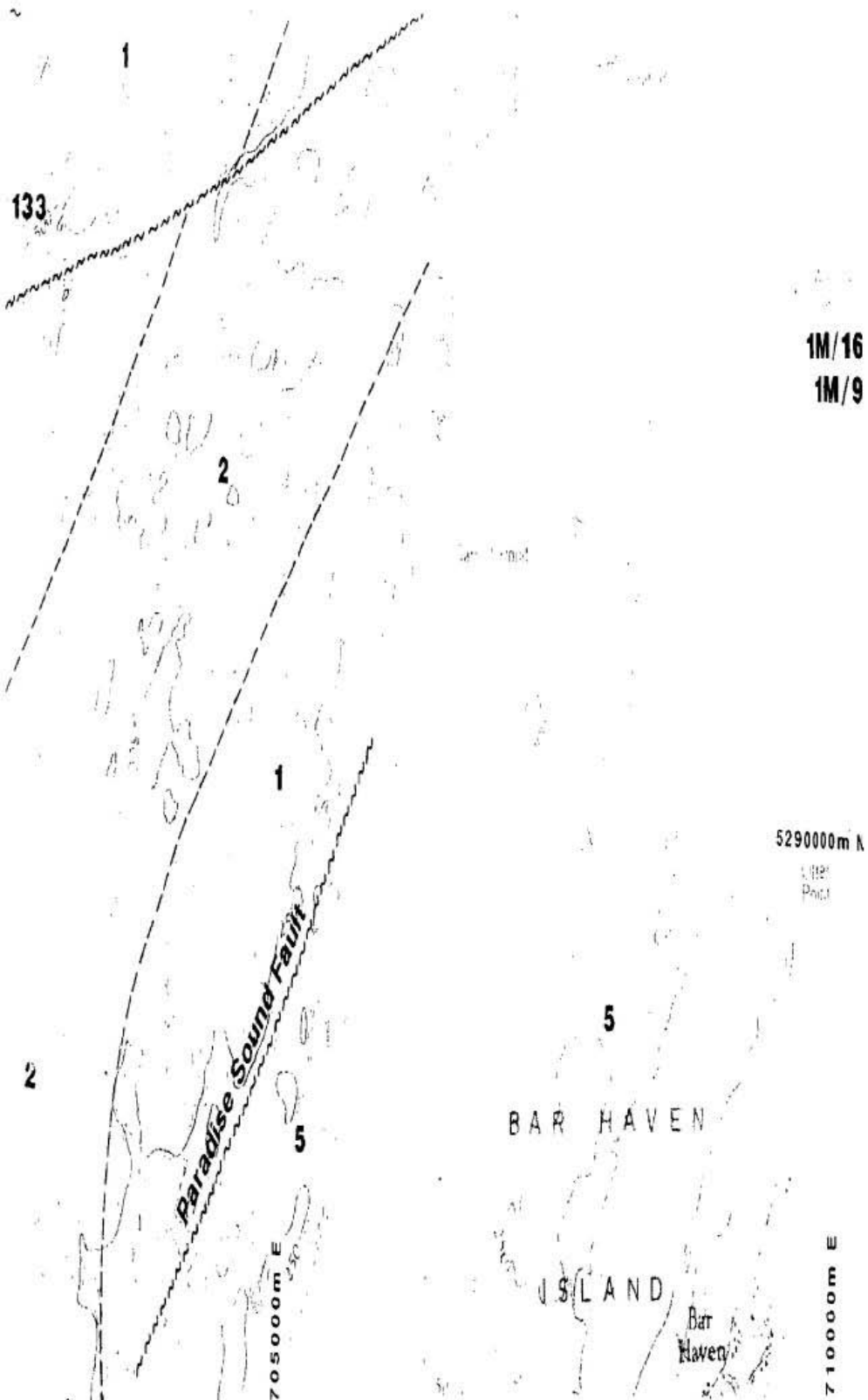

FIGURE 2 - 1
GEOLOGY OF STUDY AREA
with
mineral occurrences

FIGURE 4-30

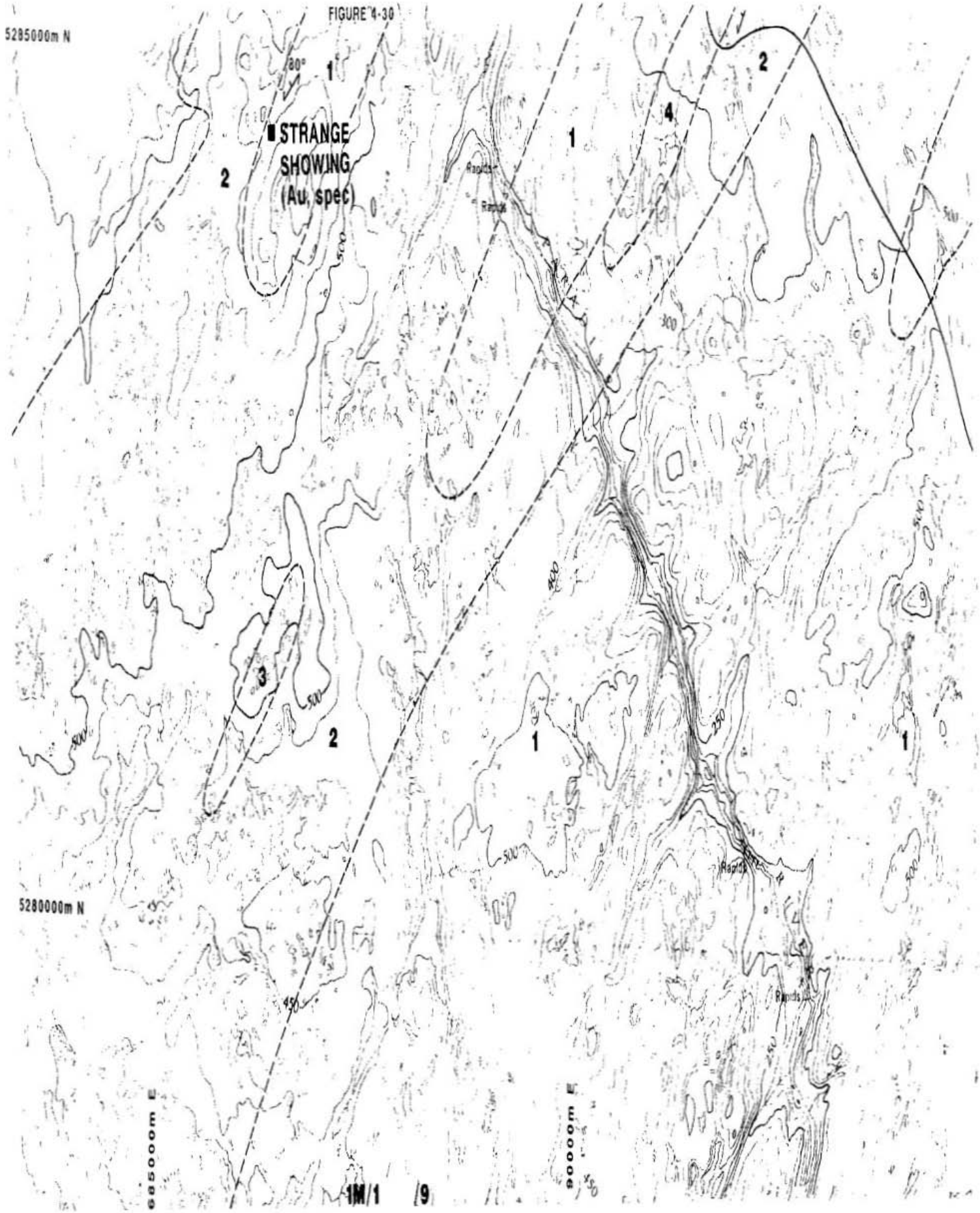
5285000m N
STRANGE SHOWING (Au, spec)
Rapids
5280000m N
685000m E
690000m E
1M/1
9

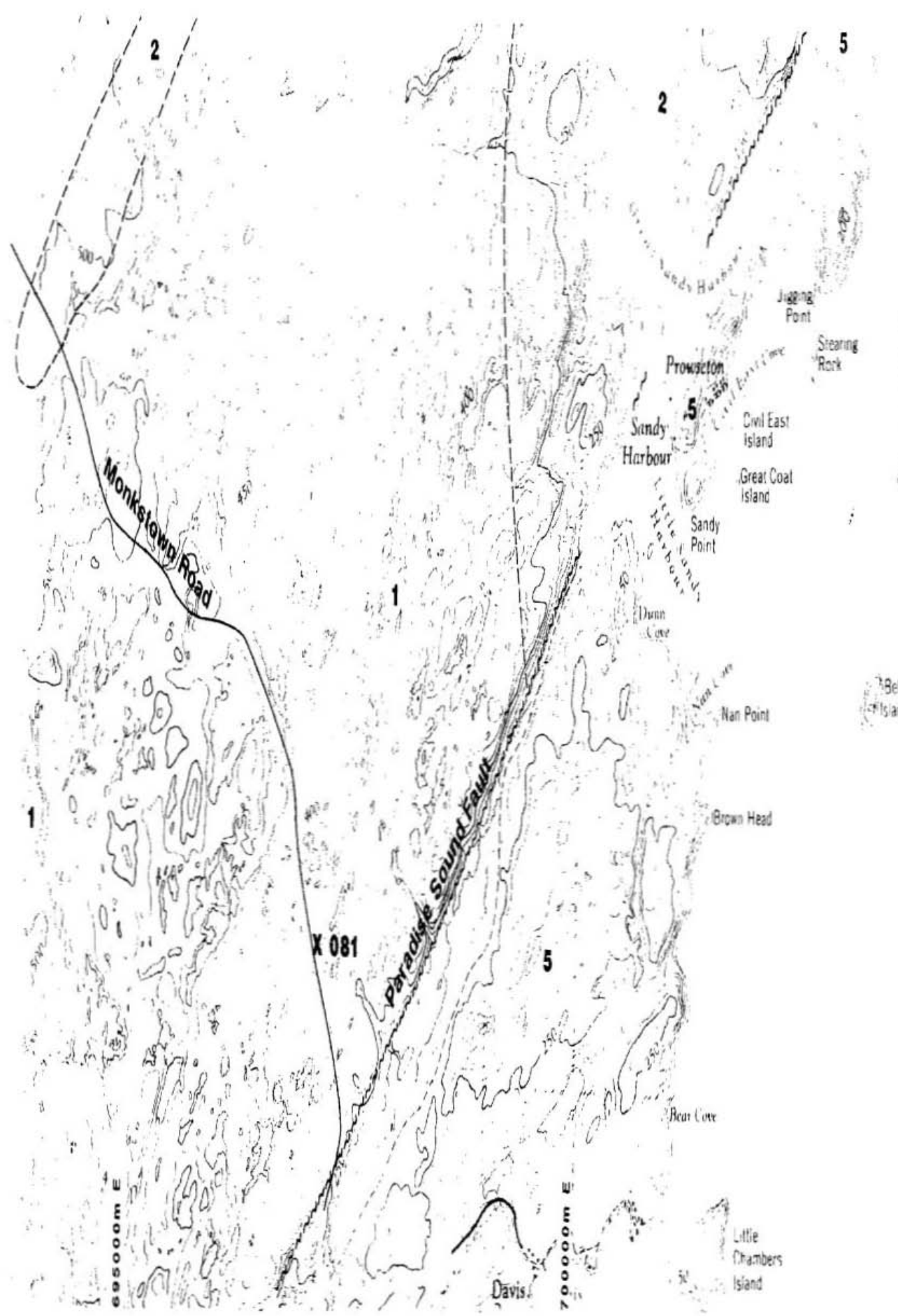

DEV
AC
6
CAMB
MU
5
HADR
SW
4
LO
3
2
1

Geoche
Mineral
Major al-
Geologic
Fault
Cleavage

Referenc
1M/9: mo
1M/10: n
1M/15: Ir
1M/16:

0

and geochemical sample sites

5285000m N

DEVONIAN

ACKLEY GRANITE

6 Massive, feldspar-megacrystic biotite granite.

CAMBRIAN AND EARLIER

MUSGRAVETOWN GROUP

5 Green to purple clastic sediments, minor mafic flows.

HADRYNIAN

SWIFT CURRENT GRANITE

4 Medium-grained, foliated hornblende-biotite granite and granodiorite.

LOVE COVE GROUP

3 Green to grey graywacke, siltstone, arkosic sandstone and conglomerate.

2 Predominantly felsic pyroclastics and flows. Minor mafic flows, tuffs and dykes.

1 Predominantly mafic flows, tuffs and dykes. Minor intercalated felsic tuffs.

Geochemical sample site X
Mineral occurrence ..... ■
Major al-pph-spec-py showing .....
Geological contact .....
Fault .....
Cleavage ..... 70°

Au ..... gold
al ..... alunite
ba ..... barite
laz ..... lazulite
pph ..... pyrophyllite
py ..... pyrite
ser ..... sericite
spec ..... specularite

References:
1M/9: modified from O'Driscoll, 1978
1M/10: modified from O'Brien et al., 1984a
1M/15: from O'Brien et al., 1984b
1M/16: modified from O'Driscoll and Hussey, 1978

5280000m N

0 1 2 3 4 5 km

SCALE = 1:25 000

to accompany M.Sc. thesis (M.U.N.) by A. Huard (1989)

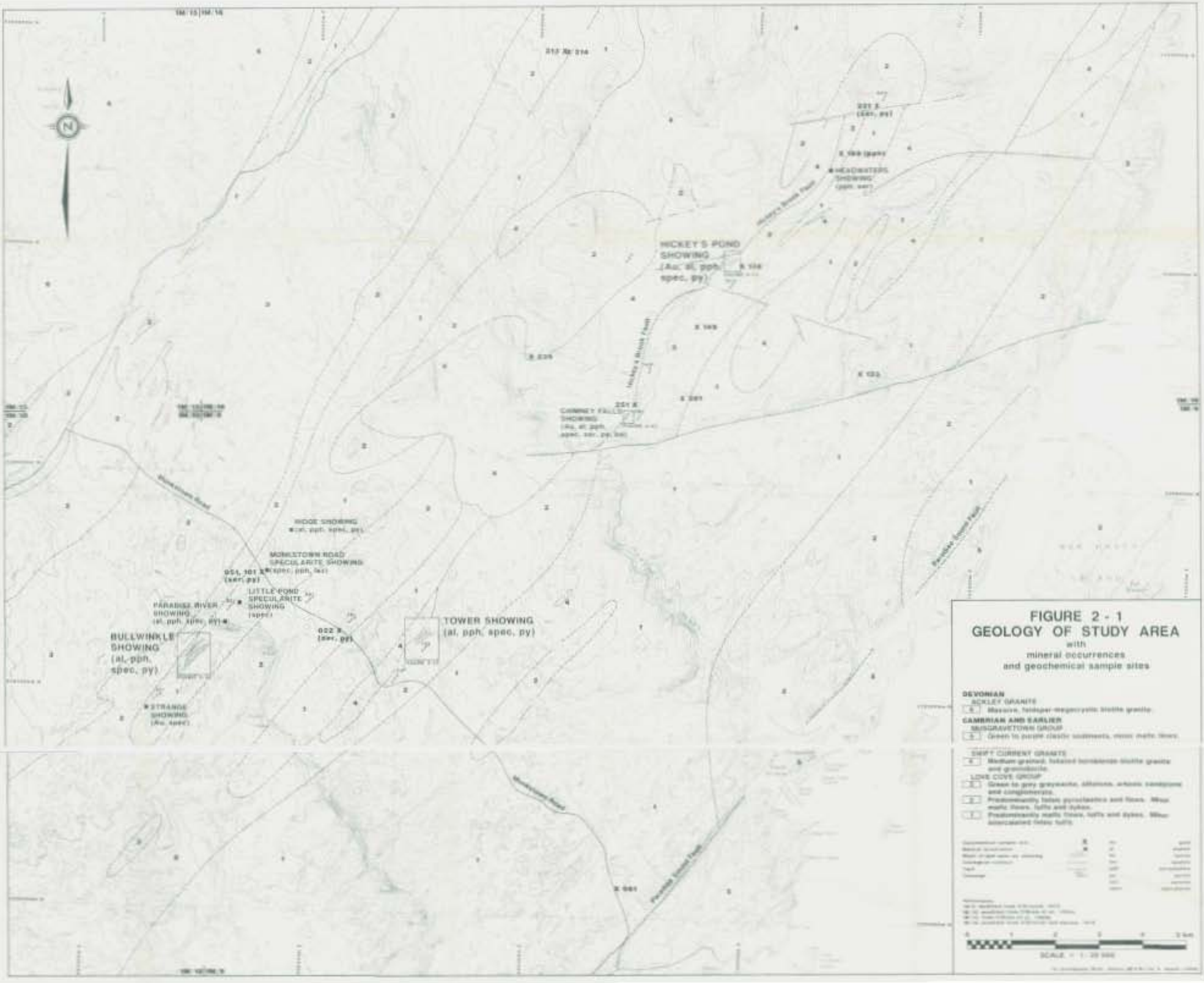
HICKEY'S POND SHOWING (Au, al, pph, spec, py)
CHIMNEY FALLS SHOWING (Au, al, pph, spec, sec, py, bo)
HEADWATERS SHOWING (pph, sec)
RIDGE SHOWING (al, pph, spec, py)
MONKSTOWN ROAD SPECULARITE SHOWING (spec, pph, bo)
LITTLE POND SPECULARITE SHOWING (spec)
PARADISE RIVER SHOWING (al, pph, spec, py)
BULLWINKLE SHOWING (al, pph, spec, py)
STRANGE SHOWING (Au, spec)
TOWER SHOWING (al, pph, spec, py)
Monkstown Road
Hickey's Brook Fault
Paradise River Fault
FIGURE 2 - 1
GEOLOGY OF STUDY AREA
with
mineral occurrences
and geochemical sample sites
DEVONIAN
ACKLEY GRANITE
Massive, feldspar-megacrystic biotite granite.
CAMBRIAN AND EARLIER
MUSGRAVETOWN GROUP
Green to purple clastic sediments, minor mafic flows.
SWIFT CURRENT GRANITE
Medium-grained, foliated hornblende-biotite granite and granodiorite.
LOVE COVE GROUP
Green to grey greywacke, siltstone, arkosic sandstone and conglomerate.
Predominantly felsic pyroclastics and flows. Minor mafic flows, tuffs and dykes.
Predominantly mafic flows, tuffs and dykes. Minor associated felsic tuffs.
SCALE 1 : 25 000